

# **Characterizing the Integrin-mediated Adhesion Profile of Single Cells by AFM-based Force Spectroscopy**

Zur Erlangung des akademischen Grades eines

**DOKTORS DER NATURWISSENSCHAFTEN**

(Dr. rer. Nat.)

Fakultät für Chemie und Biowissenschaften

Karlsruher Institut für Technologie (KIT) – Campus Süd

genehmigte

**DISSERTATION**

von

**Lu DAO**

aus

Jiangsu, China

Dekan: Prof. Dr. Martin Bastmeyer

Referent: Prof. Dr. Martin Bastmeyer

Co-Referent: Prof. Dr. Doris Wedlich

Tag der mündlichen Prüfung: 20.07.2012

Der experimentelle Teil der vorliegenden Arbeit wurde im Center for Functional Nanostructures und am Institut für Zell- und Neurobiologie (Zoologie I) des Karlsruher Instituts für Technologie (KIT) in der Zeit von April 2008 bis Mai 2012 durchgeführt.

Ich versichere, dass ich diese Arbeit selbstständig verfasst und keine anderen als die angegebenen Quellen und Hilfsmittel verwendet habe.

Lu DAO, 01. Juni 2012

# Table of Contents

---

<b>Abbreviations, symbols and units</b>	<b>- 1 -</b>
<b>Summary</b>	<b>- 4 -</b>
<b>Zusammenfassung (German)</b>	<b>- 6 -</b>
<b>1 Introduction and motivation</b>	<b>- 9 -</b>
1.1 Extracellular Matrix	- 9 -
1.1.1 Collagens	- 10 -
1.1.1.1 Fibrillar collagens	- 11 -
1.1.1.2 Network-forming type IV collagen	- 13 -
1.1.2 Laminins	- 14 -
1.2 Integrin-mediated cell adhesion to the ECM	- 16 -
1.2.1 Integrin structure	- 17 -
1.2.2 Conformational change involved in integrin activation	- 20 -
1.2.3 Integrin signaling	- 21 -
1.2.4 Collagen-binding integrins	- 22 -
1.2.5 Laminin-binding integrins	- 24 -
1.2.6 Integrin crosstalk	- 24 -
1.3 Microcontact printing ( $\mu$ CP)	- 26 -
1.4 Atomic force microscopy	- 30 -
1.4.1 Imaging mode	- 30 -
1.4.1.1 Basic principle	- 30 -
1.4.1.2 Forces between the AFM tip and sample surfaces	- 32 -
1.4.1.3 Imaging modes	- 33 -
1.4.2 Force spectroscopy mode	- 35 -
1.4.2.1 Basic principle	- 35 -
1.4.2.2 AFM based single cell force spectroscopy	- 37 -
1.5 Cell adhesion assays	- 41 -
1.5.1 Bulk assays	- 41 -
1.5.2 Single cell assays	- 42 -
1.5.2.1 Glass microneedle	- 42 -
1.5.2.2 Biomembrane force probe	- 43 -
1.5.2.3 Optical tweezers	- 43 -
1.5.2.4 Magnetic tweezers	- 43 -
1.6 Motivation	- 46 -
<b>2 Materials and Methods</b>	<b>- 47 -</b>
2.1 Materials	- 47 -
2.1.1 Reagents and Kits	- 47 -
2.1.2 Antibodies and labeling reagents list	- 49 -
2.1.3 Buffers and solutions	- 50 -
2.1.4 Software	- 50 -

2.1.5	Apparatus	- 51 -
2.2	Methods	- 52 -
2.2.1	Cell adhesion substrate preparation	- 52 -
2.2.1.1	Protein/PEG bifunctional substrates	- 52 -
2.2.1.2	Laminin/fibrillar collagen I bifunctional substrates	- 53 -
2.2.1.3	Monomeric/fibrillar collagen I bifunctional substrates	- 54 -
2.2.1.4	Preparation of collagen IV/fibrillar collagen I bifunctional substrates	- 54 -
2.2.2	Cell culture	- 55 -
2.2.3	Cell cycle synchronization	- 56 -
2.2.4	Immunostaining	- 56 -
2.2.5	Microscopy techniques	- 57 -
2.2.5.1	AFM imaging	- 57 -
2.2.5.2	AFM based single-cell force spectroscopy	- 57 -
2.2.5.3	Scanning electron microscopy (SEM)	- 57 -
2.2.6	Flow cytometry	- 58 -
2.2.7	Statistical analysis	- 58 -
2.2.8	Thermal noise of the cantilever	- 58 -
2.2.9	Reverse transcription real time PCR	- 59 -
2.2.9.1	Primer design	- 59 -
2.2.9.2	Total RNA isolation and cDNA synthesis	- 59 -
2.2.9.3	Real-time qPCR	- 60 -
2.2.10	Protein preparation and analysis	- 60 -
2.2.10.1	Cell lysates preparation	- 60 -
2.2.10.2	SDS-PAGE	- 60 -
2.2.10.3	Western blot	- 60 -
<b>3</b>	<b>Comparative Single-Cell Force Spectroscopy on Different Bifunctional Substrates</b>	<b>- 62 -</b>
3.1	Abstract	- 62 -
3.2	Introduction	- 63 -
3.3	Results	- 65 -
3.3.1	Experimental setup for quantifying differential cell adhesion to ECM components by comparative single-cell force spectroscopy	- 65 -
3.3.2	Producing protein/PEG bifunctional substrates	- 66 -
3.3.3	Comparative SCFS on laminin/PEG bifunctional substrates	- 67 -
3.3.4	Differential CHO cell adhesion is not caused by different mechanical properties of the laminin and PEG surfaces	- 69 -
3.3.5	Comparative SCFS on BSA /PEG bifunctional substrates	- 70 -
3.3.6	Producing laminin/fibrillar collagen I bifunctional substrates for comparative SCFS	- 70 -
3.3.7	Comparative SCFS on laminin/fibrillar collagen I bifunctional substrates	- 72 -
3.3.8	Investigating the effect of substrate contact history on cell adhesion	- 75 -

3.3.9	Producing bifunctional substrates featuring monomeric/fibrillar collagen I for comparative SCFS	- 78 -
3.3.10	Elucidating the affinity of integrins $\alpha_1\beta_1$ and $\alpha_2\beta_1$ to monomeric and fibrillar collagen I	- 80 -
3.3.11	Producing bifunctional substrates featuring collagen IV/fibrillar collagen I for comparative SCFS	- 81 -
3.3.12	Elucidating the affinity of integrins $\alpha_1\beta_1$ and $\alpha_2\beta_1$ to collagen IV and fibrillar collagen I	- 82 -
3.4	Discussion	- 84 -
<b>4</b>	<b>Revealing Adhesive Variation in Clonal Population by Comparative Single-Cell Force Spectroscopy</b>	<b>- 88 -</b>
4.1	Abstract	- 88 -
4.2	Introduction	- 89 -
4.3	Results	- 91 -
4.3.1	Comparing CHO cell adhesion to homogeneous laminin and fibrillar collagen I surfaces by conventional SCFS	- 91 -
4.3.2	Determining single-cell adhesion profiles on laminin/fibrillar collagen I substrates	- 93 -
4.3.3	Superimposing force distributions from individual cells generates broad force distribution	- 95 -
4.3.4	Independent regulation of cell adhesion to laminin and collagen I	- 95 -
4.3.5	Non-genetic and cell-cycle independent adhesion variability in <i>in vitro</i> cell cultures	- 97 -
4.3.6	Variation of integrin $\alpha_6$ cell surface expression and adhesion variability	- 99 -
4.4	Discussion	- 101 -
<b>5</b>	<b>Inverse Regulation between Integrin <math>\alpha_2\beta_1</math> and Laminin Receptors</b>	<b>- 104 -</b>
5.1	Abstract	- 104 -
5.2	Introduction	- 105 -
5.3	Results	- 106 -
5.3.1	Integrin $\alpha_2\beta_1$ is a collagen I receptor in both CHO-A2 and SAOS-A2 cells	- 106 -
5.3.2	Integrin $\alpha_2\beta_1$ is not a functional laminin receptor in either CHO-A2 or SAOS-A2 cells	- 107 -
5.3.3	Integrin $\alpha_2\beta_1$ expression suppresses cell spreading on laminin	- 108 -
5.3.4	Integrins containing the $\alpha_6$ subunit are laminin receptors in both CHO-WT and SAOS-WT cells	- 112 -
5.3.5	Transcription and expression levels of integrin $\alpha_6$ and $\beta_4$ are downregulated in $\alpha_2\beta_1$ -expressing cells	- 113 -
5.3.6	Integrin $\alpha_6$ and $\beta_4$ expression decreases in SAOS-WT cells transiently expressing integrin $\alpha_2\beta_1$	- 115 -
5.4	Discussion	- 117 -

<b>6</b>	<b>Summary of the projects</b>	<b>- 122 -</b>
<b>7</b>	<b>Concluding remarks</b>	<b>- 123 -</b>
7.1	Bifunctional substrates expand the scope of SCFS	- 123 -
7.2	Multifunctional ECM adhesion substrates for comprehensive single-cell adhesion profiling	- 124 -
7.3	The cell/substrate contact history has no influence on subsequent adhesion measurements by SCFS at short contact times	- 126 -
7.4	Determining integrin affinities to different collagen subtypes may facilitate the selection of suitable coatings for biomaterials	- 127 -
7.5	Adhesion receptor variation within cell populations as a potential strategy to cope with evolutionary pressure	- 127 -
7.6	AFM-based SCFS as a versatile tool to characterize integrin-mediated adhesion profile of single cells	- 130 -
	<b>Bibliography</b>	<b>- 132 -</b>
	<b>Appendix</b>	<b>- 151 -</b>
	Movie (included in CD)	- 151 -
	Curriculum Vitae	- 152 -
	List of publications	- 153 -
	Acknowledgements	- 154 -

## List of Figures

---

Fig. 1.1	Macromolecular organization of the extracellular matrix.	- 10 -
Fig. 1.2	Collagen triple helix.	- 11 -
Fig. 1.3	Axial structure of D-periodic collagen I fibrils.	- 12 -
Fig. 1.4	Collagen type IV network formation.	- 14 -
Fig. 1.5	Laminin $\alpha$ , $\beta$ and $\gamma$ chains and the structure of laminin-111.	- 15 -
Fig. 1.6	Integrins.	- 17 -
Fig. 1.7	Integrin structure and activation process.	- 19 -
Fig. 1.8	Location of integrin-binding sites in three different collagen IV heterotrimers.	- 23 -
Fig. 1.9	Si master fabrication and $\mu$ CP techniques.	- 27 -
Fig. 1.10	Schematic representation of the atomic force microscope.	- 32 -
Fig. 1.11	Variation of the Van der Waals interaction with the separation distance between the AFM tip and the sample.	- 33 -
Fig. 1.12	Idealized force-distance curve describing a single approach-retract cycle of the AFM tip.	- 36 -
Fig. 1.13	Capturing a suspended cell with the AFM cantilever.	- 38 -
Fig. 1.14	AFM-SCFS.	- 39 -
Fig. 1.15	Schematic illustrations of events causing force steps and the unbinding of membrane tethers.	- 40 -
Fig. 1.16	Cell adhesion bulk assays.	- 42 -
Fig. 1.17	Single cell adhesion assays.	- 44 -
Fig. 2.1	Fabrication of bifunctional protein/PEG substrates.	- 53 -
Fig. 2.2	Fabrication of bifunctional ECM protein substrates.	- 55 -
Fig. 3.1	Comparison between conventional SCFS and comparative SCFS.	- 66 -
Fig. 3.2	Selective cell adhesion on laminin/PEG substrates.	- 67 -
Fig. 3.3	Comparative SCFS on laminin/PEG substrates.	- 68 -
Fig. 3.4	Overlap of force curves taken on the laminin or the PEG part of a laminin/PEG bifunctional substrate.	- 69 -
Fig. 3.5	Laminin/fibrillar collagen I bifunctional substrates.	- 71 -
Fig. 3.6	Addition of fluorescent marker protein does not influence CHO cell adhesion to laminin significantly.	- 72 -
Fig. 3.7	Comparative SCFS of a single CHO cell on laminin/fibrillar collagen I bifunctional substrates mirrors long term differential spreading of CHO cells on laminin and collagen I.	- 74 -

Fig. 3.8	Detachment forces and accumulative SD analysis.	- 77 -
Fig. 3.9	Linear fit of detachment forces and relative standard deviations of 3 individual cells.	- 78 -
Fig. 3.10	Morphology of monomeric/fibrillar collagen I bifunctional substrates.	- 80 -
Fig. 3.11	Detachment forces of CHO-WT, CHO-A1 and CHO-A2 cells on monomeric/fibrillar collagen I bifunctional substrates.	- 81 -
Fig. 3.12	Collagen IV/fibrillar collagen I bifunctional substrates.	- 82 -
Fig. 3.13	Detachment forces of CHO-WT, CHO-A1 and CHO-A2 cells on collagen IV/fibrillar collagen I bifunctional substrates.	- 83 -
Fig. 4.1	AFM-SCFS of CHO cells on collagen and laminin.	- 93 -
Fig. 4.2	CHO cell detachment forces on laminin/fibrillar collagen I bifunctional substrates.	- 94 -
Fig. 4.3	Pooled detachment forces from cell population and individual cells.	- 95 -
Fig. 4.4	Detachment forces analysis.	- 96 -
Fig. 4.5	Detachment force distribution of CHO cells on laminin.	- 97 -
Fig. 4.6	Synchronization of CHO cells.	- 99 -
Fig. 4.7	Analyzing integrin $\alpha_6$ cell surface expression by flow cytometry.	- 100 -
Fig. 5.1	Integrin $\alpha_2\beta_1$ is a collagen receptor in both CHO-A2 and SAOS-A2 cells.	- 107 -
Fig. 5.2	Integrin $\alpha_2\beta_1$ expression suppresses laminin binding in CHO and SAOS cells.	- 108 -
Fig. 5.3	Adhesion of CHO-A2 and SAOS-A2 cells on collagen and laminin.	- 108 -
Fig. 5.4	CHO-WT and CHO-A2 cells spreading on LM/Col substrates.	- 110 -
Fig. 5.5	Quantification of CHO-WT and A2 cell alignment on LM/fCol I substrates.	- 112 -
Fig. 5.6	Adhesion of SAOS-WT and CHO-WT to laminin in the presence of blocking antibodies.	- 113 -
Fig. 5.7	Transcription and expression levels of integrin subunits in SAOS-WT and -A2 cells.	- 115 -
Fig. 5.8	Integrin $\beta_4$ and $\alpha_6$ expression level of SAOS-WT, SAOS-A2 and transient transfected SAOS-WT cells.	- 116 -
Fig. 7.1	Printing micropatterns consisting of three different proteins.	- 125 -
Fig. 7.2	Intrinsic variation and extrinsic regulation of laminin-binding integrins.	- 129 -



## List of tables

---

Table 1.1	Comparison of various microscopy techniques for biological applications.	- 30 -
Table 1.2	comparison of different imaging modes.	- 34 -
Table 1.3	Overview of different cell adhesion assays.	- 45 -
Table 2.1:	Reagents and Kits.	- 48 -
Table 2.2	Primary antibodies and isotype control.	- 49 -
Table 2.3	Secondary antibodies and staining reagents.	- 50 -
Table 2.4	Buffers and solutions.	- 50 -
Table 2.5	Software.	- 50 -
Table 2.6	Apparatus.	- 51 -
Table 2.7	Primers targeting human integrins.	- 59 -

## Abbreviations, symbols and units

---

<b>Å</b>	angstrom ( $10^{-10}$ m)
<b>°C</b>	degree Celsius
<b>Ø</b>	diameter
<b>µCP</b>	microcontact printing
<b>µg</b>	microgramm ( $10^{-6}$ g)
<b>µl</b>	microliter ( $10^{-6}$ l)
<b>µm</b>	micrometer ( $10^{-6}$ m)
<b>AFM</b>	atomic force microscopy
<b>b2MG</b>	beta-2-microglobulin
<b>BMP</b>	biomembrane force probe
<b>BSA</b>	bovine serum albumin
<b>BrdU</b>	bromodeoxyuridine
<b>CHO</b>	Chinese hamster ovary
<b>CHO-A1</b>	Chinese hamster ovary cells stably expressing integrin $\alpha$ 1
<b>CHO-A2</b>	Chinese hamster ovary cells stably expressing integrin $\alpha$ 2
<b>CLSM</b>	confocal laser scanning microscopy
<b>Col I</b>	collagen type I
<b>Col IV</b>	collagen type IV
<b>Conc.</b>	concentration
<b>DMEM</b>	Dulbecco's modified Eagle medium
<b>DNA</b>	deoxyribonucleic acid
<b>ECM</b>	extracellular matrix
<b>EDTA</b>	ethylenediaminetetraacetic acid
<b>EG3O-Me</b>	ethyleneglycol-3-O-mercaptan
<b>EHS</b>	Engelbreth-Holm-Swarm
<b>EMT</b>	epithelial mesenchymal transition
<b>fCol I</b>	fibrillar collagen type I
<b>FC</b>	flow cytometry
<b>FCS</b>	fetal calf serum
<b>F-D curve</b>	force-distance curve
<b>Fig.</b>	figure
<b>FITC</b>	fluorescein isothiocyanate
<b>GFOGER</b>	glycine-phenylalanine-hydroxyproline- glycine-glutamate-arginine

<b>h</b>	hour
<b>H<sub>2</sub>O<sub>2</sub></b>	hydrogen peroxide
<b>H<sub>2</sub>SO<sub>4</sub></b>	sulfuric acid
<b>HSP</b>	heat shock protein
<b>IF</b>	immunofluorescence
<b>ITG</b>	integrin
<b>K<sub>4</sub>[Fe(CN)<sub>6</sub>]·3H<sub>2</sub>O</b>	potassium hexacyanoferrate(II) trihydrate
<b>K<sub>3</sub>[Fe(CN)<sub>6</sub>]</b>	potassium hexacyanoferrate(III)
<b>KOH</b>	potassium hydroxide
<b>K<sub>2</sub>S<sub>2</sub>O<sub>3</sub></b>	potassium thiosulfate
<b>LM</b>	laminin
<b>M</b>	molar (mol/l)
<b>m</b>	meter
<b>mCol I</b>	monomeric collagen type I
<b>min</b>	minute
<b>mM</b>	millimolar
<b>MAD</b>	median absolute deviation
<b>MEM</b>	minimal essential medium
<b>N</b>	Newton (kg·m/s <sup>2</sup> )
<b>NC</b>	non-collageneous
<b>nm</b>	nanometer (10 <sup>-9</sup> m)
<b>nN</b>	nanonewton (10 <sup>-9</sup> N)
<b>ODM</b>	octadecylmercaptan
<b>PBS</b>	phosphate buffered saline
<b>PD</b>	photodiode
<b>PDMS</b>	polydimethylsiloxane
<b>PEG</b>	polyethylene glycol
<b>PFA</b>	paraformaldehyde
<b>pN</b>	piconewton (10 <sup>-12</sup> N)
<b>PSI</b>	plexin-sempahorin-integrin
<b>PVDF</b>	polyvinylidene difluoride
<b>RBC</b>	red blood cell
<b>RT-PCR</b>	reverse transcription polymerase chain reaction
<b>RGD</b>	arginine-glycine-aspartate
<b>RNA</b>	ribonucleic acid

<b>s</b>	second
<b>SAOS</b>	sarcoma osteogenic
<b>SCFS</b>	single-cell force spectroscopy
<b>SEM</b>	scanning electron microscopy
<b>STM</b>	scanning tunneling microscopy
<b>Si</b>	silicon
<b>Si<sub>3</sub>N<sub>4</sub></b>	silicon nitride
<b>SDS-PAGE</b>	sodium dodecyl sulfate polyacrylamide gel electrophoresis
<b>TEM</b>	transmission electron microscopy
<b>VdW</b>	Van der Waals
<b>v/v</b>	volume per volume
<b>WB</b>	western blot
<b>w/v</b>	weight per volume
<b>WT</b>	wild type
<b>YIGSR</b>	tyrosine-isoleucine-glycine-serine-arginine

## Summary

---

In tissues cells are surrounded by the extracellular matrix (ECM), a structurally and chemically complex mixture of macromolecules, including collagen fibrils and laminin glycoproteins. Cells bind to the ECM using a large number of different receptors and these interactions are of great importance for maintaining tissue structure and function. Among these receptors, integrins are responsible for the mechanical coupling of the ECM to the cytoskeleton, as well as for transducing extracellular signals influencing cell adhesion, migration and proliferation. By sensing intra- and extracellular signals, cells can furthermore modulate the transcription and expression levels of different integrins, and thus adapt to changes in their surroundings. Better understanding integrin-mediated adhesion processes is therefore essential for more comprehensively understanding cellular interactions with the ECM. Over the last years different techniques have been developed to quantify receptor-mediated cell adhesion. In AFM-based single force spectroscopy (SCFS), a living cell is attached to a functionalized cantilever and approached to an adhesive substrate. During the subsequent cell retraction, rupture forces between the cell and the substrate are recorded and provide a measure of the cell adhesion strength. The ability to measure forces with high resolution over a wide range makes SCFS a unique tool to study cellular adhesion across dimensions from the single-molecule level to that of the entire cell.

This dissertation is composed of three parts studying different aspects of integrin-mediated cell adhesion to ECM proteins using SCFS. In the first part, a “comparative SCFS” technique was established to directly compare the adhesion strength of single cells to two different ECM components presented on a single bifunctional adhesion substrate fabricated by microcontact printing ( $\mu$ CP). Individual Chinese hamster ovary (CHO) cells immobilized on an AFM cantilever were then alternatively pressed onto the two coatings and the adhesion forces were measured. All tested CHO cells displayed comparatively low adhesion to collagen, but strong adhesion to laminin. When restricting the cell-substrate contact time to 10 sec, cells exhibited a consistent, surface-specific adhesion response even over a large number of force cycle repetitions ( $>30$ ), demonstrating that meaningful differential adhesion data can be acquired using SCFS and short contact times. Furthermore, by comparing adhesion of wild-type CHO cells and CHO cells stably transfected with integrin  $\alpha_1\beta_1$  (CHO-A1) or  $\alpha_2\beta_1$  (CHO-A2) on bifunctional monomeric/fibrillar collagen I or collagen IV/collagen I substrates, the binding preferences of integrin  $\alpha_1\beta_1$  and  $\alpha_2\beta_1$  to different collagen subtypes were elucidated. Performing comparative SCFS on heterofunctional adhesion surfaces

therefore provides quantitative and directly comparative information regarding the binding strength of specific integrin receptors to different ECM components.

In the second project, the significance of adhesive cell-to-cell variations in cell populations was investigated. Testing many ( $n=30$ ) CHO cells on collagen- or laminin-functionalized surfaces yielded a wide variation of adhesion forces across the cell population. In contrast, repeatedly testing the same cell ( $>30$ ) revealed a comparatively narrow force distribution, indicating that adhesion to different ECM proteins is precisely yet differently set in each cell of the population. Thus, broad adhesion force distributions within cell populations originate from cell-to-cell variations rather than from fluctuations in the adhesive response of individual cells. Adhesion variability to laminin was non-genetic and cell cycle-independent but scaled with the range of  $\alpha_6$  integrin expression on the cell surface. Adhesive cell-to-cell variations due to varying receptor expression levels therefore appear to be an inherent feature of cell populations and should to be considered when fully characterizing population adhesion.

Although widely regarded as a collagen receptor, integrin  $\alpha_2\beta_1$  has also been suggested to function as a laminin receptor. In the third part of this thesis, integrin  $\alpha_2\beta_1$ -mediated adhesion to collagen I and laminin was compared in CHO and human osteosarcoma SAOS cells. Cell spreading assays and SCFS on laminin/collagen substrates confirmed integrin  $\alpha_2\beta_1$  as a collagen I but not a laminin receptor in both cell types. Instead, transient or stable expression of integrin  $\alpha_2\beta_1$  led to an unexpected downregulation of the laminin receptors integrin  $\alpha_6\beta_1$  and  $\alpha_6\beta_4$ , indicating an inverse regulation between the collagen receptor integrin  $\alpha_2\beta_1$  and laminin receptors. Since integrin  $\alpha_2\beta_1$  and  $\alpha_6\beta_1/\alpha_6\beta_4$  also have important and opposing roles during metastasis, these results may also provide new insights into adhesive changes occurring during cancer progression. In summary, comparative AFM-based SCFS was used as a novel tool to characterize integrin-mediated adhesion profiles of single cells to different ECM components. By performing SCFS on multifunctional adhesion substrates, quantitative single-cell information could be generated not previously obtainable from population-averaging measurements on homogeneous adhesion substrates.

## Zusammenfassung (German)

---

In Geweben eingebettete Zellen sind von extrazellulärer Matrix (extracellular matrix, ECM) umgeben, einem strukturell und chemisch komplexen Gemisch aus verschiedenen Makromolekülen, wie zum Beispiel fibrillären Kollagenen und Laminin-Glykoproteinen. Zellen binden an die ECM mithilfe verschiedener Rezeptoren und diese Interaktionen sind von allgemeiner Bedeutung für die Erhaltung der Gewebestruktur und -funktion. Unter diesen Rezeptoren sind Integrine verantwortlich für die mechanische Ankopplung der ECM an das Zytoskelett, sowie für die Übermittlung extrazellulärer Signale in das Zellinnere zur Steuerung vielfältiger Prozesse, wie der Zelladhäsion, -wanderung und -proliferation. Über das Detektieren extra- und intrazellulärer Signale können Zellen darüberhinaus die Transkription und Expression von Integrinen modulieren und sich somit Änderungen in ihrer Umgebung anpassen. Ein besseres Verständnis der Integrin-vermittelten Bindungen ist somit essentiell auch für ein umfassendes Verständnis zellulärer Interaktionen mit der ECM. In den letzten Jahren wurden eine Reihe neuer Methoden zur quantitativen Messungen der Rezeptor-vermittelten Adhäsion entwickelt. In der AFM-basierten Einzelkraftspektroskopie (single-cell force spectroscopy, SCFS) wird eine lebende Zelle an einer funktionalisierten AFM-Spitze immobilisiert und einem adhäsiven Substrat angenähert. Während der folgenden Zellretraktion können aus den resultierenden Abrisskräfte die Zellhaftungseigenschaften bestimmt werden. Die Möglichkeit, Kräfte über einen großen Bereich mit hoher Auflösung zu messen, macht SCFS zu einem einzigartigen Werkzeug zur Bestimmung zellulärer Adhäsionskräfte vom Einzel-Molekülbereich bis hin zu Zellgesamtkräften.

Diese Dissertation besteht aus drei Teilen, in denen verschiedene Aspekte der Integrin-vermittelten Zelladhäsion zu ECM-Proteinen untersucht wurden. Im ersten Teil wird die Etablierung einer neuartigen „komparativen SCFS“-Technik beschrieben, mit deren Hilfe die Haftkräfte einer einzelnen Zelle zu zwei verschiedenen ECM-Komponenten direkt verglichen werden kann. Dazu werden beide ECM-Komponenten auf einem im Mikrokontakt-Druckverfahren (microcontact printing,  $\mu$ CP) hergestellten einzelmem Adhäsionssubstrat direkt nebeneinander präsentiert. Einzelne CHO-Zellen wurden dann abwechselnd auf beide Beschichtungen gedrückt und die resultierenden Adhäsionskräfte gemessen. Alle getesteten Zellen zeigten eine erhöhte Adhäsion zu Laminin im Vergleich zu Kollagen. Wenn die Substrat-Kontaktzeit auf 10 Sekunden beschränkt wurde, zeigten die Zellen ein konsistentes, Substrat-spezifisches Adhäsionsverhalten selbst bei einer großen Zahl von Kraftzyklus-Wiederholungen (>30). Dadurch wurde gezeigt, dass mithilfe der SCFS Aussagen über das

differenzielle Adhäsionsverhalten von Zellen selbst bei Verwendung kurzer Kontaktzeiten getroffen werden können. Desweiteren wurden mit Hilfe bifunktionaler monomerer/fibrillärer Kollagen I- oder Kollagen I/Kollagen IV-Substrate die unterschiedlichen Bindungsstärken der beiden Integrine  $\alpha_1\beta_1$  and  $\alpha_2\beta_1$  zu verschiedenen Kollagen-Subtypen verglichen. Die komparative SCFS auf heterofunktionalen Adhäsionssubstraten liefert somit quantitative und direkt-vergleichbare Informationen über die Bindungsstärke bestimmter Integrin-Rezeptoren zu verschiedenen ECM-Komponenten.

Im zweiten Teil der Arbeit wurde die Bedeutung adhäsiver Unterschiede zwischen einzelnen Zellen einer CHO Zellpopulation untersucht. Die Messung vieler ( $n=30$ ) Zellen auf Kollagen- oder Lamininsubstraten offenbarte dabei eine große Bandbreite der Adhäsionskräfte. Im Gegensatz dazu ergab das wiederholte Messen ( $>30$  mal) einzelner Zellen eine vergleichsweise enge Verteilung der Adhäsionskräfte. Diese Ergebnisse zeigen, dass die große Streuung der Adhäsionseigenschaften innerhalb der Zellpopulation auf adhäsiven Unterschieden zwischen den Zellen und nicht auf Schwankungen in der Adhäsionsantwort einzelner Zellen in wiederholten Messungen beruht. Die Variabilität der Adhäsion zu Laminin beruht nicht auf genetischen oder Zellzyklus-bedingten Unterschieden, sondern skaliert mit der Spanne der Integrin  $\alpha_6$  Expression auf der Zelloberfläche. Das Auftreten adhäsiver Unterschiede zwischen einzelnen Zellen aufgrund unterschiedlicher starker Rezeptorexpression erscheint somit als eine inhärente Eigenschaft von Zellpopulationen. Dieser Sachverhalt sollte bei der vollständigen Charakterisierung der Adhäsionseigenschaften von Zellpopulationen beachtet werden.

Obwohl Integrin  $\alpha_2\beta_1$  hauptsächlich als Kollagen-Rezeptor bekannt ist, weisen einige Studien darauf hin, dass dieses Integrin auch als Laminin-Rezeptor fungiert. Im dritten Teil dieser Arbeit wurde daher die  $\alpha_2\beta_1$ -vermittelte Adhäsion zu Kollagen I und Laminin in CHO und der humanen Zelllinie SAOS untersucht. Zell-Spreit-Versuche und SCFS auf bifunktionalen Kollagen/Laminin-Oberflächen bestätigten die Rolle von  $\alpha_2\beta_1$  als Kollagen-, aber nicht als Laminin-Rezeptor. Im Gegenteil führt die transiente oder stabile Expression von  $\alpha_2\beta_1$  zu einer unerwarteten Herunterregulierung der Lamininrezeptoren  $\alpha_6\beta_1$  and  $\alpha_6\beta_4$ , was für eine inverse Regulierung zwischen dem Kollagen-Rezeptor  $\alpha_2\beta_1$  und verschiedenen Laminin-Rezeptoren spricht. Da  $\alpha_2\beta_1$  und  $\alpha_6\beta_1/\alpha_6\beta_4$  auch wichtige und entgegengesetzte Rollen während der Metastasierung zugeschrieben werden, könnte diese Ergebnisse auch neue Einsichten in adhäsive Veränderungen während der Krebsentstehung liefern. Zusammenfassend wurde in dieser Arbeit die AFM-basierte SCFS verwendet, um die Integrin-vermittelte Adhäsion einzelnen Zellen in einer neuartigen Weise zu charakterisieren. Insbesondere durch die Verwendung multifunktionaler Adhäsionssubstrate konnte die differenzielle Haftung einzelner



Zellen präzise quantifiziert werden, was bisher unter Verwendung populationsmittelnder Verfahren und homogener Substrate nicht möglich war.

# **1 Introduction and motivation**

---

## **1.1 Extracellular Matrix**

Within tissues, animal cells are surrounded by the extracellular matrix (ECM) which is a three dimensional network of macromolecules, including glycoproteins, proteoglycans, polysaccharides and non-matrix proteins (Bosman and Stamenkovic, 2003) (**Fig. 1.1**). Many of these macromolecules are first secreted locally by cells embedded within the ECM and later organized into fibers, layers or sheet-like structures. The ECM does not only provides mechanical support for the cells, but also plays an active role in transmitting environmental signals to cells, thus regulating their survival, proliferation and differentiation (Hay, 1991; HAY, 1999; Berrier and Yamada, 2007; Alberts et al., 2008; Karp, 2010). Structural glycoproteins such as collagens and elastin provide mechanical support for the cells. Proteoglycans and polysaccharides attract water and form porous hydrated gels, thereby maintaining a hydrated environment and serving as selective filters to regulate the traffic of molecules and cells (Vakonakis and Campbell, 2007). Non-matrix proteins are also indispensable for ECM function: growth factors are capable of stimulating cell proliferation and differentiation; cytokines are responsible for intercellular communication; metalloproteinases and serine proteases are necessary for matrix degradation. Variations in the relative amount of the different macromolecules give rise to different tissues and organs (Werb and Chin, 1998).

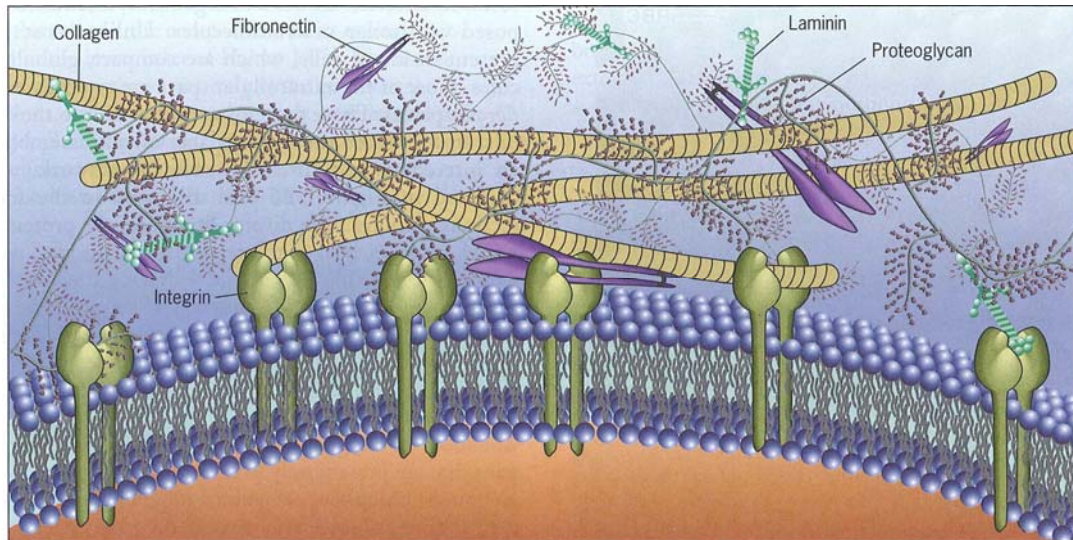


**Fig. 1.1 Macromolecular organization of the extracellular matrix.**

The main components of the ECM are glycoproteins and proteoglycans. The proteins shown here (collagen, laminin and fibronectin) bind to each other and also have binding sites for matrix-embedded cells. Proteoglycans occupy large amounts of extracellular space. Figure taken from (Karp, 2010).

### 1.1.1 Collagens

Collagens form the major protein component of the ECM. In vertebrates the collagen family contains at least 28 (Kadler et al., 2007). All collagen monomers comprise 3  $\alpha$ -chains which feature repeated Gly-X-Y motifs, in which X and Y can be any amino acid but are commonly proline and hydroxyproline. The Gly-X-Y motif allows the 3  $\alpha$ -chains to form right-handed triple helical structures held together by hydrogen bonds in a manner so that all glycine residues are buried within the core and all X and Y residues are exposed at the surface (**Fig. 1.2**). Depending on the type of collagen, the triple-helical motifs can constitute either major or minor parts of the collagen monomer. Additional non-collagenous (NC) domains are usually located at the N- and C- termini. These NC domains are often important for collagens to interact with other matrix molecules (van der Rest and Garrone, 1991; Fratzl, 2008; Gordon and Hahn, 2010).

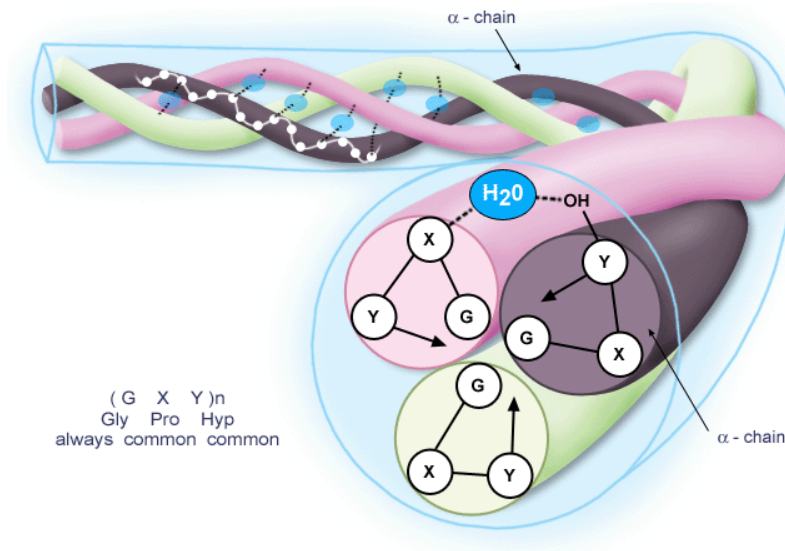


**Fig. 1.2 Collagen triple helix.**

Collagen monomers are composed of 3  $\alpha$ -chains which are featured with Gly-X-Y motifs. Gly-X-Y motifs enable collagen monomers to organize into a right-handed triple helical structure with the glycine residue being buried within the core and X and Y residues at the surface. Figure taken from (Roughley, 2008).

The members of the collagen family can be further grouped into different subfamilies (Myllyharju and Kivirikko, 2001; Ricard-Blum et al., 2005; Kadler et al., 2007; Gordon and Hahn, 2010), according to their subsequent polymeric forms. For instance, collagen type I, II, III, V and XI are fibrillar collagens (Kadler et al., 1996); collagen type IV, VI, VIII, and X form networks of different kinds (Knupp and Squire, 2005); type XIII, XVII, XXIII, and XXV collagens are trans-membrane collagens inserted in the plasma membrane in a type II orientation (Franzke et al., 2003; Franzke et al., 2005) and collagen type XV and XVIII are endostatin precursor collagens (Sasaki et al., 2000).

### 1.1.1.1 Fibrillar collagens

In mammals, fibrillar collagens are encoded by 11 genes (Huxley - Jones et al., 2007). Some collagens like collagen type II are homotrimers while others, such as collagen I (Col I) and V are heterotrimers. These monomers are about 300 nm long and 1.5 nm in diameter and feature a continuous long Gly-X-Y triple helical region, which is composed of around 1000 amino acids (Smith, 1968). There are short NC non-helical telopeptides at the N- and C- termini, which are important for fibril formation (Prockop

and Fertala, 1998; Hulmes, 2002). Fibrillar collagen monomers are capable of assembling into highly oriented long fibrils, with a length in the  $\mu\text{m}$  to  $\text{mm}$  range and a diameter of 12 to 500 nm. As seen by electron microscopy, those fibrils are characterized by an axial D-periodic 67 nm banding (Gross and Schmitt, 1948; Miller and Wray, 1971). The D-bands result from alternating overlap and gap regions of the regular quarter-staggered collagen monomers (**Fig. 1.3**) (Mould et al., 1990; Kadler et al., 1996).

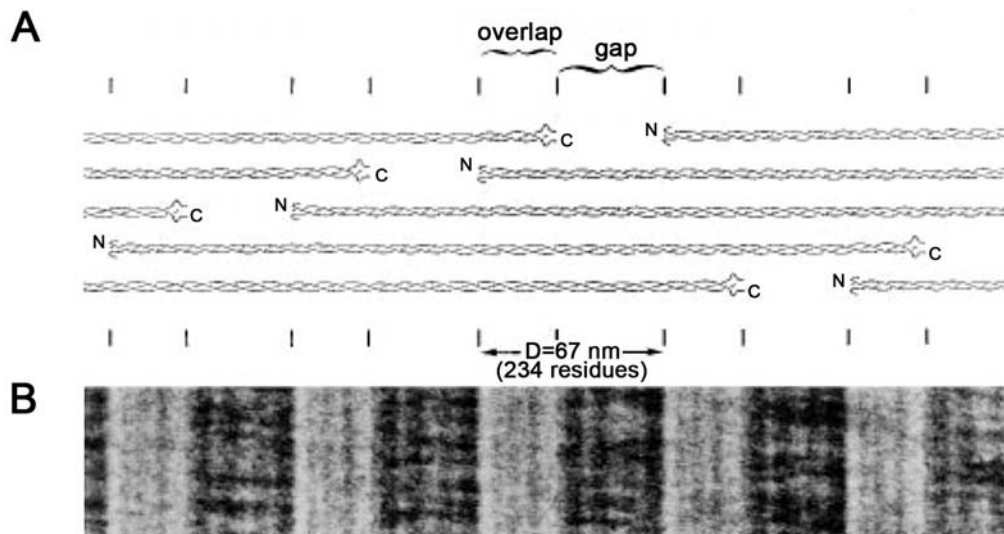


**Fig. 1.3** Axial structure of D-periodic collagen I fibrils.

(A) Schematic representation of the axial packing arrangement of triple-helical collagen molecules in a fibril. The 67 nm D-bands are composed of overlap and gap region of staggered collagen I monomers. (B) Electron microscopy image of a negatively stained collagen I fibril. The repeating broad dark and light zones are produced by preferential stain penetration into the gap regions and overlap regions. Figure taken from (Kadler et al., 1996).

Fibrillar collagens are synthesized as soluble procollagens with large propeptides at both ends of the triple helical domain (Myllyharju, 2005). The C-propeptides are afterwards cleaved by special metalloproteinases, leaving the short C-telopeptides (Greenspan, 2005). The extend of the N-propeptide cleavage depends on the collagen type (Colige et al., 2005). In principle, the process of fibril formation is entropy-driven: since the collagen molecules are more than a thousand fold less soluble than procollagen, the loss of solvent molecules from the surface of collagen results in assemblies with a circular cross-section, which minimizes the surface area/volume ratio of the fibril (Kadler et al., 1987). However, several additional

proteins are indispensable for collagen fibrillogenesis *in vivo*: fibronectin and fibronectin- and collagen-binding integrins function as organizers determining the sites of collagen assembly, while collagens type V and XI in particular are suggested to serve as nucleators for the fibril formation (Kadler et al., 2008). After the fibrils have formed in the extracellular space, the telopeptide lysine residues and triple-helical hydroxylysines of the constituent collagen molecules react to form covalent cross-links, which gives rise to the high tensile strength of the collagen fibrils (Eyre et al., 1984; Canty and Kadler, 2005).

Type I collagen [ $\alpha 1(I)$ ]<sub>2</sub> $\alpha 2(I)$  constitutes up to 90% of the skeletons of mammals and is also widespread in tendon, skin, ligaments, cornea, and many interstitial connective tissues. *In vivo*, type I collagen is mostly incorporated into composites with either collagen type III (Fleischmajer et al., 1990) or type V (Niyibizi and Eyre, 1989) and provides tensile stiffness for many of these tissues. Due to its wide distribution in the body, different degradation products of collagen type I are frequently used to monitor physiological or pathological changes in tissues. Furthermore, owing to its superior structural and mechanical properties, as well as ability to interact with over 50 molecules (Di Lullo et al., 2002), collagen I is currently used in a number of tissue engineering applications (Lee et al., 2001; Ramshaw et al., 2009).

#### **1.1.1.2 Network-forming type IV collagen**

Type IV collagen is also known as basement membrane collagen (Hudson et al., 2003). It is a major component of the basal lamina and is essential for stabilizing this compound macromolecular network, for filtering molecules in the basement membrane, as well as storage of growth factors (Göhring et al., 1998). Six different  $\alpha$ -chains combine into three isoforms of collagen IV heterotrimers [ $\alpha 1(IV)$ ]<sub>2</sub> $\alpha 2(IV)$ ,  $\alpha 3(IV)\alpha 4(IV)\alpha 5(IV)$  and [ $\alpha 5(IV)$ ]<sub>2</sub> $\alpha 6(IV)$  (Zhou and Reeders, 1996). [ $\alpha 1(IV)$ ]<sub>2</sub> $\alpha 2(IV)$ , however, is the most common isoform of collagen IV and was discovered first. The structure of collagen IV is characterized by 3 distinct motifs: a globular C-terminal NC1 domain, a lysine- and cysteine-rich N-terminal 7S domain and a long triple helical domain with several interruptions alongside (Brazel et al., 1988). Collagen IV molecules form three-dimensional irregular polygonal arrays in a stepwise process: two trimeric NC1 domains interact with each other in a head-to-head manner and the

covalent crosslink between a methionine and a lysine residue from opposite trimers stabilize this link (Than et al., 2002); the 7S domain from 4 collagen molecules connect to each other via disulfide bonds and lysyl oxidase-mediated crosslinks (Bailey et al., 1984); the lateral association of the two-dimensional aggregates through different interactions (e.g. supercoil formation by supramolecular twisting) give rise to the higher order of supramolecular organization (**Fig. 1.4**) (Yurchenco and Ruben, 1988; Barge et al., 1991).

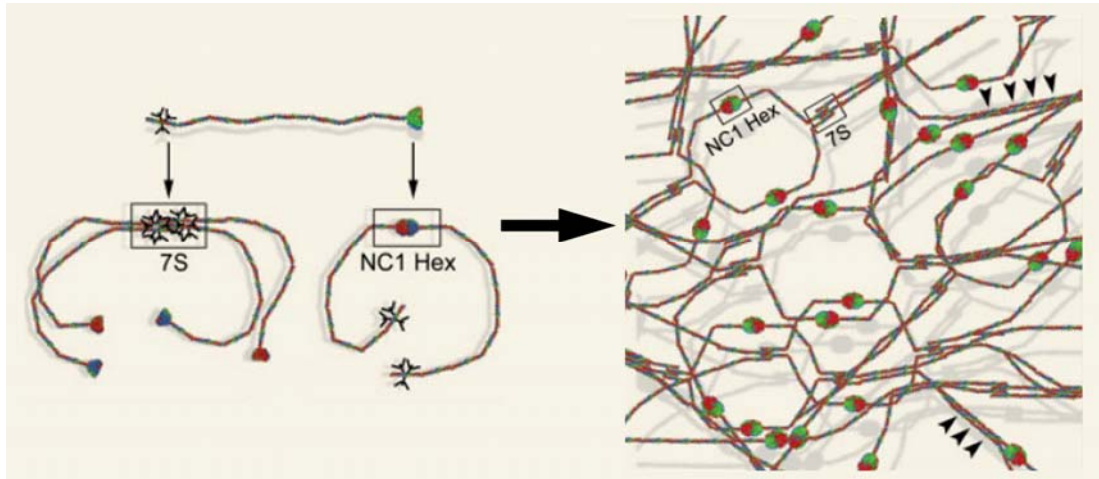


**Fig. 1.4 Collagen type IV network formation.**

Collagen IV molecules are able to form dimers or tetramers by crosslinking their NC1 domains or 7S domains. The lateral association of collagen IV polymers enables collagen IV network formation. Figure adapted from (Khoshnoodi et al., 2008) and modified.

### 1.1.2 Laminins

Laminins (LMs) are the major component of the basal lamina, and they serve as the primary organizer of their typical sheet-like structure (Timpl, 1989; Alberts et al., 2008). In 1979, laminin was first isolated and purified from mouse Engelbreth-Holm-Swarm (EHS) tumor, and recognized as heterotrimers linked by disulfide bonds (Timpl et al., 1979). EHS laminin was originally named laminin-1 and later laminin-111 and identified as the first member of the big family of laminins (Burgeson et al., 1994; Aumailley et al., 2005). So far, five  $\alpha$ , three  $\beta$  and three  $\gamma$  chains have been identified in vertebrates, making up 15 isoforms of laminin (**Fig. 1.5 A**) (Koch et al., 1999; Miner and Yurchenco, 2004).



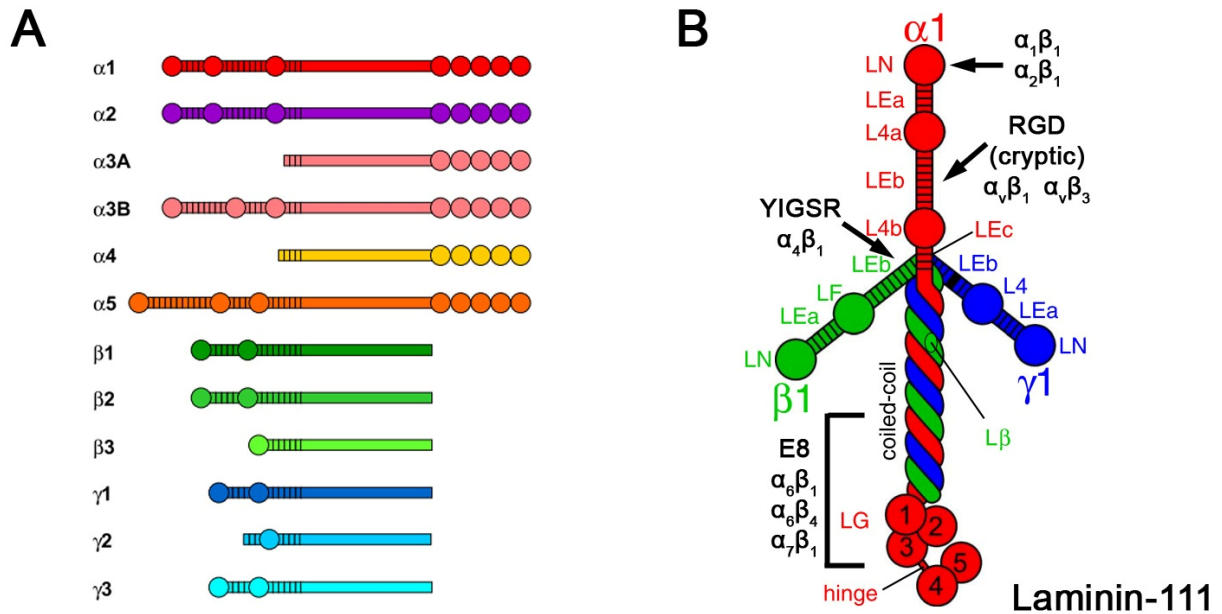


**Fig. 1.5 Laminin  $\alpha$ ,  $\beta$  and  $\gamma$  chains and the structure of laminin-111.**

(A) Five  $\alpha$  chains, three  $\beta$  chains and three  $\gamma$  chains are able to form 15 laminin types. (B) The structure of laminin-111. Different domains of the  $\alpha$ (red),  $\beta$ (green) and  $\gamma$ (blue) chains are indicated. Integrin binding sites are labeled in black. Figure modified after (Durbeej, 2010).

LM-111 is composed of an  $\alpha 1$  (~400 kDa), a  $\beta 1$  (~220 kDa), and a  $\gamma 1$  (~200 kDa) chains (Engel et al., 1981; Beck et al., 1990). The C-termini of all 3 chains are held together by disulfide bonds, producing an  $\alpha$ -helical coiled-coil domain (long arm) with five homologous globular domains (LG domains, each of which approximately 20 kDa) at the far end of the  $\alpha$  chain (Scheele et al., 2007). The N-termini of the  $\alpha 1$ ,  $\beta 1$  and  $\gamma 1$  chains remain separated. Therefore, the LM-111 molecule takes the shape of an asymmetric bouquet, similar to a bunch of three flowers whose stems are twisted together (**Fig. 1.5 B**) (Cognato and Yurchenco, 2000). The amino-terminal sequences of the three short arms are composed of two domain types: a cysteine-rich 60 amino acid domain (laminin epidermal growth factor like (LE) motif) which is rod-like and arranged into rows; a laminin N-terminal domain (LN), and laminin4 (L4) and laminin four domains (LF), which are cysteine-poor globular domains interspaced by LE motifs (Tunggal et al., 2000). In vitro, LM-111 self-associates by intermolecular interactions between LN domains and forms roughly hexagonal networks in a cation-dependent polymerization process (Yurchenco et al., 1985; Paulsson, 1988; Yurchenco et al., 1992).



## **1.2 Integrin-mediated cell adhesion to the ECM**

The majority of cells interact with the ECM either transiently or constantly, and this interaction influences cell behavior profoundly (Hynes, 2009). For instance, the change of ECM dimensionality strongly influences cell morphology and migration behavior (Doyle et al., 2009); a varying elasticity of the ECM can direct mesenchymal stem cell differentiation into neurons, myocytes or osteoblasts, respectively (Engler et al., 2006); cells often proliferate faster on stiff compared to soft substrates (Peyton et al., 2006); ECM geometry influences cell cytoskeleton distribution, spreading area and even control cell life or death (Chen et al., 1997; Lehnert et al., 2004). Although the influence of mechanical properties of the ECM on cell behavior receives increasing attention (Discher et al., 2009), cell-ECM interactions are usually built through adhesion receptors such as integrins (Hynes, 1987, 2002).

Most cells interact with ECM via focal adhesions, which are integrin-containing, multiprotein structures that bridges intracellular actin bundles to ECM mechanically (Abercrombie and Dunn, 1975). With a lateral size less than 200 nm and a height around 40 nm (Chen and Singer, 1982; Franz and Muller, 2005; Kanchanawong et al., 2010), focal adhesions have been identified to consist of more than 150 components (Zaidel-Bar et al., 2007). They coordinate with one another and regulate many biological processes (Geiger et al., 2009). Depending on the type of ECM and cells, integrin-mediated cell-matrix adhesions can exist in other forms varying in shape, size, localization and composition (Geiger et al., 2001). For example, fibrillar adhesions are essential for fibronectin matrix formation (Pankov et al., 2000; Zamir et al., 2000) and podosomes play significant roles in various malignant cells, macrophages and osteoclasts (Gimona et al., 2008). However, those two adhesion structures are outside the scope of this dissertation and therefore not going to be discussed.

### 1.2.1 Integrin structure

Integrins are  $\alpha\beta$  heterodimeric transmembrane proteins that function as the major receptors mediating dynamic cell-cell and cell-ECM interactions. They physically bridge ECM proteins with the intracellular cytoskeleton and were originally named “integrins” to demonstrate their significance in maintaining the integrity of the ECM-cytoskeleton linkage (Fig. 1.6 A) (Barczyk et al., 2010; Campbell and Humphries, 2011). The  $\alpha$  and  $\beta$  subunits of integrins are non-covalently associated with each other. In mammals, 18  $\alpha$  subunits and 8  $\beta$  subunits make up 24 different integrins (Takada et al., 2007). According to their ligand specificities, integrins can be sub-grouped into collagen receptors, RGD receptors, laminin receptors and leukocyte-specific receptors (Fig. 1.6 B) (Hynes, 2002).

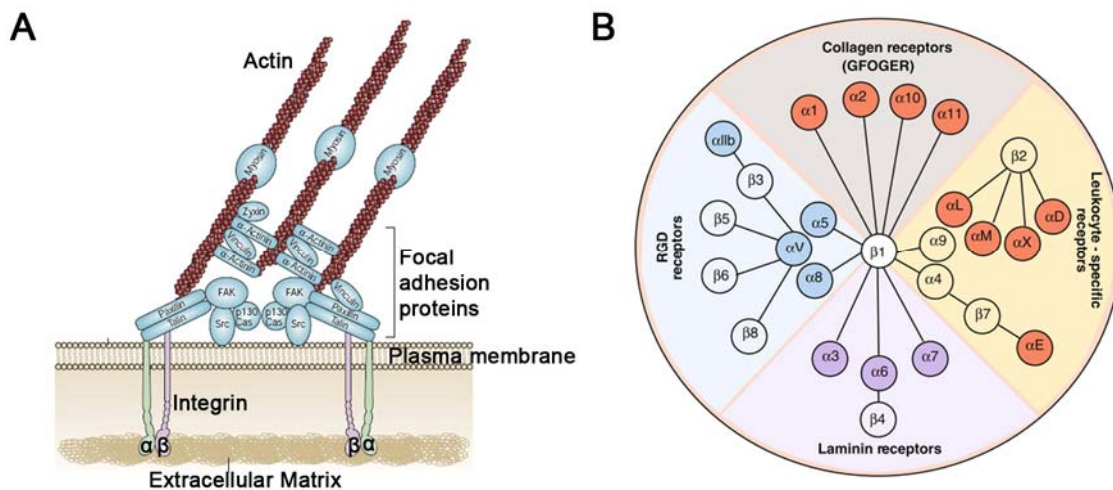


**Fig. 1.6 Integrins.**

(A) Integrins bridge the ECM with the cytoskeleton (modified after (Mitra et al., 2005)). (B) Overview of integrin  $\alpha$  and  $\beta$  subunits (adapted from (Barczyk et al., 2010)).

The  $\alpha$  and  $\beta$  subunits of integrins show no homology to each other, while all the  $\alpha$  subunits and all the  $\beta$  subunits share some characteristic motifs (**Fig. 1.7 A**) (Arnaout et al., 2005). The N-terminal region of  $\alpha$  subunits contains a seven-bladed structure comprising seven repeats of about 60 amino acids each, called the  $\beta$  propeller domain. Nine  $\alpha$  subunits have an additional I-domain inserted between the second and the third blade of the  $\beta$  propeller (Larson et al., 1989). The  $\alpha$  I-domain adopts a specific Rossmann-fold configuration with five  $\beta$ -sheets surrounded by seven  $\alpha$ -helices. Ligand binding occurs via a coordinating  $Mg^{2+}$  ion in the metal-ion-dependent

adhesion site (MIDAS) motif (Lee et al., 1995). In integrins that have no  $\alpha$  I-domain, the  $\beta$  propeller directly participates in the ligand binding process (Humphries, 2000). The C-terminal region to the  $\beta$  propeller domain comprises a large portion of the  $\alpha$  subunit extracellular domain of about 500 residues. Three  $\beta$ -sandwich domains are presented in this region, designated as the thigh, calf-1, and calf-2 domains (Xiong et al., 2001).

The N-terminal region of the  $\beta$  subunit contains four different domains. The cysteine-rich plexin-sempahorin-integrin (PSI) domain is important for restraining the integrin in the active conformation (Zang and Springer, 2001). The I-like domain in  $\beta$  subunit is homologous to the I-domain in  $\alpha$  subunit. It contains a  $Mg^{2+}$ -coordinating MIDAS and a site adjacent to MIDAS (ADMIDAS), able to bind an inhibitory  $Ca^{2+}$  ion. This ADMIDAS site can also bind to  $Mn^{2+}$ , leading to a conformational change resulting in an active form of the integrin (Humphries et al., 2003). In integrins that lack I-domains, the I-like domain directly binds the ligand together with the  $\beta$  propeller domain in the  $\alpha$  subunit, while in integrins that contain I-domains, the I-like domain regulates ligand binding indirectly (Xiong et al., 2001). The hybrid domain resembles a  $\beta$ -sandwich domain that is folded from both sides of the I-like domain. The swing motion of the hybrid domain is necessary for integrin activation (Takagi and Springer, 2002). The four epithelial growth factor (EGF) domains are cysteine-rich and play a significant role in signal transduction (Takagi et al., 2001b; Beglova et al., 2002). The cytoplasmic domains of the  $\beta$  subunits are usually very short (40 to 70 amino acids) except for the  $\beta$ 4 subunit (over 1000 amino acids) (de Pereda et al., 1999).

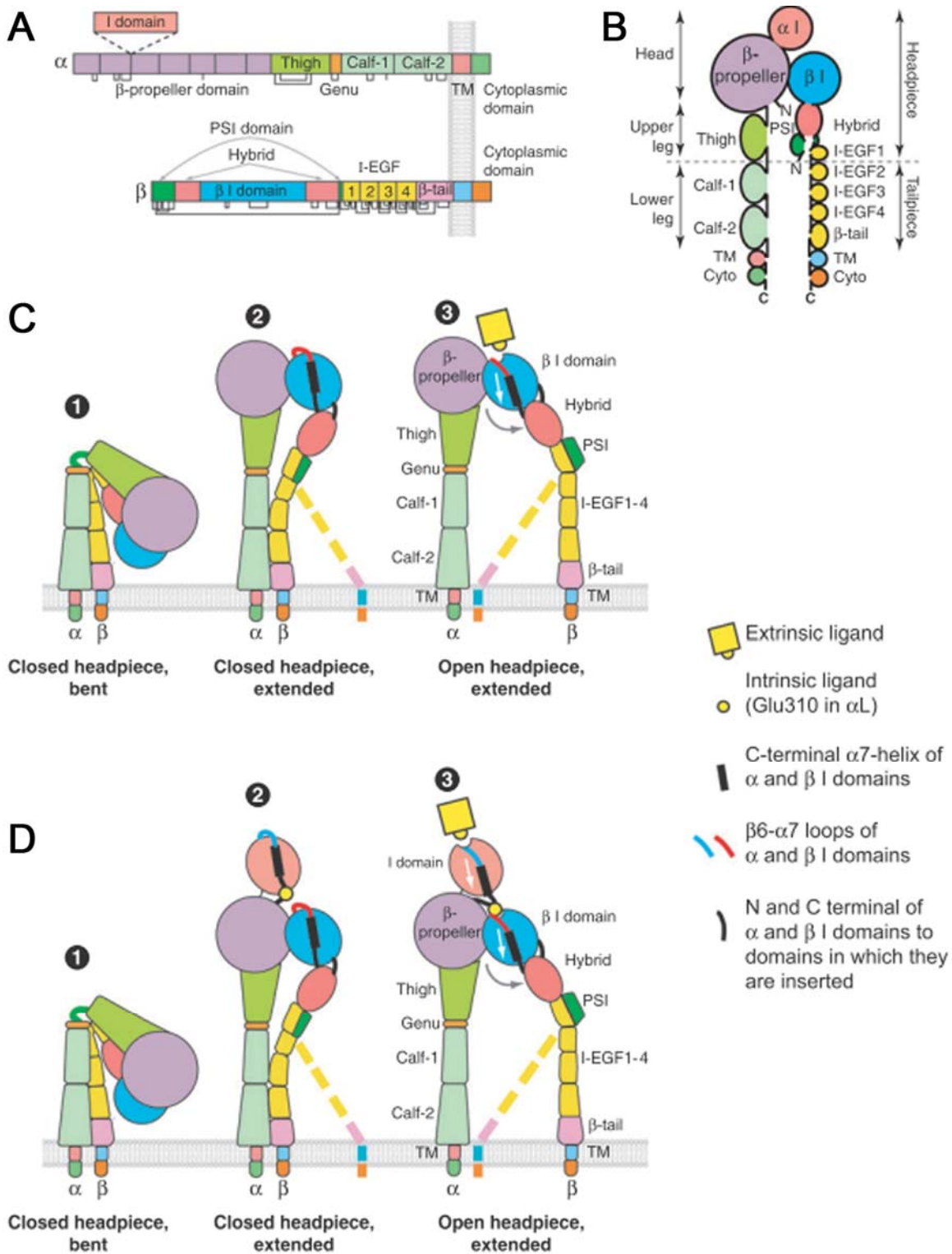


**Fig. 1.7 Integrin structure and activation process.**

(A) Integrin domain organization. (B) Schematic depiction of integrin domain arrangement from N to C terminus. (C–D) Domain rearrangement during activation of integrins that lack (C) or contain (D) an  $\alpha$  I-domain. The  $\beta$  subunit lower legs are flexible and are therefore shown in what may be the predominant (solid representation) and the less predominant (dashed lines) orientations. Figure adapted from (Luo et al., 2007).

### **1.2.2 Conformational change involved in integrin activation**

The affinity of integrins to their ligands is strictly related to their conformation. In the low affinity (inactive) state, a non-ligand occupied integrin is bent at the hinge region, which is located between the  $\beta$  propeller and thigh of the  $\alpha$  subunit, and the EGF repeat 1 and 2 of the  $\beta$  subunit (**Fig. 1.7 B, C1 and D1**) (Takagi and Springer, 2002). The headpiece of the integrin is closed and faces down towards the membrane. The cytoplasmic domains of the  $\alpha$  and  $\beta$  subunits are tightly associated with each other. As a result, the inactive integrin adopts a V shape, as observed in EM images (Lu et al., 2001; Xiong et al., 2001).

According to the “switchblade” model, transition of integrins from the low to the high affinity state is accompanied by a protein stretching process (**Fig. 1.7 C and D**) (Luo et al., 2007). Cytoplasmic signals caused by different protein binding (such as talin binding to  $\beta$  subunit cytoplasmic tail) disrupt the association between the cytoplasmic domain, the transmembrane domain and the lower leg part of the  $\alpha$  and  $\beta$  subunits. This destabilizes the interaction between the lower leg and the headpiece and further results in the integrin standing up (Takagi et al., 2001a; Beglova et al., 2002; Takagi et al., 2002). The conformational change of the  $\beta_6$ - $\alpha_7$  loop and the MIDAS in the I-like domain then exposes the ligand-binding site. The C-terminal  $\alpha_7$  helix of the I-like domain moves downward, pulling the hybrid domain approximately  $80^\circ$  away with respect to the I-like domain. In consequence, integrins are able to bind extrinsic ligands with high affinity (Takagi et al., 2002; Carman and Springer, 2003).

For I-domain-containing integrins, conformational changes that transmit allostery from the I-like domain to the I-domain are indispensable for integrin activation. (**Fig. 1.7 D**). A Glu residue in the linker between the C-terminal  $\alpha_7$  helix of the I-domain and the  $\beta$ -sheet 3 of the  $\beta$ -propeller domain is required for I-domain activation (Huth et al., 2000; Alonso et al., 2002). This Glu residue might work as an intrinsic ligand and bind to the MIDAS in the I-like domain when it is activated. It pulls down the C terminal  $\alpha_7$  helix of the I-domain and activates the integrin receptor (Alonso et al., 2002; Yang et al., 2004).

Nevertheless, some evidence is incompatible with the “switchblade” model. For instance, the crystal structure of the integrin  $\alpha_v\beta_3$  ectodomain is found to be V-shaped

rather than linear or extended, despite of the active or inactive state of the receptor (Xiong et al., 2001; Luo and Springer, 2006). Therefore another model called the “deadbolt” model has been put forward (Xiong et al., 2003). In this model, integrins adopt the bent conformation no matter whether they are in an inactivated or activated state. Instead, the elongated CD loop of the  $\beta$  transmembrane domain serves as a “deadbolt”. It shields the I-like domain from binding to the ligand in the inactive state. Upon inside-out signaling transmitted from the cytoplasmic domain, the transmembrane domain moves to unlock the “deadbolt” by sliding it 0.3 nm away and sets the I-like domain free for ligand binding. This model is energetically favored and allows a faster transition from the inactive to active state (Arnaout et al., 2005). However, the validity of those two models is currently under debate.

### **1.2.3 Integrin signaling**

Integrin signaling involves an ordered series of events including integrin activation, integrin engagement and initial signaling, integrin clustering and focal adhesion assembly, and integrin inactivation (Harburger and Calderwood, 2009). Integrins are activated in response to inside-out signaling. The cytoplasmic protein talin, which binds to actin as well as to multiple cytoskeletal and signaling proteins, is recruited to the integrin  $\beta$  subunit cytoplasmic domain. This leads to the dissociation of the integrin  $\alpha$  and  $\beta$  cytoplasmic domains and subsequently to a conformational change of the integrin and integrin activation (Tadokoro et al., 2003; Wegener et al., 2007). Several other proteins have also been suggested to be indispensable for integrin activation such as kindlins (Ma et al., 2008b; Harburger et al., 2009) and the integrin-linked kinase (Honda et al., 2009).

The binding of integrins to their ligands completes the coupling from the cytoskeleton to the ECM via talin. Forces are transmitted through a nascent adhesion site and facilitate the reinforcement of the ECM-cytoskeleton link. As a result, additional cytoskeletal and signaling proteins are recruited to the adhesion sites (Ginsberg et al., 2005). Association between integrin transmembrane domains induces integrin clustering (Li et al., 2003). As adhesions mature, more than 150 proteins assemble at the cytoplasmic domain of clustered and ligand-bound integrins, and are responsible for force and signal transmission from the ECM to the cytoskeleton (Zaidel-Bar et al., 2007).

Integrin disengagement is necessary for cell body relocation (Lauffenburger and Horwitz, 1996). This process is initialized by integrin phosphorylation and binding of competing proteins to integrin followed by talin disconnection from the integrin  $\beta$  subunit cytoplasmic domain (Millon-Fremillon et al., 2008). Afterwards, integrins can be internalized and recycled (Bretscher, 1992; Lawson and Maxfield, 1995) or left behind on the substrates as “footprints” (Palecek et al., 1998).

#### **1.2.4 Collagen-binding integrins**

The four I-domain-containing integrins  $\alpha_1\beta_1$ ,  $\alpha_2\beta_1$ ,  $\alpha_{10}\beta_1$  and  $\alpha_{11}\beta_1$  are collagen type I receptors (White et al., 2004). They bind to the hexapeptide GFOGER (O=hydroxyproline) of the collagen type I triple helix using their I-domain in the  $\alpha$  subunit (Knight et al., 2000; Zhang et al., 2003). Those four integrins have different distribution patterns in tissues. Integrin  $\alpha_1\beta_1$  and  $\alpha_2\beta_1$  are both abundant in mesenchymal cells (Zutter and Santoro, 1990; Voigt et al., 1995). However, they are reported to have opposite functions in some signaling pathways regulating collagen synthesis (Riikonen et al., 1995; Ivaska et al., 1999). Thus, the cell response to collagen may rely on the abundance of either integrin. Integrins  $\alpha_{10}\beta_1$  and  $\alpha_{11}\beta_1$  participate in the metabolism of bone and cartilage (Camper et al., 2001; Tiger et al., 2001).

The major collagen IV-binding integrins are  $\alpha_1\beta_1$  and  $\alpha_2\beta_1$  (Aumailley and Gayraud, 1998; Leitinger and Hohenester, 2007). In the CB3 fragment of Collagen type IV, which is 100 nm away from the N-terminus, there are two binding sites for integrin  $\alpha_2\beta_1$  and one binding site for integrin  $\alpha_1\beta_1$  (**Fig. 1.8**) (Vandenberg et al., 1991; Kern et al., 1993). Spatial vicinity of Asp461 on  $\alpha_1(\text{IV})$  chain to Arg461 on  $\alpha_2(\text{IV})$  chain is critical for the binding of integrin  $\alpha_1\beta_1$  (Eble et al., 1993), while GFOGER sequences are the binding sites for integrin  $\alpha_2\beta_1$  (Knight et al., 2000). There is an additional integrin binding site in the triple helical domain of Collagen type IV: residue 531-543 of  $\alpha_1(\text{IV})$  chain has been suggested as the binding site for integrin  $\alpha_3\beta_1$  (Lauer et al., 1998). In addition, several integrin binding sites are located in the NC1 domain of Collagen type IV: integrin  $\alpha_1\beta_1$  for  $\alpha_1(\text{IV})$  NC1,  $\alpha_v\beta_3$ ,  $\alpha_v\beta_5$  and  $\alpha_3\beta_1$  for  $\alpha_2(\text{IV})$  NC1,  $\alpha_v\beta_3$  and  $\alpha_v\beta_5$  for  $\alpha_3(\text{IV})$  NC1,  $\alpha_v\beta_3$  for  $\alpha_6(\text{IV})$  NC1 domains (**Fig. 1.8**) (Pedchenko et al., 2004; Khoshnoodi et al., 2008). Binding of integrins  $\alpha_{10}\beta_1$  and  $\alpha_{11}\beta_1$  to Collagen

type IV has also been reported (Tiger et al., 2001; Tulla et al., 2001). However, the binding sites of these integrins on Collagen type IV are still unclear.

In addition to the GER sequences, there are also RGD sequences present in collagens. However, the RGD sequences cryptic in native fibrillar collagen I (fCol I) and Collagen type IV. After thermal denaturation or proteolytic degradation, RGD sequences in the triple helical domain are exposed (Xu et al., 2001) and serve as the binding site for RGD-binding integrins such as  $\alpha_5\beta_1$  (Davis, 1992; Gullberg et al., 1992).

Although integrins  $\alpha_1\beta_1$ ,  $\alpha_2\beta_1$ ,  $\alpha_{10}\beta_1$  and  $\alpha_{11}\beta_1$  are both collagen type I- and type IV-binding integrins, their binding specificities are different (Leitinger, 2011). Integrin  $\alpha_1\beta_1$  binds basement membrane collagen IV with a higher affinity than fibrillar collagen I, whereas  $\alpha_2\beta_1$  integrins display higher affinity towards collagen I as compared to collagen IV (Kern et al., 1994; Tuckwell et al., 1995; Dickeson et al., 1999; Tiger et al., 2001; Tulla et al., 2001). Integrin  $\alpha_2\beta_1$  is more efficient as a fibrillar collagen binding integrin while  $\alpha_1\beta_1$  has a higher affinity for monomeric collagen (Jokinen et al., 2004). The binding preferences of  $\alpha_{10}\beta_1$  and  $\alpha_{11}\beta_1$  are similar to  $\alpha_1\beta_1$  and  $\alpha_2\beta_1$ , respectively (Tiger et al., 2001; Tulla et al., 2001; Zhang et al., 2003).

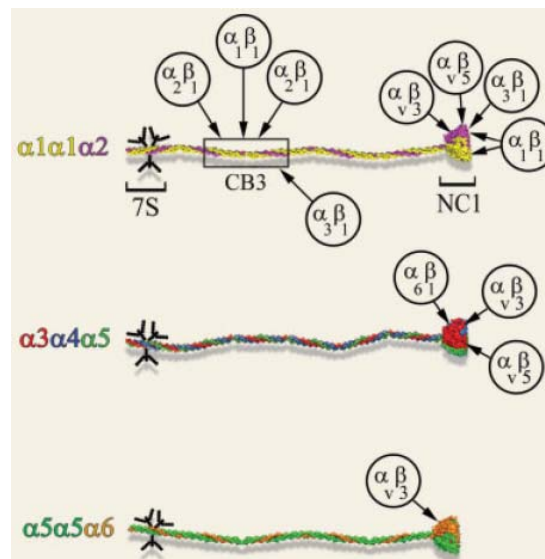


**Fig. 1.8 Location of integrin-binding sites in three different collagen IV heterotrimers.**

NC1 domains are the main integrin-binding sites in collagen IV molecules. In addition, integrins  $\alpha_1\beta_1$ ,  $\alpha_2\beta_1$  and  $\alpha_3\beta_1$  are able to bind CB3 domain in  $[\alpha_1(I)]_2\alpha_2(I)$ . Figure is adapted from (Khoshnoodi et al., 2008)



### **1.2.5 Laminin-binding integrins**

There are various integrin binding sites on LM-111 (**Fig. 1.5 B**). The binding sites for  $\alpha_1\beta_1$  (Goodman et al., 1991) and  $\alpha_2\beta_1$  (Languino et al., 1989) are located on the LN motif of the LM  $\alpha_1$  chain (Pfaff et al., 1994; Colognato-Pyke et al., 1995). Integrin  $\alpha_{10}\beta_1$  has been reported as a LM-111 receptor and the binding site has been suggested to be similar to the  $\alpha_1\beta_1$  integrin binding site (Tulla et al., 2001). The major cell binding domain of LM-111 corresponds to the proteolytic fragment E8 (240 kDa, composed of a triple stranded helix formed by the  $\alpha_1$ ,  $\beta_1$  and  $\gamma_1$  chains together with the G1-G3 domain of the  $\alpha_1$  chain) for most cell types (Aumailley et al., 1987; Goodman et al., 1987). This adhesion is mediated largely by integrins  $\alpha_6\beta_1$  (Aumailley et al., 1990a; Sonnenberg et al., 1990b),  $\alpha_6\beta_4$  (De Luca et al., 1990; Sonnenberg et al., 1991) or  $\alpha_7\beta_1$  (Kramer et al., 1991; von der Mark et al., 1991), depending on the cell type.

An RGD sequence located on the LEB motif of the LM  $\alpha_1$  chain is also responsible for cell adhesion (**Fig. 1.5 B**) (Aumailley et al., 1990b). The sequence is cryptic in native LM-111 and becomes accessible to cells only after proteolytic degradation of the adjacent L4b domain (Nurcombe et al., 1989). Integrin  $\alpha_v\beta_1$  and  $\alpha_v\beta_3$  are the binding partners of this motif (Aumailley et al., 1990b; Kramer et al., 1990; Sonnenberg et al., 1990b; Goodman et al., 1991).

The pentapeptide YIGSR is located in the LEB domain of the LM-111  $\beta_1$  chain (Fig. 1.5 B). It was found to be one of the principle sites in LM-mediated cell attachment, migration and receptor binding (Graf et al., 1987a). One of the main receptor for the YIGSR motif is the high affinity 67-kDa non-integrin laminin receptor (Graf et al., 1987b). It associates with vinculin and  $\alpha$ -actinin when YIGSR-mediated cell spreading occurs (Massia et al., 1993). Furthermore, the YIGSR motif may exert its cell-adhesive activity through interaction with  $\beta_1$  integrins, especially  $\alpha_4\beta_1$  (Maeda et al., 1994; Hopker et al., 1999).

### **1.2.6 Integrin crosstalk**

Integrins interact with one another and crosstalk with a multitude of other adhesion molecules. Trans-dominant interactions, indicating an inhibitory effect of one integrin on another have been widely reported (Diaz-Gonzalez et al., 1996; Hodivala-Dilke et

al., 1998; Baciú et al., 2003; Abair et al., 2008). Crosstalk between integrins, Src-family kinases and Rho-family GTPases regulate a range of cellular processes that are important for cell adhesion, spreading, migration and mechanotransduction (Huveneers and Danen, 2009). Integrin-mediated cell-ECM adhesion can also regulate cadherin-mediated cell-cell adhesion (Monier-Gavelle and Duband, 1997; Gimond et al., 1999). Coordination between integrins and growth factor receptors are also crucial for specific cellular responses to stimuli originating in the ECM (Porter and Hogg, 1998; Eliceiri, 2001; Alam et al., 2007).

### **1.3 Microcontact printing ( $\mu$ CP)**

The microcontact printing ( $\mu$ CP) technique was invented in 1993 by Whitesides and colleagues (Kumar and Whitesides, 1993). During the last two decades, it has been developed into a convenient, effective, and low-cost method for manufacturing micro- and nanostructures for various applications (Quist et al., 2005). Given the cell dimensions of tens of micrometers,  $\mu$ CP-generated substrates are particularly suitable for evaluating cell-based systems.

Structured silicon (Si) masters and elastomeric poly(dimethylsiloxane) (PDMS) stamps are essential for  $\mu$ CP. The Si masters carrying the micropatterns are produced by standard photolithography (**Fig. 1.9 A**). A Si wafer is spin-coated with a thin layer of photoresist and baked. After exposure to high energy UV light through a photolithographic mask, the photoresist will be degraded and the designed patterns are generated. Afterwards the uncured photoresist is removed and the remaining photoresist is used as resist in the subsequent etching step, yielding a patterned Si surface (Wallraff and Hinsberg, 1999). Si masters can be used to cast PDMS with complementary structures. As a less hydrophobic material compared to PDMS, Si master can also adsorb proteins from smooth PDMS cuboids (von Philipsborn et al., 2006a; Coyer et al., 2007). PDMS stamps are produced by mixing fluidic elastomer with curing agent and solidifying afterwards, during which time they are able to conform to different surface topographies (Kumar et al., 1994; Armani et al., 1999). PDMS is highly hydrophobic with a water contact angle around  $110^\circ$ . In contrast, many proteins are hydrophilic, as are glass and silicon. Therefore, the binding affinity of proteins to PDMS is lower than to glass and silicon, which makes PDMS a powerful tool for transferring proteins to glass and silicon (Tan et al., 2001).

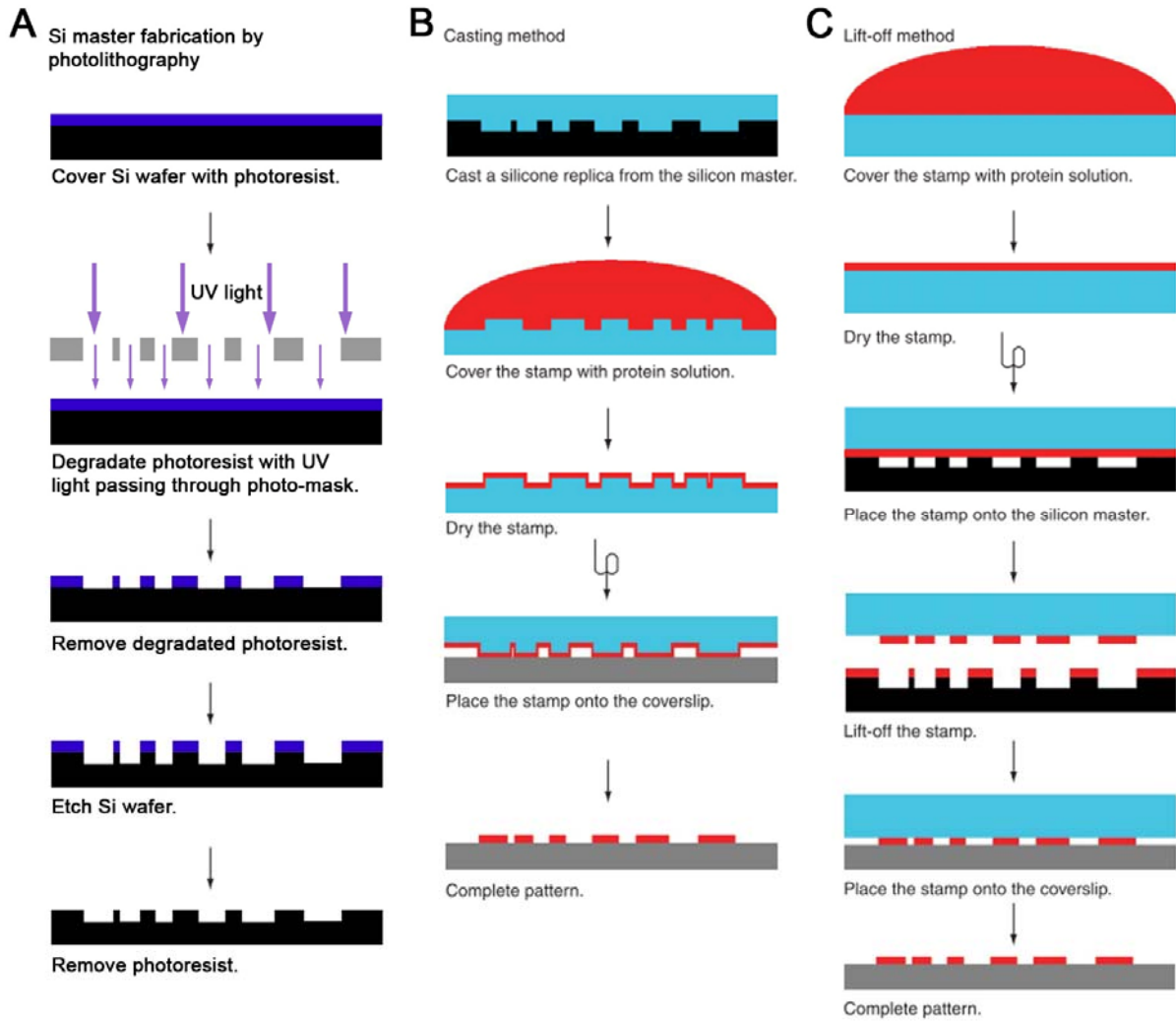


**Fig. 1.9 Si master fabrication and  $\mu$ CP techniques.**

(A) Si masters are fabricated by standard photolithography. (B) Patterned PDMS stamps are used in casting method for printing micropatterns. (C) Smooth PDMS cuboids are used in lift-off methods to generate micropatterns. (B) and (C) are taken from (von Philipsborn et al., 2006a).

The basic principle of  $\mu$ CP is straightforward. A stamp is fabricated by curing PDMS against a featured Si master. The stamp will assume a complementary topography to the master. The stamp is then coated with the desired molecules and brought into contact with the substrate. Molecules on the raised parts of the stamp relief will transfer to the substrate if they interact more strongly with the substrate than with the stamp (**Fig. 1.9 B**) (Alom Ruiz and Chen, 2007). By using the “casting method”, alkanethiols can be printed on gold covered surfaces (Kumar and Whitesides, 1993), alkylsilane can be transferred to glass or Si surfaces (Xia et al., 1995), and various

proteins and peptides can be delivered from hydrophobic (PDMS) to less hydrophobic surfaces (Kane et al., 1999; Tan et al., 2001; Li et al., 2009).

The mechanical properties of PDMS allow for printing of structures as small as 500 nm (Sotomayor Torres, 2003). However, the aspect ratio of the stamps has to be carefully chosen. The raised structures may collapse if they are too high; and the stamps will sag if the raised structures are too far away from each other (Delamarche et al., 1997; Hui et al., 2002). In addition, micro patterns composed of different types of molecules can not be easily generated by the casting method without a precise positioning system. As a consequence, molecules printed in a second step may be placed on top of the first printed layer or the original printed molecules may be removed by the second stamping step.

The lift-off method is capable of printing small, sparse structures with unlimited distance in between without the risk of stamp deformation or collapse. Multiple types of molecules can also be printed easily without any additional specialized equipment (**Fig. 1.9 C**) (von Philipsborn et al., 2006a; Coyer et al., 2007; Desai et al., 2011). Here, a smooth PDMS cuboid is inked with the desired molecule and placed onto a featured Si wafer. The molecules on the PDMS stamp will then be subtracted by the raised structure of the master. Afterwards, a second molecule (which does not bind to the first one) can be added to the PDMS cuboid, filling the gaps on the PDMS. A second Si master can also be used to subtract molecules from the PDMS, introducing additional patterns on the stamp. The inking and subtraction process can be repeated several times. At the last step, all the molecules are transferred to the substrate by the normal printing procedure. Although many proteins can be successfully printed by the lift-off method and retain their biological activity (von Philipsborn et al., 2006a), some proteins such as fibronectin may lose activity due to conformational changes caused by sandwiching between surfaces of very different hydrophilic/hydrophobic properties during contact (Anderson and Robertson, 1995; Biasco et al., 2005).

Compared to other systems which take advantage of physical barriers to direct cell adhesion and spreading (Jungbauer et al., 2004),  $\mu$ CP uses only chemical cues to direct cells. ECM proteins such as fibronectin (Chen et al., 1997; They et al., 2006),

laminin (Mendelsohn et al.), vitronectin (Gupta et al.) and collagen (Hou et al., 2009; Monroe et al., 2009) are relevant to cell adhesion and migration research and are therefore commonly used as “ink” for  $\mu$ CP. Such patterned ECM protein substrates have provided novel insight into the mechanisms underlying cell spreading within confined geometries. Chen and his colleagues showed that it is not the total area of the ECM protein but its distribution which controls cell life or death (Chen et al., 1997). Various patterns of ECM proteins give rise to similar cell morphology but distinct cytoskeleton arrangement (They et al., 2006). Furthermore, cell migration on “one-dimensional” (linear) ECM protein patterns may mimic cell behavior in the three-dimensional state, while cell migration on two-dimensional ECM substrates is slower and random directional (Doyle et al., 2009).  $\mu$ CP has also been used to fabricate protein gradients for chemotaxis research. Not only the steepness of  $\mu$ CP ephrin gradients but also the total amount of ephrin regulate axon outgrowth (von Philipsborn et al., 2006b). While many studies have been based on single ECM protein patterns backfilled with a non-adhesive material, such as polyethylene glycols (PEG) (Brock et al., 2003), studies of cell behavior on multiple ECM protein substrates have just recently started to emerge (Desai et al., 2011).

## 1.4 Atomic force microscopy

### 1.4.1 Imaging mode

#### 1.4.1.1 Basic principle

The atomic force microscope (AFM) belongs to the family of scanning probe microscope (SPM) (Binnig et al., 1986). Compared to other microscopy techniques, AFM imaging can achieve single atom resolution but without harsh demands for the scanning environment, sophisticated sample preparation steps (Nicholas A; von Ardenne, 1938; Binnig et al., 1982; Binnig et al., 1987; Egerton, 2005; Pawley, 2006). All these advantages make AFM a versatile tool for detecting the morphology of biological specimens in real time, under physiological condition and with submolecular resolution (Hoh and Hansma, 1992; Braga and Ricci, 2011).

	<b>CLSM</b>	<b>SEM</b>	<b>TEM</b>	<b>STM</b>	<b>AFM</b>
<b>Sample preparation</b>	fluorescent labeling	dehydration and metallic coating	sample staining and cross-sectioning	dehydration and metallic coating	No
<b>Operating environment</b>	physiological environment	vacuum	vacuum	vacuum	physiological environment
<b>Imaging speed</b>	fast	fast	fast	fast	fairly slow
<b>Working distance</b>	$\mu\text{m}$ -mm	mm	mm	nm	nm
<b>XY-resolution</b>	200 nm	nm	Å	Å	Å
<b>Z-resolution</b>	$\mu\text{m}$	-	-	Å	Å
<b>3D image from single scan</b>	no	no	no	yes	yes
<b>Maximum scanning Size</b>	$\text{mm}^2$	$\text{mm}^2$	$\text{mm}^2$	$\text{nm}^2$	100x100 $\mu\text{m}$
<b>Inner structure visible</b>	no	no	yes	no	no
<b>Combination with florescent microscopy</b>	-	no	no	no	yes
<b>Sample damage after imaging</b>	photobleaching	mass loss due to electron beam irradiation	mass loss due to electron beam irradiation	no	no

**Table 1.1 Comparison of various microscopy techniques for biological applications.**

CLSM: confocal laser scanning microscopy, SEM: scanning electron microscopy, TEM: transmission electron microscopy, STM: scanning tunneling microscopy.

In AFM a sharp tip interacts weakly with the sample and scans line by line over it while interaction is measured and controlled. In this way, the tip moves up and down as it tracks the surface morphology. The xyz position of the tip is recorded and controlled by an electronic feedback circuit. From the recorded tip movement a 3D reconstruction of the sample can be obtained (**Fig. 1.10**). There are three components of the AFM which are crucial for high resolution imaging (Kaupp, 2006; Morris et al., 2010). A micro-fabricated, sharp stylus, or tip, determines the resolving power of the AFM (Tortonese, 1997). The tip is usually made of hard materials, such as Si or Si<sub>3</sub>N<sub>4</sub>. The radius of the apex is usually in the range of several nanometers. The stylus is mounted on a micrometer-sized cantilever, whose spring constant can vary from several mN/m to tens of N/m. Therefore, any small force variation between AFM tip and the sample surface will lead to a strong deformation of the cantilever. The second key element of the AFM is the scanning mechanism (Binnig and Smith, 1986; Taylor, 1993). In many AFM setups, a piezo transducer moves with the sample in a three dimensional manner and the cantilever remains stationary. The sample motion is driven by the electric voltage applied to the top and bottom, left and right, front and back of the piezoelectric transducer. Within a certain range, the expansion of the transducer is proportional to the potential difference with an accuracy of atomic dimensions, so that the xyz position of the sample can be precisely controlled. The third essential element is the detection mechanism for the cantilever deflection (Meyer and Amer, 1988). Most commonly, a laser beam is focused at the end of the cantilever above the tip and reflected towards a photodiode. Movement of the cantilever following variations in the sample surface topography will lead to a laser path change and finally to a large displacement of the laser spot position on the photodiode. The laser intensity difference between the left and right or top and bottom segment of the photodetector quantifies the lateral or vertical movement of the AFM tip respectively. The feedback loop collects cantilever movement information from the photodetector and adjusts the sample position accordingly to maintain either a constant force or a constant height between the AFM tip and sample. The three-dimensional motion of piezo transducer is recorded and later integrated into the sample topography image.



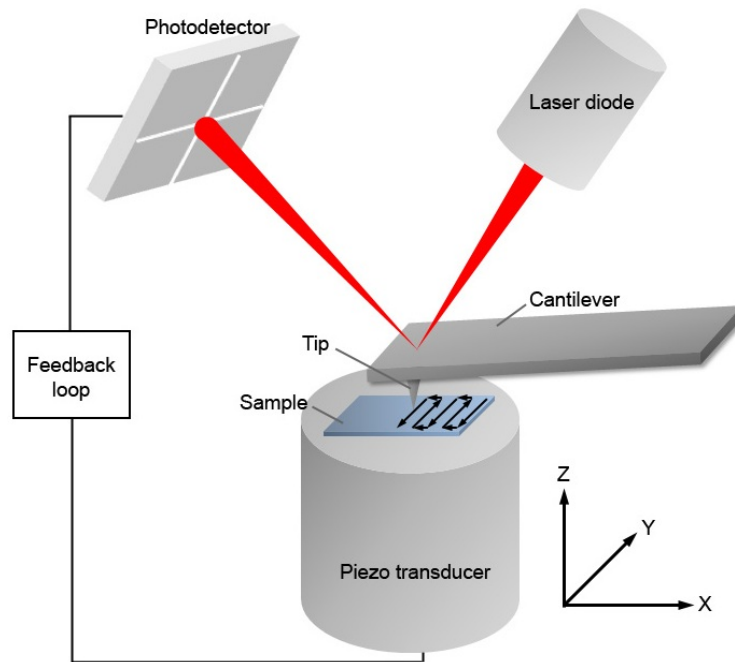


**Fig. 1.10 Schematic representation of the atomic force microscope.**

An AFM tip sweeps the sample line by line and the tip-sample interaction is under control: a laser light is focused on the AFM cantilever just above the tip and reflected to a photodetector. Any force variations between AFM tip and the sample will lead to cantilever bending followed by dislocation of laser spot on the photodetector. A feedback loop processes cantilever movement information and adjusts the sample position accordingly.

#### 1.4.1.2 Forces between the AFM tip and sample surfaces

When AFM tip and sample are far away from each other (a few hundred nm), long-range interactions such as capillary, electrostatic and magnetic interactions are significant, while the attractive Van der Waals (VdW) force is too small to exhibit any significant effect (**Fig. 1.11**) (Binnig and Rohrer, 1999). As the AFM tip is getting closer to sample surface, the attractive VdW force increases drastically, leading to downward bending of AFM cantilever. When the tip-sample separation reduces even further, repulsive VdW forces increase. At first VdW forces compensate for the attractive force and then become the dominant force between tip and sample, resulting in the upward bending of the cantilever (**Fig. 1.11**).

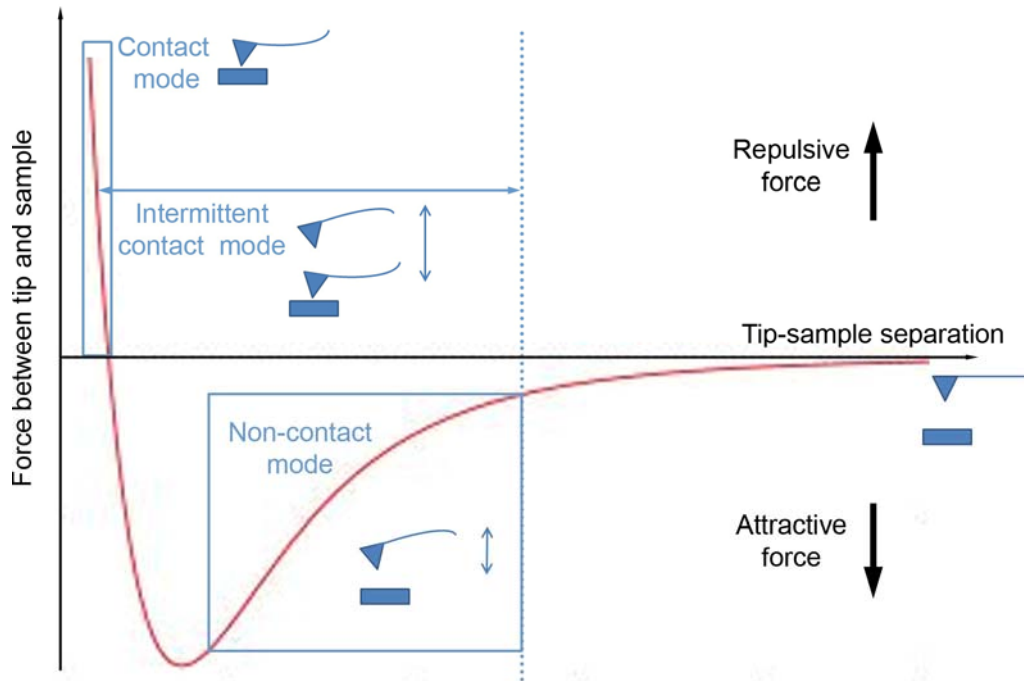


**Fig. 1.11** Variation of the Van der Waals interaction with the separation distance between the AFM tip and the sample.

With the decrease of tip-sample separation, the VdW forces changes from attractive to repulsive. Different imaging modes and the corresponding cantilever bending are indicated.

#### 1.4.1.3 Imaging modes

Depending on the distance between AFM tip and sample surfaces, three AFM imaging modes can be distinguished: contact mode, with  $<0.5$  nm tip-sample separation, tapping mode (intermittent contact mode), with  $0.5\text{--}2$  nm tip-sample separation, and non-contact mode with  $0.1\text{--}10$  nm tip-sample separation (Wang et al., 2007; Michler, 2008). In contact mode, the AFM tip is so close to the sample surface that the repulsive VdW force dominates (**Fig. 1.11**). The AFM tip moves on the sample in a raster pattern, while the force between tip and sample is maintained constant at a user-defined set point. Any change of sample topography will lead to the variation of tip-sample separation, causing force deviation from the set point. The feedback loop senses the deviation and adjusts the Z-position of the piezo transducer, compensating the height change of the sample at that point (Le Grimmelc et al., 1998; Schimmel et al., 1999). Capillary force caused by a thin water film on the sample surface is a major problem for contact mode imaging in air. In this case, the AFM tip is strongly glued to the sample surface by a liquid meniscus, often resulting

in sample damage during scanning. A sealed chamber filled with dry air can decrease the humidity and solve this problem.

In intermittent contact mode, the cantilever is driven by an acoustic wave to oscillate up and down near its resonance frequency with an amplitude of up to 200 nm. The tip resonates up and down during scanning and intermittently touches the sample surface at each point. When the tip-sample separation decreases, elastic and inelastic interactions cause a change in the oscillation amplitude and a phase shift relative to the driving signal of the cantilever. Both amplitude and phase shift can be used by the feedback loop to track the surface topography (García and Pérez, 2002; Paulo and García, 2002). Intermittent contact mode in air not only significantly decreases the effect of capillary forces but also reduces lateral forces causing sample damage.

In non-contact mode, the cantilever oscillates with an amplitude of a few nm, without touching the sample surface. The increased attractive VdW forces between the tip and sample caused by the shortened tip-sample separation leads to a damping effect of the cantilever. This signal is then used by the feedback loop to construct AFM images (Martin et al., 1987).

	<b>Cantilever spring constant</b>	<b>Resonance frequency</b>	<b>Scanning force</b>	<b>Merits and drawbacks</b>
<b>Contact mode</b>	0.01-1.0 N·m <sup>-1</sup>	7-50 kHz	nN-μN	+ high speed + high resolution + suitable for scanning rough samples - lateral force causes damage - strong capillary force when scanning performed in air
<b>Tapping mode</b>	30-60 N·m <sup>-1</sup>	250-350 kHz	nN	+ high lateral resolution + eliminates lateral forces + minimizes capillary forces - slightly slower than contact mode
<b>Non- contact mode</b>	0.5-5 N·m <sup>-1</sup>	50-120 kHz	pN	+ no force exerted on the sample - lower lateral resolution, limited by tip-sample separation - slowest scan speed - usually only works on extremely hydrophobic sample

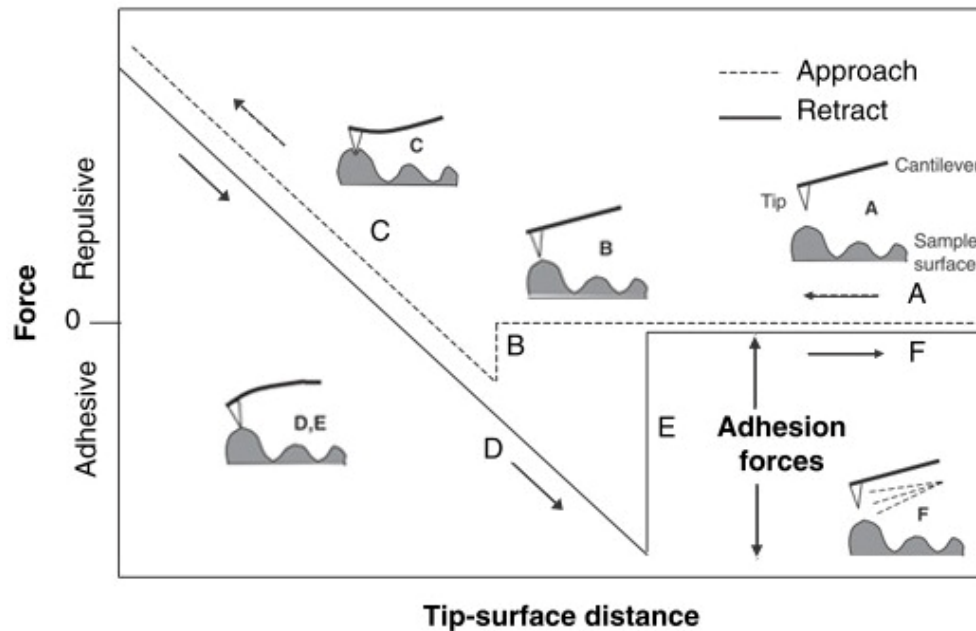
**Table 1.2 comparison of different imaging modes.**

Table summarized based on (Morris et al., 2010) and (Thornton, 1998).

## **1.4.2 Force spectroscopy mode**

### **1.4.2.1 Basic principle**

The high accuracy and sensitivity with which the AFM scanner can be controlled in xyz-directions allows for a precise manipulation of very small forces not only during imaging but also force spectroscopy mode (Butt et al., 2005; Hinterdorfer and Dufrene, 2006). During force spectroscopy, the XY-position of the AFM cantilever is fixed, whereas the Z-position is changed in a controlled manner. During this process the height changes of the z-piezo element and the vertical deflection of the cantilever detected by the photodiode are recorded, resulting in a so-called force-distance curve (**Fig. 1.12**). First the height of the cantilever is decreased without interacting with the sample. At this time point, there is no cantilever deflection but a declining distance between tip and sample (**Fig. 1.12 A**). The initial contact between the tip and the surface is mediated by attractive VdW forces that lead to an attraction of the tip towards the surface (**Fig. 1.12 B**). When the cantilever is moved even further down, the cantilever is bent upwards in direct proportion to the z-piezo height until the preset deflection point is reached (**Fig. 1.12 C**). Afterwards, the cantilever is withdrawn and progressively relaxes. Due to the tip-sample adhesion, the cantilever may then start bending in the opposite direction (**Fig. 1.12 D and E**), until it eventually loses contact with the sample (**Fig. 1.12 F**).



**Fig. 1.12** Idealized force-distance curve describing a single approach-retract cycle of the AFM tip.

(A-C) The cantilever is brought into contact with the sample surface until a preset force is reached. (D-F) When the cantilever is withdrawn, adhesion forces between the sample and the AFM tip hinder tip retraction, resulting in the downward bending of the cantilever until the tip and sample are totally separated. Figure is modified from (Shahin et al., 2005).

After cantilever calibration, the force  $F$  exerted by the cantilever on a sample can be calculated using Hooke's law:  $F=k \cdot s$ , where  $k$  is the spring constant of the cantilever and  $s$  is the deflection of the cantilever (Butt et al., 2005). Depending on the cantilever stiffness, the range of forces that the AFM can detect in force spectroscopy mode spans from the pN to the  $\mu$ N range (Benoit and Gaub, 2002). This range encompasses subtle interactions such as single thermal collision of proteins in liquid and hydrogen bonds, covalent and electrostatic bonds, as well as receptor-ligand and antibody-antigen recognition (Grandbois et al., 1999; Evans, 2001; Muller et al., 2009a). Furthermore, force spectroscopy can be performed under physiological conditions at unparalleled spatial resolution. That makes it particularly suitable for a wide range of biological applications, such as quantifying inter-cellular or cell-ECM adhesion (du Roure et al., 2006; Taubenberger et al., 2007).

#### **1.4.2.2 AFM based single cell force spectroscopy**

By combining AFM and optical microscopy, cells can be manipulated to assess cellular adhesion at a given location on a functionalized surface, tissue or on another cell (Benoit et al., 2000; Benoit and Gaub, 2002). This method was later termed AFM-based single-cell force spectroscopy (AFM-SCFS) (Benoit et al., 2000). Several modifications to the conventional AFM set up are necessary for AFM-SCFS. An optical microscopy allows for precise positioning of the cell, while simultaneously observing cell contact behavior during measurement. For probing mammalian cells, a temperature-controlled chamber filled with cell culture medium is usually implemented. In addition, in order to guarantee complete cell-substrate or cell-cell separation, an extended Z-range up to 100  $\mu\text{m}$  is required (Puech et al., 2006).

AFM-SCFS can be performed in two ways, by probing either the adhesion of a cantilever-attached cell to a functionalized surface (Zhang et al., 2002) or the adhesion of an immobilized cell to a ligand-coated cantilever (Lehenkari and Horton, 1999). Since only the former approach is adopted in this thesis, it will be expanded here.

In order to ensure stable cell attachment to the AFM cantilever during force measurements, the cantilever surface has to be functionalized with an adhesive coating. Concanavalin A or wheat germ agglutinin, lectins that bind carbohydrate groups on the cell surface, are commonly used to immobilize various cell types (Benoit et al., 2000; Wojcikiewicz et al., 2004). To capture a single cell onto the functionalized cantilever, a small volume of cell suspension is added to the fluid chamber. A single cell settling on the support is then approached (**Fig. 1.13 A**) and gently pressed with the functionalized AFM cantilever (**Fig. 1.13 B**). After a short time (in the range of seconds), the cantilever is elevated to separate the cell from the support (**Fig. 1.13 C**). This converts the cantilever with a living cell into a probe, which can subsequently be brought into contact with the functionalized surface or another cell.

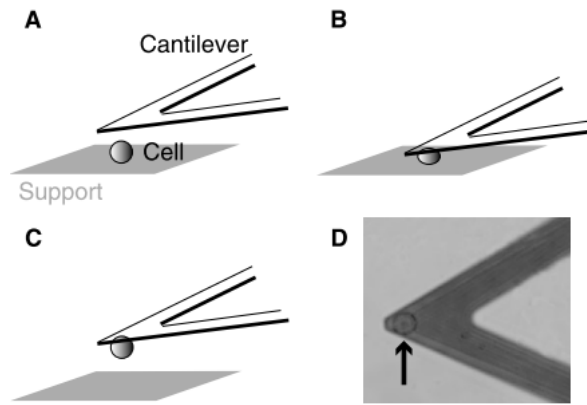


**Fig. 1.13** Capturing a suspended cell with the AFM cantilever.

(A) The apex of a lectin-functionalized AFM cantilever is positioned above a cell. (B) The cantilever is then gently pushed onto the cell. (C) The cantilever-bound cell is separated from the support and the cell is allowed to adhere firmly. (D) A phase-contrast image of a cell (arrow) bound to a tip-less cantilever. Figure adapted from (Helenius et al., 2008).

To measure adhesion of a single cell to a substrate of interest, the cell attached to the cantilever is lowered with a constant speed until the cell is in contact with the substrate and a preset force is reached. After a given contact time, the cantilever is elevated until the cell completely detaches from the substrate (**Fig. 1.14 A**). During this retraction process, the cantilever deflection, which is proportional to the vertical force that indicates cell-substrate adhesion, is recorded in a force-distance (F-D) curve (**Fig. 1.14 B**). By varying the preset contact force and contact time, both overall cell adhesion and the contribution of single-molecule binding can be detected.

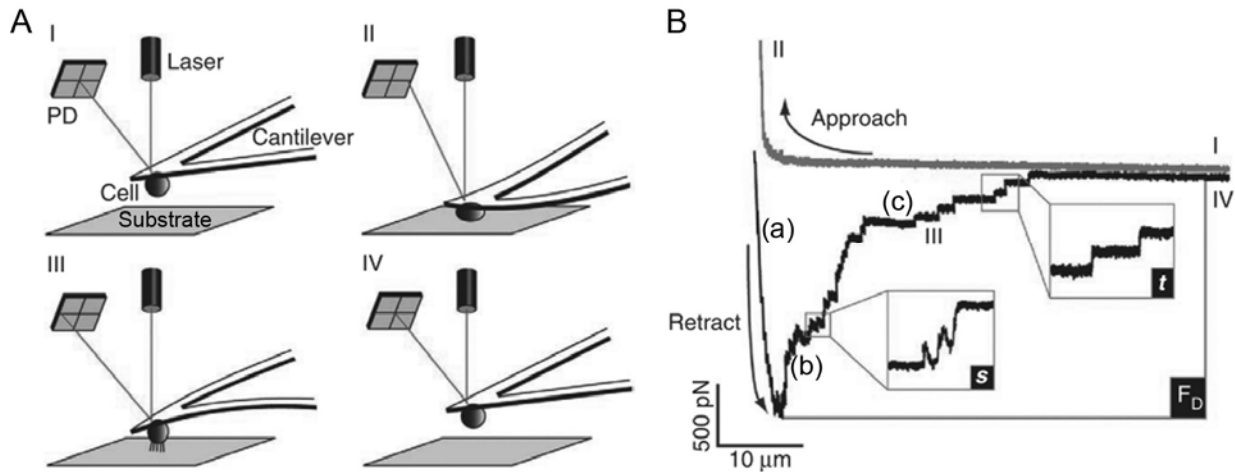


**Fig. 1.14 AFM-SCFS.**

(A) Depiction of a cell-adhesion force measurement. To measure the force acting on the cell attached to a cantilever, the cantilever deflection is determined using a laser beam reflected by the back of the cantilever onto a multisegment photodiode (PD). The cantilever-bound cell is lowered towards the substrate (I) until a preset force is reached (II). After a given contact time, the cantilever is retracted from the substrate (III) until cell and substrate are completely separated (IV). (B) Force-distance (F–D) curve showing steps (I), (II), (III) and (IV) corresponding to those outlined in (A). Several unbinding events can be observed (s, force steps; t, unbinding of membrane tethers;  $F_D$ , maximal detachment force). Figure adapted and slightly modified from (Friedrichs et al., 2010).

The retraction F-D curve can be divided into three phases (Helenius et al., 2008). During the initial phase (**Fig. 1.14 B a**), the withdrawal of the cantilever inverts the force applied on the cell from pushing to pulling. Cell-substrate contact points bear stronger forces as the overall pulling force increases, leading to cell cortex deformation. The binding strength of individual receptors, their total number and distribution geometry, determines at what force the cell will start to detach from the substrate. The cell detachment force  $F_D$ , which corresponds to the distance from the lowest point of the retraction F-D curve to the base line (**Fig. 1.14 B**), represents the maximum strength of cell-substrate binding.

During the second phase (**Fig. 1.14 B b**), receptors either detach from the substrate surface or are pulled away from the cell cortex at the tip of a membrane tether (**Fig. 1.15 A**). As a result, individual force steps occur. During the final phase of detachment (**Fig. 1.14 B c**), the cell body is no longer in contact with the substrate and attachment is mediated exclusively by tethers (**Fig. 1.15 B**) (Sun et al., 2005). The lipid composition of the membrane and the mechanical properties of the cell



cortex determine the force required for tether extension, while the receptor-ligand interaction at the end of the tether only influences the tether life-time but not the detachment force (Marcus et al., 2004). Therefore, once tether extension initiates, this force remains constant independently of tether length (Hochmuth et al., 1996). When the receptor-ligand bond at the tip of the tether dissociates due to the end of its lifetime, the tether separates from the surface.

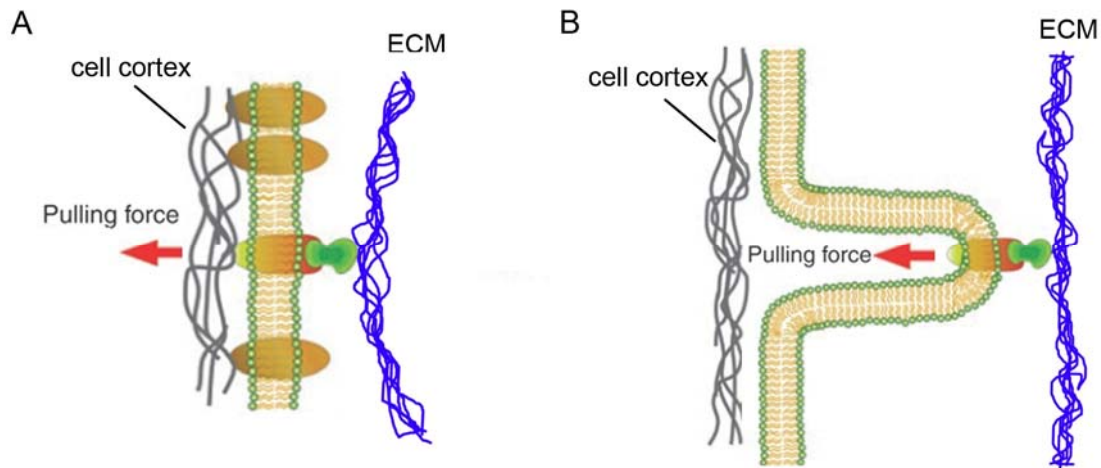


**Fig. 1.15 Schematic illustrations of events causing force steps and the unbinding of membrane tethers.**

(A) Pulling force leads to the receptor-ECM or receptor-cell cortex separation which is indicated as force steps in the force curves. (B) After the cell body totally separated from ECM, the receptor-ECM interaction anchors specific point of cell membrane and the pulling force causes membrane extension until the life time of receptor-ECM bonds is over. This event is named tether. Figures taken from (Muller et al., 2009a) and modified.

## **1.5 Cell adhesion assays**

Controlled adhesion of cells to their environment (e.g. the ECM or to other cells) is of great importance for many biological processes such as embryonic development, immune response, wound healing and tumor metastasis (Lauffenburger and Wells, 2001; Adams, 2002). In order to understand the mechanism of cell adhesion, several qualitative and quantitative cell adhesion assays have been established over the past years. Some of them are bulk assays able to measure the adhesive behavior of large cell populations in a single experiment. Other assays measure the adhesive behavior of individual cells and are thus called single-cell assays.

### **1.5.1 Bulk assays**

In bulk assays, cells are usually cultured on the substrates of interest for a certain time before forces are applied to detach the cells from their substrates. Washing assays utilize the shear force of hydrodynamically-streamed physiological buffer to flush away non-adherent cells from the substrates, where the percentage of remaining cells provides a measurement for the cell-substrate adhesion strength (**Fig. 1.16 A**) (Klebe, 1974). Although this method lacks reproducibility, it has enabled the elucidation of important cell adhesion mechanisms (Yamada and Kennedy, 1984; Sieg et al., 2000). Other semi-quantitative methods, such as the flow chamber (**Fig. 1.16 B**) (Kaplanski et al., 1993), spinning disc (**Fig. 1.16 C**) (García et al., 1997) and centrifuge assay (**Fig. 1.16 D**) (Reyes and García, 2003) make use of either well defined hydrodynamic shear forces or centrifugal forces to detach cells from the substrate. As a result, these three assays generate reproducible results regarding the adhesion strength of the whole cell population. However, since cell spreading area and topography can significantly influence cell resistance to shear or centrifugal forces, reproducing those assays requires precise control of cell-seeding density and spreading time.

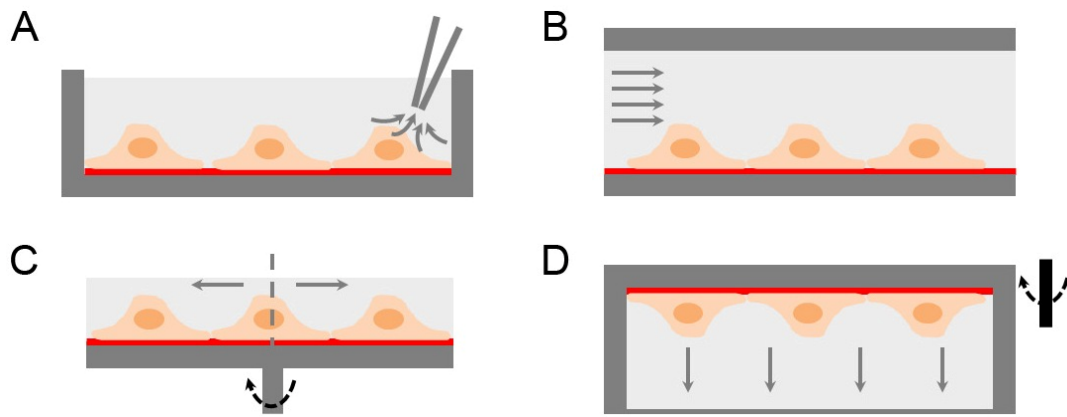


**Fig. 1.16 Cell adhesion bulk assays.**

Washing Assays (A), flow chamber (B), spinning disc (C) and centrifuge assay (D) are shown schematically. The directions of the applied forces are indicated by arrows.

## 1.5.2 Single cell assays

In contrast to bulk assays which can obtain statistically relevant data from large number of cells within short time frames, single cell assays are usually more time-consuming. However, the adhesion behavior of individual cells within a population can be detected and compared in a quantitative manner. Within the last years, several single-cell assays, such as AFM-based SCFS, have been developed to measure cell adhesion down to detecting single-molecule adhesion/rupture events. They are often combined with optical microscopy to monitor the movement of the cells or the probes, however, the principles of force determination vary from method to method (Neuman et al., 2007; Helenius et al., 2008; Neuman and Nagy, 2008).

### 1.5.2.1 Glass microneedle

Glass microneedle assays are conceptually similar to the AFM (**Fig. 1.17 A**) (Kishino and Yanagida, 1988; Ishijima et al., 1996). Here, a soft glass microneedle functions as a force transducer. The stiffness of this transducer can be controlled by manipulating its radius and length. The applied force can be determined by measuring the deflection of the microneedle by optical microscopy. The force resolution of this method is limited by the optical resolution of the light microscope. Consequently, an alternative experiment setup has been implemented using an optical fiber replacing the soft needle as force transducer (Cluzel et al., 1996). The light emitted from the end of the optical fiber is received by a position-sensitive

photodetector, which allows for the precise determination of the force transducer's deflection.

### **1.5.2.2 Biomembrane force probe**

In the biomembrane force probe (BFP), a swollen red blood cell (RBC) usually serves as force sensor (**Fig. 1.17 B**) (Evans et al., 1995). Its membrane stiffness is flexibly controllable over orders of magnitude by micropipette suction. To measure cell adhesion to an ECM protein, a ligand-coated bead is adhered to the RBC and approached by a cell which is held by another micropipette. After a preset time, the bead and cell separation takes place and the position of the bead attached to the force sensor is closely monitored by optical microscopy. The detachment force is then obtained by multiplying the RBC stiffness by the bead displacement, which stands for the change in extension of the membrane (Simson et al., 1998; Zarnitsyna et al., 2007).

### **1.5.2.3 Optical tweezers**

The setup of optical tweezers utilizes a trapped micron-sized bead in the focus of a powerful laser beam. For small displacements (~150 nm), the optical trap acts as a linear spring, with a spring constant that depends on the dielectric property of the bead and the laser intensity (**Fig. 1.17 C**) (Gordon, 1973; Ashkin et al., 1986). For cell adhesion measurements, a functionalized bead is placed on the dorsal side of an adherent cell and afterwards withdrawn. Any cell-bead interaction will lead to the dislocation of the beads from the optical trap. This dislocation is detected by differential interference contrast and correlated to the adhesion force (Andersson et al., 2007).

### **1.5.2.4 Magnetic tweezers**

Magnetic tweezers make use of a gradient magnetic field generated by permanent magnets or electromagnets and of magnetic beads (**Fig. 1.17 D**). The magnetic force can be controlled by changing the position of the magnet or adjusting the current which generates the magnetic field. Biomolecule-coated-beads are then brought into contact with the cell for a certain time before they are withdrawn by means of the applied magnetic force (Kollmannsberger and Fabry, 2007). Alternatively, a bead-cell

couple can be placed onto the functionalized surfaces and detached by pulling on the magnetic bead (Walter et al., 2006).

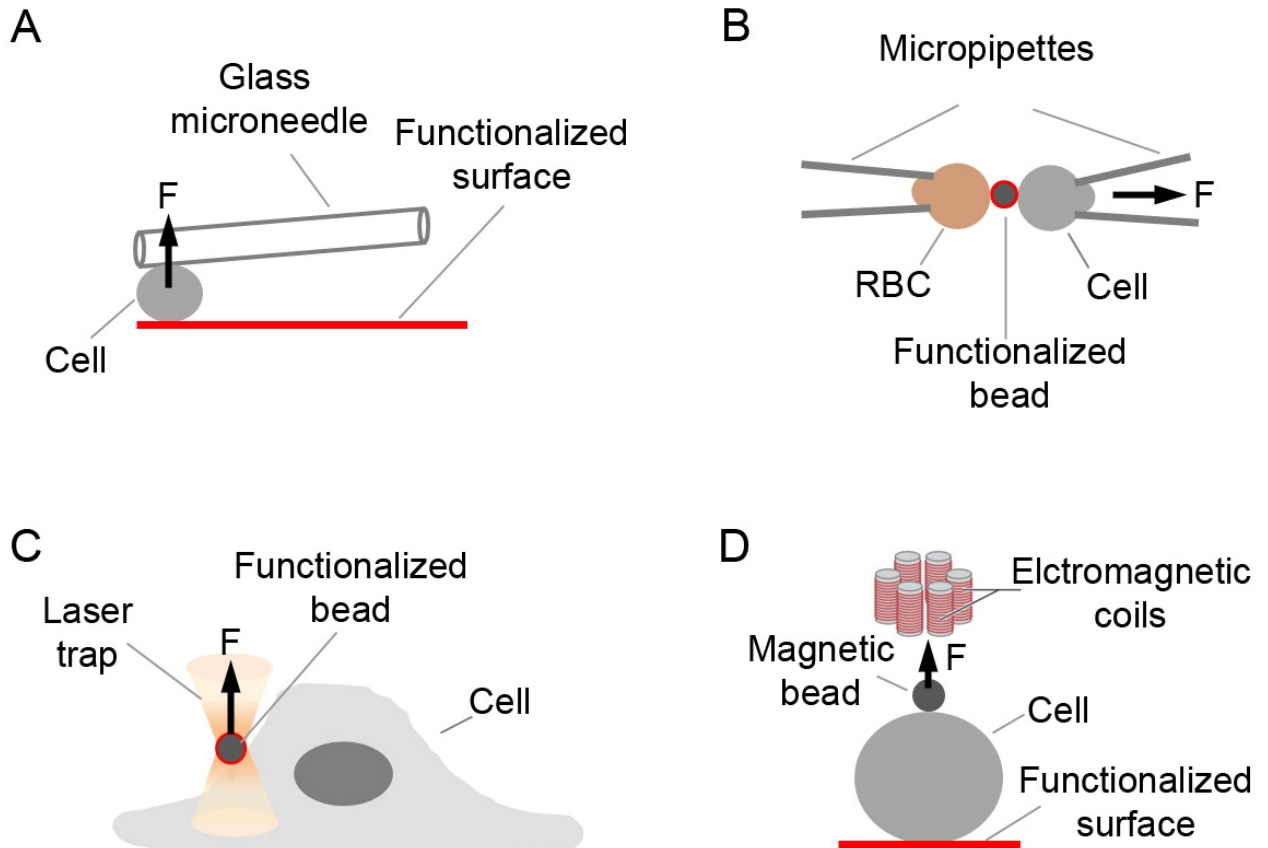


**Fig. 1.17 Single cell adhesion assays.**

The principles of glass microneedle (A), BMP (B), optical tweezers (C) and magnetic tweezers (D) are shown schematically. The directions of the applied forces are indicated by arrows.

	Cell adhesion assay	Force type	Force range	Dynamic range	Pros vs. cons
<b>Bulk assay</b>	Washing assay	hydrodynamic shear force	-	-	+ simple - low reproducibility - no quantitative data
	Flow chamber	hydrodynamic shear force	~pN	-	+ reproducible ± semiquantitative - cell spreading area and topography dependent
	Spinning disc	hydrodynamic shear force	up to $\mu\text{N}$	-	+ wide applicable force range + reproducible ± semiquantitative - complex experimental setup - cell spreading area and topography dependent
	Centrifuge assay	centrifugal force	up to $\mu\text{N}$	-	+ wide applicable force range + reproducible ± semiquantitative - cell spreading area and topography dependent
<b>Single cell assay</b>	Glass microneedles	pulling force	0.001-1000pN	$\geq 100$ ms	+ small spring constants - low spatial resolution
	BFP	pulling force	0.01–1000 pN	$\geq 1$ ms	+ high force resolution + good temporal control - cell deformation by aspiration
	Optical tweezer	pulling force	0.1–200 pN	$\geq 10$ ms	+ high force resolution - restricted to low detachment forces - local heating
	Magnetic tweezer	pulling force	0.001–100 pN	$\geq 1$ s	+ high force resolution - weak temporal and spacial control
	AFM SCFS	pulling force	1 pN-1 $\mu\text{N}$	$\geq 10$ $\mu\text{s}$	+ wide applicable force range + high force resolution + good control of contact conditions + commercially available - time and cost intensive

**Table 1.3 Overview of different cell adhesion assays.**

Table is summarize after (Bustamante et al., 2000; Clausen-Schaumann et al., 2000; Taubenberger, 2009; Brenner et al., 2011).

## 1.6 Motivation

AFM-SCFS offers the opportunity to quantify adhesion forces from the single molecule to the single cell scale. However, as indicated by its name, this technique is only able to measure a single cell per adhesion experiment, making it a relatively time-consuming technique. When characterizing cell adhesion to multiple ECM components mimicking a particular *in vivo* adhesion niche, many individual cells have to be measured separately on individual substrates, significantly prolonging the quantification procedure. The aim of my first project (Chapter 3) is therefore to incorporate several ECM components onto the same surface and to compare directly adhesion of single cells to these ECM components with minimized spatial and temporal differences. Fundamental questions regarding the appropriate quantification of the obtained SCFS data are to be addressed, such as regarding the number of possible force cycle repetitions offered by this setup, the number of force cycles repetitions sufficient for obtaining a solid statistical evaluation of the adhesion properties of a single cell, whether single cell adhesion forces are influenced by preceding measurements and whether the adhesion strength of individual cells to different ECM components is independently regulated.

In contrast to broad force distributions obtained from cell populations, force distribution from single cells measured several times are usually narrow. My second project (Chapter 4) is intended to elucidate mechanisms underlying adhesive variations between individual cells in populations. Three possibilities will be investigated: the presence of different subclones with different adhesion properties due to genetic changes, adhesion variation at different cell cycle stages and variation of adhesion receptor numbers on the surface of different cells.

Particular integrins often specifically bind to several different extracellular ligands, but the binding affinities to these ligands are difficult to compare in the context of a living cell. In the third project (Chapter 5), the affinity of  $\alpha_2\beta_1$  integrin to collagen and laminin will be compared in single cells. Moreover, the influence of expressing exogenous integrins on the expression of endogenous integrins will be investigated.

Together, all three projects are intended to provide new insight into mechanisms underlying integrin-mediated cell adhesion to the ECM on the level of single cells.

## 2 Materials and Methods

### 2.1 Materials

#### 2.1.1 Reagents and Kits

Reagents and Kits	Company	Applications
(3-glycidyloxypropyl)trimethoxysilane	www.sigmaaldrich.com	glass passivation
7.5% Mini-PROTEAN® TGX™ precast polyacrylamide gels	www.bio-rad.com	SDS-PAGE
acetic acid	www.carlroth.de	0.25% (v/v)
amino-PEG2000	www.rapp-polymere.com	glass passivation
Bio-Rad protein assay	www.bio-rad.com	protein concentration determination
cell surface protein isolation kit	www.piercenet.com	surface protein isolation
collagen type I	www.advancedbiomatrix.com	50-100 µg/ml in glycine buffer, surface coating
collagen type IV	www.sigmaaldrich.com	100 µg/ml in acetic 0.25% (v/v) acid solution, surface coating
CO <sub>2</sub> independent medium	www.invitrogen.com	SCFS
DMEM	www.invitrogen.com	cell culture
ethanol/EtOH (>99.8%)	www.carlroth.de	washing, solvent
FITC conjugated collagen type I	www.sigmaaldrich.com	20 µg/ml in PBS, surface coating
fluorescent mounting medium	www.dako.com	fluorescence microscopy
gel blotting paper	www.whatman.com	Western blotting
Geneticin/G-418 Sulfate	www.invitrogen.com	cell culture
glycine	www.carlroth.de	50 mM, collagen buffer
hydrogen peroxide (H <sub>2</sub> O <sub>2</sub> )	www.carlroth.de	piranha solution (H <sub>2</sub> SO <sub>4</sub> :H <sub>2</sub> O <sub>2</sub> =3:1)
hydroxyurea	www.sigmaaldrich.com	2 mM, cell cycle synchronization
KAPA SYBR® Fast qPCR Kit	www.peqlab.de	real time PCR
laminin-111	www.invitrogen.com	20 µg/ml in PBS, surface coating
L-glutaminie	www.invitrogen.com	2 mM, cell culture medium supplement
isopropanol/2-propanol	www.carlroth.de	washing
MEM alpha medium	www.paa.com	cell culture
minimum essential medium (MEM)	www.invitrogen.com	cell culture
Nanofectin Kit	www.paa.com	cell transfection
octadecylmercaptan (ODM)	www.sigmaaldrich.com	1.5 mM in EtOH, µCP
oligonucleotides	www.eurofinsdna.com	PCR
paraformaldehyd/PFA	www.sigmaaldrich.com	4% (m/v) in PBS, fixation
penicillin-streptomycin	www.invitrogen.com	cell culture
silicone elastomer kit/PDMS	www.dowcorning.com	µCP stamps
potassium chloride	www.sigmaaldrich.com	200 mM in glycine buffer, collagen buffer



Reagents and Kits	Company	Applications
potassium hexacyanoferrate(II) trihydrate ( $K_4[Fe(CN)_6] \cdot 3H_2O$ )	www.sigmaaldrich.com	0.76 mM, gold etching
potassium hexacyanoferrate(III) ( $K_3[Fe(CN)_6]$ )	www.sigmaaldrich.com	10 mM, gold etching
potassium thiosulfate ( $K_2S_2O_3$ )	www.sigmaaldrich.com	0.2 M, gold etching
potassium hydroxide (KOH)	www.sigmaaldrich.com	0.9 M, gold etching
proteinase inhibitor cocktail	www.roche.de	0.1 tablet/ml
purified bovine collagen solution	www.advancedbiomatrix.com	25 or 50 $\mu$ g/ml in PBS, surface coating
PVDF membrane (Immobilon)	www.millipore.com	Western blot
RNeasy kit	www.qiagen.com	RNA extraction
sulfuric acid ( $H_2SO_4$ )	www.carlroth.de	piranha solution ( $H_2SO_4:H_2O_2=3:1$ )
SuperSkript III RT	www.invitrogen.com	cDNA synthesis
The Precision Plus Protein™ Kaleidoscope™ standards	www.bio-rad.com	SDS-PAGE
thymidine	www.sigmaaldrich.com	5 mM, cell cycle synchronization
Triton X-100	www.carlroth.de	0.2% (v/v) in PBS, permeabilizing
trypsin/EDTA	www.invitrogen.com	cell detachment
trypsin inhibitor	www.sigmaaldrich.com	inhibits trypsin after cell passaging
Western Lightning Plus-ECL substrate	www.perkinelmer.com	develop western blots
YIGSR	www.sigmaaldrich.com	100 $\mu$ g/ml, adhesion blocking
Zeocin	www.invitrogen.com	150 $\mu$ g/mL, cell culture

Table 2.1: Reagents and Kits.

## 2.1.2 Antibodies and labeling reagents list

Primary antibodies and isotype control	Company	React with	Applications	Dilution/Conc.
mouse monoclonal anti- $\beta$ - <i>tubulin</i> , clone TUB 2.1	www.sigmaaldrich.com	human	WB	1:8000
mouse monoclonal anti- <i>collagen, type I</i> , clone COL-1	www.sigmaaldrich.com	bovine	IF	1:100
mouse monoclonal anti- <i>Hsp90</i> , clone AC88	www.abcam.com	human	WB	1:1000
mouse monoclonal anti <i>integrin <math>\alpha</math>1</i> I domain, clone FB12	www.millipore.com	human	WB	1:500
mouse monoclonal anti- <i>CD49b (integrin <math>\alpha</math>2)</i> , clone 2/CD49b	www.bdbiosciences.com	human	WB	1:1000
rabbit polyclonal anti- $\alpha$ 6	www.abcam.com (article number: ab75737)	human	WB and FC	5 $\mu$ g/ml
rat monoclonal anti- <i>CD49f (integrin <math>\alpha</math>6)</i> , clone GoH3	www.bdbiosciences.com	human, hamster	adhesion blocking, IF	5 $\mu$ g/ml
mouse monoclonal Anti- <i>ITGA7</i> , clone 8G2	www.sigmaaldrich.com	human	WB	1:250
mouse monoclonal anti- <i>CD29 (integrin <math>\beta</math>1)</i> , clone 18/CD29	www.bdbiosciences.com	human	WB	1:2000
mouse monoclonal anti- <i>integrin <math>\beta</math>1</i> , clone 6S6	www.millipore.com	human	adhesion blocking	10 $\mu$ g/ml
mouse monoclonal anti- <i>Integrin <math>\beta</math>4</i> , clone M126	www.abcam.com	human	WB	1:1000
mouse monoclonal anti- <i>integrin <math>\beta</math>4</i> , clone ASC-8	www.millipore.com	human	adhesion blocking	10 $\mu$ g/ml
rabbit polyclonal anti- <i>laminin</i>	www.sigmaaldrich.com	mouse	IF	1:100
mouse monoclonal anti- <i>paxillin</i> , clone 349/paxillin	www.bdbiosciences.com	human, hamster	IF	1:500
mouse monoclonal anti- <i>vinculin</i> , clone hVIN-1	www.sigmaaldrich.com	human, hamster	IF	1:50
purified rabbit IgG	www.invitrogen.com	-	FC	25 $\mu$ g/ml
purified rat IgG2a, $\kappa$ isotype control	www.bdbiosciences.com	-	control for adhesion blocking	5 $\mu$ g/ml

Table 2.2 Primary antibodies and isotype control.

WB=Western blot; IF=immunofluorescence; FC=flow cytometry.

Secondary antibodies and staining reagents	Company	Dilution/Conc.
<b>Alexa Fluor® 488 phalloidin</b>	www.invitrogen.com	1:200
goat anti- <b>human</b> IgG (H+L)- <b>Alexa Fluor® 594</b>	www.invitrogen.com	2 µg/ml
goat anti- <b>mouse</b> IgG (H+L)- <b>Alexa Fluor® 488</b>	www.invitrogen.com	1:200
goat anti- <b>mouse</b> IgG (H+L)- <b>AMCA</b>	www.dianova.com	1:200
donkey anti- <b>mouse</b> IgG (H+L)- <b>Cy3</b>	www.dianova.com	1:500
Sheep anti- <b>mouse</b> IgG (H+L)- <b>HRP</b>	www.abcam.com	1:1000
goat anti- <b>rabbit</b> IgG (H+L)- <b>Alexa Fluor® 488</b>	www.invitrogen.com	1:200
goat anti- <b>rabbit</b> IgG (H+L)- <b>AMCA</b>	www.dianova.com	1:200
goat anti- <b>rabbit</b> IgG (H+L)- <b>Cy3</b>	www.dianova.com	1:500
donkey anti- <b>rabbit</b> IgG (H+L)- <b>HRP</b>	www.gelifesciences.com	1:1000

**Table 2.3 Secondary antibodies and staining reagents.**

### 2.1.3 Buffers and solutions

5x SDS-PAGE loading buffer	250mM Tris-HCl pH 6.8, 50% (v/v) glycerol, 5% (m/v) SDS, 0.2% (m/v) bromophenol blue, 5% (v/v) 2-mercaptoethanol
cell lysis buffer	1% (v/v) triton x-100, 150 mM NaCl, 10 mM Tris buffer (pH 7.5), 1mM EDTA (pH 8.0) and 0.1 tablet/ml proteinase inhibitor cocktail
etching solution	0.76 mM $K_4[Fe(CN)_6] \cdot 3H_2O$ , 10 mM $K_3[Fe(CN)_6]$ , 0.2 M $K_2S_2O_3$ and 0.9 M KOH
PBS	137 mM NaCl, 3 mM KCl, 8 mM $Na_2HPO_4$ , 2 mM $K_2HPO_4$
running buffer	25 mM Tris-HCl (pH 8.8), 192 mM glycine, 0.1% SDS
TBST	120 mM Tris-HCl, pH 7.4, 150 mM NaCl, and 0.05% Tween-20
transfer buffer	20% (v/v) methanol, 1.44% (w/v) glycine, 0.3025% (w/v) Tris
stripping buffer	1.5% (w/v) glycine, 0.1% (w/v) SDS, 1% (v/v) Tween 20, adjust to pH 2.2

**Table 2.4 Buffers and solutions.**

### 2.1.4 Software

BLAST	www.ncbi.nlm.nih.gov/BLAST
Igor Pro	www.wavemetrics.com
InStat	www.graphpad.com/instat/
JPK-IP software	www.jpk.com
NetPrimer	www.premierbiosoft.com/netprimer/index.html
OriginPro 8.1G	www.originlab.de
REST	www.qiagen.com

**Table 2.5 Software.**

### 2.1.5 Apparatus

Apparatus	Company	Applications
AxioObserver inverted microscope	www.zeiss.com	optical imaging
BioCell	www.jpk.com	SCFS
CellHesion module	www.jpk.com	SCFS
EM CPD030	www.leica.com	critical point drying
Laser scanning microscope, LSM 510	www.zeiss.com	optical imaging
Nanodrop	www.nanodrop.com	RNA concentration measurement
NanoWizard II AFM	www.jpk.com	SCFS and scanning
Petridish heater	www.jpk.com	control temperature during SCFS
RotorGene 6000	www.qiagen.com	real time PCR
Scanning electron microscope, SUPRA25	www.zeiss.com	imaging
Tipless v-shaped cantilever, NP-O	www.veeco.com	SCFS
V-shaped Si <sub>3</sub> N <sub>4</sub> cantilever, MLCT	www.veeco.com	AFM scanning

**Table 2.6**     **Apparatus.**

## 2.2 Methods

### 2.2.1 Cell adhesion substrate preparation

#### 2.2.1.1 Protein/PEG bifunctional substrates

Si wafers carrying groove/ridge structures were designed according to experiment requirements and fabricated by Dr. Mario Hauser (Karlsruher Institut für Technologie) using standard photolithography. PDMS stamps with complementary patterns were cast from Si wafers using a thin stamp technique as described previously (James et al., 1998; Geissler et al., 2000). Stamps were inked with 1.5 mM octadecylmercaptan (ODM) in ethanol and pressed onto gold-coated glass coverslips. As a result, ODM was transferred from the protruding parts of the stamps to the gold surface, forming a micropatterned, self-assembled monolayer (**Fig. 2.1 A**). By immersing the coverslips in 10 ml aqueous solution containing 0.76 mM potassium hexacyanoferrate(II) trihydrate ( $K_4[Fe(CN)_6] \cdot 3H_2O$ ), 10 mM potassium hexacyanoferrate(III) ( $K_3[Fe(CN)_6]$ ), 0.2 M potassium thiosulfate ( $K_2S_2O_3$ ) and 0.9 M potassium hydroxide (KOH), the ODM unprotected gold layer was etched away (Kumar and Whitesides, 1993) (**Fig. 2.1 B**). After treatment with piranha solution (a 3:1 mixture of concentrated sulfuric acid ( $H_2SO_4$ ) with hydrogen peroxide ( $H_2O_2$ )) for 30 min, the substrate was covered with (3-glycidyloxypropyl)trimethoxysilane for 1 h in a nitrogen atmosphere. After addition of amino-PEG2000, the silanized substrate was baked at 85°C for 60 h (**Fig. 2.1 C**). Afterwards, the substrate was intensively rinsed with water and incubated with 20 µg/ml natural mouse laminin (laminin-111) or 10 µg/ml BSA in PBS at 4°C for 1 h. As a result, the gold micropatterns were covered by laminin or BSA and the remaining transparent areas were passivated with PEG2000 (**Fig. 2.1 D**).

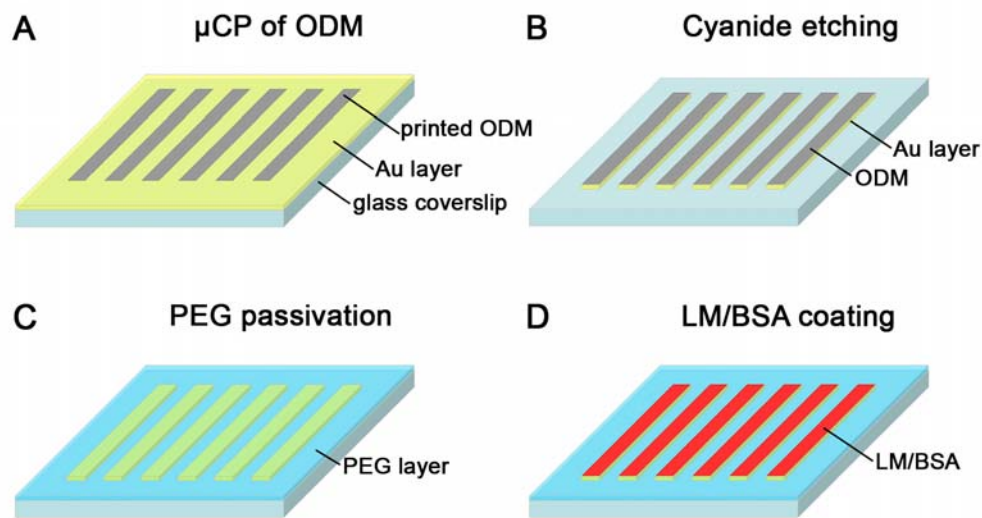


**Fig. 2.1 Fabrication of bifunctional protein/PEG substrates.**

(A) Transferring ODM stripes onto a gold-sputtered coverslip by microcontact printing. (B) Removing ODM-unprotected areas of the gold layer by cyanide etching. (C) Passivation of the exposed glass surface of with PEG-2000. (D) Laminin or BSA adsorbs specifically to the gold stripes, while PEG2000-covered areas remain passivated.

### 2.2.1.2 Laminin/fibrillar collagen I bifunctional substrates

Laminin stripes were produced by a modification of the lift-off method (von Philipsborn et al., 2006a). Briefly, PDMS cuboids with a top surface area of  $\sim 1 \text{ cm}^2$  were covered with 250  $\mu\text{l}$  of a solution containing 20  $\mu\text{g/ml}$  laminin-111 and 2  $\mu\text{g/ml}$  Alexa594-conjugated goat anti-human IgG as a fluorescent marker. After incubation in a humidified chamber at 37°C for 1h, the PDMS cuboid was rinsed twice with distilled water and briefly dried under nitrogen flow. The cuboid was then pressed shortly onto a structured Si wafer (**Fig. 2.2 A**) and transferred onto a freshly cleaved mica disc ( $\text{\O}8 \text{ mm}$ ) glued onto a 24 mm round glass coverslip (**Fig. 2.2 B**). The remaining protein-free areas on the mica surface were backfilled with collagen by adding a solution containing 50  $\mu\text{g/ml}$  collagen type I in 50 mM glycine, pH 9.2 and 200 mM KCl (**Fig. 2.2 C**). After incubation in a humidified chamber at room temperature for 4 h, the substrates were rinsed with PBS, if required immunofluorescence-stained for collagen type I and inspected under a fluorescent microscope.

### **2.2.1.3 Monomeric/fibrillar collagen I bifunctional substrates**

Monomeric collagen stripes were produced by a modification of the lift-off method (von Philipsborn et al., 2006a). PDMS cuboids with a top surface area of  $\sim 1 \text{ cm}^2$  were covered with 250  $\mu\text{l}$  of acetic acid (pH=3) containing 25  $\mu\text{g/ml}$  collagen type I and 25  $\mu\text{g/ml}$  FITC-conjugated collagen type I. After incubation in a humidified chamber at 4°C for 1 h, the PDMS cuboid was rinsed twice with distilled water and briefly dried under nitrogen flow. The cuboid was then pressed onto a structured Si wafer, left on the wafer for 1 min (**Fig. 2.2 A**) and transferred onto a freshly cleaved mica disc ( $\text{\O}8 \text{ mm}$ ) glued onto a round glass coverslip ( $\text{\O}24 \text{ mm}$ ) and left in contact with mica for 1 min (**Fig. 2.2 B**). The remaining protein-free areas on the mica surface were backfilled with collagen by adding a solution containing 50  $\mu\text{g/ml}$  collagen type I in 50 mM glycine, pH 9.2 and 200 mM KCl (**Fig. 2.2 C**). After incubation in a humidified chamber at room temperature for 30 min, the substrates were rinsed with PBS.

### **2.2.1.4 Preparation of collagen IV/fibrillar collagen I bifunctional substrates**

Collagen IV stripes were produced by a modification of the lift-off method (von Philipsborn et al., 2006a). PDMS cuboids with a top surface area of about  $1 \text{ cm}^2$  were covered with 250  $\mu\text{l}$  of 0.25% (v/v) acetic acid containing 100  $\mu\text{g/ml}$  collagen type IV. After incubation in a humidified chamber at room temperature for 1h, the PDMS cuboid was rinsed twice with distilled water and briefly dried under nitrogen flow. The cuboid was then pressed shortly onto a structured Si wafer (**Fig. 2.2 A**) and transferred onto a freshly cleaved mica disc ( $\text{\O}8 \text{ mm}$ ) glued onto a 24 mm round glass coverslip (**Fig. 2.2 B**). The remaining protein-free areas on the mica surface were backfilled with collagen by adding a solution containing 25  $\mu\text{g/ml}$  collagen type I and 25  $\mu\text{g/ml}$  FITC conjugated collagen type I in 50 mM glycine, pH 9.2 and 200 mM KCl (**Fig. 2.2 C**). After incubation in a humidified chamber at room temperature for 30 min, the substrates were rinsed with PBS.

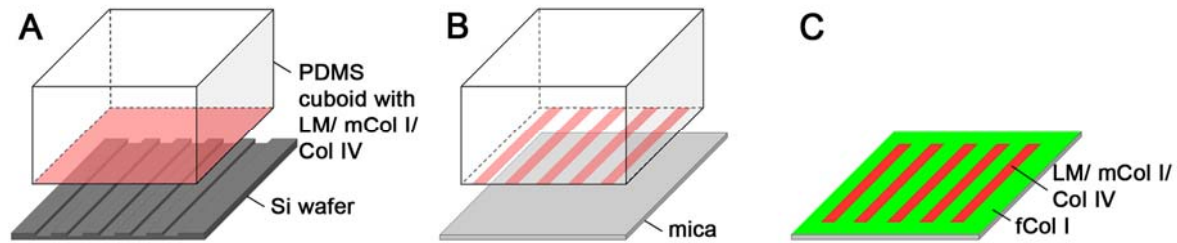


**Fig. 2.2 Fabrication of bifunctional ECM protein substrates.**

(A) A PDMS cuboid coated with LM, mCol I or Col IV is pressed onto a structured Si wafer. The ECM protein adsorbs to ridge structures on the wafer. (B) When the PDMS cuboid is subsequently pressed onto a freshly cleaved mica disc, ECM protein stripes are transferred to the mica surface. (C) After adding collagen solution to the mica, the remaining surface is covered by fCol I.

### 2.2.2 Cell culture

CHO cells and CHO cells stably transfected with human integrin  $\alpha 1$  (CHO-A1) and  $\alpha 2$  (CHO-A2) subunits together with human osteosarcoma SAOS cells and SAOS cells stably transfected with human  $\alpha 2$  (SAOS-A2) subunit are kindly provided by Professor Jyrki Heino (University of Turku, Finland). CHO cells were cultured in  $\alpha$ -MEM containing 10% fetal bovine serum, 100 IU/ml penicillin, and 100  $\mu$ g/ml streptomycin at 37°C and with 5% CO<sub>2</sub>. CHO-A2 cells were cultured with additional 0.4 mg/ml geneticine to maintain the stable expression of integrin  $\alpha 2$ . CHO-A1 cells were cultured in  $\alpha$ -MEM containing 5% fetal bovine serum, 2 mM L-glutamine, 100 IU/ml penicillin, 100  $\mu$ g/ml streptomycin with an additional 150  $\mu$ g/ml Zeocin to maintain the stable expression of integrin  $\alpha 1$ . SAOS-WT cells were cultured in DMEM containing 10% fetal bovine serum, 100 IU/ml penicillin, and 100  $\mu$ g/ml streptomycin at 37°C and with 5% CO<sub>2</sub>. SAOS-A2 cells were cultured with 0.25 mg/ml geneticine to maintain the stable expression of integrin  $\alpha 2$ . All cells were passaged every 2-3 days or before reaching confluency. For cell adhesion assays, cells were washed with PBS (Ca<sup>2+</sup>- and Mg<sup>2+</sup>-free) and removed from the tissue culture flask with Hank's buffered salt solution containing 0.05% trypsin and 0.53 mM EDTA. Dissociated cells were centrifuged, resuspended in serum-free  $\alpha$ -MEM, seeded on the patterned substrates and cultured. For SCFS experiments, cells were transferred to CO<sub>2</sub>-independent medium supplemented with 4 mM L-glutamine, 100 IU/ml penicillin, and 100  $\mu$ g/ml streptomycin for 1h and trypsinized briefly. Trypsin was subsequently inactivated by adding soybean trypsin inhibitor. After centrifugation at 100x *g* for 5



min, the supernatant was removed and cells were resuspended in CO<sub>2</sub>-independent medium. For integrin-blocking experiment, cells were pre-incubated with the blocking antibody or peptide at 37°C for 30 min in suspension prior to SCFS. The measurements were then performed in the presence of the blocking antibody or peptide (concentration indicated in materials part) in the heated sample holder. CHO-WT cells were transiently transfected with human integrin  $\alpha$ 2 subunits using the Nanofectin Kit. The cell lysate of transfected cells was collected 24 hours after transfection.

### **2.2.3 Cell cycle synchronization**

CHO cells were synchronized using a double thymidine block, followed by mitotic shake-off and a hydroxyurea block (Cao et al., 1991). Cells at about 30% confluency were incubated with thymidine (5 mM) and incubated for 9 h and afterwards released from the thymidine block by culture in normal growth medium for 5.5 h. Subsequently, cells were cultured again in 5 mM thymidine for 9 h. Six hours after thymidine release, mitotic cells were selectively detached from the CHO cell monolayer by gentle agitation (shake-off) and collected from the decanted medium. The shake-off procedure was repeated 4 times in 20 min time intervals. The dislodged mitotic cells were pooled and kept at 4°C during collection. After centrifugation, mitotic CHO cells were cultured in growth medium containing 2 mM hydroxyurea for 9 h. As assessed by phase contrast time-lapse microscopy, a burst of mitosis occurred after 8-13 h and SCFS was performed after 15-19 h.

### **2.2.4 Immunostaining**

Cells were fixed for 30 min with 4% paraformaldehyde, permeabilized with PBS containing 0.2% Triton X-100 for 5 min and incubated with primary antibodies for 1 h at room temperature. After 5 washes with PBS, probes were incubated with the corresponding secondary antibodies for 1 h at room temperature. Actin filaments were labeled with Alexa488-coupled phalloidin. Slides were mounted in fluorescent mounting medium and analyzed with a confocal laser scanning microscope LSM 510.

## **2.2.5 Microscopy techniques**

### **2.2.5.1 AFM imaging**

All AFM experiments were performed using a NanoWizard II AFM mounted on top of an AxioObserver A1 inverted light microscope. AFM contact mode images were obtained in PBS at room temperature using V-shaped Si<sub>3</sub>N<sub>4</sub> cantilevers (MLCT) with a nominal spring constant of 0.01 N/m and a line scan rate of 0.8 Hz.

### **2.2.5.2 AFM based single-cell force spectroscopy**

SCFS experiments were performed with a NanoWizard II AFM featuring a CellHesion module with an extended vertical range of 100 µm. All measurements were performed at 37°C using a temperature-controlled sample chamber (BioCell) and tipless 205 µm long V-shaped cantilevers (NP-O, type D) with a nominal spring constant of 0.06 N/m. To facilitate cell capture, plasma-cleaned cantilevers were functionalized with concanavalin A (Puech et al., 2005). After determining the sensitivity of the optical lever system and the spring constant of the cantilever by the thermal noise method (Hutter and Bechhoefer, 1993), cells were pipetted into the sample chamber. A single cell was captured by pressing the functionalized cantilever onto the cell with a contact force of 500 pN for 3 s and elevating the cantilever subsequently. To measure cell detachment forces, the cantilever was lowered at a constant speed of 5 µm/s (unless stated otherwise) until the cell made contact with the substrate and a preset force of 1.5 nN was reached. Afterwards, the cantilever was held at a constant height for the preset contact time. Finally the cantilever was elevated about 80 µm above the substrate surface to separate cell and surface. In some experiments cell-substrate contact positions were preprogrammed in the JPK software before starting force cycles. Detachment forces were analyzed using the JPK-IP software and custom-programmed macros in Igor Pro.

### **2.2.5.3 Scanning electron microscopy (SEM)**

To analyze monomeric/fibrillar collagen substrates by SEM, substrates were fixed overnight in PBS containing 4% paraformaldehyde and 1% glutaraldehyde. Following extensive washing in PBS and distilled water, samples were dehydrated in ethanol series (20%, 30%, 50%, 70%, 90%, 95%, 100% two times each for 5 min), transferred into acetone and critical point dried (Leica EM CPD030). Dried samples were sputtered with platinum and analyzed with a scanning electron microscope

(SUPRA 25; Zeiss). SEM images were taken by Dr. Anna Müller (Karlsruher Institut für Technologie).

### 2.2.6 Flow cytometry

Flow cytometry was performed by Dr. Irina Nazarenko (Universitätsklinikum Freiburg). CHO cells plated 48 hours prior to flow cytometry measurements were harvested, counted and distributed into 96-well plate at  $3 \times 10^5$  cells/well. Cells were washed three times with 1% BSA/PBS by centrifugation at  $1000 \times g$  for 5 min at  $4^\circ\text{C}$ . Cells were incubated with primary antibody (rabbit anti  $\alpha 6$ -Integrin (ab75737), www.abcam.com) or a corresponding isotype control (purified rabbit IgG, www.invitrogen.com) in 1% BSA/PBS at a final concentration of 5 or 25  $\mu\text{g/ml}$ , respectively, at  $4^\circ\text{C}$  for 30 min. Cells were washed 3 times with cold 1% BSA/PBS as described above and incubated with the secondary antibody (anti-rabbit-PE, www.sigma-aldrich.com) at a concentration of 6  $\mu\text{g/ml}$  in 1% BSA/PBS at  $4^\circ\text{C}$  in the dark for 30 min. Subsequently, cells were washed 3 times with cold 1% BSA/PBS, resuspended in 150  $\mu\text{l}$  1% BSA/PBS and analyzed in a flow cytometer.

### 2.2.7 Statistical analysis

From the collected force-distance curves, the maximum detachment forces (maximum cantilever deflection) were determined and plotted as median $\pm$ MAD (median absolute deviation,  $\text{MAD} = \text{median}_i(|X_i - \text{median}_j(X_j)|)$ ) using OriginPro 8.1G. Statistical significance of experiments was tested with a Wilcoxon-based Mann-Whitney U-test using InStat. The accumulative standard deviation ( $SD$ ) was defined as the  $SD$  of the first  $i$  detachment forces ( $2 \leq i \leq 33$ ) on either collagen ( $SD_{icol}$ ) or laminin ( $SD_{iLM}$ ) substrates during alternating force measurements. The relative  $SD$  was defined as the difference between the accumulative  $SD$  for a given force cycle number and an  $SD_{imax}$  value incorporating the maximum number of force cycles.

### 2.2.8 Thermal noise of the cantilever

Disregarding electronic noise introduced by the AFM control system, the ultimate force resolution of the AFM cantilever is limited by its thermal noise. The minimal detectable force  $F_{min}$  can be expressed as follows:

$$F_{min} = \sqrt{\frac{4kk_BTB}{2\pi f_0 Q}}$$

in which  $k$  is the spring constant of the cantilever,  $k_B$  is the Boltzmann constant,  $T$  is the absolute temperature,  $B$  is the bandwidth of the measurement,  $f_0$  is the resonance frequency of the cantilever, and  $Q$  is the quality factor (Yasumura et al., 2000). Given a measured cantilever spring constant of about 0.12 N/m, a band width (sampling rate) of 10 kHz, a resonance frequency of 4.8 kHz and a quality factor of 1.7, the calculated  $F_{min}$  is about 20 pN.

## 2.2.9 Reverse transcription real time PCR

### 2.2.9.1 Primer design

Primers were targeted against integrin alpha6 (ITG $\alpha$ 6), alpha7 (ITG $\alpha$ 7), beta1 (ITG $\beta$ 1), beta4 (ITG $\beta$ 4) and beta-2-microglobulin (b2MG). The primers specifically target human sequences and were selected based on the following requirements: (i) high percentage of mismatch in the 3' region with at least 1 nucleotide mismatch at the 3' end, (ii) a primer melting temperature of approximately 60°C, (iii) a GC content of approximately 55%, (iv) preferably no G at the 5' end, (v) avoiding runs of more than three identical nucleotides, (vi) an amplicon length of approximately 150 nucleotides. Specificity and cross-reactivity were checked with the Basic Local Alignment Search Tool (BLAST), and the specific melting point of the amplicons was analyzed using NetPrimer. All primers were synthesized by Eurofins MWG Operon.

Target	Forward primer (5' - 3')	Reverse primer (5' - 3')
ITG $\alpha$ 6	TTGAATATACTGCTAACCCC	TCGAAACTGAACTCTTGAGGATAG
ITG $\alpha$ 7	TGTTTCAGCTACATTGCAGTCC	GCCTGGTGCTTGGGTTCT
ITG $\beta$ 1	CAAAGGAACAGCAGAGAAGC	ATTGAGTAAGACAGGTCCATAAGG
ITG $\beta$ 4	GGGTCCAGGAAGATCCATTT	AGTCGCAATACGGGTACAGG
b2MG	TCCATCCGACATTGAAGTTG	CGGCAGGCATACTCATCTT

**Table 2.7 Primers targeting human integrins.**

ITG=integrin, b2MG=beta-2-microglobulin.

### 2.2.9.2 Total RNA isolation and cDNA synthesis

Three hundred thousand SAOS-WT or A2 Cells were seeded in 6-well plates and incubated for 24 hours at 37°C and 5% CO<sub>2</sub>. mRNA isolation was performed from 5×10<sup>5</sup> cells using the RNeasy kit. Total RNA concentration was measured in a Nanodrop analyzer, and 1.5 µg RNA were used for cDNA synthesis. RNA was stored

at -80°C. cDNA was synthesized from 1.5 µg total RNA with SuperScript III RT for 5 min at 25°C, 60 min at 50°C, 15 min at 75°C in a thermocycler.

### **2.2.9.3 Real-time qPCR**

Real-time qPCR was performed in a RotorGene 6000 using the KAPA SYBR® Fast qPCR Kit. The PCR profile was as follows: 10 min at 95°C, followed by 40 cycles of 10 s at 95°C, 15 s at 60°C and 20 s at 72°C. Subsequently, a melting curve analysis was performed to ensure the purity of the product. The concentration of primers was 200-500 nM. The b2MG gene was used as control and the data was analyzed by the REST software. After normalization against b2MG expression, the transcriptional activity of each gene was calculated in relative amount, such as SAOS-A2 versus SAOS-WT, and then presented in the relative fold change (log base 2).

## **2.2.10 Protein preparation and analysis**

### **2.2.10.1 Cell lysates preparation**

Cells were cultured in Ø10 cm petridishes until 90% confluent. After washing once with ice cold PBS, 1 ml of cell lysis buffer was added, and the cells were incubated on ice for 5 min. The cells were then detached using a cell scraper, transferred to an micro-centrifuge tube and centrifuged at 13,000× *g* at 4°C for 10 min. The supernatant was collected and used for further analysis. Cell surface protein was extracted using the Pierce cell surface protein isolation kit according to the manufacturer's instruction.

### **2.2.10.2 SDS-PAGE**

Total protein concentration was determined with the Bio-Rad protein assay. Equal amounts of protein were mixed with SDS-PAGE loading buffer and denatured at 95°C for 5 min. Samples were then loaded along with a molecular weight marker (Precision Plus Protein™ Kaleidoscope™ standards) into the wells of 7.5% Mini-PROTEAN® TGX™ precast polyacrylamide gels. Gels were run at 120 V in an electrophoresis container filled with running buffer.

### **2.2.10.3 Western blot**

PVDF membranes (Immobilon-P) were immersed in methanol for 1 min. After equilibration in transfer buffer, gels and PVDF membranes were sandwiched between two pieces of Whatman gel blotting paper and two sponges. Proteins were

transferred at 100 V for 1 h. Then membranes were blocked with 5% milk in TBST for 1 h at room temperature, incubated with the respective antibodies and then probed with an HRP-conjugated secondary antibody. Blots were developed using Western Lightning Plus-ECL substrate.  $\beta$ -tubulin or heat shock protein HSP90 served as a loading control. The expression of each integrin subunit was calculated as relative amounts, such as SAOS-A2 versus SAOS-WT and then presented as the relative fold expression change (log base 2), after normalization against  $\beta$ -tubulin or HSP90 expression. In order to reprobe the proteins, PVDF membranes were incubated in stripping buffer for 1 h at room temperature. After washing with PBS and TBST, PVDF membranes were reblocked in 5% milk in TBST before proceeding to the antibody incubation.

### **3 Comparative Single-Cell Force Spectroscopy on Different Bifunctional Substrates**

---

#### **3.1 Abstract**

In tissues, cells are exposed to a complex mixture of ECM molecules with which they interact in a spatially and temporally controlled manner. While the sum of the cellular interactions to all ECM molecules determines overall cell adhesion strength, the individual receptor-mediated cell-ECM interactions regulate different aspects of cell behavior. However, so far the influence of differential adhesion to different ECM components is only poorly understood on the single-cell level, partially because suitable measurement techniques are missing. To directly compare single-cell adhesion to different ECM components, a comparative SCFS setup was developed utilizing bifunctional substrates fabricated by different  $\mu$ CP methods. As proof of concept, substrates consisting of alternating laminin-111 and collagen I stripes were produced. Single living CHO cells immobilized on an AFM cantilever were then alternately pressed on either protein and detachment forces were measured. When using 10 s contact time, all tested cells showed higher adhesion to laminin than collagen I, even when the measurement was conducted continuously for over 60 cycles. Cells displayed no adhesion fatigue or reinforcement indicating that later measurements were not influenced by preceding ones. To further demonstrate adhesion specificity, two substrates featuring both adhesive and non-adhesive areas were produced. When tested on BSA/PEG surfaces, CHO cells showed minimized adhesion on PEG but high forces on BSA, suggesting that BSA is not a suitable passivation material for SCFS. Finally, to directly compare the affinity of integrin  $\alpha_1\beta_1$  and  $\alpha_2\beta_1$  to different collagen subtypes, adhesion of CHO cells stably expressing integrin  $\alpha_1\beta_1$  (CHO-A1) and  $\alpha_2\beta_1$  (CHO-A2) was tested on monomeric/fibrillar collagen I and collagen IV/fibrillar collagen I substrates by SCFS. The results showed that integrin  $\alpha_1\beta_1$  has high affinity to all collagen subtypes, while integrin  $\alpha_2\beta_1$  only preferentially binds fibrillar collagen I. SCFS performed on bifunctional adhesion substrates therefore offers a sensitive technique to measure differential adhesion of single cells and allows for directly comparing receptor affinities in the same cell.

### **3.2 Introduction**

The ECM, a 3D structure composed of different molecules, serves as a microenvironment for the cells live inside. While the sum of the cell-ECM interactions determines the overall strength of cell-matrix adhesion, cell interaction with individual ECM components using specific integrin receptors is crucial for many biological processes such as cell differentiation during early embryo development (Darribere et al., 2000; Ma et al., 2008a), overall adhesion receptor expression during wound healing (Gingras et al., 2003; Gaudreault et al., 2007) and cell invasion during cancer progression (Jinka et al., 2012). A better understanding of how the complex ECM environment regulates the behavior of embedded cell requires more knowledge of the relative contribution of individual ECM components to adhesion of a cell. For instance, to obtain directly comparable adhesion information, special techniques should be developed to analyze single cell adhesion to two or several ECM components in the same experimental setup.

Over the last years AFM-based SCFS has been developed to quantify single cell adhesion to surfaces homogeneously coated with single ECM component with a versatile force range (about 10 pN to 100 nN) (Helenius et al., 2008; Muller et al., 2009b). In addition, the precise positioning system of the AFM allows excellent control over the contact conditions, such as interaction force, time and position. At the same time, advances in  $\mu$ CP have made it possible to print multiple ECM proteins on the same substrate (Desai et al., 2011). By performing AFM-based SCFS on heterofunctional adhesion substrates, it should therefore be possible to test single-cell adhesion to at least two different ECM components directly, but this approach has so far not been implemented.

In this work, several modified  $\mu$ CP protocols are used to fabricate different bifunctional substrates either featuring a single ECM protein and PEG or two different ECM proteins. These structurally defined surfaces are suitable for sensitive and quantitative adhesion force measurements using SCFS. Importantly, because of the proximity of two different coatings, a single cell can be alternately brought into contact with either surface and the adhesion strength to both surfaces can be directly compared. The high cell adhesion blocking efficiency of PEG could be verified, while BSA is no suitable working as passivation material for AFM-based SCFS. For



relatively short contact times (10 s), individual CHO cells retained specific adhesion to each ECM component for over 60 force cycles without being influenced by the preceding measurements. Measuring the same cell repeatedly for 20-25 times is therefore sufficient to obtain solid force measurement statistics in this system. Furthermore, to demonstrate the usefulness of bifunctional substrates to investigate differential adhesion processes,  $\alpha_1\beta_1$  and  $\alpha_2\beta_1$ -mediated adhesion of single CHO cells to monomeric and fibrillar collagen I and to collagen IV and fibrillar collagen I were compared. Similar to the results obtained by  $\alpha$  I domain solid phase binding assay and cell spreading assay (Tulla et al., 2001; Jokinen et al., 2004), integrin  $\alpha_1\beta_1$  binds with high affinity to both monomeric and fibrillar collagen I, while integrin  $\alpha_2\beta_1$  preferentially binds fibrillar collagen I. In addition, integrin  $\alpha_1\beta_1$  binds better to collagen IV than integrin  $\alpha_2\beta_1$ . These experiments established the binding preferences of integrin  $\alpha_1\beta_1$  and  $\alpha_2\beta_1$  to different collagen subtypes.

### **3.3 Results**

#### **3.3.1 Experimental setup for quantifying differential cell adhesion to ECM components by comparative single-cell force spectroscopy**

Differential cell adhesion to different ECM components plays a significant role in regulating different sub-aspects of cell behavior, including proliferation, differentiation and migration (Meighan and Schwarzbauer, 2008). To compare the affinity of a particular cell type to two different ECM molecules by conventional AFM-based SCFS on homogeneously-coated substrate, a number of cells have to be tested in separate, subsequent measurements on both surfaces (**Fig. 3.1 A**). Consequently, only population-averaged detachment forces are obtained. These measurements emphasize adhesion properties averaged over the whole cell population while it provides no information about the relative scale of adhesion of an individual cell to both substrates.

To perform directly-comparative single-cell adhesion measurements requires bifunctional adhesion substrates displaying both adhesive coating next to each other so that a single cell can be tested on both substrates in a single experiment. The bifunctional substrates have to meet several requirements. First, both substrates should be in close proximity (less than 100  $\mu\text{m}$ ) so that they can be alternately reached by the xy-positioning system of the AFM (100  $\mu\text{m}$   $\times$  100  $\mu\text{m}$ ). Substrates featuring alternating stripe patterns of both substrates are particularly suitable. Given a typical cell diameter of 10 to 20  $\mu\text{m}$ , a stripe width of 50  $\mu\text{m}$  allows for definite cell positioning on either stripe type and places at least two adjacent stripes within the cantilever positioning range of the AFM (**Fig. 3.1 B**). Secondly, both substrates must be distinguishable by light microscopy so that the cell can be positioned with confidence above either substrate.

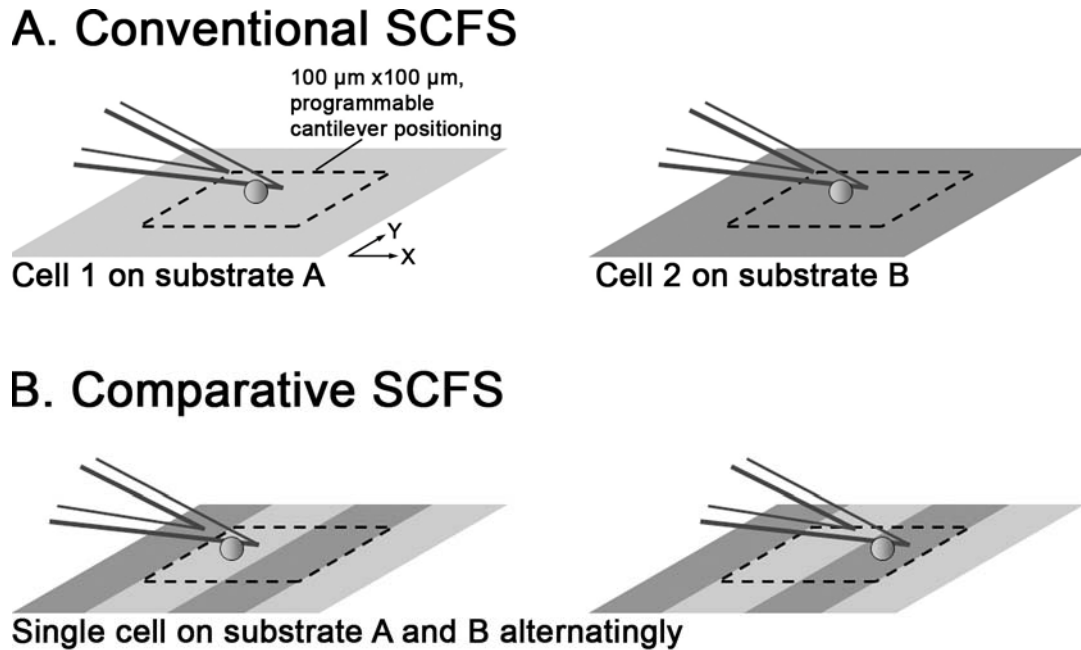


**Fig. 3.1 Comparison between conventional SCFS and comparative SCFS.**

(A) To compare cell adhesion of specific cell type to two different substrates by conventional SCFS, several cells have to be measured on each substrate subsequently. (B) By using bifunctional substrates, single-cell adhesion on different substrates can be compared directly. Multiple contact positions can be pre-programmed within a 100  $\mu\text{m}$   $\times$  100  $\mu\text{m}$  area (indicated by the dashed square).

### 3.3.2 Producing protein/PEG bifunctional substrates

Laminin is a ECM proteins facilitating integrin-mediated CHO cell adhesion (Danilov and Juliano, 1989). PEG forms brush-like monolayer preventing protein adsorption and therefore widely used as cell adhesion passivation material (Prime and Whitesides, 1993). As a model system incorporating both adhesive and non-adhesive areas on the same substrate, bifunctional substrates featuring alternating laminin (adhesive) and PEG (non-adhesive) stripes were fabricated by  $\mu\text{CP}$  (Fig. 2.1, and section 2.2.1.1). First, ODM stripes were printed on a gold-sputtered coverslip to protect the underlying gold layer from subsequent cyanide etching. Piranha treatment then removed the protecting ODM layer from the gold layer and a two-step PEG passivation protocol rendered the interjacent glass areas protein-resistant. Consequently, laminin in solution adsorbs only to the gold stripes, but not to the PEG-passivated areas. To test adhesion specificity, CHO cells were seeded on the laminin/PEG substrates. After overnight incubation CHO cells were strictly confined to laminin-functionalized stripes (Fig. 3.2 A), indicating efficient passivation of the PEG-coated areas. Furthermore, cells formed mature focal adhesions on the laminin

stripes (**Fig. 3.2 B**), demonstrating the biological activity of the laminin layer. Thus, the laminin/PEG bifunctional stripe substrates fulfill all requirements for directly-comparative SCFS (section 3.3.1). Alternatively, laminin can be substituted for other proteins, such as BSA by changing the solution used to coat the gold stripes (**Fig. 2.1**, section 2.2.1.1).

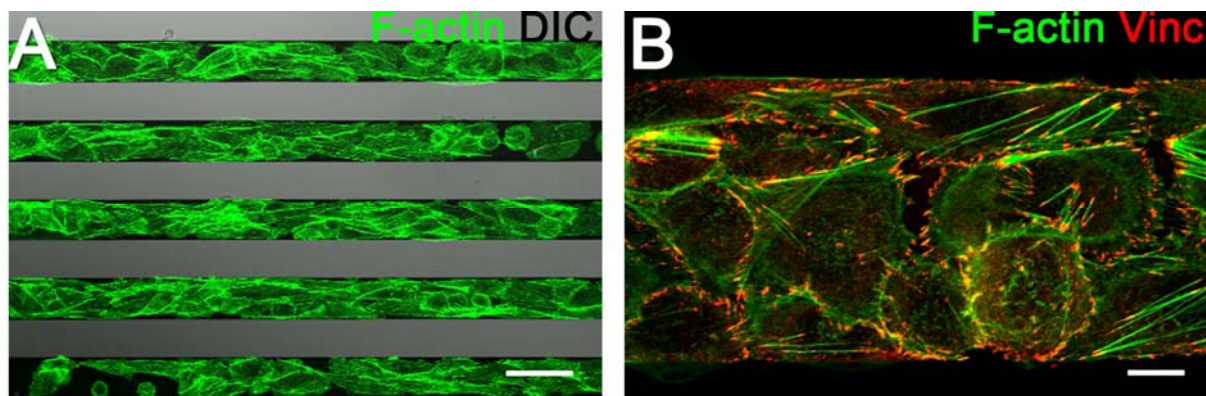


**Fig. 3.2 Selective cell adhesion on laminin/PEG substrates.**

(A) CHO cells adhere and spread exclusively on laminin-coated areas. Actin filaments labeled with Alexa488-Phalloidin (green). Laminin-coated stripes appear dark in transmission light microscopy due to the underlying gold layer. Scale bar: 50  $\mu\text{m}$ . (B) Higher magnification image of CHO cells on laminin stripes. Focal adhesions visualized by vinculin staining (red), F-actin in green. Scale bar: 10  $\mu\text{m}$ .

### 3.3.3 Comparative SCFS on laminin/PEG bifunctional substrates

To quantify and compare adhesion forces on laminin and PEG-functionalized surfaces by SCFS, a single CHO cell is attached to a concanavalin A-coated AFM cantilever. The cell is then pushed onto PEG or laminin (**Fig. 3.3 A**) areas in a preset, alternating sequence and the corresponding force curves are recorded (**Fig. 3.3 B**). Even for a relatively short contact time of 10 s, cell adhesion differs significantly between both surfaces. Detachment forces generated on laminin are comparatively high (about 1-2.5 nN), while only minimal forces build-up on PEG (less than 200 pN). Furthermore, with increasing contact time, integrin-mediated CHO cell adhesion on laminin increased but cell adhesion remains low on PEG (**Fig. 3.3 D**), confirming the excellent passivation properties of PEG for SCFS.

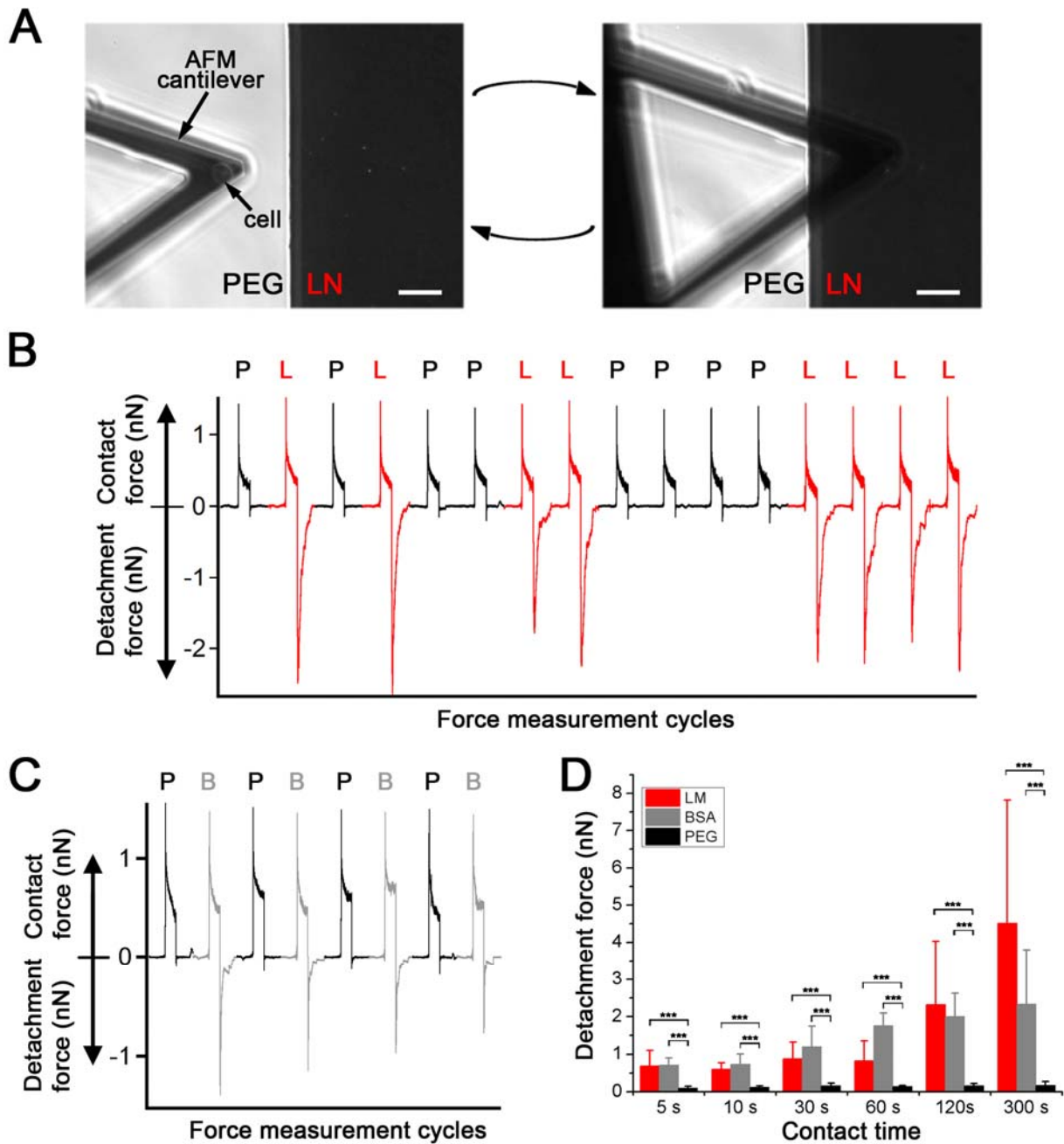


**Fig. 3.3 Comparative SCFS on laminin/PEG substrates.**

(A) A single CHO cell attached to an AFM cantilever is alternately approached to PEG (left) and laminin (right) areas. Systematic variation of the interaction position ensures that each substrate location is contacted only once. (B) 16 force curves generated in a preprogrammed sequence of force cycles alternating between the PEG-passivated (“P”, black) and the laminin-coated (“L”, red) areas. (C) 8 force curves generated in a preprogrammed sequence of force cycles alternating between PEG-passivated (“P”, black) and BSA-coated (“B”, grey) areas. (D) Detachment forces on laminin (red bars), BSA (grey bars) and PEG (black bars). Forces are given as median±MAD. At least 10 cells were measured for each condition. (\*\*\*:  $p < 0.001$  by Mann-Whitney test.)

### 3.3.4 Differential CHO cell adhesion is not caused by different mechanical properties of the laminin and PEG surfaces

Differences in the scale of cell adhesion forces forming on different substrates could also result from different micromechanical properties of the surfaces. Each force cycle is characterized by an initial step increase in force upon establishment of cell/substrate contact, a subsequent drop in effective contact force due to viscoelastic relaxation of the cell during contact, and a negative de-adhesion force peak upon cell removal (for details see **Fig. 3.4**). In the approach and contact phase, force-distance curves contain information about the nature of the mechanical interaction between cell and surface. However, comparing the shape of force curves obtained on laminin and PEG surfaces showed no difference in the approach and contact phases, while the detachment forces differed significantly (**Fig. 3.4**). Thus the variation of the detachment forces on laminin and PEG is not due to different mechanical properties of both surfaces.

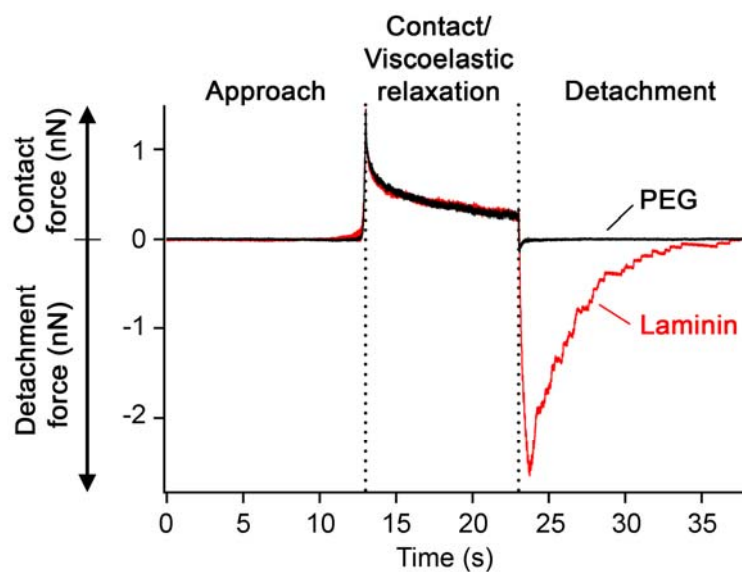


**Fig. 3.4** Overlap of force curves taken on the laminin or the PEG part of a laminin/PEG bifunctional substrate.

Both force curves taken on laminin (in red) and PEG (in black) overlap well during the approach and contact phases (displaying viscoelastic relaxation of the cell), and only diverge during the detachment phase due to different detachment forces.

### **3.3.5 Comparative SCFS on BSA /PEG bifunctional substrates**

BSA is widely used as a passivation material to prevent cell adhesion (McDevitt et al., 2002; Weghuber et al., 2010). In agreement, cell spreading on alternative fibronectin and BSA stripes only assemble focal adhesion on fibronectin but not on BSA (Johnston et al., 2008). This indicates that BSA is an efficient cell adhesion blocking protein in cell spreading assay. AFM-based SCFS, however, is an ultrasensitive method capable of quantifying cell adhesion with pN accuracy. Passivation materials used for this technique therefore require superior cell-repellent efficiency to distinguish specific from unspecific adhesion. PEG has been proved to be one of them. Dependent on the molecular weight, PEG can provide maximum entropic repulsion between the proteins and PEG surfaces (Jeon et al., 1991; Prime and Whitesides, 1993; Yang et al., 1999), therefore cell adhesion to PEG is constantly low independent of contact time (**Fig. 3.3 D**). In order to test whether BSA provides equally excellent passivation as PEG, BSA/PEG bifunctional substrates were produced for directly comparing the adhesion forces of CHO cells on two passivation materials by SCFS.

Single CHO cells were pressed on PEG and BSA surfaces alternately using contact time 10 s (**Fig. 3.3 C**). The detachment forces of CHO cells on BSA were about 1 nN while the forces on PEG were below 200 pN. Measuring 10 cells on BSA for 10s contact time gives a median detachment force of 705 pN, as high as CHO cell adhesion to laminin (687 pN, **Fig. 3.3 C**). With the increase of contact time, CHO cells adhesion on BSA increases even further. In contrast, CHO cell adhesion on PEG was constantly low, independent of contact time. Although BSA is usable as an adhesion blocking protein in cell spreading assay, it is not a suitable option for passivation in AFM-based SCFS.

### **3.3.6 Producing laminin/fibrillar collagen I bifunctional substrates for comparative SCFS**

After establishing comparative SCFS on adhesive/non-adhesive bifunctional substrates, adhesion of single cell to two types of ECM molecules are ready for comparing using substrates featuring two ubiquitous ECM protein laminin and fibrillar collagen I.  $\mu$ CP technique was used to produce bifunctional substrates with alternating stripes of those two ECM components. First, laminin was transferred from



a PDMS cuboid onto a mica surface using a lift-off technique (**Fig. 2.2**). Addition of low levels (10%) of a fluorescently-labeled, cell adhesion irrelevant protein (Alexa594-conjugated antibody) to the laminin solution allowed for visual identification of the laminin stripes (**Fig. 3.5 A and B**) but had no effect on cell adhesion (**Fig. 3.6**). In a second step, the areas between the printed ECM stripes were backfilled with fibrillar collagen I by incubation with a collagen I solution. Collagen I adsorbed exclusively on the vacant mica surfaces, as seen by immunofluorescence staining using an anti-collagen type I antibody (**Fig. 3.5 A**). AFM images of the different bifunctional substrates showed clear boundaries between the printed laminin and the backfilled collagen I fibers (**Fig. 3.5 C and D**). The height of the laminin/fibrillar collagen I interfaces obtained by AFM imaging is around 15 nm for laminin and 3 nm for fibrillar collagen I (**Fig. 3.5 C-E**), consistent with the formation of 1-2 molecular layers of ECM proteins. Thus, a bifunctional cell adhesion substrate carrying two clearly-separated and distinguishable laminin and collagen I was generated.

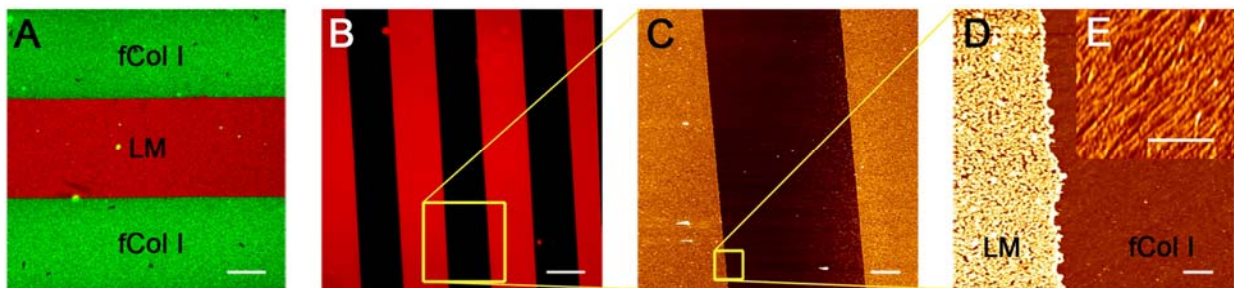


**Fig. 3.5 Laminin/fibrillar collagen I bifunctional substrates.**

(A) Fluorescent image of a laminin stripe (LM, red) backfilled with fibrillar collagen I (fCol I, green). Laminin was visualized by addition of a low concentration (10%) of a fluorescently-labeled protein (Alexa594-conjugated antibody) into the solution. Fibrillar collagen I was immunostained using a monoclonal anti-collagen antibody. Scale bar: 20  $\mu\text{m}$ . (B) Fluorescent image of the LM/fCol I bifunctional substrate. Scale bar: 50  $\mu\text{m}$ . (C) AFM image of the square area indicated in (B). The full range of the height scale corresponds to 58 nm. Scale bar: 10  $\mu\text{m}$ . (D) Higher resolution scan of the square area indicated in (C). The full range of the height scale corresponds to 37 nm. Scale bar: 1  $\mu\text{m}$ . (E) Zoom into the fibrillar collagen I part in bifunctional LM/fCol I substrates. The height is 3 nm. Collagen fibers are visible at this resolution. Scale bar: 1  $\mu\text{m}$ .



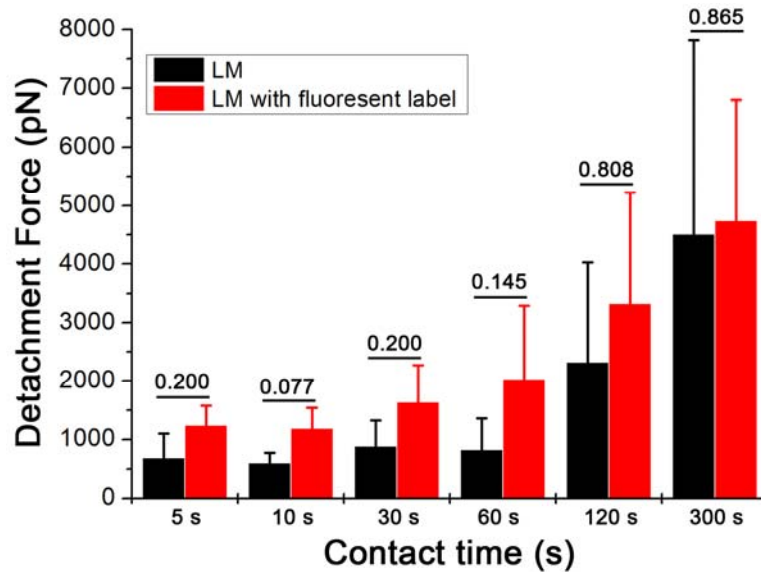


**Fig. 3.6** Addition of fluorescent marker protein does not influence CHO cell adhesion to laminin significantly.

CHO cell detachment forces (median $\pm$ MAD) on pure laminin (black bars) and on laminin containing 10% of a fluorescent marker protein (Alexa594-labeled antibody, red bars). At least 11 cells were measured for each time point. p-values (Mann-Whitney test) are indicated.

### 3.3.7 Comparative SCFS on laminin/fibrillar collagen I bifunctional substrates

To directly quantify and compare adhesion forces on laminin and collagen I surfaces by SCFS, a single CHO cell attached to an AFM cantilever was approached onto laminin (**Fig. 3.7 A**) or collagen I (**Fig. 3.7 B**) areas in a preset sequence. The corresponding detachment force was recorded and plotted over time (**Fig. 3.7 C** and **Movie 1**). To avoid possible matrix defects introduced during cell removal, different contact positions along the laminin and collagen I stripes were set for each force cycle. Since CHO cells express laminin-binding integrin (Danilov and Juliano, 1989; Furtado et al., 1992), but extremely low level of collagen-binding integrin (Nykqvist et al., 2000; Xu et al., 2011), detachment forces differed significantly between both surfaces even for a relatively short contact time of 10 s: detachment forces generated on laminin were comparatively high (about 1 nN), while only small forces built-up on collagen I (less than 300 pN). Thus, using this setup, the adhesion strength to laminin and collagen I of a single cell could be directly compared.

### *Comparative SCFS on Different Bifunctional Substrates*

To understand the general adhesion behavior of CHO cells on laminin/fibrillar collagen I bifunctional substrates, cell spreading experiments were performed using the same substrates used for SCFS. After 16 hours, CHO cells had spread and polarized almost exclusively on the laminin areas, avoiding the collagen I surface altogether (**Fig. 3.7 D-F**). The clear selective spreading behavior of CHO cells highlights the quality of the surface fictionalization procedure and mirrored well the enhanced initial adhesion forces on laminin established by SCFS. Adhesion measurements at relatively short contact times (10 s) can therefore provide useful information explaining more long-term differential adhesion responses of cells.

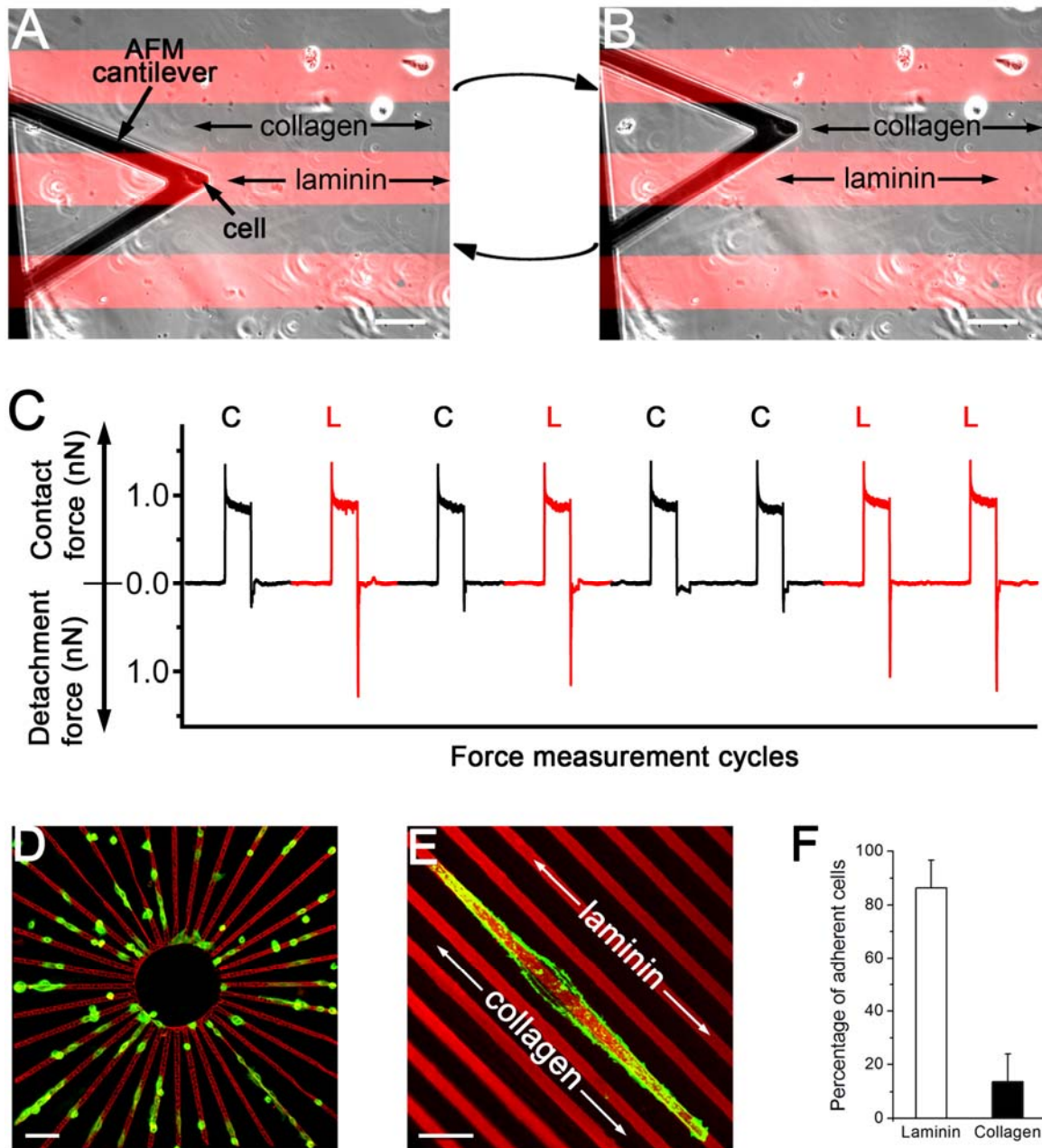


**Fig. 3.7 Comparative SCFS of a single CHO cell on laminin/fibrillar collagen I bifunctional substrates mirrors long term differential spreading of CHO cells on laminin and collagen I.**

(A-B) A single CHO cell attached to an AFM cantilever is alternately approached onto laminin (A) and collagen I (B) areas. Scale bar: 50  $\mu\text{m}$ . (C) Sequence of 8 force curves generated in a preset sequence (C-L-C-L-C-C-L-L) of force cycles alternating between laminin ("L", red) and collagen I-coated ("C") areas. Systematic variation of the interaction position along the functionalized stripes ensures that each substrate location is contacted only once. (D) CHO cells cultured on a star-patterned laminin/fibrillar collagen I substrate for 16 h. Laminin stripe width is 10  $\mu\text{m}$ . Cells were visualized by staining for F-actin (green). Laminin stripes are labeled in red. Scale bar 100  $\mu\text{m}$ . (E) Higher magnification image of a single CHO cell polarizing on a 2.5  $\mu\text{m}$ -wide laminin stripe. Scale bar 10  $\mu\text{m}$ . (F) Quantification of cell attachment to laminin or collagen I areas. Data obtained from 563 cells on 7 different substrates.

### 3.3.8 Investigating the effect of substrate contact history on cell adhesion

SCFS is usually performed several times sequentially for each contact time in order to achieve better statistics. However, in this case it has to be tested that whether preceding measurements influence later measurements. To test whether cells continued to display substrate-specific adhesion responses even after undergoing extended force cycle repetitions, single cells were subjected to over 60 force cycles, establishing cell contact with laminin and collagen I on laminin/fibrillar collagen I substrates (section 3.3.7) for more than 30 times each (**Fig. 3.8 A, C and E**). The interaction sequence pattern was varied systematically throughout the measurements in order to avoid potential artifacts arising from a repeated interaction sequence. In each force cycle, CHO cells developed high maximal and mean adhesion forces on laminin ( $F_{max} < 1800$  pN,  $F_{mean} = 850$  pN), while adhesion forces on collagen were consistently lower ( $F_{max} < 450$  pN,  $F_{mean} = 230$  pN), independently of the interaction sequence (**Fig. 3.8 A, C and E**). Detachment forces vary between force cycles but do not systematically increase or decrease with increasing force cycle number (**Fig. 3.9 A**). Therefore, for a contact time of 10 s, cells retain specific adhesion to different ECM components without being influenced by the preceding measurements.

The possibility to measure a single cell repeatedly raises the question how extending the force cycle number impacts adhesion force statistics. To investigate the influence of increased force cycle numbers on statistical parameters in detail, a single cell was subjected to over 60 alternating force cycles on collagen I and laminin (contact time 10 s) and the accumulative standard deviation ( $SD_i$ ) of the first  $i$  detachment forces ( $2 \leq i \leq 33$ ) on laminin ( $SD_{iLM}$ ) or collagen I ( $SD_{icoll}$ ) was determined. Consistent with the large fluctuation of detachment forces on laminin compared to collagen I,  $SD_{iLM}$  was consistently higher than  $SD_{icoll}$  (**Fig. 3.8 B, D and F**). However, compared to  $SD$  values obtained from the entire cell population (440 pN), single cell  $SD$  values were low on both laminin (less than 250 pN) and collagen I (less than 150 pN). The  $SD$  values initially fluctuated in response to occasional force outliers but normally stabilized after 15-20 cycles (**Fig. 3.8 B, D and F**). Next, the accumulated  $SD$  value obtained in the maximal number of force cycle ( $SD_{imax}$ ) was considered the closest approximation of the true adhesion force  $SD$  value of an individual cell and the

relative  $SD_r$  ( $SD_r = SD_r - SD_{imax}$ ) for each force cycle was plotted for 3 individual cells (**Fig. 3.9 B**). After a critical number of force cycles  $N_c$  (25 for laminin and 18 for collagen) the  $SD_r$  value of all tested cells fell within a range set by the thermal noise of the AFM cantilever, equivalent to the physical limit of AFM force resolution (20 pN, see section **2.2.8**). Progressing beyond 20 to 25 force cycles therefore does not consolidate force measurement statistics in this system.

## Comparative SCFS on Different Bifunctional Substrates

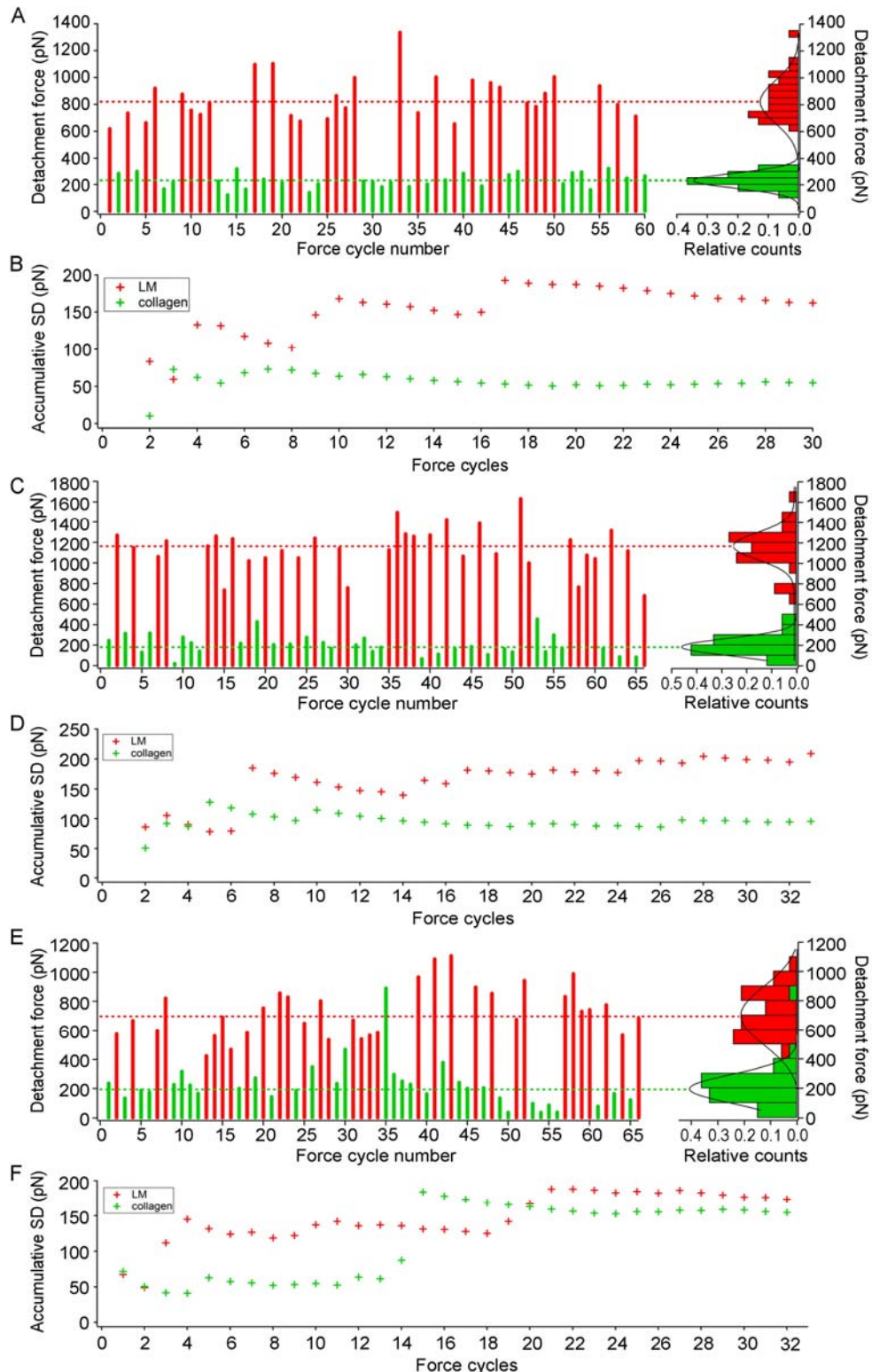


**Fig. 3.8 Detachment forces and accumulative SD analysis.**

(A, C and E) Force spectroscopy of a single CHO cell on a bifunctional laminin/collagen substrate. A total of 60 or 66 alternating force cycles were performed using a contact time of 10 s in each cycle. Cell detachment forces on laminin (red) and collagen (green) are plotted in sequence (left) or in histograms (right). Dashed lines indicate the most probable detachment force obtained from Gaussian fits to the histograms. (B, D and F) Accumulative standard deviation plotted versus force cycle number.



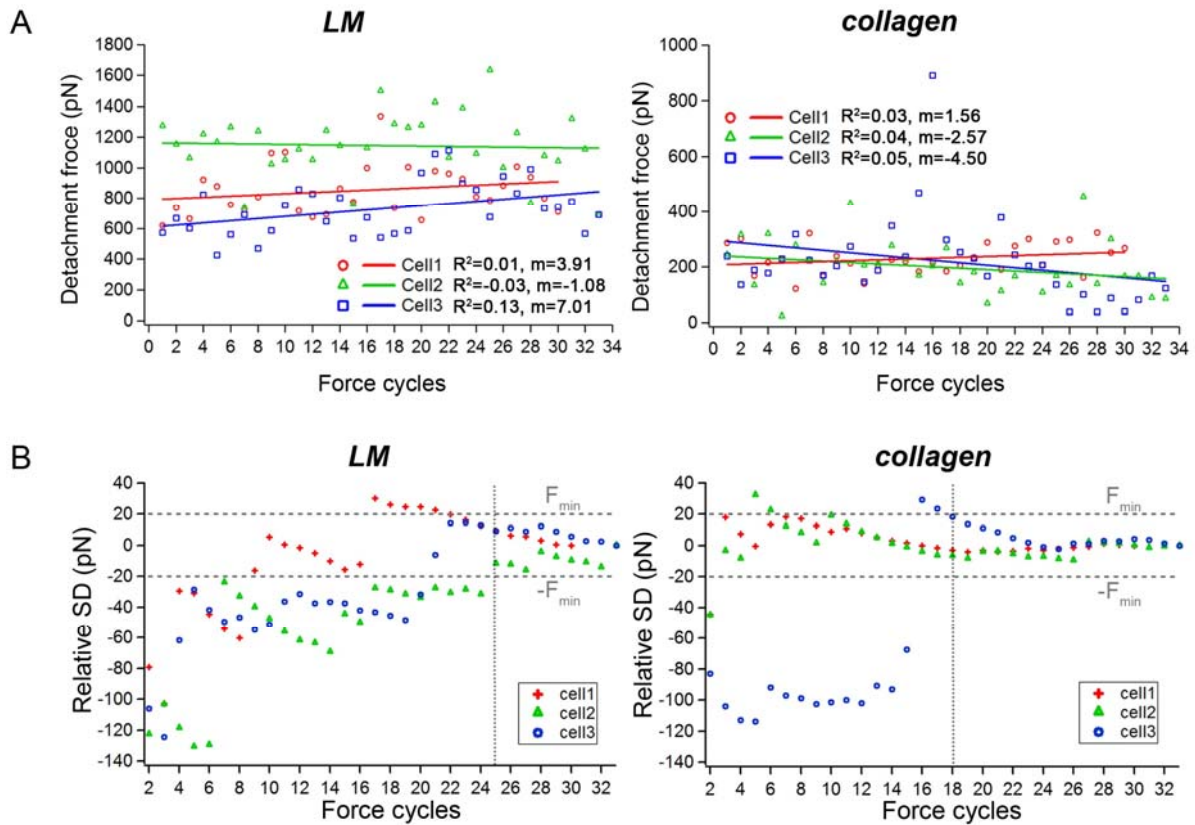


**Fig. 3.9 Linear fit of detachment forces and relative standard deviations of 3 individual cells.**

(A) Detachment forces of three LM cells on laminin (left panel) and collagen I (right panel), were plotted versus the corresponding force cycle number. Low  $R^2$  and slope ( $m$ ) values indicate independence of detachment forces from force cycle number. (B) Each cell was measured over 30 force cycles on laminin (left panel) and collagen I (right panel), respectively. The force range contained between the horizontal dashed lines describes an interval set by  $\pm$  the minimal detectable force of 20 pN around the SD<sub>max</sub> value. The vertical dashed line indicates the minimal force cycle number required to bring the relative SD within the minimal detectable force range.

### 3.3.9 Producing bifunctional substrates featuring monomeric/fibrillar collagen I for comparative SCFS

Integrin  $\alpha_1\beta_1$  and  $\alpha_2\beta_1$  are both major receptors for collagen I (Barczyk et al., 2010). However, previous studies suggest that they may have different binding preferences for different collagen subtypes:  $\alpha_1\beta_1$  was suggested to have higher affinity to monomeric collagen I while  $\alpha_2\beta_1$  prefers binding to fibrillar collagen I (Jokinen et al., 2004). CHO (CHO-WT) cells which do not express  $\alpha_2\beta_1$  and  $\alpha_1\beta_1$  (Nykqvist et al., 2000), were stably transfected with human integrin  $\alpha_1$  or  $\alpha_2$  subunit to express integrin  $\alpha_1\beta_1$  (CHO-A1) or  $\alpha_2\beta_1$  (CHO-A2) (kindly provided by Professor Jyrki Heino

from University of Turku, Finland (Jokinen et al., 2004)). To directly compare the binding affinity of integrin  $\alpha_1\beta_1$  and  $\alpha_2\beta_1$  to monomeric and fibrillar collagen I, both forms of collagen were incorporated on the same substrates by  $\mu$ CP for performing comparative SCFS.

First, monomeric collagen I stripes were transferred from a PDMS cuboid onto a mica surface using a lift-off technique. In a second step, the areas between the printed ECM stripes were backfilled with fibrillar collagen I by incubating with a collagen I solution (**Fig. 2.2**, details are described in section **2.2.1.3**). Addition of FITC conjugated collagen I allowed for visual identification of the laminin of collagen I stripes. AFM and SEM images of the different bifunctional substrates showed clear boundaries between the printed ECM protein and the backfilled collagen I fibers (**Fig. 3.10 A-E**). The height of the ECM protein interfaces obtained by AFM imaging is around 6 nm for monomeric collagen I and 3 nm fibrillar collagen I (**Fig. 3.10 B and C**), consistent with the formation of 1-2 molecular layers for collagen I. Thus, bifunctional cell adhesion substrates carrying two clearly-separated and distinguishable collagen configurations were generated.



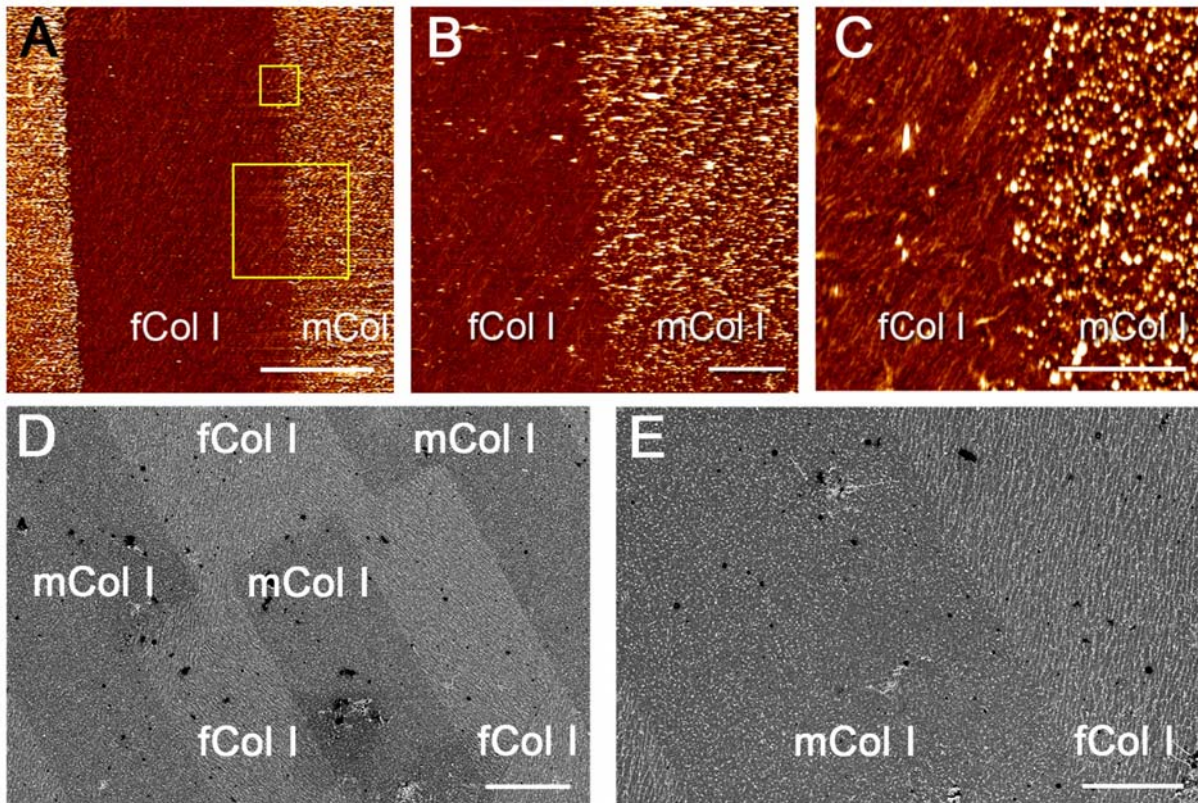


**Fig. 3.10 Morphology of monomeric/fibrillar collagen I bifunctional substrates.**

(A) AFM image of a 35  $\mu\text{m}$  x 35  $\mu\text{m}$  area with monomeric and fibrillar collagen I stripes. The full range of the height scale corresponds to 9 nm. Scale bar: 10  $\mu\text{m}$ . (B and C) AFM image of the indicated areas in (A). The full range of the height scale corresponds to 9 nm. Scale bar in L: 2  $\mu\text{m}$ ; in J: 1  $\mu\text{m}$ . (D and E) SEM image of monomeric and fibrillar collagen I stripes. Collagen fibers are visible in E. Scale bar in D: 20  $\mu\text{m}$ ; in E: 10  $\mu\text{m}$ .

### 3.3.10 Elucidating the affinity of integrins $\alpha_1\beta_1$ and $\alpha_2\beta_1$ to monomeric and fibrillar collagen I

Detachment forces of single CHO cells were compared on monomeric and fibrillar collagen I using different contact times. Considering that CHO-WT cells show only very low background adhesion to collagen, the binding affinity of integrin  $\alpha_1\beta_1$  and  $\alpha_2\beta_1$  to different collagen substrates can be directly compared by measuring single CHO-A1 or CHO-A2 cell detachment forces on bifunctional collagen substrates. CHO-A1 cells showed similar detachment forces on monomeric and fibrillar collagen I (**Fig. 3.11 B**). On both substrates, adhesion of CHO-A1 cells was significantly higher than CHO-WT and CHO-A2 cells (**Fig. 3.11 D and E**), indicating that integrin  $\alpha_1\beta_1$  is an efficient receptor for both monomeric and fibrillar collagen type I. In contrast, CHO-A2 cells adhered significantly stronger to fibrillar than to monomeric collagen I

(Fig. 3.11 C), suggesting that integrin  $\alpha_2\beta_1$  has a higher affinity for fibrillar than monomeric collagen I. Therefore, by performing comparative SCFS on monomeric/fibrillar collagen I substrates using different CHO cells, the binding preferences of integrin  $\alpha_1\beta_1$  and  $\alpha_2\beta_1$  are clarified.

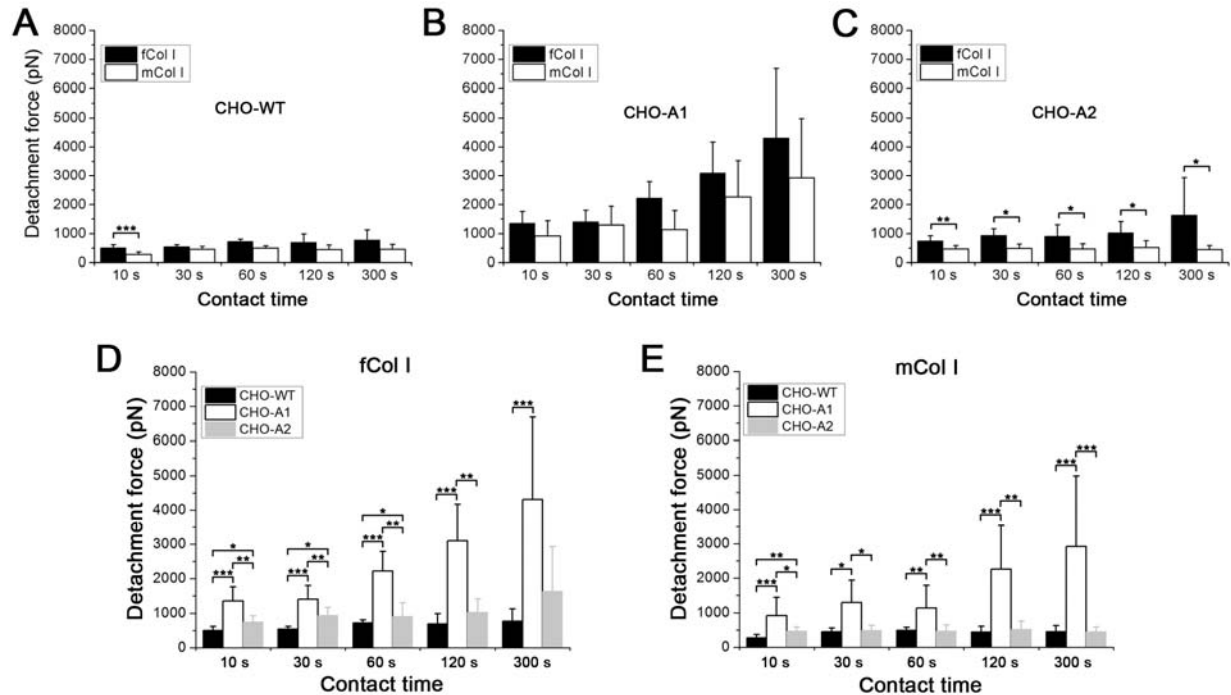


**Fig. 3.11 Detachment forces of CHO-WT, CHO-A1 and CHO-A2 cells on monomeric/fibrillar collagen I bifunctional substrates.**

(A-C) Detachment forces of CHO cells on mCol I/fCol I substrates.. (D and E) Detachment forces are replotted and grouped by substrate type. Detachment forces are plotted as median $\pm$ MAD. At least 11 cells were measured for each time point. (\*:0.01 < p < 0.05, \*\*:0.001 < p < 0.01, \*\*\*: p < 0.001 by Mann-Whitney test.)

### 3.3.11 Producing bifunctional substrates featuring collagen IV/fibrillar collagen I for comparative SCFS

Not only function as collagen I receptor, integrins  $\alpha_1\beta_1$  and  $\alpha_2\beta_1$  have also been reported as collagen IV receptors (Leitinger and Hohenester, 2007). Nevertheless, the binding specificity of those two integrins has been measured by solid phase binding assay and reported to be quite different: integrin  $\alpha_1\beta_1$  has a higher affinity for collagen IV, while  $\alpha_2\beta_1$  binds stronger to collagen I (Kern et al., 1993; Tulla et al., 2001). To directly compare the binding preference of integrins  $\alpha_1\beta_1$  and  $\alpha_2\beta_1$  to collagen IV and collagen I, substrates featuring with those two types of collagen were

fabricated by  $\mu$ CP and used for comparative SCFS of CHO-WT, CHO-A1 and CHO-A2 cells. Collagen IV microstripes were brought onto a mica disc by PDMS stamp using lift-off method. Afterwards, the remaining areas on the mica surface were backfilled with fibrillar collagen I by incubating with a collagen I solution (**Fig. 2.2**, details are described in section **2.2.1.4**). In order to make collagen I structures visible, FITC-conjugated collagen I were mixed into collagen I solution (**Fig. 3.12 A**). AFM images showed that the printed ECM proteins are clearly separated from each other. The height of the both collagen types obtained by AFM imaging is around 3 nm (**Fig. 3.12 C**), consistent with the formation of single molecular layers of collagen I and IV. Bifunctional substrates with two types of collagen were therefore generated for comparative SCFS.

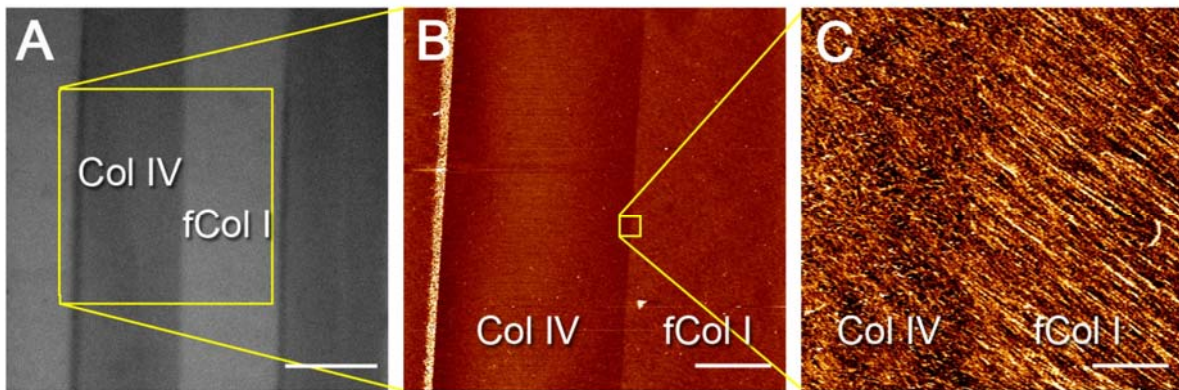


**Fig. 3.12** Collagen IV/fibrillar collagen I bifunctional substrates.

(A) Fluorescent image of the collagen IV/fibrillar collagen I bifunctional substrate. Scale bar: 50  $\mu$ m. (B) AFM image of the square area indicated in (A). The full range of the height scale corresponds to 13 nm. Scale bar: 10  $\mu$ m. (C) Higher resolution AFM images of the square areas indicated in (B). The full range of the height scale corresponds to 3 nm. Collagen I fibers are visible. Scale bar: 1  $\mu$ m.

### 3.3.12 Elucidating the affinity of integrins $\alpha_1\beta_1$ and $\alpha_2\beta_1$ to collagen IV and fibrillar collagen I

There is no significant difference between CHO-A1 adhesion on collagen IV and fibrillar collagen I (**Fig. 3.13 B**). Likewise, detachment forces of CHO-A2 cells on both collagen types are quite similar (**Fig. 3.13 C**). CHO-A1 cells adhered significantly stronger on collagen IV than CHO-WT cells while CHO-A2 and CHO-WT cells showed no difference (**Fig. 3.13 E**), indicating that integrin  $\alpha_1\beta_1$  is a collagen IV receptor while  $\alpha_2\beta_1$  is not. For different contact times, CHO-WT cells displayed

equally minimized detachment forces on surfaces coating with both collagen types, confirming that CHO-WT cells contains only low levels of endogenous collagen I and IV receptors (**Fig. 3.13 A**). Measuring adhesion of CHO-WT, CHO-A1 and CHO-A2 cells by comparative SCFS on collagen IV/fibrillar collagen I substrates therefore elucidated the affinity of integrin  $\alpha_1\beta_1$  and  $\alpha_2\beta_1$  for both types of collagen.

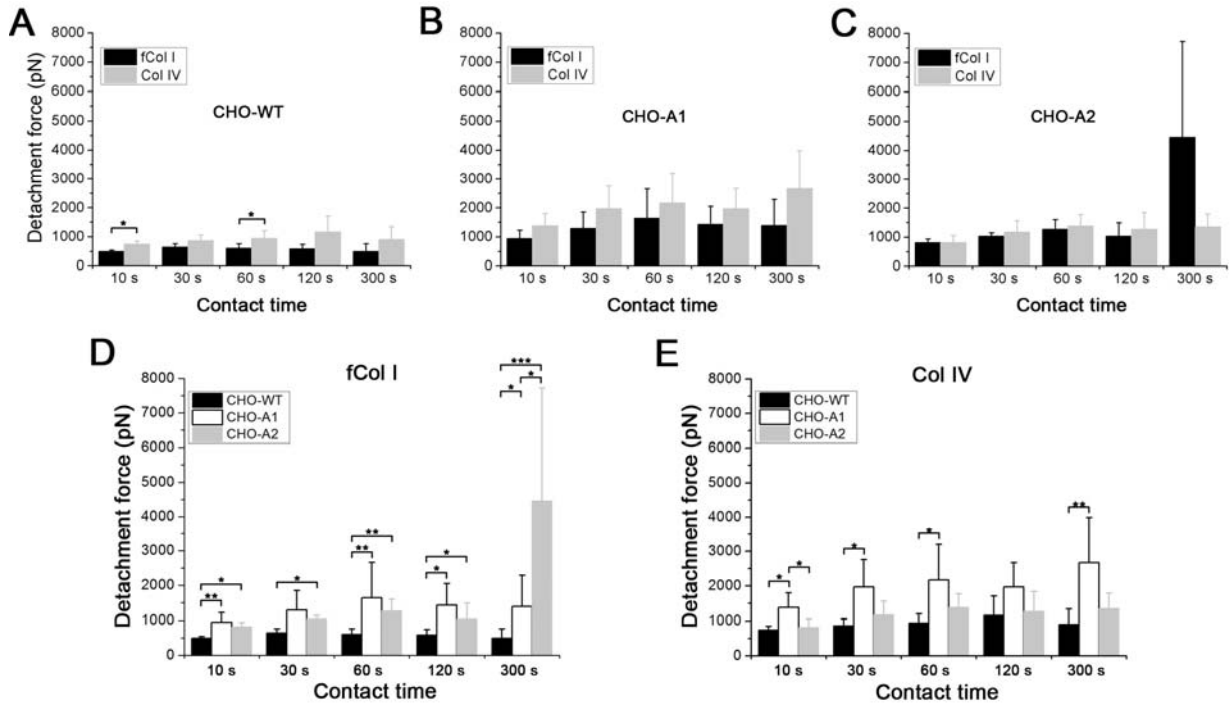


**Fig. 3.13 Detachment forces of CHO-WT, CHO-A1 and CHO-A2 cells on collagen IV/fibrillar collagen I bifunctional substrates.**

(A-C) Detachment forces of CHO cells on Col IV/fCol I substrates.. (D and E) Detachment forces are replotted and grouped by substrate type. Detachment forces are plotted as median $\pm$ MAD. At least 10 cells were measured for each time point. (\*:0.01< p<0.05, \*\*:0.001<p<0.01, \*\*\*: p<0.001 by Mann-Whitney test.)

### **3.4 Discussion**

In this chapter, two modified protocols based on alkanethiol printing followed by chemical etching (Kumar and Whitesides, 1993) and the lift-off method (von Philipsborn et al., 2006a) were used to generate microcontact printed substrates for direct comparison of single cell adhesion to two different molecules by SCFS. In contrast to the versatile geometry of microcontact printed structures used for cell spreading assays (Alom Ruiz and Chen, 2007), bifunctional substrates for comparative SCFS have to fulfill several requirements in order to ensure accurate cell placement within in the programmable cantilever positioning area ( $100 \times 100 \mu\text{m}^2$ ) (detail see section 3.3.1). All five bifunctional substrates presented in this project are validated to be suitable for this innovative application. Furthermore, this is the first printing technique capable of producing collagen type I microstructures composed of nano-scale fibrils, which is the common morphology of collagen I in many biological environments (Bigi et al., 1997).

Under physiological conditions, cell adhesion to the surface of biomaterials is affected by the adsorption of proteins at the interface. This process highly depends on the chemical and physical properties of the substrate (Dewez et al., 1997). Since PEG molecules with specific length can form brush-like monolayer which provides maximum entropic repulsion to proteins (Jeon et al., 1991; Prime and Whitesides, 1993) and BSA has no known roles in specific cell adhesion, those two molecules are widely used as passivation agents preventing cell adhesion (McDevitt et al., 2002; Brock et al., 2003). In order to test whether both PEG and BSA can be used as a passivation coating for sensitive AFM-based SCFS measurements, CHO cells adhesion was compared on laminin/PEG and BSA/PEG bifunctional substrates. PEG surfaces provided constantly low forces independent of the cell-substrate contact time. In contrast, BSA produced non-specific adhesion forces on a comparable scale to specific, integrin-mediated CHO cell adhesion to laminin, indicating that BSA is not a suitable passivation material for SCFS.

However, why does BSA function as a suitable passivation material in long term spreading assay but not for SCFS? A recent publication suggests that the cantilever pressing during cell-surface contact in SCFS may lead to a quick unfolding of BSA



(within seconds). The increased molecular surface in the unfold state contributes to the cell-BSA non-specific cell adhesion which is dominated by surface area related hydrophobic interactions and electrostatic attractions (Celik and Moy, 2012). In contrast, in cell seeding assay no extra forces are applied between the cells and the BSA thereby the protein unfolding event is negligible. Furthermore, the adhesion inhibition performance of BSA highly depends on the physiochemical properties of the substrate underneath. Surfaces functionalized with alkylsilanes terminated with amino group exhibit a significant residue level of adhesion despite being coated with a BSA layer. Nevertheless, surfaces functionalized with alkylsilanes terminated with carboxyl or methyl groups become completely non-adhesive with BSA coating (Lee et al., 2005). This research therefore highlights the importance of application-specific passivation material selection.

Integrin-mediated cell adhesion is initialized by the activation and ligand binding of individual integrin molecules followed by the lateral assembly of integrins into larger adhesion complexes, such as focal adhesions (Lotz et al., 1989; Gallant and García, 2007). However, the initial stages of this process are difficult to monitor by light microscopy. AFM-based SCFS provides a technique to monitor the formation of integrin-mediated cell adhesion contacts on the force level. Initial cell/substrate interactions are dominated by single integrin-mediated adhesion events, followed by progressive receptor aggregation and establishment of cooperative adhesion after 60 to 120 s of ECM contact (Taubenberger et al., 2007). In the experiments presented in this chapter, a comparatively short cell-substrate contact time of 10 s was used when comparing CHO cell adhesion to laminin and fibrillar collagen I. In this time frame cell-ECM interaction are dominated by single-integrin adhesion events. Despite the relatively short contact time, all CHO cells displayed consistently lower adhesion on collagen I than on laminin. CHO cells express low numbers of collagen receptors but they express the laminin-binding integrin  $\alpha_6\beta_1$  (Furtado et al., 1992). The differential adhesion response therefore apparently corresponds to the integrin receptor expression profile of these cells. This indicated that even the earliest cellular adhesion events are governed by the particular receptor repertoire of the cell. Short contact times are sufficient to determine the specific adhesion properties of CHO cells to different ECM components.

To properly interpret the results of repeated force cycles with the same cell requires testing whether preceding measurements influence the outcome of subsequent measurements. For up to 60 force cycles and a 10 s contact time CHO cell detachment forces remained highly substrate-specific on laminin/collagen substrates, displayed neither enhancement nor fatigue with increasing force cycle number and were independent of the cellular contact history. Therefore, the ligand-specific cell adhesion is able to build up and disassemble rapidly without being affected by the previous measurements.

SCFS is a sensitive yet comparatively slow adhesion assay requiring a specialized AFM setup. AFM-based SCFS therefore depends on a well-thought-out experimental strategy to obtain statistically meaningful data within practicable time scales. A basic experimental question is whether it is sufficient to test a small number cells several times or whether larger number of cells need to be tested. Because cantilever calibration and cell attachment requires substantial time, it may be attractive to measure a single cell several times upon successful immobilization on a calibrated cantilever. Using short contact times, cells continued to respond specifically to both laminin and collagen I substrates over a large number of force cycles. Over the entire force measurement procedure, cell adhesion remained robust. Therefore, extended force measurement routines are compatible with cell function and survival. However, extending measurements for more than 20-25 cycles failed to further improve single-cell adhesion force statistics due to intrinsic limits of AFM force resolution originating from the thermal noise of the cantilever. In order to fully characterizing the overall adhesion behavior of a cell population, experimental resources should be directed towards measuring a higher number of cells

Integrin  $\alpha_1\beta_1$  and  $\alpha_2\beta_1$ , both major collagen binding receptors, show distinct affinity to different collagen subtypes. To directly comparing the binding preferences of both integrins in living cells, adhesion of CHO-WT, CHO-A1 and CHO-A2 cells was quantified on different bifunctional collagen substrates. The obtained data suggests that integrin  $\alpha_1\beta_1$  is a receptor for monomeric and fibrillar collagen I and for collagen type IV while integrin  $\alpha_2\beta_1$  has high affinity for fibrillar collagen I but not for monomeric collagen I or collagen type IV. Previous studies produced similar results by analyzing the binding preference of recombinant integrins  $\alpha_1$  and  $\alpha_2$  I domains (Kern et al.,

1993; Nykvist et al., 2000; Tulla et al., 2001; Zhang et al., 2003). According to these studies,  $\alpha_1\beta_1$  prefers the basement membrane type IV collagen over fibril forming collagens, such as collagen type I. This is in contrast to  $\alpha_2\beta_1$ , which preferentially binds to collagen I over collagen IV (Nykvist et al., 2000). CHO-A1 cell adhesion on collagen IV is substantially higher than on fibrillar collagen I by comparative SCFS (**Fig. 3.13 B**), however, no significant difference was observed. The detachment forces of CHO-A2 cells were similar on both collagen types for shorter contact times, whereas for 300 s, collagen I rendered much higher adhesion than collagen IV (**Fig. 3.13 C**). This strong force enhancement from 120 s to 300 s indicates that an integrin clustering events may happen within this time frame (Gallant and García, 2007). Using CHO-A1 and CHO-A2 cells in spreading experiments, it was shown that integrin  $\alpha_1\beta_1$  prefers monomeric collagen I, while integrin  $\alpha_2\beta_1$  prefers fibrillar collagen I (Jokinen et al., 2004). By comparative SCFS, CHO A1 exhibited equal adhesion on both monomeric and fibril collagen I while CHO-A2 cells adhered significantly stronger on monomeric ones. As a complement to the solid-phase I domain binding assay and cell spreading assay, comparative SCFS using  $\alpha_1\beta_1$ - or  $\alpha_2\beta_1$ -expressing cell on bifunctional collagen substrates were performed to further clarify the binding preference of integrin  $\alpha_1\beta_1$  and  $\alpha_2\beta_1$  to different collagen types.

In conclusion, bifunctional adhesion substrates are an efficient tool for characterizing differential adhesion processes both of individual cells and within cell populations. Comparative SCFS can also be combined with other adhesion receptor quantification assay on gene, mRNA and protein levels in order to fully understand the cell adhesion regulation mechanism in the future. This could shed new light into creating new biomaterials with better biocompatibility and developing new therapy against metastatic cell transferring and invasion.



## **4 Revealing Adhesive Variation in Clonal Population by Comparative Single-Cell Force Spectroscopy**

---

### **4.1 Abstract**

Cell populations often display heterogeneous behaviour, including cell-to-cell variations in morphology, adhesion and spreading. Better understanding the significance of cell variations for the function of the population as a whole requires quantitative single-cell assays. To investigate adhesion variability in a CHO cell population in detail, integrin-mediated CHO cell adhesion to laminin and collagen I, were measured by AFM-based SCFS. All tested CHO cells adhered more strongly to laminin than collagen I, but population adhesion force distributions to both ECM components were broad and partially overlapped. Testing many (n=30) CHO cells on collagen- or laminin-functionalized surfaces yielded a wide variation of adhesion forces across the cell population. In contrast, repeatedly testing the same cell (>30 force cycles) revealed a comparatively narrow adhesion force distribution. Thus, broad adhesion force distributions within cell populations originate from cell-to-cell variations rather than from fluctuations in the adhesive response of individual cells. Adhesion variability to laminin was non-genetic and cell cycle-independent but scaled with the range of  $\alpha 6$  integrin expression on the cell surface. To determine the levels of laminin and collagen I binding in individual cells directly, single CHO cells were measured alternately on adjacent microstripes of laminin and collagen I on the same adhesion substrate. Again all tested cells bound laminin more strongly, but the scale of laminin over collagen binding varied between cells. Together, this demonstrates that CHO cell adhesion to different ECM components is precisely yet differently set in each cell of the population. Adhesive cell-to-cell variations due to varying receptor expression levels thus appear to be an inherent feature of cell populations and should to be considered when fully characterizing population adhesion.

## **4.2 Introduction**

Despite sharing a common origin and function, cells in clonal populations are often surprisingly heterogeneous in different cellular properties (Altschuler and Wu, 2010; Spiller et al., 2010), such as cell size (Rubin and Hatie, 1968), multiplication rate (Grundel and Rubin, 1988) or protein expression (Cai et al., 2006). Frequently, population variability increases when cells are transferred from their natural surrounding into *in vitro* cell culture (Heppner, 1984; Grundel and Rubin, 1988; Rubin, 1990), but the underlying molecular mechanisms are largely unknown. Likewise, the biological significance of many *in vivo* cell-to-cell variations is still unclear (Altschuler and Wu, 2010). Despite the inherent heterogeneities in many aspects of cell behaviour, cell populations are stable and function reliably. Cell-to-cell variations may be beneficial by increasing population diversity and enhancing survival in the face of changing environmental conditions (Kussell and Leibler, 2005). During development, cell variability may be advantageous for robust cell line expansion (Grundel and Rubin, 1988). Cell variability may also confer drug-resistance to populations (Singh et al., 2010).

Better understanding the mechanisms and consequences of cell variability requires suitable assays for analyzing single cell behavior (Ryan et al., 2011). Phenotypic variation linked to morphological changes, such as variations in cell size or spreading area can usually be assessed by standard light microscopy, while variation in protein expression levels between individual cells can be analyzed by fluorescent microscopy or flow cytometry. In contrast, determining functional properties that do not involve morphological changes are usually more difficult to measure. As a consequence, less is known about functional heterogeneities, including adhesive or mechanical variations within populations. Many cell adhesion assays, such as washing assays, generate only population-averaged adhesion data. Subtle variations in adhesion between individual cells, which may be of potential biological significance, are therefore usually impossible to detect with these assays. At the same time, carefully analyzing adhesive properties of individual cells may be crucial for better understanding the behavior of the entire population. For instance, in a cancer cell population extreme adhesive properties of a single aberrant cell may be sufficient to lead to dissemination and metastasis (Chambers et al., 2002) (Poste et al., 1982).

*Revealing Adhesive Variations in Clonal Populations by Comparative SCFS*

Furthermore, conventional adhesion assays usually permit only testing cell adhesion to a single type of ECM component at a time, whereas information about differential adhesion of a particular cell to two or more different types of ECM may be desirable.

Here SCFS was performed on bifunctional laminin/collagen substrates to investigate adhesion variability in a CHO cell population. Substantial variability in adhesion to collagen I and laminin was observed between individual cells. Furthermore, adhesion variability was proven to be non-genetic and cell cycle-independent but that it scales with the variation of integrin receptor expression within the population. Adhesion to laminin and collagen is independently regulated and correlates with a differential adhesion and spreading behavior on mixed laminin/collagen adhesion substrates. Therefore, cell-to-cell adhesion variation due to differential integrin expression levels is an intrinsic property of clonal cell population and may serve as an important mechanism to cope with the evolutionary pressure.

## **4.3 Results**

### **4.3.1 Comparing CHO cell adhesion to homogeneous laminin and fibrillar collagen I surfaces by conventional SCFS**

To compare CHO cell adhesion to two ubiquitous ECM components collagen and laminin by AFM-based SCFS, muscovite mica surfaces homogeneously coated with collagen type I and laminin-111 were prepared. Collagen I substrates were produced by adsorbing collagen type I monomers onto muscovite mica (**Fig. 4.1 A**). Under suitable buffer conditions, collagen monomers assemble into a thin layer of aligned collagen fibrils on this surface (Jiang et al., 2004). In a similar fashion, laminin surfaces were produced by adsorbing laminin-111 to mica. In this case, a homogenous layer of laminin forms (**Fig. 4.1 A**). Adhesion of CHO cells on collagen I and laminin was subsequently quantified by AFM-based SCFS using a 10 s contact time. On collagen 22 CHO cells were measured on collagen and 31 CHO cells were measured on laminin.

CHO cell detachment forces on collagen were comparatively low ( $213 \pm 57$  pN) (**Fig. 4.1 B**). CHO cells do not express  $\alpha_2\beta_1$  integrin, a major receptor for collagen type I (Nykqvist et al., 2000), but possibly low levels of other collagen binding integrins (Xu et al., 2011). Removing extracellular  $Mg^{2+}$  significantly reduced CHO cell adhesion on collagen, suggesting that the weak adhesion of CHO cells on collagen is mediated by other  $Mg^{2+}$ -dependent collagen receptors, such as  $\alpha_1\beta_1$ ,  $\alpha_{10}\beta_1$  and/or  $\alpha_{11}\beta_1$  (**Fig. 4.1 C**). In contrast, cells displayed significantly elevated adhesion forces on laminin using the same contact time ( $738 \pm 298$  pN). CHO cells adhesion to laminin is thought to be integrin-mediated (Danilov and Juliano, 1989), involving  $\alpha_6\beta_1$  and  $\alpha_6\beta_4$  (Aumailley et al., 1990a; Sonnenberg et al., 1990a; Furtado et al., 1992). To prove specific, integrin-mediated CHO cell adhesion to laminin, SCFS was performed in the presence of an inhibitory peptide (YIGSR), which competes with major receptor binding sites on laminin for integrin receptors (Mecham, 1991). In presence of the YIGSR peptide, detachment forces on laminin were drastically reduced and did not increase with contact time (**Fig. 4.1 D**). Adding an anti- $\alpha_6$  integrin blocking antibody (clone GoH3) significantly reduced CHO cell adhesion on laminin, while adding a rat IgG isotype control had no effect, confirming specific,  $\alpha_6$  integrin-mediated laminin binding.

Comparing population-averaged detachment forces suggests that CHO cells adhere stronger on laminin than collagen. However, plotting the detachment force values of all tested cells in a probability histogram (**Fig. 4.1E**) revealed a more complex picture of the adhesion properties within the population. CHO cells displayed relatively wide force distributions on both collagen (20-900 pN) and laminin (100-2000 pN), indicating large cell-to-cell variations in adhesion within the population. Interestingly, while the laminin distribution was strongly shifted to higher forces, both force distributions overlapped considerably: More than 90% of the collagen rupture forces fell within the force range covered by the laminin distribution, while about 60% of the laminin distribution overlapped with the collagen distribution. The extensive detachment force overlap demonstrated that some cells bind laminin less strongly than other cells bind collagen. Thus, the clear preference of CHO cells for laminin over collagen established based on population-averaged data does not necessarily apply to all individual cells within the population. In fact, the population may contain individual cells in which the preference for laminin and collagen is reversed. A reversal of the binding preference for laminin and collagen in individual cells, however, could have important functional implication for overall population behavior. The adhesion force variation furthermore raises the question whether cells displaying relatively high adhesion to laminin also show relatively higher adhesion to collagen, or whether the relative adhesion strength to laminin and collagen are unrelated in a particular cell. However, using separate collagen and laminin substrates does not allow for testing the relative scale of laminin over collagen binding for individual cells. Therefore, new setup for comparing single cell adhesion on two substrates is in demand.

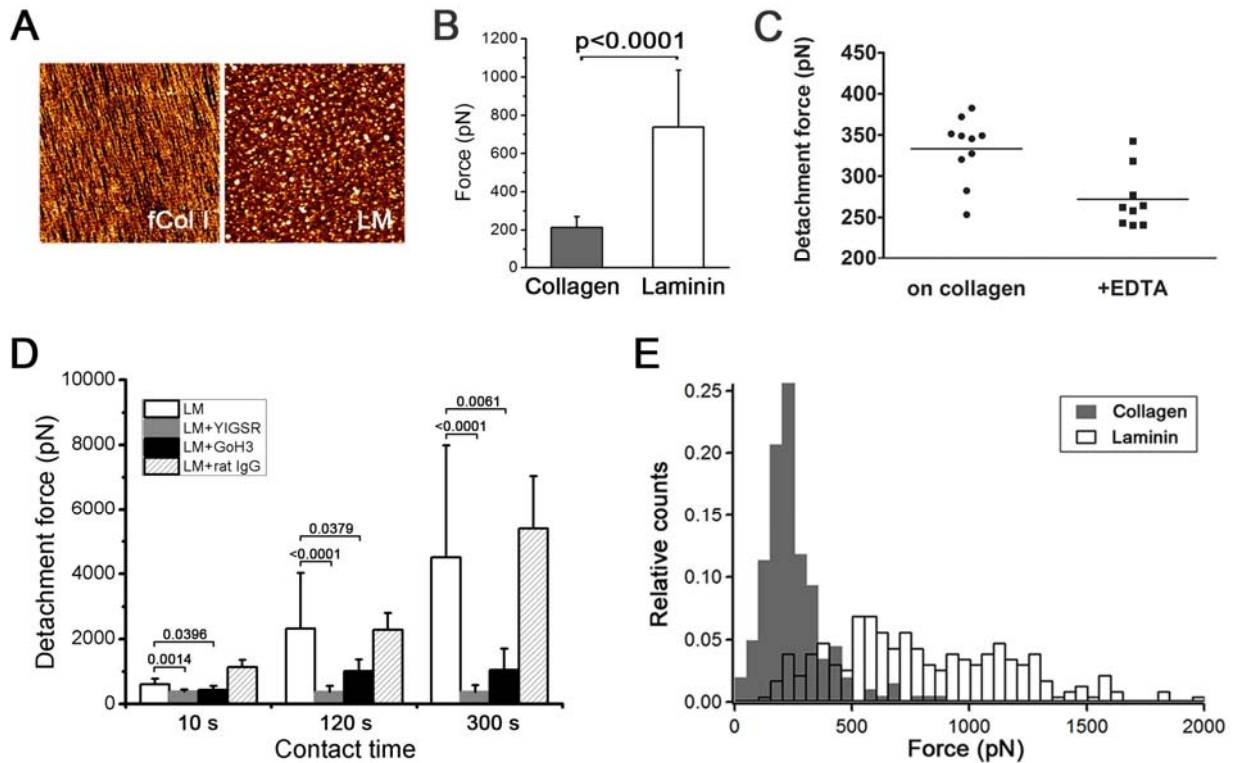


**Fig. 4.1 AFM-SCFS of CHO cells on collagen and laminin.**

(A) AFM images of fibrillar collagen I and laminin on mica substrates. Image sizes: 3  $\mu\text{m}$  x 3  $\mu\text{m}$ , height scales of collagen and laminin images are 0-3 nm and 0-8 nm, respectively. (B) CHO cell detachment forces on fibrillar collagen I and laminin after a contact time of 10 s plotted in a bar chart (median $\pm$ MAD). (C) Detachment force distribution of a single CHO cell measured on fibrillar collagen I. Adding 10 mM EDTA to remove extracellular  $\text{Mg}^{2+}$  significantly reduces adhesion of the same cell ( $p=0.0109$ ), according to paired t test. (D) Detachment forces on laminin (white bars) and on laminin in the presence of a specific blocking peptide (dark grey bars) or the anti-integrin  $\alpha 6$  subunits antibody GoH3 (black bars) or the rat IgG isotype control (patterned bars). Forces are given as median $\pm$ MAD. At least 11 cells were measured for each condition. p-values (Mann-Whitney test) are indicated. (E) CHO cell detachment forces on fibrillar collagen and laminin after a contact time of 10 s plotted as probability distributions. 22 cells were measured on collagen and 31 cells were measured on laminin.

#### 4.3.2 Determining single-cell adhesion profiles on laminin/fibrillar collagen I substrates

To quantify individual cell adhesion to laminin and collagen I directly, single CHO cells were measured alternately on adjacent microstripes of laminin and fibrillar collagen I on the same adhesion substrate (also shown in section 3.3.8 and Fig. 3.7 A-C to investigate the influence of preceding measurements to later ones). CHO cells were subjected to over 60 force cycles, establishing cell contact with laminin and collagen I for more than 30 times each (Fig. 4.2). The interaction sequence pattern was varied systematically throughout the measurements in order to avoid potential

systematic effects arising from a monotonous interaction sequence. Although the adhesion forces fluctuated with each force cycle, CHO cells always developed high adhesion forces on laminin while adhesion forces on collagen I were consistently lower (**Fig. 4.2**), which corresponds to the adhesive repertoire of the cell. Detachment forces distributed normally on both substrates (**Fig. 4.2**), but again measurements on laminin surfaces yielded higher forces than on collagen I surfaces, indicating that CHO cells respond specifically to the presented ECM substrate regardless of interaction sequence and force cycle number. Single cell the detachment force distributions on laminin and collagen I (**Fig. 4.2**) are much narrower than the distributions of the whole cell population (**Fig. 4.1E**), raising questions regarding the underlying reasons for the wide force distribution in the cell population.

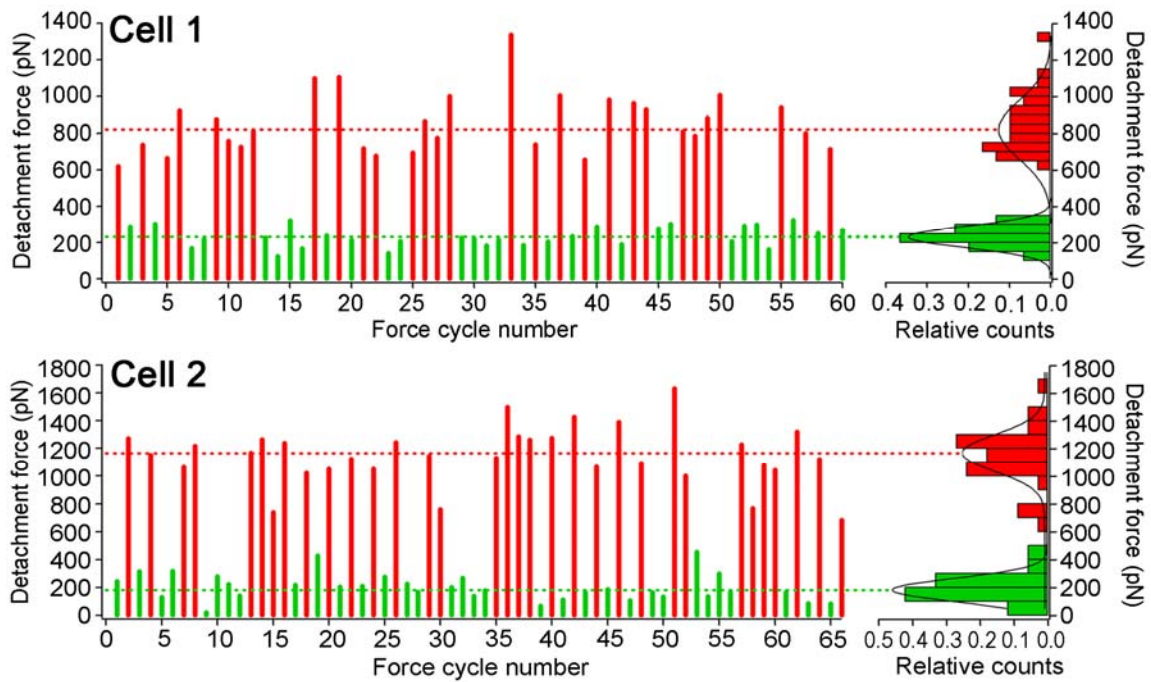


**Fig. 4.2** CHO cell detachment forces on laminin/fibrillar collagen I bifunctional substrates.

Force spectroscopy of two individual CHO cells on a bifunctional laminin/fibrillar collagen I substrate. A total of over 60 alternating force cycles were performed using a contact time of 10 s in each cycle. Cell detachment forces on laminin (red) and collagen I (green) are plotted in sequence (left) or in histograms (right). Dashed lines indicate the most probable detachment force obtained from Gaussian fits to the histograms. Figure is replotted of Fig. 3.8.

### 4.3.3 Superimposing force distributions from individual cells generates broad force distribution

To understand the reason for the broad force distribution of the whole cell population, several cells are measured on laminin for 30 times consecutively using contact time 10 s. The resulting detachment force distributions are comparatively narrow, but the mean value varied considerably between cells (**Fig. 4.3 A and B**). This indicated that the adhesion potential of individual cells is precisely set and that it remains constant for the duration of the entire experiment (about 1h). Superimposing single-cell force distribution from 3 cells generated a broad distribution similar to the distribution obtained from 30 cells (**Fig. 4.3 A and B**). Therefore, broad adhesion force distributions within cell populations originate from cell-to-cell variations rather than fluctuations in the adhesive response of individual cells in repeated adhesion force measurements.

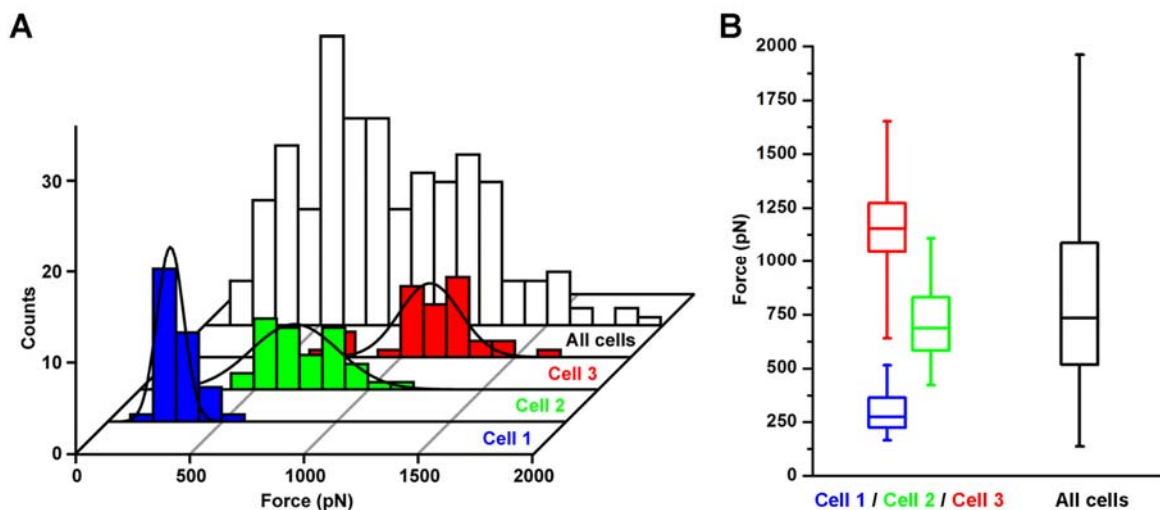


**Fig. 4.3 Pooled detachment forces from cell population and individual cells.**

(A) Pooled detachment force distribution of 30 single CHO cells on laminin after a contact time of 10 s (white bars). The distributions from 3 individual cells, each measured 30 times using a 10 s contact time, are shown in red, green or blue bars. Gaussian fits to the single cell force distributions are also plotted. (B) Box-whisker plots of the data presented in (A).

### 4.3.4 Independent regulation of cell adhesion to laminin and collagen I

While different integrin types interact with different ligands via their extracellular domain, they may interact with the same cytoskeletal linker proteins, such as talin, vinculin or paxillin inside the cell (Zaidel-Bar et al., 2007). Thus, variations in integrin



adhesion between cells could in principle be due to variations in the levels of the intracellular interaction partners. Additional intracellular factors, such as PKC activation (Schreiner et al., 1991) or heterogeneities in the actin cytoskeleton (Volk et al., 1984), may also influence integrin function. However, if intracellular factors were primarily responsible, laminin and collagen I binding would be equally affected by these variations, yielding cells more or less competent in all integrin-mediated adhesion processes. To test for a possible correlation between adhesion to laminin and collagen I, different adhesion levels were compared in five individual cells (**Fig. 4.2 A**). Although all cells exhibited elevated adhesion to laminin as compared to collagen I (on average 3.1-fold), the relative degree of preference to laminin in comparison to collagen I varied considerably between cells, ranging from 1.4 to 5.6-fold, or by a factor of four. Plotting detachment forces on laminin versus collagen I showed no correlation between both parameters (**Fig. 4.4 B**), indicating that adhesion strength to different ECM components is independently regulated in individual CHO cells.

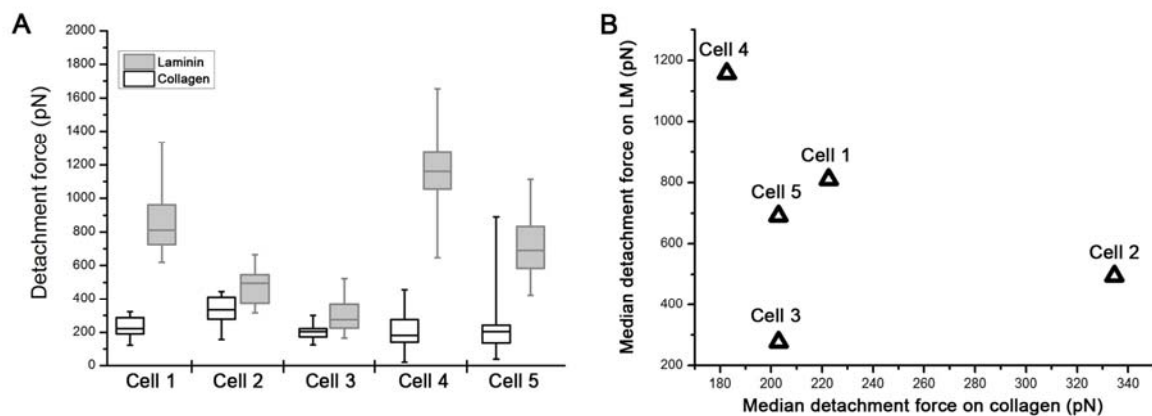


**Fig. 4.4 Detachment forces analysis.**

(A) Directly-comparative adhesion measurement of individual CHO cells on laminin and collagen. Detachment forces (box-whisker plots) of 5 cells on laminin (grey boxes) and collagen (clear boxes). Single cells were alternately approached onto the laminin- and collagen-functionalized part of a laminin/collagen adhesion substrate (at least 20 cycles per cell, contact time 10 sec). (B) Laminin versus collagen median detachment force values plotted for the same 5 cells shown in (A). The detachment force scales on LM and collagen do not correlate in individual cells.

#### 4.3.5 Non-genetic and cell-cycle independent adhesion variability in *in vitro* cell cultures

The CHO cell population showed a remarkable variation in adhesion to laminin. One possible explanation could be the presence of different subpopulations with different adhesive potentials, for instance due to mutations in adhesion-relevant proteins. To test for the possible presence of subpopulations, single cells from the original population were isolated and expanded into new cell populations. Testing adhesion to laminin of 3 different subclones (more than 13 cells per subclone) again yielded wide population force distributions (**Fig. 4.5 B-D**) indistinguishable from the original population (**Fig. 4.5 A**). Because the subclones underwent only about 20-30 cell divisions before being tested in SCFS, genetic changes between cells cannot account for widespread cell-to-cell variability within subcloned populations.

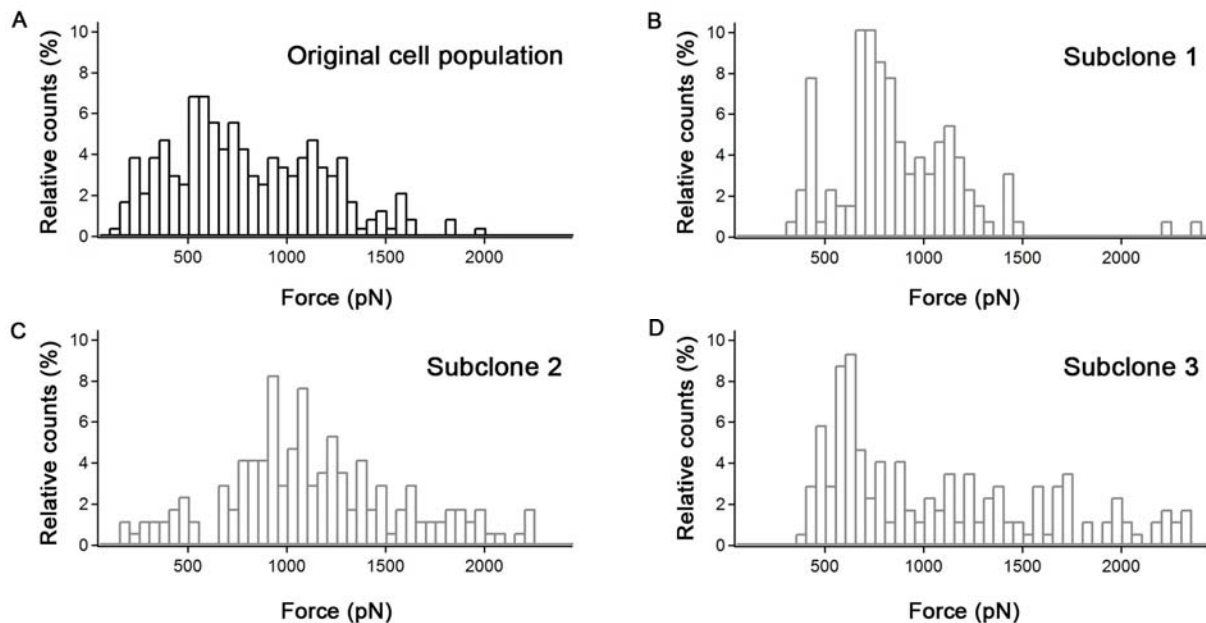


**Fig. 4.5 Detachment force distribution of CHO cells on laminin.**

(A) Original population (31 cells) and (B-D) 3 subcloned populations generated from the original population (13 cells each).

All adhesion measurements were performed in cell cycle-unsynchronized populations, as this state may better represent population behavior under typical cell culture conditions. However, during the cell cycle, especially M phase, cells undergo large cytoskeletal rearrangements and membrane refolding, which are likely to affect their

adhesive and mechanical properties. In agreement, adhesive changes during M phase have been previously demonstrated by SCFS (Weder et al., 2009). A washing step was involved when preparing cell suspensions for adhesion measurements to remove the majority of mitotic cells (about 7% of cells at any given time) due to their weak attachment to tissue culture plastic. Most mitotic cells were therefore excluded from the analysis. Nevertheless, adhesion variability may originate from testing cells in other cell cycle states. To investigate possible cell cycle effects, CHO cells were synchronized using a double thymidine block, followed by a mitotic shake-off and a hydroxyurea block. This protocol arrests cells at the end of G1 phase (Cao et al., 1991). Consistent with a complete cell cycle arrest of the entire population at this stage, there were no mitotic cells left judged by the absence of rounded-up cells in phase contrast microscopy (**Fig. 4.6 A**) and the absence of cells with condensed chromosomal DNA after Hoechst staining (not shown). Hydroxyurea removal produced a sharp burst of mitosis starting after 8 h and peaking after 10 h (**Fig. 4.6 B**). By 13 h after release, more than 93% of all cells had divided and re-entered G1 phase without having progressed into S phase as indicated by the absence of BrDU-positive nuclei (data not shown). Cells had therefore completed one complete cell cycle round before being tested by SCFS during a time window of 15-19 h post-release (**Fig. 4.6 B**). Cells in G1 displayed the same degree of adhesion variability as cells in an unsynchronized population, as judged by a similar spread of the adhesion force distributions (**Fig. 4.6 C and D**). Adhesion variability therefore occurs even in cells in the same cell cycle phase, ruling out different cell cycle phases as the main reason for variability in this assay.

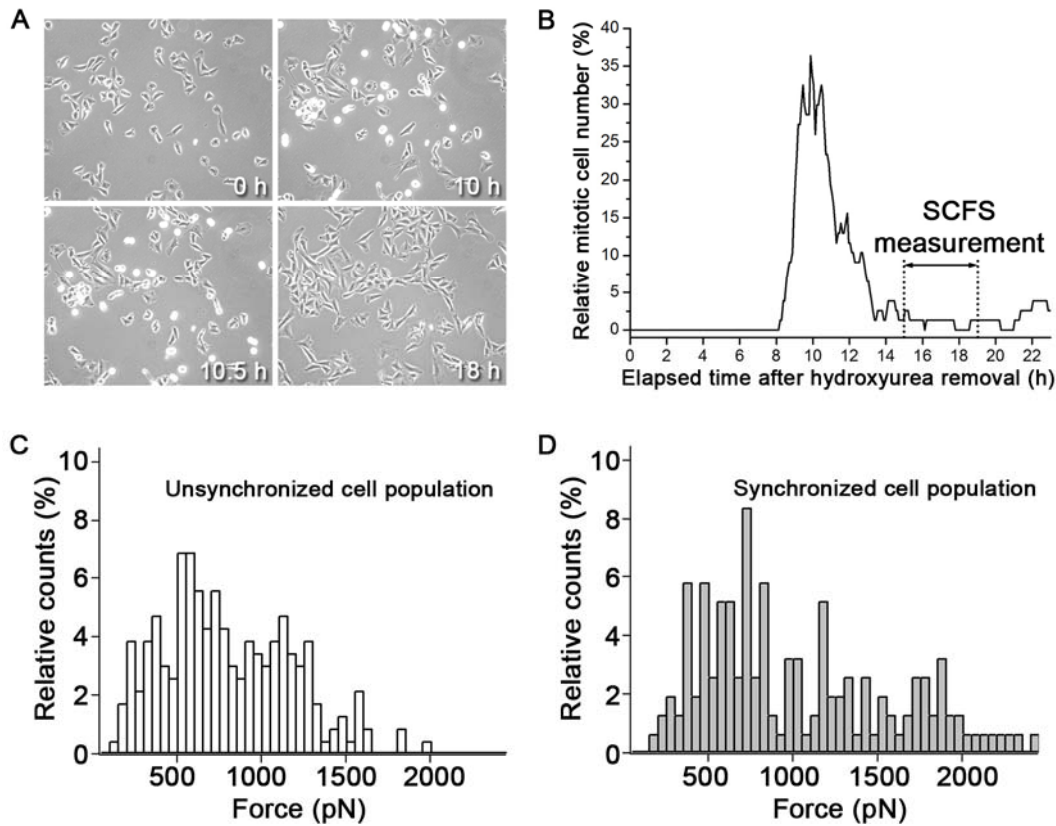


**Fig. 4.6 Synchronization of CHO cells.**

(A) Phase contrast images of a synchronized CHO cell population at indicated time points of release from cell cycle arrest. (B) Relative number of mitotic cells after release from cell cycle arrest. The time span for SCFS experiments is indicated. Similar adhesion force distributions in unsynchronized (C) and synchronized (D) populations. The distribution in (C) corresponds to the graph shown in Fig. 3.11 A.

#### 4.3.6 Variation of integrin $\alpha 6$ cell surface expression and adhesion variability

The peptide and antibody blocking experiments identified  $\alpha 6$  subunit-containing integrins as the main laminin receptor in CHO cells (**Fig. 4.1 D**). To investigate a possible link between adhesion strength and the expression of integrin  $\alpha 6$ , the main mediator of laminin binding in CHO cells, flow cytometry experiments were performed by Dr. Irina Nazarenko, Universitätsklinik Freiburg, to determine  $\alpha 6$  cell surface levels. In the parental CHO cell population,  $\alpha 6$  expression varied about 100-fold across all measured cells and about 15-fold when excluding the 5% of cells with the highest expression levels (**Fig. 4.7 A**). Cell surface expression of  $\alpha 6$  in the bulk of the cell population thus correlated well with the scale of adhesion variability (200-2500 pN, ~12.5-fold) in the same population. Given that adhesion strength may scale with the

number of integrin receptors on the cell surface (Keely et al., 1995; Garcia et al., 1998), cell-to-cell variations in adhesion to laminin may be primarily due to variations of the number of  $\alpha_6$  integrin receptors on the cell surface. On the cell surface the  $\alpha_6$  subunit combines with  $\beta_4$  or  $\beta_1$  subunits to form the functional laminin receptors  $\alpha_6\beta_1$  and/or  $\alpha_6\beta_4$ . Variations in the expression levels of the corresponding  $\beta$  subunits may further contribute to the observed adhesion variability. However,  $\beta$  subunit expression levels could not be determined due the unavailability of antibodies recognizing hamster proteins. Expression of  $\alpha_6$  also showed a similar spread in the parental population and the three subclones (**Fig. 4.7 B-D**), suggesting that expression variability was equally non-genetic and established during cell expansion after subcloning. Adhesion variability caused by variation of the receptor number on the cell surface therefore appears to be an intrinsic feature of CHO cells populations cultured *in vitro*.

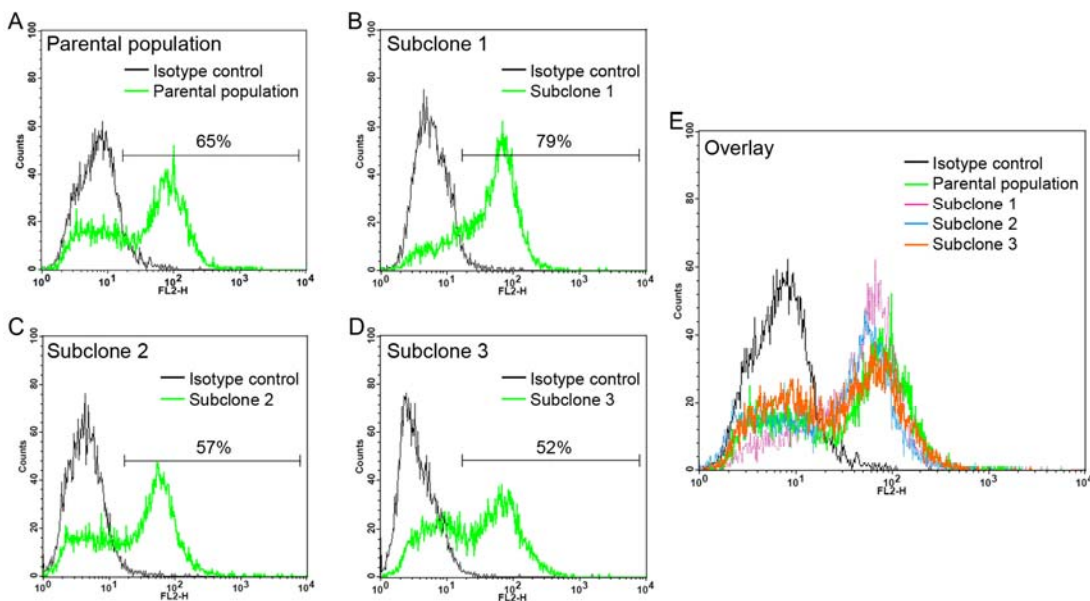


**Fig. 4.7 Analyzing integrin  $\alpha_6$  cell surface expression by flow cytometry.**

Integrin  $\alpha_6$  cell surface expression in parental CHO cell population (A) and three subclones (B-D) are analyzed by flow cytometry. Black curves indicate isotype controls. The percentages of cells showing specific  $\alpha_6$  integrin staining are indicated. (E) Overlay of curves (A-D) to highlight their overlap.

#### **4.4 Discussion**

Using a single-cell adhesion assay demonstrated considerable adhesion variability across the population, while single cells display markedly narrow force distributions when tested repeatedly. Cell cycle-related effects could be a possible cause for the observed cell-to-cell adhesion variations, so could be the presence of subpopulations with different adhesive properties or different integrin receptor expression levels. However, subcloning from a single cell produced a detachment force spectra indistinguishable from the original population. Subclones grew into new populations over the course of around 20 days. At the time of testing, subcloned cells had therefore progressed through an estimated about 30 cell cycles. Given average mutation rates in mammalian cells on the order of about  $1 \times 10^{-8}$  per genetic locus and generation (Lynch, 2010), genetic variations are unlikely to account for the wide spread of adhesion forces across the expanded subclonal populations over this cell culture period. Therefore genetic changes are unlikely to account for the population variability. Likewise, a cell cycle-synchronized CHO cell population displayed the same degree of adhesion variability as an unsynchronized population, ruling out cell cycle phases as the primary cause for the observed variation in this case.

Adhesion variability to laminin in parental and subclonal populations correlated well with the scale of  $\alpha 6$  integrin expression variability in these populations as shown by flow cytometry. In flow cytometry several thousand cells per experiment are measured, analyzing heterogeneous expression within the population with high statistical significance. However, single cells cannot be analyzed in this technique, preventing directly comparing the expression and adhesion profiles of individual cells. However, as the spread of integrin expression in the subcloned populations mirrored a similar spread of adhesion strength in these populations, the variations in adhesion is attributed to variations in integrin expression levels. Integrin receptor levels have been previously shown to vary across CHO cell populations (Laukaitis et al., 2001; Azab and Osterrieder, 2012). The transition from well-defined single-cell adhesion levels to broad adhesion variations in the subclones suggests rapid diversification of expression levels during population expansion. Fast re-establishment of cell heterogeneity after population expansion from single cells has been observed in other cell types and behavioral aspects. For instance, parental and subcloned NIH

3T3 cell populations display similar degrees of heterogeneity in regard to multiplication rates (Grundel and Rubin, 1988).

The mechanisms underlying variable protein expression levels in genetically identical populations are not fully understood. Even when growing in the same environment, cells from clonal populations can exhibit different behavior (Kaern et al., 2005; Maheshri and O'Shea, 2007) and the random production and/or degradation of mRNA may contribute to these variations in some case (Maamar et al., 2007; Suel et al., 2007). In CHO cells the random cycling between inactive and active states of genes is also known to cause variations in mRNA and, as a result, protein levels (Niepel et al., 2009). However, reversible epigenetic events, such as DNA methylation and histone modifications, are increasingly proving to be highly dynamic processes (Rando and Verstrepen, 2007; Spiller et al., 2010) and may play a dominant role in governing non-heritable variations in mammalian cells. In any case, cell adhesion properties, and likely integrin expression levels, remained constant in the tested cells over the entire SCFS measurement interval (~1h), indicating relatively temporal stable receptor expression levels in individual cells.

Despite the inherent heterogeneities in many aspects of cell behaviour, cell populations are stable and function reliably. In fact, cell-to-cell variations may be beneficial by increasing population diversity and enhancing survival in the face of changing environmental conditions (Kussell and Leibler, 2005). On the other hand, heterogeneity in cancer cell population may affect the effectiveness of anti-cancer treatments. Individual cells within tumor cell populations are often highly heterogeneous in their ability to metastasize and in their sensitivity to anti cancer drugs (Rubin, 1990). Many of the behavioural differences between tumor cells have been shown to be non-heritable (Snijder and Pelkmans, 2011) and frequently correlate with variations in antigen expression, including changes in the number of specific adhesion receptors exposed at the cell membrane. As cell-matrix interactions play an important role in the invasive and metastatic behaviour of tumor cells (Schreiner et al., 1991), inhibitory antibodies to adhesion molecules, including integrin receptors, are presenting themselves as promising tools for suppressing tumor growth and spreading (Lu et al., 2008). However, non-genetic variations in cell surface expression of the targeted receptors may contribute to the resistance of

individual cells to these treatments (Taupier et al., 1983). Analyzing the adhesive properties of individual cells within tumor populations may provide important information about the full adhesive spectrum present in a population and thereby improve the effectiveness of inhibitor-based cancer treatments.

In summary, large adhesion variations between individual cells in a genetically homogenous cell population results from varying integrin receptor expression. Bifunctional substrates are useful tool to quantify single cell adhesion to two integrin ligands. Substrates featuring more types of ECM components mimicking the real tissue are in demand thereby the impact of differential adhesion variability on population behaviour can be interpreted in a more comprehensive manner.



## **5 Inverse Regulation between Integrin $\alpha_2\beta_1$ and Laminin Receptors**

---

### **5.1 Abstract**

Integrin  $\alpha_2\beta_1$ , a well-characterized collagen I receptor, has been repeatedly reported to also be a laminin-111 receptor, but its relative binding strengths to collagen and laminin have not been determined in the context of living cells. To compare  $\alpha_2\beta_1$ -mediated adhesion, bifunctional adhesion substrates were produced consisting of alternating collagen and laminin microstripes. CHO-WT cells, which express only low levels of endogenous collagen-binding integrins, adhered exclusively on laminin stripes, whereas CHO-A2 cells stably expressing  $\alpha_2\beta_1$  adhered and polarized strongly on collagen I, indicating a general preference of  $\alpha_2\beta_1$  for collagen over laminin. To directly compare the  $\alpha_2\beta_1$ -mediated adhesion strength to collagen I and laminin in the same cell, adhesion forces were quantified on both substrates using AFM-based SCFS. As expected, CHO-A2 cells adhered more strongly to collagen I than CHO-WT cells. Comparable results were obtained for  $\alpha_2\beta_1$ -expressing (SAOS-A2) and  $\alpha_2\beta_1$ -deficient wild type (SAOS-WT) human osteosarcoma cells. Surprisingly however, CHO-WT and SAOS-WT cells showed significantly stronger adhesion to laminin than the corresponding  $\alpha_2\beta_1$ -expressing cells, pointing towards a suppressing effect of  $\alpha_2\beta_1$  expression on laminin-binding. In agreement, RT-qPCR and western blot analysis of cells stably expressing  $\alpha_2\beta_1$  revealed a downregulation of integrin subunits  $\alpha_6$  and  $\beta_4$ , both components of the major laminin-binding integrin receptors  $\alpha_6\beta_1$  and  $\alpha_6\beta_4$ . Likewise, SAOS-WT transiently transfected to express  $\alpha_2\beta_1$  showed decreased  $\alpha_6$  and  $\beta_4$  expression. In conclusion, these results demonstrate that  $\alpha_2\beta_1$  is an efficient receptor for collagen I but not for laminin in these cell types. Instead,  $\alpha_2\beta_1$  expression suppresses  $\alpha_6$  and  $\beta_4$  expression and laminin binding, suggesting an inverse regulation of  $\alpha_2\beta_1$  and laminin receptors.

## **5.2 Introduction**

Integrin  $\alpha_2\beta_1$  is widely expressed in many cell types such as epithelial cells, platelets, endothelial cells, fibroblasts and chondrocytes (Zutter and Santoro, 1990) and it has been reported to control mammary gland branching morphogenesis and collagen remodeling within the ECM (Heino, 2000; Chen et al., 2002). The integrin  $\alpha_2$  I-domain recognizes a GOFGER hexapeptide within the collagen triple helix in a  $Mg^{2+}$ - and  $Mn^{2+}$ -dependent manner. As a consequence,  $\alpha_2\beta_1$  integrin is often primarily regarded as a collagen receptor (Dickeson et al., 1997; Knight et al., 2000). However, depending on the cell type in which it is expressed, integrin  $\alpha_2\beta_1$  has also been reported to bind to the LN motif of the laminin  $\alpha_1$  chain (Pfaff et al., 1994) and to be a functional laminin receptor (Elices and Hemler, 1989; Languino et al., 1989).

In addition to integrin  $\alpha_2\beta_1$ , other integrin receptors are known to bind to laminin, such as integrin  $\alpha_6\beta_1$  and  $\alpha_6\beta_4$ . Both of these integrins bind to the E8 domain close to the C-terminal of the laminin  $\alpha_1$  chain (Sonnenberg et al., 1990b), thereby controlling cell adhesion and migration on laminin. In contrast to  $\alpha_2$  integrin,  $\alpha_6$  subunits are cleaved by furin into a heavy and a light chain connected by a disulfide bridge (Lehmann et al., 1996). In cells expressing the  $\alpha_6$ ,  $\beta_1$ , and  $\beta_4$  subunits,  $\alpha_6\beta_4$  integrin forms as the dominant heterodimer (Mercurio, 1995).

The original motivation for this study was to compare  $\alpha_2\beta_1$  integrin-mediated cell adhesion to collagen and laminin and to determine the relative binding strength of this receptor to both ECM components. To achieve this goal, two complimentary cell systems were used:  $\alpha_2\beta_1$ -deficient CHO-WT together with  $\alpha_2\beta_1$ -expressing CHO-A2 cells, and wild type,  $\alpha_2\beta_1$ -deficient human osteosarcoma cells (SAOS-WT) together with  $\alpha_2\beta_1$ -expressing SOAS cells (SAOS-A2) (Vihinen et al., 1996; Nykvist et al., 2000). The spreading behavior of  $\alpha_2\beta_1$ -deficient and expressing cells on laminin/collagen I bifunctional substrates was investigated and cell adhesion strength to both coatings was determined by SCFS. These experiments demonstrated that integrin  $\alpha_2\beta_1$  is an efficient collagen receptor but not laminin receptor in both cell systems. Moreover, RT-PCR and western blots results indicate that stable or transient expression of  $\alpha_2\beta_1$  effectively downregulates the expression of the laminin receptor  $\alpha_6\beta_4$ , suggesting an inhibitory effect of integrin  $\alpha_2\beta_1$  on laminin binding.

## **5.3 Results**

### **5.3.1 Integrin $\alpha_2\beta_1$ is a collagen I receptor in both CHO-A2 and SAOS-A2 cells**

Integrin  $\alpha_2\beta_1$  is a well-established collagen receptor (Emsley et al., 2000; White et al., 2004). Nevertheless, this integrin has also been reported to be a laminin receptor (Languino et al., 1989; Lotz et al., 1990). However, the relative contribution of  $\alpha_2\beta_1$  to laminin and collagen binding in a particular cell type has not been established. SCFS was therefore used to compare the binding strength of  $\alpha_2\beta_1$  to collagen and laminin in living cells. To ensure measuring specific  $\alpha_2\beta_1$ -dependent adhesion, two cell line pairs were used: CHO-WT and SAOS-WT cells, which do not express endogenous  $\alpha_2$  integrin (Vihinen et al., 1996; Nykvist et al., 2000), thus serve as a negative control for  $\alpha_2\beta_1$ -mediated adhesion. CHO-A2 and SAOS-A2 cells stably express the  $\alpha_2$  subunit, which combines with endogenous  $\beta_1$  subunits to form functional  $\alpha_2\beta_1$  receptors (**Fig. 5.1 A and B**).

If  $\alpha_2\beta_1$  integrin is a receptor for both collagen and laminin, one would expect elevated adhesion forces on both ECM components in CHO-A2 and SAOS-A2 cells compared to the corresponding wild-type cells. To confirm that integrin  $\alpha_2\beta_1$  is a functional collagen I receptor in CHO-A2 and SAOS-A2 cells, AFM based SCFS was performed and the adhesion forces of  $\alpha_2\beta_1$ -deficient and  $\alpha_2\beta_1$ -expressing cells were quantified on collagen I. For different contact time, both CHO-A2 and SAOS-A2 cells showed significantly higher adhesion than the corresponding wild-type cells (**Fig. 5.1C and D**), demonstrating that integrin  $\alpha_2\beta_1$  is an efficient collagen I receptor in both cell systems. Due to weak residual expression of the collagen I receptor integrin  $\alpha_1\beta_1$  in SAOS-WT cells (Vihinen et al., 1996), SAOS-WT cells adhere slightly stronger on collagen I than CHO-WT cells, which do not express  $\alpha_1\beta_1$  integrin (Nykvist et al., 2000). Efficient collagen I binding through  $\alpha_2\beta_1$  in CHO-A2 cells confirmed previous  $\alpha_2\beta_1$  studies (Taubenberger et al., 2007; Tulla et al., 2008a).

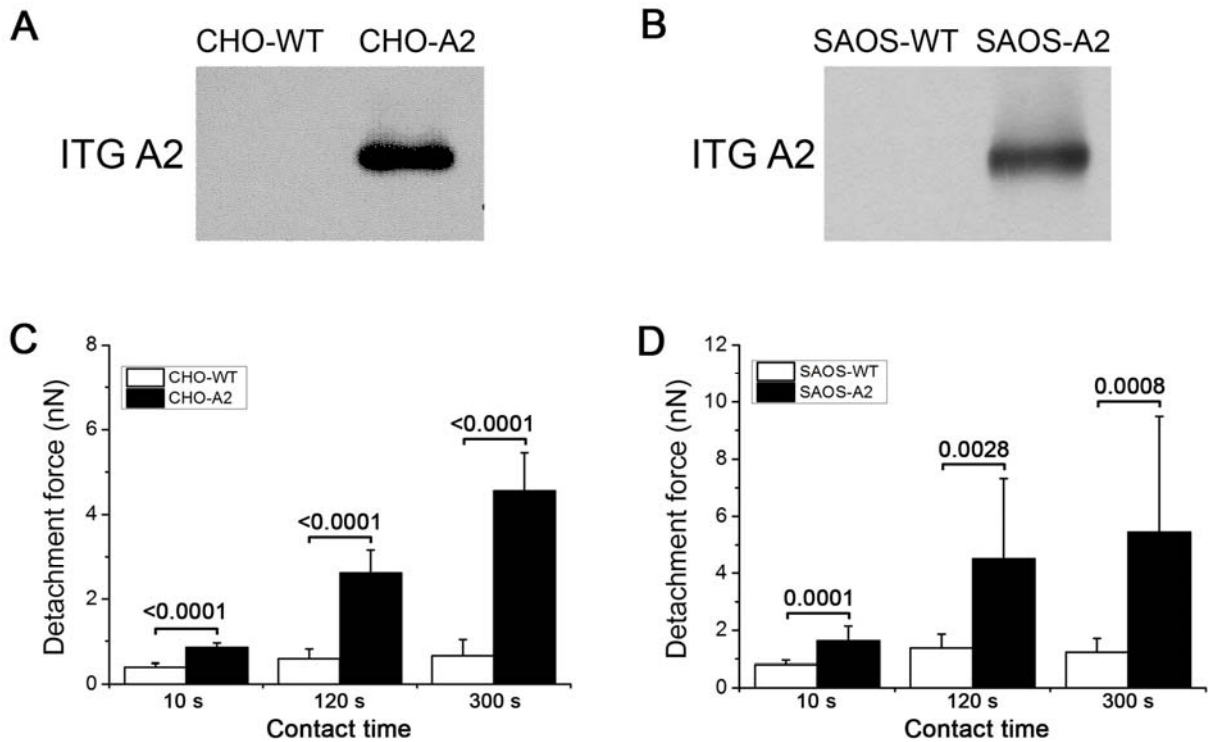


**Fig. 5.1 Integrin  $\alpha_2\beta_1$  is a collagen receptor in both CHO-A2 and SAOS-A2 cells.**

Western blots of human integrin  $\alpha_2$  subunit in CHO-WT/CHO-A2 (A) and SAOS-WT/SAOS-A2 (B) cells. CHO-WT/CHO-A2 (C) and SAOS-WT/SAOS-A2 (D) cell adhesion on collagen I was quantified by SCFS. The data are presented in median $\pm$ MAD. At least 10 cells were measured for each time point. p-values (Mann-Whitney test) are indicated.

### 5.3.2 Integrin $\alpha_2\beta_1$ is not a functional laminin receptor in either CHO-A2 or SAOS-A2 cells

Next, adhesion of integrin  $\alpha_2\beta_1$ -deficient and -expressing cells to laminin was compared. If integrin  $\alpha_2\beta_1$  also mediates laminin binding, one would again expect higher adhesion of CHO-A2 and SAOS-A2 cells to laminin compared to the corresponding WT cells. Otherwise, if  $\alpha_2\beta_1$  does not bind laminin, adhesion of  $\alpha_2\beta_1$ -deficient and expressing cells to laminin should be similar. Surprisingly,  $\alpha_2\beta_1$ -expressing cells showed significantly lower adhesion to laminin than the corresponding  $\alpha_2\beta_1$ -deficient cells (Fig. 5.2 A and B), suggesting that integrin  $\alpha_2\beta_1$  is not a laminin receptor in either CHO-A2 or SAOS-A2 cells. Moreover, the comparatively low adhesion of the A2 cells to laminin compared to collagen (Fig. 5.3 A and B) indicated that integrin  $\alpha_2\beta_1$  is at most a poor laminin receptor in either CHO-A2 or SAOS-A2 cells. Together, the results established that integrin  $\alpha_2\beta_1$  is an

efficient collagen I but not laminin receptor in both cell systems and indicated that  $\alpha_2$  integrin expression in fact suppresses laminin-binding, possibly by downregulation of other laminin receptors.

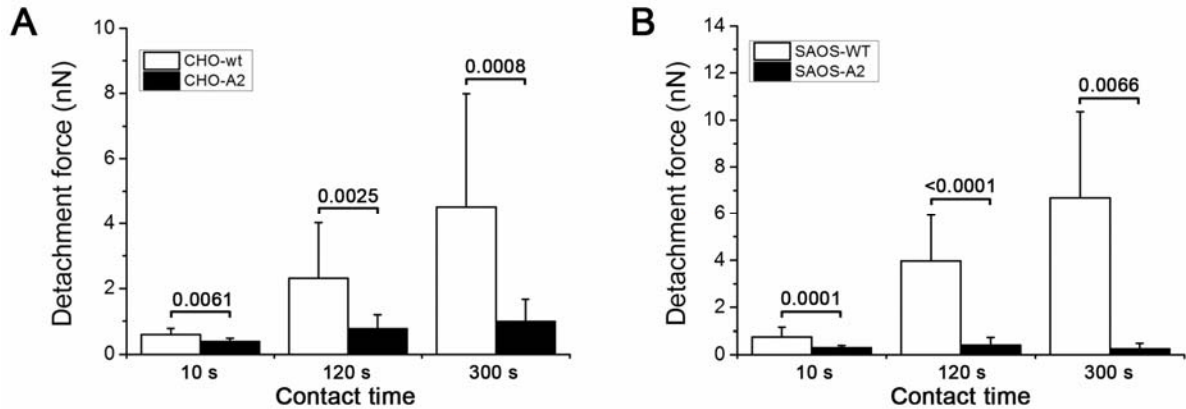


**Fig. 5.2 Integrin  $\alpha_2\beta_1$  expression suppresses laminin binding in CHO and SAOS cells.**

CHO-WT/CHO-A2 (A) and SAOS-WT/SAOS-A2 (B) cell adhesion on laminin was quantified by SCFS. The data are presented in median $\pm$ MAD. At least 15 cells were measured for each time point. p-values (Mann-Whitney test) are indicated.

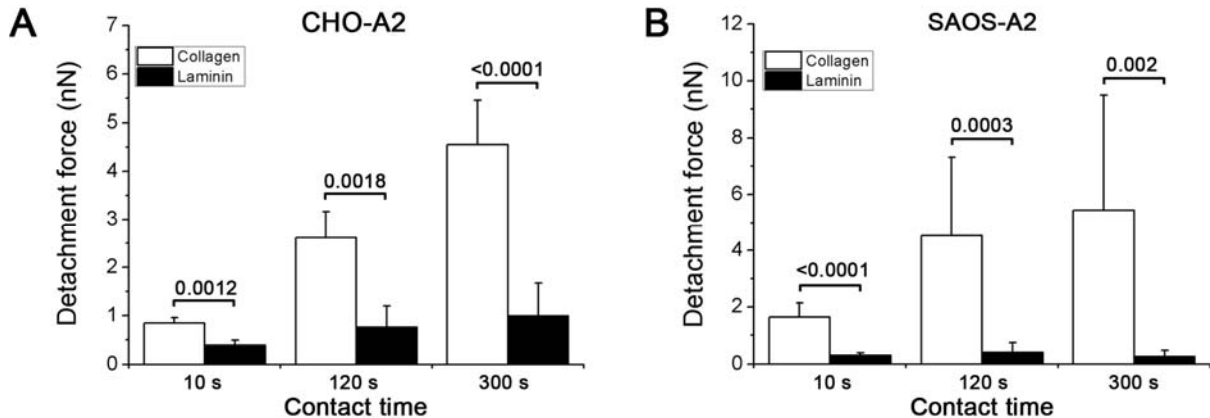


**Fig. 5.3 Adhesion of CHO-A2 and SAOS-A2 cells on collagen and laminin.**

CHO-A2 (A) and SAOS-A2 (B) cell adhesion data (median $\pm$ MAD) on collagen and laminin presented in **Fig. 5.1** and **Fig. 5.2** are replotted to highlight differential binding to collagen and laminin. At least 10 cells were measured for each time point. p-values (Mann-Whitney test) are indicated.

### 5.3.3 Integrin $\alpha_2\beta_1$ expression suppresses cell spreading on laminin

The SCFS measurements demonstrated enhanced adhesion to collagen and reduced adhesion to laminin of  $\alpha_2\beta_1$ -expressing cells. To complement the adhesion

measurements with a spreading assay, CHO-WT and CHO-A2 cells were seeded on bifunctional substrates featuring alternating laminin and collagen I stripes and grown overnight. Spreading on either ECM protein should provide a direct read-out of the cells' differential adhesion behavior. CHO-WT cells, consistent with high adhesion to laminin and their low levels of endogenous collagen receptors (Nykqvist et al., 2000), spread predominantly on the laminin stripes (**Fig. 5.4 A-C, H**). More than 75% of all CHO-WT cells adhered on single laminin stripes and oriented their long axis parallel with the stripe, assuming a highly polarized morphology (**Fig. 5.5 A and B**). The remaining CHO-WT cells spanned several laminin stripes (**Fig. 5.4 C**). As a consequence, the cell long axis sometimes deviated somewhat from the laminin orientation. Nevertheless, the clear preference of CHO-WT cells for the laminin-coated stripes corroborated the results from the adhesion measurements and indicated that these cells express endogenous laminin receptors which facilitate adhesion and spreading on laminin.

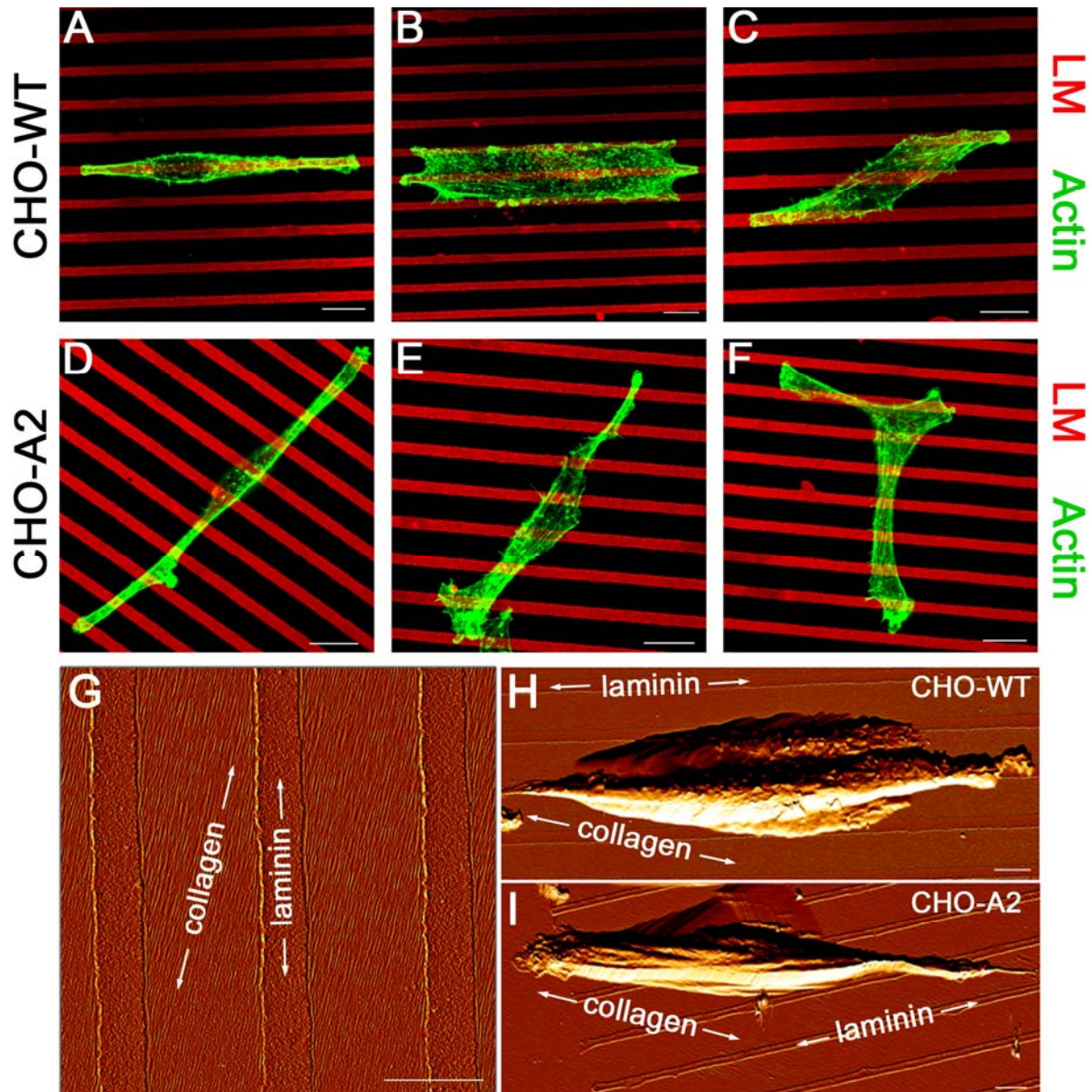


**Fig. 5.4 CHO-WT and CHO-A2 cells spreading on LM/Col substrates.**

Fluorescent (A-F) and AFM (G-H) images of CHO-WT (A-C and H) and CHO-A2 (D-F and I) on LM/fCol I substrates (G). (A-F) Actin filaments of the cells are labeled in green and LM stripes are labeled in red. Scale bar: 10  $\mu\text{m}$ . (G-H) The orientation of collagen I fibers and laminin stripes are indicated by arrows. Scale bar: 5  $\mu\text{m}$ .

In contrast, CHO-A2 cells, which stably express integrin  $\alpha_2\beta_1$ , rarely spread on or parallel to the laminin stripes (**Fig. 5.4 D-F**). AFM scanning showed that some of CHO-A2 cells aligned well with the direction of the collagen fibers (**Fig. 5.4 I**), consistent with the spreading behavior of these cells on pure collagen surfaces (Friedrichs et al., 2007). Many CHO-A2 cells partially aligned with the collagen fibrils in some areas of the cell, and with laminin stripes in other areas of the cell, leading to



a wide distribution of cell orientations falling in between the direction of the collagen I fibers and the laminin stripes. This indicated that CHO-A2 cells are able to interact with both collagen and laminin. Cell alignment on ordered collagen substrates requires integrin-mediated contraction forces (Friedrichs et al., 2007). Likewise, strong polarization along thin laminin stripes will depend on the formation of integrin-mediated cell adhesion and cell contraction forces. An intermediate polarization between the collagen fibril and the laminin stripe orientation could reflect different balances between integrin-mediated adhesion processes to both ECM components. The cell alignment relative to the collagen and laminin direction was therefore analyzed. However, because the orientation of the self-assembling collagen fibrils on mica depends on the random orientation of the mica crystal, which could not be determined or controlled prior to the printing of the laminin stripes, the bifunctional substrates contain different angles between the laminin stripes and the collagen fibrils. Therefore, all substrates were first imaged by AFM to determine the angle between the laminin stripes and the collagen fibrils, and cell orientations were subsequently determined by light microscopy. Substrates displaying a laminin to collagen angle of  $30\pm 5$  or  $60\pm 5$  degrees were grouped and the cell orientations were analyzed. In both groups the alignment distribution peak is closer to the collagen fiber direction than to the laminin stripe direction (**Fig. 5.5 C and D**), suggesting a dominant role of collagen over laminin on cell alignment. The preferential alignment of CH-A2 cells with the collagen fibers on the LM/Col substrates indicates that even if integrin  $\alpha_2\beta_1$  mediated some laminin binding in these cells, it functioned much less efficiently than mediating collagen binding.



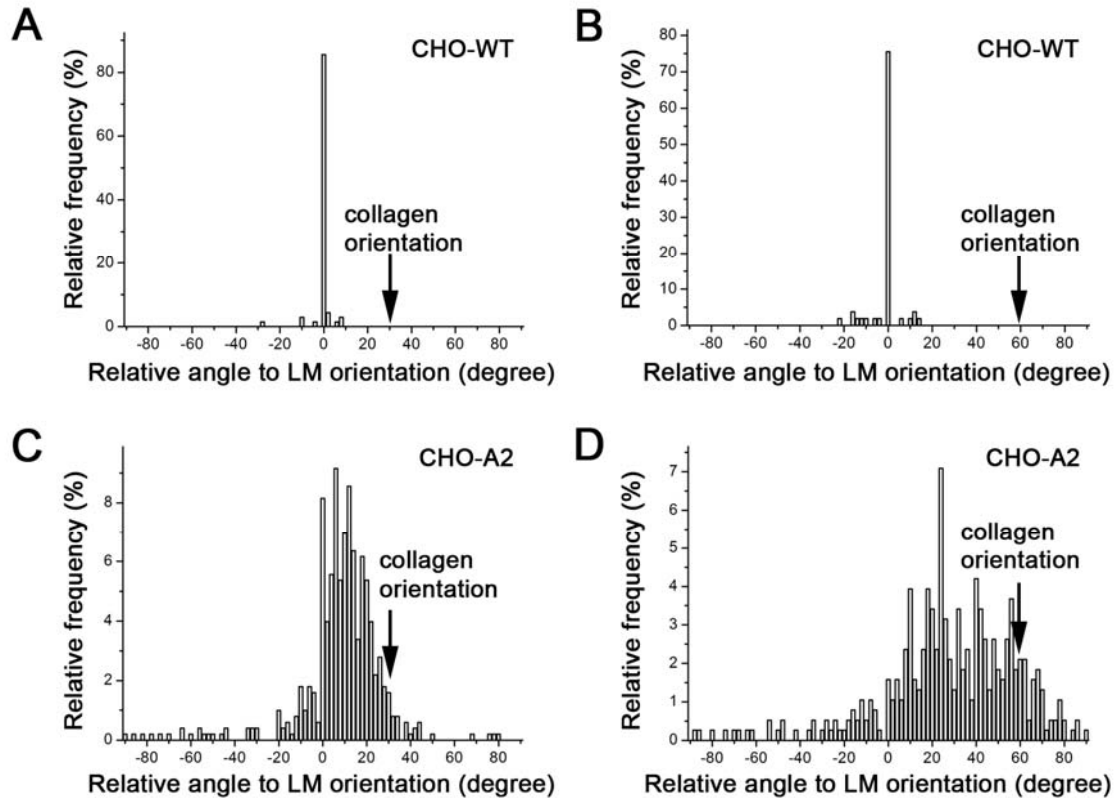


**Fig. 5.5 Quantification of CHO-WT and A2 cell alignment on LM/fCol I substrates.**

LM/Col substrates displaying a laminin to collagen angle of  $30\pm 5$  (A and C) or  $60\pm 5$  (B and D) degrees were grouped. The alignment of CHO-WT (A and B) and CHO-A2 (C and D) cells on the bifunctional substrates are quantified. Orientations of laminin stripes are set to zero, and the angles between the collagen I fibers and the laminin stripes are indicated by black arrows.

### **5.3.4 Integrins containing the $\alpha 6$ subunit are laminin receptors in both CHO-WT and SAOS-WT cells**

CHO-WT and SAOS-WT cells show enhanced adhesion to laminin compared to the corresponding A2 cell lines, suggesting that integrins other than  $\alpha 2\beta 1$  mediate laminin-binding in these cells. For instance, integrin  $\alpha 6\beta 1$  (Aumailley et al., 1990a; Sonnenberg et al., 1990b),  $\alpha 6\beta 4$  (De Luca et al., 1990; Sonnenberg et al., 1990b; Sonnenberg et al., 1991) and  $\alpha 7\beta 1$  (Kramer et al., 1991; von der Mark et al., 1991) are additional receptors for laminin (Belkin and Stepp, 2000). In order to identify the laminin receptors in SAOS-WT cells, SCFS was performed on laminin in the presence of various integrin blocking antibodies. Blocking either the integrin  $\beta 1$  (antibody clone 6S6) or  $\beta 4$  (antibody clone ASC-8) subunits in SAOS-WT does not completely inhibit cell adhesion, however blocking the  $\beta 1$  and  $\beta 4$  subunits leads to a significant reduction of detachment forces. Furthermore, in the presence of the  $\alpha 6$

blocking antibody GoH3, adhesion forces of SAOS-WT on laminin also decreased drastically (**Fig. 5.6 A**). Together, these results indicate that SAOS-WT cells use both integrin  $\alpha_6\beta_1$  and  $\alpha_6\beta_4$  as laminin receptors.

For CHO-WT cells, blocking integrin  $\alpha_6$  subunits also lowers the detachment force on laminin significantly (**Fig. 5.6 B**). However, due to the limited availability of hamster integrin antibodies, the  $\beta$  subunits coupling with the  $\alpha_6$  subunit to form laminin receptors could not be identified. Integrin  $\alpha_7\beta_1$  does not appear to mediate laminin-binding in either cell type, since blocking  $\beta_1$  and  $\beta_4$  together or  $\alpha_6$  alone almost completely prevented laminin binding.

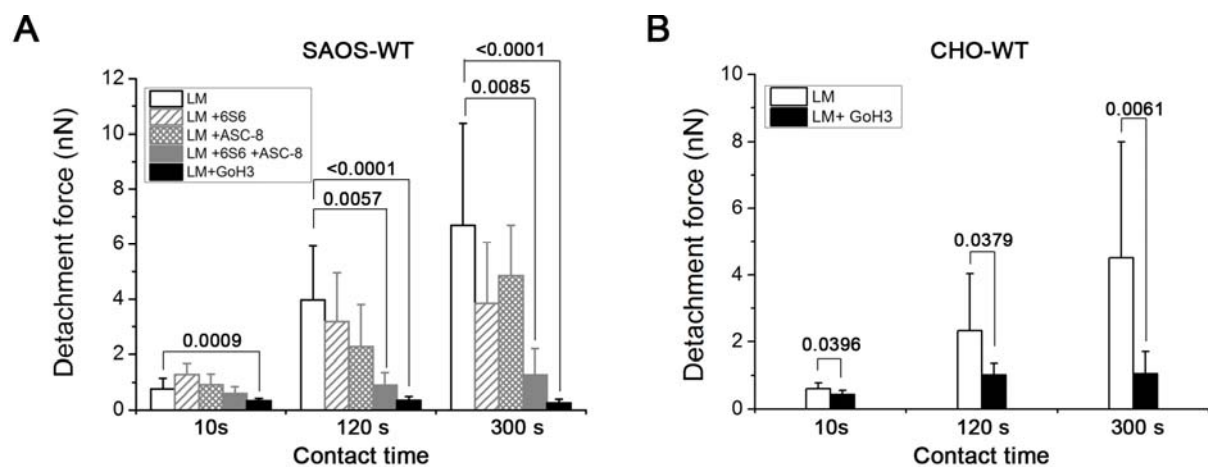


**Fig. 5.6 Adhesion of SAOS-WT and CHO-WT to laminin in the presence of blocking antibodies.**

SAOS-WT (A) and CHO-WT (B) cell adhesion was quantified by SCFS with either the integrin  $\beta_1$  subunit blocking antibody 6S6,  $\beta_4$  subunit blocking antibody ASC-8 or  $\alpha_6$  subunit blocking antibody GoH3. The data are presented in median $\pm$ MAD. At least 10 cells were measured for each time point. p-values (Mann-Whitney test) are indicated.

### 5.3.5 Transcription and expression levels of integrin $\alpha_6$ and $\beta_4$ are downregulated in $\alpha_2\beta_1$ -expressing cells

To elucidate whether reduced adhesion of  $\alpha_2\beta_1$ -expressing cells to laminin results from a lower amount of laminin receptors, the transcription and expression levels of the laminin-binding receptors  $\alpha_6\beta_1$  and  $\alpha_6\beta_4$  cells were analyzed in SAOS-WT and SAOS-A2 cells. This analysis could only be performed in the human SAOS cell line, since suitable antibodies recognizing hamster integrins are not available and DNA sequence information is still missing for the hamster genome. Using quantitative RT-PCR, the mRNA levels of integrin  $\alpha_6$  and  $\beta_4$  were demonstrated to be 5- and 3-fold

lower in  $\alpha_2\beta_1$ -expressing cells than in  $\alpha_2\beta_1$ -deficient ones (**Fig. 5.7 A**). Transcription of the  $\beta_1$  subunit was slightly enhanced (1.4 fold) in A2 cell. In order to analyze the expression levels of both integrins, SAOS-WT and SAOS-A2 cell surface proteins were isolated using the Pierce cell surface protein isolation kit according to the manufacturer's instruction. Together with the total protein extracted from both cell types, cell surface protein was probed for integrin  $\alpha_6$ ,  $\alpha_7$ ,  $\beta_1$  and  $\beta_4$  by SDS-PAGE and western blot. Both surface and total protein levels of integrin  $\alpha_6$  and  $\beta_4$  are more than 4 times lowered in SAOS-A2 cells (**Fig. 5.7 B and C**), corresponding to a similar decrease of the mRNA levels of both integrins. The expression level of  $\beta_1$  showed almost no difference between  $\alpha_2\beta_1$ -expressing and -deficient cell. Thus, a decreased expression of integrin receptors may contribute to the adhesion decrease on laminin in SAOS-A2 cells. Interestingly, integrin  $\alpha_7$  subunit, which plays no role in SAOS-WT cells adhesion to laminin based on the antibody blocking experiments, showed strong upregulation on the mRNA level (**Fig. 5.7 A**) but downregulation in surface and total protein in SAOS-A2 cells (**Fig. 5.7 B and C**). Considering that laminin-111 is the main ligand for integrin  $\alpha_7\beta_1$  (Barczyk et al., 2010), the functional relevance of these opposing changes on the transcription and expression level needs to be further investigated.

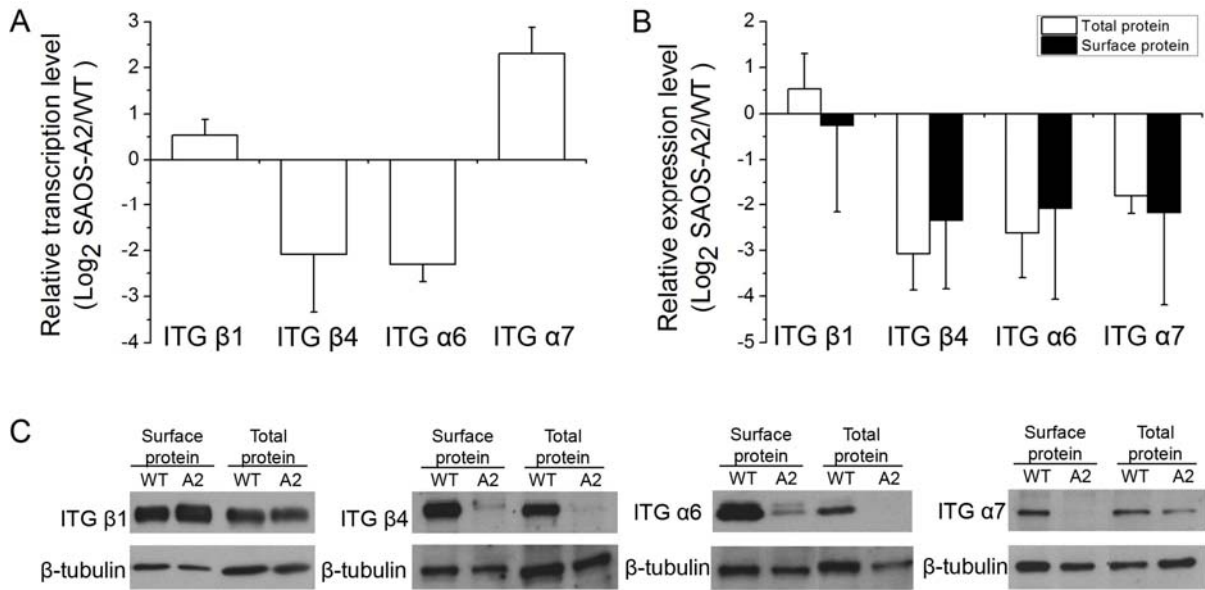


**Fig. 5.7** Transcription and expression levels of integrin subunits in SAOS-WT and -A2 cells.

Quantitative real time RT-PCR (A) and Western blots (B and C) of integrin  $\beta_1$ ,  $\beta_4$ ,  $\alpha_6$  and  $\alpha_7$  subunits of SAOS-WT and SAOS-A2 cells. The transcription and expression levels of the target genes were calculated, as described in Materials and Methods. Data are presented as mean $\pm$ SD. At least 4 independent experiments were performed for each integrin subunits.

### 5.3.6 Integrin $\alpha_6$ and $\beta_4$ expression decreases in SAOS-WT cells transiently expressing integrin $\alpha_2\beta_1$

To exclude that the downregulation of laminin receptors was due to possible cloning artifacts during the establishment of the SAOS-A2 cell line (Ivaska et al., 1999), SAOS-WT cells were transiently transfected with the integrin  $\alpha_2$  subunit, and after 24 h, cell lysates were collected and analyzed for the expression levels of laminin-binding integrins by western blotting. The transiently transfected cells expressed 8 times less integrin  $\alpha_2$  than SAOS-A2 cells (**Fig. 5.8 A**). Despite the comparatively modest  $\alpha_2$  expression level following transient transfection, integrin  $\alpha_6$  and  $\beta_4$  expression was decreased (**Fig. 5.8 A and B**). Corresponding to the lower transient  $\alpha_2$  expression levels,  $\beta_4$  expression was not as strongly reduced from the wild-type level as in the stable SAOS-A2 cells. Apparently, in SAOS cells the extent of laminin receptor downregulation scales with the strength of integrin  $\alpha_2$  expression. In conclusion, stable or transient expression of integrin  $\alpha_2\beta_1$  causes a downregulation of laminin receptors integrin  $\alpha_6\beta_1$  and  $\alpha_6\beta_4$ .

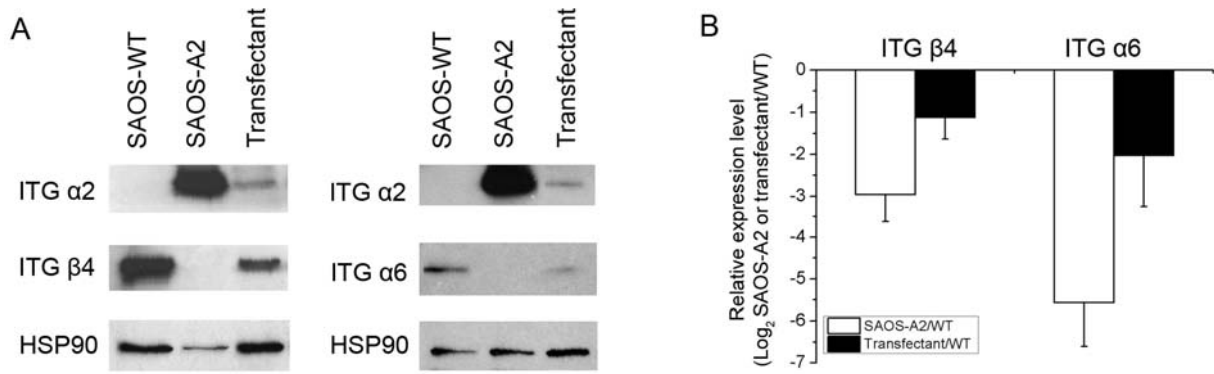


**Fig. 5.8 Integrin  $\beta 4$  and  $\alpha 6$  expression level of SAOS-WT, SAOS-A2 and transiently transfected SAOS-WT cells.**

(A) Western blots against integrin  $\beta 4$  and  $\alpha 6$  in lysates from SAOS-WT, SAOS-A2 and transiently  $\alpha 2$ -transfected SAOS-WT cells. HSP90 was used as a loading control. (B) Relative expression levels of the target (mean $\pm$ SD) were calculated as described in Materials and Methods. At least 3 independent experiments were performed for each integrin subunit.

## **5.4 Discussion**

Many integrin types have several ligands within the ECM. For instance, integrin  $\alpha_3\beta_1$  binds to collagen, laminin and fibronectin, while integrin  $\alpha_v\beta_3$  binds to vitronectin, fibrinogen and laminin (Darribere et al., 2000). Likewise, integrin  $\alpha_2\beta_1$  has been reported as a collagen I and a laminin receptor (Elices and Hemler, 1989; Tulla et al., 2008b). However, the ligand-binding specificity of integrins, including  $\alpha_2\beta_1$ , also depends on the cell type where they are expressed. While integrin  $\alpha_2\beta_1$  binds both laminin and collagen in endothelial cells (Languino et al., 1989) and LOX melanoma cells (Elices and Hemler, 1989), it mediates cellular adhesion solely to collagen in platelets (Kirchhofer et al., 1990) and MeWo melanoma cells (Kramer and Marks, 1989). These findings suggest that the ligand-binding specificity of integrin  $\alpha_2\beta_1$  is modulated by unknown cell-type specific factors. Better understanding the role of a particular integrin receptor, such as  $\alpha_2\beta_1$ , in a certain cell type therefore requires techniques which allow for directly comparing the binding strength of the receptor to its different ligands.

In this context, CHO-WT and -A2 and SAOS-WT and -A2 cells were used to determine the binding strength of integrin  $\alpha_2\beta_1$  to two of its known ligands, laminin-111 and collagen I. Both CHO-A2 and SAOS-A2 cells, which express integrin  $\alpha_2\beta_1$ , adhere stronger to collagen compared to their corresponding  $\alpha_2\beta_1$ -deficient WT cells, indicating that integrin  $\alpha_2\beta_1$  functions as a collagen receptor in both cell types. These results are consistent with previous research performed by Friedrichs et al., (Friedrichs et al., 2007). The A2 cell lines also adhered more strongly to collagen than to laminin, indicating that  $\alpha_2\beta_1$  is a far better collagen than laminin receptor in these cells. However, surprisingly, the  $\alpha_2\beta_1$ -expressing A2 cell lines show lower adhesion to laminin than the WT cells, suggesting that integrin  $\alpha_2\beta_1$  expression in fact downregulates laminin binding.

It has been established that the affinity of the  $\alpha_2$  I-domain to its ligands can increase due to conformational activation (Shimaoka et al., 2001). For example,  $\alpha_2$  I-domain was shown being capable of binding to collagen but barely to laminin by solid phase binding assay. Activation of the  $\alpha_2$  I-domain by locking it in an open conformation through the point mutation E318W not only leads to a significant enhancement of collagen binding ability but also endows  $\alpha_2$  I-domain with remarkably increased

laminin binding ability (Tulla et al., 2008b). As the activation state of integrin  $\alpha_2\beta_1$  has been reported to be dependent on the cell type in which the integrin is expressed (Van de Walle et al., 2005), it is possible that expressed integrin  $\alpha_2\beta_1$  in CHO-A2 and SAOS-A2 cells is only in a semi-open conformation which is sufficient for collagen binding but not laminin binding.

Most cells express multiple integrins to interact with numerous ligands in their environment. The coordination of integrin signaling in to a net effect that influences cell behavior has been named integrin crosstalk (Blystone et al., 1999). Integrin crosstalk has been demonstrated in many cell types such as epithelial cells (Tomatis et al., 1999), Keratinocytes (Goldfinger et al., 1999) and platelets (Riederer et al., 2002). Furthermore, integrin crosstalk is usually unidirectional: the transducer integrin influences the target integrins, but not vice versa. Most of the reported integrin crosstalk requires ligation of the transducer integrin. In this case, integrin activation is closely related to the process and therefore intact integrin cytoplasmic domains are indispensable (Gonzalez et al., 2010). Several proteins like Matrix metalloproteinase (Baciu et al., 2003), calcium/calmodulin-dependent protein kinase II (Blystone et al., 1999), talin (Calderwood et al., 2004) and protein kinase A (Gonzalez et al., 2008) are reported as the key regulators of ligand-dependent integrin crosstalk.

Another class of integrin crosstalk is ligation-independent. For example, inhibition of integrin  $\alpha_3\beta_1$  in human breast carcinoma cells with an antibody that binds to the  $\beta$ -propeller domain of  $\alpha_3$  subunit increases integrin  $\alpha_2\beta_1$ -mediated cell adhesion to collagen (Lichtner et al., 1998). Also, expression of integrin  $\alpha_2\beta_1$  in the mouse breast carcinoma cell line Mm5MT results in upregulation of integrin  $\alpha_6\beta_4$  (Sun et al., 1998). So far the general mechanisms underlying ligation-independent integrin crosstalk have not been discovered. In this project, inverse integrin regulation in CHO cells and SAOS cells were conducted on the mRNA and protein level. No evidence for involvement of any signaling crosstalk has been discovered. Therefore the reported  $\alpha_2\beta_1$  and  $\alpha_6$  integrin coordination does not likely to follow either of the above mentioned integrin crosstalk mechanisms.

Transcriptional and post-transcriptional mechanisms for varying the integrin repertoire at the cell surface have been described in previous reports (Gingras et al.,

2003; Liang et al., 2004; Demetriou et al., 2008). These mechanisms either work through transcriptional regulation, altering the relative expression level of one integrin to another, or through localized regulation of integrin-ECM interactions (Meighan and Schwarzbauer, 2008). In this project, real time RT-PCR demonstrated that the mRNA levels of integrin  $\alpha_6$  and  $\beta_4$  decrease after  $\alpha_2\beta_1$  expression, suggesting that transcriptional mechanisms may underlie the inverse regulation.

Transcription requires binding of specific transcription factors to the gene promoter region (Latchman, 1997). Sp1 is a member of the Zn-finger family of transcription factors (Zhao and Meng, 2005). Six, two and five target sites for Sp1 were identified in the  $\alpha_2$ ,  $\alpha_6$  and  $\beta_4$  gene promoters respectively (Zutter et al., 1994; Lin et al., 1997; Takaoka et al., 1998; Gaudreault et al., 2007). As binding of Sp1 positively influences the activity of  $\alpha_2$ ,  $\alpha_6$  and  $\beta_4$  promoters, increased recruitment of Sp1 to the  $\alpha_2$  promoter would leave fewer Sp1 molecules for the  $\alpha_6$  and  $\beta_4$  promoters, reducing  $\alpha_6$  and  $\beta_4$  transcription activity and lowering  $\alpha_6$  and  $\beta_4$  mRNA levels. Competition for a shared transcription factor could thus explain the opposing regulation of these genes. However, the  $\alpha_2$  expression plasmid used for stable or transient transfections contains a viral promoter (Friend spleen focus-forming virus long terminal repeat) instead of the natural promoter (Ohashi et al., 1985; Riikonen et al., 1995; Baum et al., 1997). The exogenous  $\alpha_2$  gene may therefore be regulated differently than the endogenous gene. Interestingly however, there is also a Sp1 binding site located within the viral promoter of the  $\alpha_2$  plasmid, raising the possibility that competition for Sp1 regulates the collagen and laminin receptor levels also in the transfected cells. In order to see whether the introduction of extra Sp1 binding site by transfection contributes to the lowered  $\alpha_6$  and  $\beta_4$  mRNA and protein levels, small interfering RNA targeting  $\alpha_2$  integrin can be introduced into an untransfected  $\alpha_2$ -expressing cell line. If decreased  $\alpha_6$  and  $\beta_4$  transcription and expression are still observed, the inverse regulation is not ascribed to the transcription factor competition.

Integrin levels may also be regulated on the post-transcriptional level. Considering that the  $\beta_4$  subunit only associates with the  $\alpha_6$  subunit and that integrin  $\alpha_6\beta_4$  is only stable as the dimeric protein on cell surface (Rigot et al., 1999), the concurrent decrease in cell surface expression of  $\alpha_6$  and  $\beta_4$  subunits in A2 cells may be ascribed to the reduction of  $\alpha_6$  surface expression as the primary cause. A possible



explanation for reduced  $\alpha_6$  surface expression could be the competitive recruitment of  $\beta_1$  subunits from endogenous  $\alpha_6$  by high levels of transfected  $\alpha_2$ . However, the exact mechanisms by which  $\alpha_2$  expression leads to reduced  $\alpha_6$  and  $\beta_4$  subunits transcription and expression deserves further research.

Shifting the balance between collagen and laminin receptors could have significant influence on cell behavior, such as metastasis. Laminin forms a major component of the basement membrane, a thin, sheet-like structure of the ECM that serves as a carrier for the epithelium (Durbeej, 2010). During malignant cell invasion and metastasis, the basement membrane is often penetrated or dissolved, and cell adhesion to laminin is therefore of great importance in this process (Patarroyo et al., 2002). In fact, exogenous laminin enhances the metastatic potential of malignant cells (Malinoff et al., 1984; Terranova et al., 1984). Integrins  $\alpha_6\beta_1$  and  $\alpha_6\beta_4$  are the dominant laminin receptors in many cell types (Aumailley et al., 1990a), and this significance in adhesion to laminin makes them a major indicator of metastasis (Pawelek and Chakraborty, 2008). For instance, upregulation of integrin  $\alpha_6\beta_1$  endows sarcoma cells with the capability to invade basement membranes (Kielosto et al., 2009), while expression of integrin  $\alpha_6\beta_4$  is associated with the formation, migration, invasion, and survival of carcinoma cells (Mercurio and Rabinovitz, 2001; Bertotti et al., 2005). Immunohistochemical studies have colocalized laminin and integrin  $\alpha_6\beta_4$  at the invasive front of gastric carcinoma in vivo (Tani et al., 1996). Collagens, as the most abundant protein family in the ECM, together with collagen-binding integrins also play a significant role in the invasion of malignant cells (Staniszewska et al., 2009). Integrin  $\alpha_2\beta_1$  expression is decreased in adenocarcinoma of the breast, as well as other epithelial malignancies, in a manner that correlates with the degree of tumor cell differentiation (Stallmach et al., 1992; Pignatelli and Stamp, 1995). Although there are conflicting reports (Kostenuik et al., 1996), it appears that consistent diminution or loss of  $\alpha_2\beta_1$  expression corresponds to higher grade tumors (Zutter et al., 1995; Mirtti et al., 2006). Therefore,  $\alpha_2\beta_1$  could have a double role in preventing metastasis – by enhancing cell adhesion to collagen and by suppressing the expression of invasion-promoting laminin receptors. In this way, CHO-A2 and SAOS-A2 cells, which express lower amounts of laminin receptor  $\alpha_6\beta_1$  and  $\alpha_6\beta_4$  and

higher levels of collagen receptor  $\alpha_2\beta_1$  may represent a less malignant and invasive phenotype than the corresponding wild type cells.

Another possible physiological importance of the inverse regulation between integrin  $\alpha_2\beta_1$  and  $\alpha_6\beta_4$  may lie in a significant role of these receptors during epithelial-mesenchymal transition (EMT), which occurs while embryo development as well as the transition from confined tumor to invasive malignancy (Radisky, 2005). An increase in integrin  $\alpha_2\beta_1$  expression during EMT induced by fibroblast growth factor-1 has been observed in a rat bladder carcinoma cell line (Valles et al., 1996) and during hepatocyte growth factor-triggered EMT in MDCK cells (Chiu et al., 2002). On the other hand, expression of integrin  $\alpha_6\beta_4$  is lost during EMT induced by transforming growth factor- $\beta$  in mouse mammary gland cells (Yang et al., 2009). The data acquired from CHO and SAOS cells suggest that  $\alpha_2\beta_1$ -deficient and expressing cells may correspond to the cell before and after EMT.

In conclusion, it could be established that integrin  $\alpha_2\beta_1$  is an efficient collagen but not laminin receptor in CHO and SAOS cells. Furthermore, introduction of exogenous integrin  $\alpha_2\beta_1$  downregulates mRNA and protein levels of the laminin receptors integrin  $\alpha_6\beta_1$  and  $\alpha_6\beta_4$ , suggesting an inverse regulation between integrin  $\alpha_2\beta_1$  and laminin receptors. By combining cell spreading assays and single-cell force spectroscopy on bifunctional substrates with classic mRNA and protein analysis methods, new insight into mechanisms of integrin cross-talk could thus be gained. The opposing regulation of collagen and laminin receptors could play a role during metastasis and EMT, but the functional relevance of this inverse regulation still needs to be established.

## 6 Summary of the projects

---

Using SCFS as a powerful tool to quantify adhesion forces at the single cell scale, different aspects of integrin-mediated cell adhesion to ECM are investigated in the previously described projects. In Chapter 4, comparative SCFS was invented. Two ECM components were incorporated on the same surface by innovative  $\mu$ CP techniques, which allow direct comparison of a single cell adhesion to two different ECM proteins. By using relatively short contact time, single CHO cells retain specific adhesion to laminin and collagen without being influenced by the preceding measurements. The adhesion forces of individual CHO cells to different ECM do not correlate with each other, indicating that the different integrins within the same cell are independently regulated. Measuring single CHO cell on laminin many times generates narrow force distribution, while pooling the adhesion forces of CHO cell population renders broad distribution. In Chapter 5, these cell-to-cell adhesion variations are revealed to be non-genetic and cell cycle independent, but correlate with receptor number variations on the cell surface, which is suggested to be an intrinsic property of cell population cultured *in vitro*. In Chapter 6, the binding affinity of a specific integrin  $\alpha_2\beta_1$  to two ECM components laminin and collagen was investigated. This integrin was confirmed to be a collagen receptor but not a laminin receptor in both CHO and SAOS cells systems. Furthermore, the expression of integrin  $\alpha_2\beta_1$  contributes to the downregulation of endogenous laminin receptors  $\alpha_6\beta_1$  and  $\alpha_6\beta_4$  at both mRNA and protein levels. As inverse regulation between the  $\alpha_2$  and  $\alpha_6$  integrins are closely related to cancer progression, this work may shed new light into cancer treatment. In summary, not only single cell adhesion but also individual integrin affinity to different ECM proteins can be compared. Integrin expression variation, as an intrinsic property of *in vitro* cell population can also be regulated by the expression of other integrins. SCFS are the essential tool in obtaining all those conclusions.

## 7 Concluding remarks

---

### 7.1 Bifunctional substrates expand the scope of SCFS

Cell adhesion to the ECM is of great importance to many biological processes such as embryogenesis, metastasis and wound healing. Better understanding cell-ECM interactions via integrin receptors requires quantitative assays which are not only capable of distinguishing single-cell adhesion behavior against the adhesion of the whole cell population but which are also able to address the relative contribution of individual ECM components to overall adhesion of a cell. The presented work introduces a “comparative SCFS” technique which fulfills all those requirements and which can be used to compare single-cell adhesion on two different ECM molecules directly. A key element of this technique is bifunctional substrates featuring microstripes of two different ECM molecules. The substrates are designed in a way that both ECM molecules can be alternately reached by the *xy*-positioning system of the AFM.

For the first time, micropatterns were fabricated featuring fibrillar collagen I organized into nanoscale fibrils, which is the common morphology of collagen I in many tissues. Under suitable buffer conditions, collagen I self-assembles into fibrils on mica surfaces. The fibrillar arrangement presents an important advantage over previous microstructured substrates carrying monomeric and thus potentially unphysiological collagen coatings. In Chapter 4, it was validated that both integrin  $\alpha_1\beta_1$  and  $\alpha_2\beta_1$  have high binding affinities to fibrillar collagen I while only  $\alpha_1\beta_1$  binds efficiently to monomeric collagen I. However, it should be pointed out that micropatterned fibrillar collagen substrates can only be produced on mica surfaces, which limits their application in many light microscopy applications due to the poor optical properties of mica. The backfilling collagen solution only covered the areas left barren by the preceding  $\mu$ CP step. Since a key step of this printing technique is the subsequent protein adsorption to the protein-vacant areas on the substrate, it is important that both proteins do not interact with each other, as in this case the second protein would bind both to the first protein and to the remaining areas on the substrate. However, collagen I, collagen IV, laminin, or BSA do not bind each other and can thus be freely

combined to fabricate multiple protein substrates for comparative SCFS. Vitronectin and fibronectin do not bind each other but have high affinities to different types of collagen (Gebb et al., 1986; Guidry et al., 1990). Furthermore, fibronectin has been shown to lose its bioactivity during the stamping process (von Philipsborn et al., 2006a). Backfilling may therefore be a suitable approach to retain the biological activity of fibronectin in microstructured substrates. For the visualization of the printed protein microstructures, a fluorescent dye can be added, as long as the dye does not influence cell adhesion.

Besides establishing methods to produce substrates featuring alternating ECM microstripes using different  $\mu$ CP techniques, a protocol to produce protein/PEG substrates was developed. The PEG surfaces produced using this method gave consistently low cell adhesion forces for contact times of up to 5 min (longest tested time). The PEG surfaces are therefore useful for determining background adhesion of different cell types by SCFS. Here, laminin/PEG and BSA/PEG substrates were tested. In theory, the printing technique could be easily extended to fabricate any combination of protein/PEG substrates by substituting laminin or BSA with other proteins in the last manufacturing step (see section 2.2.1.1 and Fig. 2.1).

## 7.2 Multifunctional ECM adhesion substrates for comprehensive single-cell adhesion profiling

In this work integrin-mediated adhesion of a single cell to two different ECM components was compared. To more comprehensively characterize the adhesion repertoire of a cell, it would be desirable to measure adhesion to additional ligands. Multiprotein micropatterns could be achieved by performing multiple rounds of lift-off  $\mu$ CP (von Philipsborn et al., 2006a) using several Si wafers. In principle,  $N$  rounds of lift-off could generate micropatterns displaying  $N+1$  types of proteins. Fig. 7.1 depicts a possible procedure of fabricating substrates containing 3 proteins: A cuboid of PDMS is homogeneously coated with a protein  $A$  and brought into contact with a micropatterned Si wafer. The relief structure of the Si wafer comes into contact with the protein coating and locally removes protein  $A$  from the PDMS cuboid (Fig. 7.1 A). Afterwards, a solution of a protein  $B$  is added onto the PDMS cuboid, coating only the bared PDMS surfaces. A Si wafer 2 is then used to remove proteins  $A$  and  $B$  within certain regions (Fig. 7.1 B). The remaining protein  $A$  and  $B$  micropatterns are then

transferred to a mica or glass surface by stamping (**Fig. 7.1 C**). Finally, the mica or glass surface is incubated with a protein C solution so that protein C covers the remaining areas on the mica. If the geometry of the Si wafers is designed properly, all three proteins can be reached by the *xy*-positioning system of the AFM (**Fig. 7.1 D**). In this way, the adhesive repertoire of individual cells could be characterized more comprehensively by SCFS using several types of ECM components.

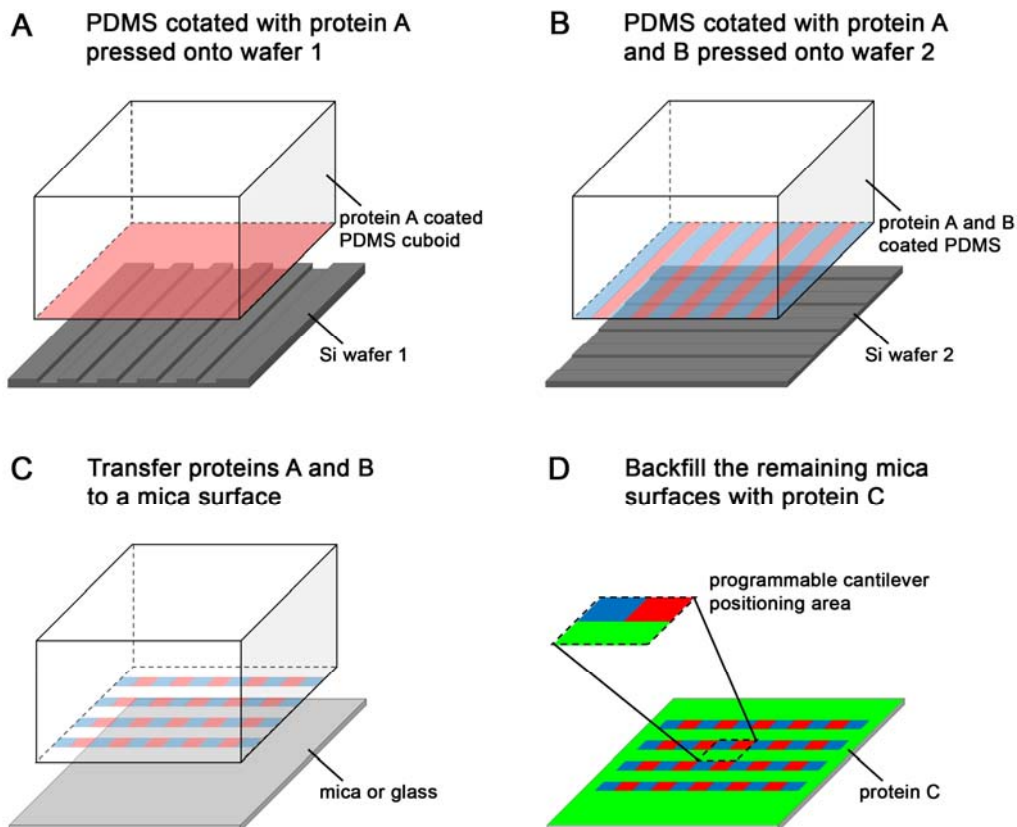


**Fig. 7.1 Printing micropatterns consisting of three different proteins.**

(A) A PDMS cuboid is covered with protein A. By contacting the cuboid with a patterned Si wafer, protein A is adsorbed onto the relief structure. (B) The PDMS cuboid is then coated with protein B, which will only cover the blank areas on the PDMS. The PDMS cuboid is then pressed onto a new structured Si wafer. Both proteins will adsorb only to ridge structures on the wafer. (C) When the PDMS cuboid is subsequently pressed onto glass or mica, the ECM proteins are transferred to the new surface. (D) After adding a protein C solution to the glass or mica, the remaining areas are covered by protein C. All three proteins are available for the *xy*-cantilever positioning system of the AFM.

In addition to  $\mu$ C-printed substrates, ECM microarrays are emerging as another promising tool for analyzing differential cell adhesion to ECM components (Kuschel et al., 2006; Hattori et al., 2010). By means of alternative micropatterning techniques,

such as piezoelectric microspotting or microfluidic patterning, micrometer-sized patterns of ECM proteins are deposited on a non-adhesive background. Cells are then seeded onto the microarray and grown for a controlled time before the unattached cells are removed by rinsing with buffers. The remaining cells on each ECM spot are then quantified. ECM microarrays permit extensive comparative cell adhesion profiling on many ECM components within a short time, using minimized cell numbers and ECM protein amount. In its latest development, the “microenvironment array chip”, different soluble factors can be freely combined with the ECM substrates, thereby creating a more versatile environment for cell adhesion screening (Hattori et al., 2011). Using such a microarray chip, CHO cell adhesion to laminin was found to be stronger than on collagen I, similar to the quantitative data obtained by SCFS in Chapters 3 and 4. However, in contrast to comparative SCFS, ECM microarray profiling is a semi-quantitative assay which focuses on cell population behavior while cell-to-cell adhesion variation cannot be studied.

### **7.3 The cell/substrate contact history has no influence on subsequent adhesion measurements by SCFS at short contact times**

Repeated measurements of individual CHO cells on laminin/collagen substrates using short contact times showed a consistent and ECM type-specific adhesion response mirroring the adhesion receptor repertoire of the cells and the longer-term spreading behavior (16 h) on the same bifunctional substrates. SCFS measurements at relatively short contact times can therefore provide useful information explaining more long-term adhesion responses of cells.

For a given contact time, in SCFS several force measurements are usually performed on the same cell to improve the statistical evidence. However, questions such as whether preceding measurements influence later measurements and how many force cycles suffice to obtain robust statistics had not been thoroughly addressed previously. By measuring CHO cell adhesion on laminin/collagen substrates for many force cycles (>60), it was validated that for short contact times (10 s), the force measurement sequence or the force cycle number has no influence on the detachment forces. However, performing more than 20-25 force cycles does not improve the statistic validity, since the standard deviation of the measurements

approach the system-inherent sensitivity limits set by the thermal noise of the cantilever. Given the large variability of cell adhesion properties in a population, the experimental resources are then better invested in testing a larger number of cells.

#### **7.4 Determining integrin affinities to different collagen subtypes may facilitate the selection of suitable coatings for biomaterials**

Integrin  $\alpha_1\beta_1$  and  $\alpha_2\beta_1$  have been reported to have different affinities to different collagen subtypes, such as monomeric and fibrillar collagen I or collagen IV. However, this conclusion was based on semi-quantitative assays testing the binding efficiency of recombinant integrin  $\alpha$  I-domains (Nykqvist et al., 2000; Tulla et al., 2001; Zhang et al., 2003). In this dissertation, adhesion of individual  $\alpha_1\beta_1$ - or  $\alpha_2\beta_1$ -expressing cells to different collagen subtypes was measured, testing the integrin receptors in their physiological environment on the membrane of living cells. Integrin  $\alpha_1\beta_1$  was shown to have a high affinity for monomeric collagen I, fibrillar collagen I and collagen IV, while integrin  $\alpha_2\beta_1$  only showed strong binding to fibrillar collagen I. Owing to its outstanding mechanical properties and universal expression in various tissues (Di Lullo et al., 2002), collagen is widely used in tissue engineering as a coating material (Lee et al., 2001; Ramshaw et al., 2009). Identifying the binding preference of different integrins may facilitate the selection of suitable collagen coatings according to the cell and tissue types and in this way further optimize the biocompatibility of the artificial material.

#### **7.5 Adhesion receptor variation within cell populations as a potential strategy to cope with evolutionary pressure**

Cell populations often display cell-to-cell variations in behavior, including adhesion to ECM components. For instance, testing the adhesion of many cells CHO cells revealed a broad force distribution. In contrast, measuring single CHO cells many times rendered much narrower force distributions. Superimposing the force distributions from individual cells measured repeatedly (30 times) generates a distribution which is as broad as a distribution collected from measuring 30 cells once each. Therefore, broad adhesion distributions in cell populations are caused by cell-to-cell variations rather by large fluctuations in the adhesive response of individual cells. It was furthermore validated that the observed adhesive variations in the cell population are non-genetic and cell cycle-independent but that they instead scale



with the range of  $\alpha 6$  integrin expression on the cell surface. Therefore, adhesion variability caused by variations of the receptor number on the cell surface appears to be an intrinsic feature of cells populations cultured *in vitro*. In nature, organisms are under constant evolutionary pressure. A stochastic expression of integrin receptors in a uniform cell population may generate a range of adhesion responses to different extracellular stresses and increase the likelihood of survival (**Fig. 7.2 A**). The absolute and relative scales of adhesion to laminin and collagen I also varied strongly between CHO cells, demonstrating that collagen and laminin binding are regulated independently for each cell and this may be ascribed to intrinsic cell-to-cell variations in integrin receptor expression.

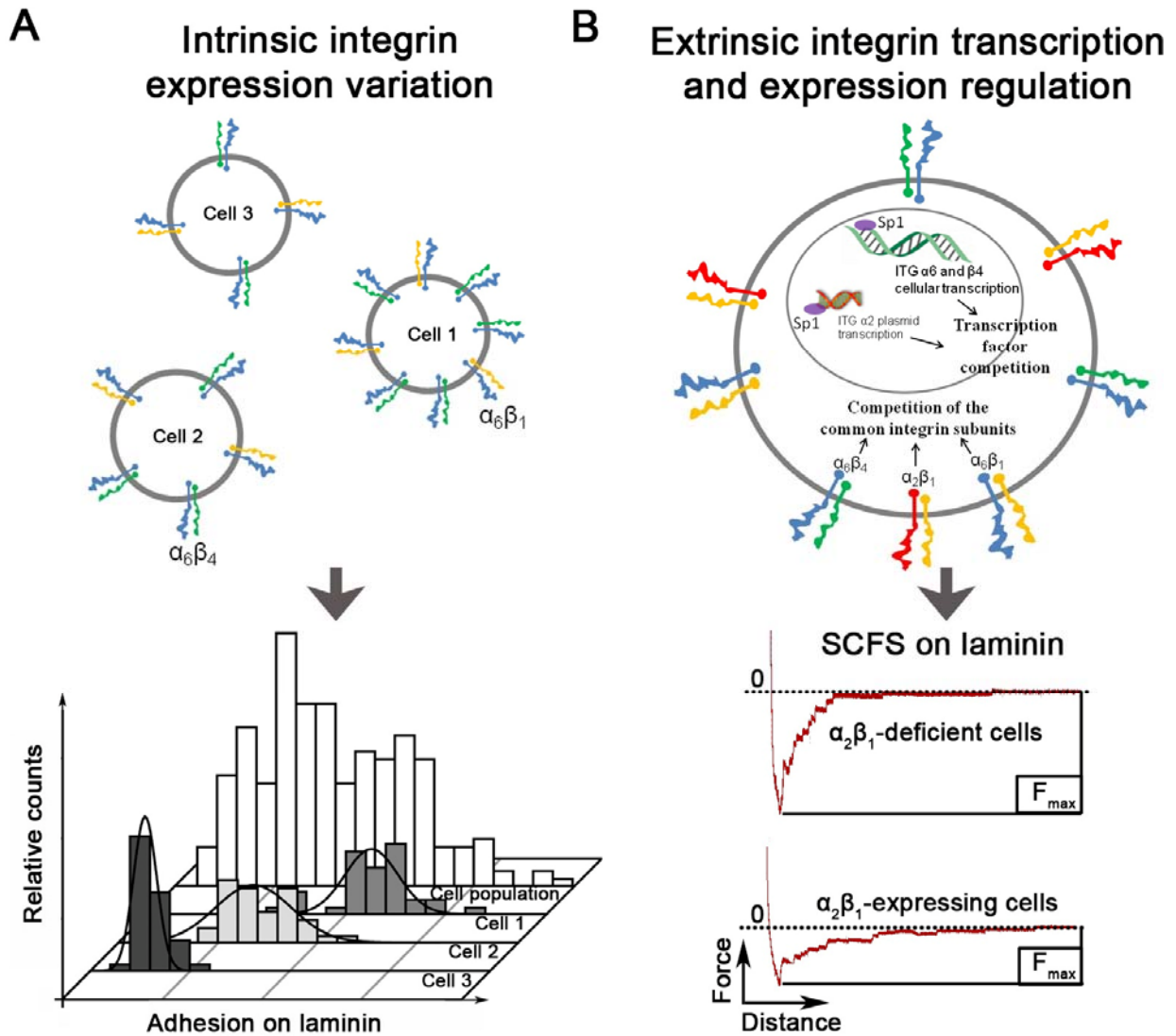


**Fig. 7.2 Intrinsic variation and extrinsic regulation of laminin-binding integrins.**

(A) Cell-to-cell variations in the expression of the laminin receptor integrin  $\alpha_6\beta_1$  and  $\alpha_6\beta_4$  are an intrinsic property of clonal cell population, leading to a broad adhesion force distribution of the CHO cell population but a narrow force distribution of individual cells. (B) The introduction of the exogenous  $\alpha_2$  gene may cause competition between transcription factors and between other shared integrin subunits, resulting in decreased  $\alpha_6\beta_1$  and  $\alpha_6\beta_4$  mRNA and protein levels. The reduced number of laminin receptors in  $\alpha_2\beta_1$ -expressing cells causes lower adhesion to laminin.

Integrin expression can not only be regulated intrinsically in a random manner, but also can be regulated extrinsically in a unidirectional way by expression of exogenous integrins. For instance, expression of integrin  $\alpha_2\beta_1$  in CHO cells and SAOS cells leads to the downregulation of mRNA and protein levels of the laminin-binding integrins  $\alpha_6\beta_1$  and  $\alpha_6\beta_4$  and further contributes to the cell adhesion decrease to laminin. This effect becomes apparent 24 h after transfection, indicating a relatively

fast feedback happening within this time frame. The cause for this unidirectional regulation may be a competition for the transcription factor Sp1 and/or the limited availability of shared integrin subunits on the cell surface (**Fig. 7.2 B**). Nevertheless, further experiments are required to identify the key molecules and signalling pathways controlling this process.

Gene transfection or knockdown is widely used to introduce exogenous integrin into cells or to eliminate endogenous integrins from cells. When comparing the behavior of wild type cells to transfected or to knockdown cells, the observed differences are usually attributed to the transfected or eliminated integrin. However, the results presented in Chapter 5 underline that the introduction or ablation of integrin genes may have profound and global influences on the cells, in particular on the transcription, expression and activity of other integrins. These possible consequences should be considered when try to elucidate the function of particular integrin subtype by transfection or knockdown.

## **7.6 AFM-based SCFS as a versatile tool to characterize integrin-mediated adhesion profile of single cells**

There is an ever increasing demand for better understanding cell adhesion processes between cells and the ECM, in particular regarding the precise contribution of individual adhesion receptor types to overall cell adhesion. During the last years several advanced adhesion techniques have been developed to characterize adhesion of single cells. Of these techniques, AFM-based SCFS features the most versatile force range and has been applied in this dissertation to characterize integrin-mediated adhesion profiles of single cells and of entire cell populations to different ECM proteins. The results demonstrate that important cell adhesion information can only be obtained by using a sensitive and quantitative single-cell technique and not from semi-quantitative bulk assays. A current drawback of SCFS is that it requires a relatively long experimental procedure to obtain statistically relevant data and that it is limited to investigating early adhesion events (<20 min). However, these drawbacks are offset by the unique ability to quantify receptor-mediated cell adhesion under physiological conditions over a unique force range starting from the single molecule level to overall adhesion in the same experimental setup. In the future, SCFS performed on complex multi-functional adhesion substrates may

harbour the unique chance to comprehensibly characterize the adhesion profile of single cells, providing important input for many biological and medical applications.

## Bibliography

---

- Abair, T.D., Sundaramoorthy, M., Chen, D., Heino, J., Ivaska, J., Hudson, B.G., Sanders, C.R., Pozzi, A., and Zent, R.** (2008). Cross-talk between integrins alpha1beta1 and alpha2beta1 in renal epithelial cells. *Exp Cell Res* **314**, 3593-3604.
- Abercrombie, M., and Dunn, G.A.** (1975). Adhesions of fibroblasts to substratum during contact inhibition observed by interference reflection microscopy. *Exp Cell Res* **92**, 57-62.
- Adams, J.C.** (2002). Regulation of protrusive and contractile cell-matrix contacts. *J Cell Sci* **115**, 257-265.
- Alam, N., Goel, H.L., Zarif, M.J., Butterfield, J.E., Perkins, H.M., Sansoucy, B.G., Sawyer, T.K., and Languino, L.R.** (2007). The integrin-growth factor receptor duet. *J Cell Physiol* **213**, 649-653.
- Alberts, B., Johnson, A., Lewis, J., Raff, M., Roberts, K., and Walter, P.** (2008). *Molecular Biology of the Cell*. (New York: Garland Science).
- Alom Ruiz, S., and Chen, C.S.** (2007). Microcontact printing: A tool to pattern. *Soft Matter* **3**, 168-177.
- Alonso, J.L., Essafi, M., Xiong, J.P., Stehle, T., and Arnaout, M.A.** (2002). Does the integrin alphaA domain act as a ligand for its betaA domain? *Curr Biol* **12**, R340-342.
- Altschuler, S.J., and Wu, L.F.** (2010). Cellular heterogeneity: do differences make a difference? *Cell* **141**, 559-563.
- Anderson, A.B., and Robertson, C.R.** (1995). Absorption spectra indicate conformational alteration of myoglobin adsorbed on polydimethylsiloxane. *Biophys J* **68**, 2091-2097.
- Andersson, M., Madgavkar, A., Stjerdahl, M., Wu, Y., Tan, W., Duran, R., Niehren, S., Mustafa, K., Arvidson, K., and Wennerberg, A.** (2007). Using optical tweezers for measuring the interaction forces between human bone cells and implant surfaces: System design and force calibration. *Rev Sci Instrum* **78**, 074302.
- Armani, D., Liu, C., and Aluru, N.** (1999). Re-configurable fluid circuits by PDMS elastomer micromachining. In *Micro Electro Mechanical Systems, 1999. MEMS '99. Twelfth IEEE International Conference on*, pp. 222-227.
- Arnaout, M.A., Mahalingam, B., and Xiong, J.P.** (2005). Integrin structure, allostery, and bidirectional signaling. *Annu Rev Cell Dev Biol* **21**, 381-410.
- Ashkin, A., Dziedzic, J.M., Bjorkholm, J.E., and Chu, S.** (1986). Observation of a single-beam gradient force optical trap for dielectric particles. *Opt Lett* **11**, 288.
- Aumailley, M., and Gayraud, B.** (1998). Structure and biological activity of the extracellular matrix. *J Mol Med (Berl)* **76**, 253-265.
- Aumailley, M., Timpl, R., and Sonnenberg, A.** (1990a). Antibody to integrin alpha 6 subunit specifically inhibits cell-binding to laminin fragment 8. *Exp Cell Res* **188**, 55-60.
- Aumailley, M., Nurcombe, V., Edgar, D., Paulsson, M., and Timpl, R.** (1987). The cellular interactions of laminin fragments. Cell adhesion correlates with two fragment-specific high affinity binding sites. *J Biol Chem* **262**, 11532-11538.
- Aumailley, M., Gerl, M., Sonnenberg, A., Deutzmann, R., and Timpl, R.** (1990b). Identification of the Arg-Gly-Asp sequence in laminin A chain as a latent cell-binding site being exposed in fragment P1. *FEBS Lett* **262**, 82-86.
- Aumailley, M., Bruckner-Tuderman, L., Carter, W.G., Deutzmann, R., Edgar, D., Ekblom, P., Engel, J., Engvall, E., Hohenester, E., Jones, J.C., Kleinman, H.K., Marinkovich, M.P., Martin, G.R., Mayer, U., Meneguzzi, G., Miner, J.H., Miyazaki, K., Patarroyo, M., Paulsson, M., Quaranta, V., Sanes, J.R., Sasaki, T., Sekiguchi, K., Sorokin, L.M., Talts, J.F., Tryggvason, K., Uitto, J., Virtanen, I., von der Mark, K., Wewer, U.M., Yamada, Y., and Yurchenco, P.D.** (2005). A simplified laminin nomenclature. *Matrix Biol* **24**, 326-332.
- Azab, W., and Osterrieder, N.** (2012). Glycoproteins D of equine herpesvirus type 1 (EHV-1) and EHV-4 determine cellular tropism independently of integrins. *J Virol* **86**, 2031-2044.

- Baciu, P.C., Suleiman, E.A., Deryugina, E.I., and Strongin, A.Y.** (2003). Membrane type-1 matrix metalloproteinase (MT1-MMP) processing of pro- $\alpha$ v integrin regulates cross-talk between  $\alpha$ v $\beta$ 3 and  $\alpha$ 2 $\beta$ 1 integrins in breast carcinoma cells. *Exp Cell Res* **291**, 167-175.
- Bailey, A.J., Sims, T.J., and Light, N.** (1984). Cross-linking in type IV collagen. *Biochem J* **218**, 713-723.
- Barczyk, M., Carracedo, S., and Gullberg, D.** (2010). Integrins. *Cell Tissue Res* **339**, 269-280.
- Barge, A., Ruggiero, F., and Garrone, R.** (1991). Structure of the basement membrane of corneal epithelium: quick-freeze, deep-etch comparative study of networks deposited in culture and during development. *Biology of the Cell* **72**, 141-147.
- Baum, C., Itoh, K., Meyer, J., Laker, C., Ito, Y., and Ostertag, W.** (1997). The potent enhancer activity of the polycythemic strain of spleen focus-forming virus in hematopoietic cells is governed by a binding site for Sp1 in the upstream control region and by a unique enhancer core motif, creating an exclusive target for PEBP/CBF. *J Virol* **71**, 6323-6331.
- Beck, K., Hunter, I., and Engel, J.** (1990). Structure and function of laminin: anatomy of a multidomain glycoprotein. *Faseb J* **4**, 148-160.
- Beglova, N., Blacklow, S.C., Takagi, J., and Springer, T.A.** (2002). Cysteine-rich module structure reveals a fulcrum for integrin rearrangement upon activation. *Nat Struct Biol* **9**, 282-287.
- Belkin, A.M., and Stepp, M.A.** (2000). Integrins as receptors for laminins. *Microscopy Research and Technique* **51**, 280-301.
- Benoit, M., and Gaub, H.E.** (2002). Measuring cell adhesion forces with the atomic force microscope at the molecular level. *Cells Tissues Organs* **172**, 174-189.
- Benoit, M., Gabriel, D., Gerisch, G., and Gaub, H.E.** (2000). Discrete interactions in cell adhesion measured by single-molecule force spectroscopy. *Nat Cell Biol* **2**, 313-317.
- Berrier, A.L., and Yamada, K.M.** (2007). Cell-matrix adhesion. *J Cell Physiol* **213**, 565-573.
- Bertotti, A., Comoglio, P.M., and Trusolino, L.** (2005).  $\beta$ 4 Integrin Is a Transforming Molecule that Unleashes Met Tyrosine Kinase Tumorigenesis. *Cancer Research* **65**, 10674-10679.
- Biasco, A., Pisignano, D., Krebs, B., Pompa, P.P., Persano, L., Cingolani, R., and Rinaldi, R.** (2005). Conformation of microcontact-printed proteins by atomic force microscopy molecular sizing. *Langmuir* **21**, 5154-5158.
- Bigi, A., Gandolfi, M., Roveri, N., and Valdré, G.** (1997). In vitro calcified tendon collagen: an atomic force and scanning electron microscopy investigation. *Biomaterials* **18**, 657-665.
- Binnig, G., and Smith, D.P.E.** (1986). Single-tube three-dimensional scanner for scanning tunneling microscopy. *Review of Scientific Instruments* **57**, 1688-1689.
- Binnig, G., and Rohrer, H.** (1999). In touch with atoms. *Reviews of Modern Physics* **71**, S324-S330.
- Binnig, G., Quate, C.F., and Gerber, C.** (1986). Atomic Force Microscope. *Physical Review Letters* **56**, 930-933.
- Binnig, G., Rohrer, H., Gerber, C., and Weibel, E.** (1982). Surface Studies by Scanning Tunneling Microscopy. *Physical Review Letters* **49**, 57-61.
- Binnig, G., Gerber, C., Stoll, E., Albrecht, T.R., and Quate, C.F.** (1987). Atomic Resolution with Atomic Force Microscope. *EPL (Europhysics Letters)* **3**, 1281.
- Blystone, S.D., Slater, S.E., Williams, M.P., Crow, M.T., and Brown, E.J.** (1999). A Molecular Mechanism of Integrin Crosstalk:  $\alpha$ v $\beta$ 3 Suppression of Calcium/Calmodulin-dependent Protein Kinase II Regulates  $\alpha$ 5 $\beta$ 1 Function. *The Journal of Cell Biology* **145**, 889-897.
- Bosman, F.T., and Stamenkovic, I.** (2003). Functional structure and composition of the extracellular matrix. *The Journal of Pathology* **200**, 423-428.
- Braga, P.C., and Ricci, D.** (2011). *Atomic Force Microscopy in Biomedical Research-Methods and Protocols.* (New York: Springer Science+Business Media).
- Brazel, D., Pollner, R., Oberbaumer, I., and Kuhn, K.** (1988). Human basement membrane collagen (type IV). The amino acid sequence of the  $\alpha$ 2(IV) chain and its comparison with the  $\alpha$ 1(IV) chain reveals deletions in the  $\alpha$ 1(IV) chain. *Eur J Biochem* **172**, 35-42.

- Brenner, M.D., Zhou, R., and Ha, T.** (2011). Forcing a connection: Impacts of single-molecule force spectroscopy on in vivo tension sensing. *Biopolymers* **95**, 332-344.
- Bretscher, M.S.** (1992). Circulating integrins: alpha 5 beta 1, alpha 6 beta 4 and Mac-1, but not alpha 3 beta 1, alpha 4 beta 1 or LFA-1. *EMBO J* **11**, 405-410.
- Brock, A., Chang, E., Ho, C.C., LeDuc, P., Jiang, X., Whitesides, G.M., and Ingber, D.E.** (2003). Geometric determinants of directional cell motility revealed using microcontact printing. *Langmuir* **19**, 1611-1617.
- Burgeson, R.E., Chiquet, M., Deutzmann, R., Ekblom, P., Engel, J., Kleinman, H., Martin, G.R., Meneguzzi, G., Paulsson, M., Sanes, J., and et al.** (1994). A new nomenclature for the laminins. *Matrix Biol* **14**, 209-211.
- Bustamante, C., Macosko, J.C., and Wuite, G.J.** (2000). Grabbing the cat by the tail: manipulating molecules one by one. *Nat Rev Mol Cell Biol* **1**, 130-136.
- Butt, H.-J., Cappella, B., and Kappl, M.** (2005). Force measurements with the atomic force microscope: Technique, interpretation and applications. *Surface Science Reports* **59**, 1-152.
- Cai, L., Friedman, N., and Xie, X.S.** (2006). Stochastic protein expression in individual cells at the single molecule level. *Nature* **440**, 358-362.
- Calderwood, D.A., Tai, V., Di Paolo, G., De Camilli, P., and Ginsberg, M.H.** (2004). Competition for talin results in trans-dominant inhibition of integrin activation. *J Biol Chem* **279**, 28889-28895.
- Campbell, I.D., and Humphries, M.J.** (2011). Integrin Structure, Activation, and Interactions. *Cold Spring Harbor Perspectives in Biology* **3**.
- Camper, L., Holmvall, K., Wangnerud, C., Aszodi, A., and Lundgren-Akerlund, E.** (2001). Distribution of the collagen-binding integrin alpha10beta1 during mouse development. *Cell Tissue Res* **306**, 107-116.
- Canty, E.G., and Kadler, K.E.** (2005). Procollagen trafficking, processing and fibrillogenesis. *J Cell Sci* **118**, 1341-1353.
- Cao, G., Liu, L.M., and Cleary, S.F.** (1991). Modified method of mammalian cell synchronization improves yield and degree of synchronization. *Exp Cell Res* **193**, 405-410.
- Carman, C.V., and Springer, T.A.** (2003). Integrin avidity regulation: are changes in affinity and conformation underemphasized? *Current Opinion in Cell Biology* **15**, 547-556.
- Celik, E., and Moy, V.T.** (2012). Nonspecific interactions in AFM force spectroscopy measurements. *J Mol Recognit* **25**, 53-56.
- Chambers, A.F., Groom, A.C., and MacDonald, I.C.** (2002). Dissemination and growth of cancer cells in metastatic sites. *Nat Rev Cancer* **2**, 563-572.
- Chen, C.S., Mrksich, M., Huang, S., Whitesides, G.M., and Ingber, D.E.** (1997). Geometric control of cell life and death. *Science* **276**, 1425-1428.
- Chen, J., Diacovo, T.G., Grenache, D.G., Santoro, S.A., and Zutter, M.M.** (2002). The alpha(2) integrin subunit-deficient mouse: a multifaceted phenotype including defects of branching morphogenesis and hemostasis. *Am J Pathol* **161**, 337-344.
- Chen, W.T., and Singer, S.J.** (1982). Immunoelectron microscopic studies of the sites of cell-substratum and cell-cell contacts in cultured fibroblasts. *J Cell Biol* **95**, 205-222.
- Chiu, S.J., Jiang, S.T., Wang, Y.K., and Tang, M.J.** (2002). Hepatocyte growth factor upregulates alpha2beta1 integrin in Madin-Darby canine kidney cells: implications in tubulogenesis. *J Biomed Sci* **9**, 261-272.
- Clausen-Schaumann, H., Seitz, M., Krautbauer, R., and Gaub, H.E.** (2000). Force spectroscopy with single bio-molecules. *Current Opinion in Chemical Biology* **4**, 524-530.
- Cluzel, P., Lebrun, A., Heller, C., Lavery, R., Viovy, J.L., Chatenay, D., and Caron, F.** (1996). DNA: an extensible molecule. *Science* **271**, 792-794.
- Colige, A., Ruggiero, F., Vandenberghe, I., Dubail, J., Kesteloot, F., Van Beeumen, J., Beschin, A., Brys, L., Lapière, C.M., and Nusgens, B.** (2005). Domains and Maturation Processes That

- Regulate the Activity of ADAMTS-2, a Metalloproteinase Cleaving the Aminopropeptide of Fibrillar Procollagens Types I–III and V. *Journal of Biological Chemistry* **280**, 34397-34408.
- Cognato-Pyke, H., O'Rear, J.J., Yamada, Y., Carbonetto, S., Cheng, Y.S., and Yurchenco, P.D.** (1995). Mapping of network-forming, heparin-binding, and alpha 1 beta 1 integrin-recognition sites within the alpha-chain short arm of laminin-1. *J Biol Chem* **270**, 9398-9406.
- Cognato, H., and Yurchenco, P.D.** (2000). Form and function: the laminin family of heterotrimers. *Dev Dyn* **218**, 213-234.
- Coyer, S.R., Garcia, A.J., and Delamarche, E.** (2007). Facile preparation of complex protein architectures with sub-100-nm resolution on surfaces. *Angew Chem Int Ed Engl* **46**, 6837-6840.
- Danilov, Y.N., and Juliano, R.L.** (1989). Phorbol ester modulation of integrin-mediated cell adhesion: a postreceptor event. *J Cell Biol* **108**, 1925-1933.
- Darribere, T., Skalski, M., Cousin, H.L., Gaultier, A., Montmory, C., and Alfandari, D.** (2000). Integrins: regulators of embryogenesis. *Biol Cell* **92**, 5-25.
- Davis, G.E.** (1992). Affinity of integrins for damaged extracellular matrix: alpha v beta 3 binds to denatured collagen type I through RGD sites. *Biochem Biophys Res Commun* **182**, 1025-1031.
- De Luca, M., Tamura, R.N., Kajiji, S., Bondanza, S., Rossino, P., Cancedda, R., Marchisio, P.C., and Quaranta, V.** (1990). Polarized integrin mediates human keratinocyte adhesion to basal lamina. *Proc Natl Acad Sci U S A* **87**, 6888-6892.
- de Pereda, J.M., Wiche, G., and Liddington, R.C.** (1999). Crystal structure of a tandem pair of fibronectin type III domains from the cytoplasmic tail of integrin alpha6beta4. *EMBO J* **18**, 4087-4095.
- Delamarche, E., Schmid, H., Michel, B., and Biebuyck, H.** (1997). Stability of molded polydimethylsiloxane microstructures. *Advanced Materials* **9**, 741-746.
- Demetriou, M.C., Stylianou, P., Andreou, M., Yiannikouri, O., Tsapralis, G., Cress, A.E., and Skourides, P.** (2008). Spatially and temporally regulated alpha6 integrin cleavage during *Xenopus laevis* development. *Biochem Biophys Res Commun* **366**, 779-785.
- Desai, R.A., Khan, M.K., Gopal, S.B., and Chen, C.S.** (2011). Subcellular spatial segregation of integrin subtypes by patterned multicomponent surfaces. *Integr Biol (Camb)* **3**, 560-567.
- Dewez, J.L., Berger, V.V., Schneider, Y.J., and Rouxhet, P.G.** (1997). Influence of Substrate Hydrophobicity on the Adsorption of Collagen in the Presence of Pluronic F68, Albumin, or Calf Serum. *J Colloid Interface Sci* **191**, 1-10.
- Di Lullo, G.A., Sweeney, S.M., Korkko, J., Ala-Kokko, L., and San Antonio, J.D.** (2002). Mapping the Ligand-binding Sites and Disease-associated Mutations on the Most Abundant Protein in the Human, Type I Collagen. *J. Biol. Chem.* **277**, 4223-4231.
- Diaz-Gonzalez, F., Forsyth, J., Steiner, B., and Ginsberg, M.H.** (1996). Trans-dominant inhibition of integrin function. *Mol Biol Cell* **7**, 1939-1951.
- Dickeson, S.K., Walsh, J.J., and Santoro, S.A.** (1997). Contributions of the I and EF hand domains to the divalent cation-dependent collagen binding activity of the alpha2beta1 integrin. *J Biol Chem* **272**, 7661-7668.
- Dickeson, S.K., Mathis, N.L., Rahman, M., Bergelson, J.M., and Santoro, S.A.** (1999). Determinants of ligand binding specificity of the alpha(1)beta(1) and alpha(2)beta(1) integrins. *J Biol Chem* **274**, 32182-32191.
- Discher, D.E., Mooney, D.J., and Zandstra, P.W.** (2009). Growth factors, matrices, and forces combine and control stem cells. *Science* **324**, 1673-1677.
- Doyle, A.D., Wang, F.W., Matsumoto, K., and Yamada, K.M.** (2009). One-dimensional topography underlies three-dimensional fibrillar cell migration. *J Cell Biol* **184**, 481-490.
- du Roure, O., Buguin, A., Feracci, H., and Silberzan, P.** (2006). Homophilic interactions between cadherin fragments at the single molecule level: an AFM study. *Langmuir* **22**, 4680-4684.
- Durbeej, M.** (2010). Laminins. *Cell Tissue Res* **339**, 259-268.



- Eble, J.A., Golbik, R., Mann, K., and Kuhn, K.** (1993). The alpha 1 beta 1 integrin recognition site of the basement membrane collagen molecule [alpha 1(IV)]2 alpha 2(IV). *EMBO J* **12**, 4795-4802.
- Egerton, R.F.** (2005). *Physical Principles of Electron Microscopy*. (New York: Springer Science + Business Media, Inc.).
- Eliceiri, B.P.** (2001). Integrin and Growth Factor Receptor Crosstalk. *Circulation Research* **89**, 1104-1110.
- Elices, M.J., and Hemler, M.E.** (1989). The human integrin VLA-2 is a collagen receptor on some cells and a collagen/laminin receptor on others. *Proc Natl Acad Sci U S A* **86**, 9906-9910.
- Emsley, J., Knight, C.G., Farndale, R.W., Barnes, M.J., and Liddington, R.C.** (2000). Structural basis of collagen recognition by integrin alpha2beta1. *Cell* **101**, 47-56.
- Engel, J., Odermatt, E., Engel, A., Madri, J.A., Furthmayr, H., Rohde, H., and Timpl, R.** (1981). Shapes, domain organizations and flexibility of laminin and fibronectin, two multifunctional proteins of the extracellular matrix. *J Mol Biol* **150**, 97-120.
- Engler, A.J., Sen, S., Sweeney, H.L., and Discher, D.E.** (2006). Matrix Elasticity Directs Stem Cell Lineage Specification. *Cell* **126**, 677-689.
- Evans, E.** (2001). Probing the relation between force--lifetime--and chemistry in single molecular bonds. *Annu Rev Biophys Biomol Struct* **30**, 105-128.
- Evans, E., Ritchie, K., and Merkel, R.** (1995). Sensitive force technique to probe molecular adhesion and structural linkages at biological interfaces. *Biophys J* **68**, 2580-2587.
- Eyre, D.R., Paz, M.A., and Gallop, P.M.** (1984). Cross-linking in collagen and elastin. *Annu Rev Biochem* **53**, 717-748.
- Fleischmajer, R., MacDonald, E.D., Perlish, J.S., Burgeson, R.E., and Fisher, L.W.** (1990). Dermal collagen fibrils are hybrids of type I and type III collagen molecules. *J Struct Biol* **105**, 162-169.
- Franz, C.M., and Muller, D.J.** (2005). Analyzing focal adhesion structure by atomic force microscopy. *J Cell Sci* **118**, 5315-5323.
- Franzke, C.-W., Bruckner, P., and Bruckner-Tuderman, L.** (2005). Collagenous Transmembrane Proteins: Recent Insights into Biology and Pathology. *Journal of Biological Chemistry* **280**, 4005-4008.
- Franzke, C.-W., Tasanen, K., Schumann, H., and Bruckner-Tuderman, L.** (2003). Collagenous transmembrane proteins: collagen XVII as a prototype. *Matrix Biology* **22**, 299-309.
- Fratzl, P.** (2008). *Collagen*. (New York: Springer Science+Business Media, LLC).
- Friedrichs, J., Helenius, J., and Muller, D.J.** (2010). Quantifying cellular adhesion to extracellular matrix components by single-cell force spectroscopy. *Nat Protoc* **5**, 1353-1361.
- Friedrichs, J., Taubenberger, A., Franz, C.M., and Muller, D.J.** (2007). Cellular remodelling of individual collagen fibrils visualized by time-lapse AFM. *J Mol Biol* **372**, 594-607.
- Furtado, G.C., Cao, Y., and Joiner, K.A.** (1992). Laminin on *Toxoplasma gondii* mediates parasite binding to the beta 1 integrin receptor alpha 6 beta 1 on human foreskin fibroblasts and Chinese hamster ovary cells. *Infect Immun* **60**, 4925-4931.
- Gallant, N.D., and García, A.J.** (2007). Model of integrin-mediated cell adhesion strengthening. *Journal of Biomechanics* **40**, 1301-1309.
- Garcia, A.J., Huber, F., and Boettiger, D.** (1998). Force required to break alpha5beta1 integrin-fibronectin bonds in intact adherent cells is sensitive to integrin activation state. *J Biol Chem* **273**, 10988-10993.
- García, A.J., Ducheyne, P., and Boettiger, D.** (1997). Quantification of cell adhesion using a spinning disc device and application to surface-reactive materials. *Biomaterials* **18**, 1091-1098.
- García, R., and Pérez, R.** (2002). Dynamic atomic force microscopy methods. *Surface Science Reports* **47**, 197-301.
- Gaudreault, M., Vigneault, F., Leclerc, S., and Guerin, S.L.** (2007). Laminin reduces expression of the human alpha6 integrin subunit gene by altering the level of the transcription factors Sp1 and Sp3. *Invest Ophthalmol Vis Sci* **48**, 3490-3505.

- Gebb, C., Hayman, E.G., Engvall, E., and Ruoslahti, E.** (1986). Interaction of vitronectin with collagen. *J Biol Chem* **261**, 16698-16703.
- Geiger, B., Spatz, J.P., and Bershadsky, A.D.** (2009). Environmental sensing through focal adhesions. *Nat Rev Mol Cell Biol* **10**, 21-33.
- Geiger, B., Bershadsky, A., Pankov, R., and Yamada, K.M.** (2001). Transmembrane crosstalk between the extracellular matrix--cytoskeleton crosstalk. *Nat Rev Mol Cell Biol* **2**, 793-805.
- Geissler, M., Bernard, A., Bietsch, A., Schmid, H., Michel, B., and Delamar, E.** (2000). Microcontact-Printing Chemical Patterns with Flat Stamps. *Journal of the American Chemical Society* **122**, 6303-6304.
- Gimona, M., Buccione, R., Courtneidge, S.A., and Linder, S.** (2008). Assembly and biological role of podosomes and invadopodia. *Current Opinion in Cell Biology* **20**, 235-241.
- Gimond, C., van Der Flier, A., van Delft, S., Brakebusch, C., Kuikman, I., Collard, J.G., Fassler, R., and Sonnenberg, A.** (1999). Induction of cell scattering by expression of beta1 integrins in beta1-deficient epithelial cells requires activation of members of the rho family of GTPases and downregulation of cadherin and catenin function. *J Cell Biol* **147**, 1325-1340.
- Gingras, M.E., Larouche, K., Larouche, N., Leclerc, S., Salesse, C., and Guerin, S.L.** (2003). Regulation of the integrin subunit alpha5 gene promoter by the transcription factors Sp1/Sp3 is influenced by the cell density in rabbit corneal epithelial cells. *Invest Ophthalmol Vis Sci* **44**, 3742-3755.
- Ginsberg, M.H., Partridge, A., and Shattil, S.J.** (2005). Integrin regulation. *Curr Opin Cell Biol* **17**, 509-516.
- Göhring, W., Sasaki, T., Heldin, C.-H., and Timpl, R.** (1998). Mapping of the binding of platelet-derived growth factor to distinct domains of the basement membrane proteins BM-40 and perlecan and distinction from the BM-40 collagen-binding epitope. *European Journal of Biochemistry* **255**, 60-66.
- Goldfinger, L.E., Hopkinson, S.B., deHart, G.W., Collawn, S., Couchman, J.R., and Jones, J.C.** (1999). The alpha3 laminin subunit, alpha6beta4 and alpha3beta1 integrin coordinately regulate wound healing in cultured epithelial cells and in the skin. *J Cell Sci* **112 ( Pt 16)**, 2615-2629.
- Gonzalez, A.M., Claiborne, J., and Jones, J.C.** (2008). Integrin cross-talk in endothelial cells is regulated by protein kinase A and protein phosphatase 1. *J Biol Chem* **283**, 31849-31860.
- Gonzalez, A.M., Bhattacharya, R., deHart, G.W., and Jones, J.C.** (2010). Transdominant regulation of integrin function: mechanisms of crosstalk. *Cell Signal* **22**, 578-583.
- Goodman, S.L., Deutzmann, R., and von der Mark, K.** (1987). Two distinct cell-binding domains in laminin can independently promote nonneuronal cell adhesion and spreading. *J Cell Biol* **105**, 589-598.
- Goodman, S.L., Aumailley, M., and von der Mark, H.** (1991). Multiple cell surface receptors for the short arms of laminin: alpha 1 beta 1 integrin and RGD-dependent proteins mediate cell attachment only to domains III in murine tumor laminin. *J Cell Biol* **113**, 931-941.
- Gordon, J.P.** (1973). Radiation Forces and Momenta in Dielectric Media. *Physical Review A* **8**, 14-21.
- Gordon, M.K., and Hahn, R.A.** (2010). Collagens. *Cell Tissue Res* **339**, 247-257.
- Graf, J., Iwamoto, Y., Sasaki, M., Martin, G.R., Kleinman, H.K., Robey, F.A., and Yamada, Y.** (1987a). Identification of an amino acid sequence in laminin mediating cell attachment, chemotaxis, and receptor binding. *Cell* **48**, 989-996.
- Graf, J., Ogle, R.C., Robey, F.A., Sasaki, M., Martin, G.R., Yamada, Y., and Kleinman, H.K.** (1987b). A pentapeptide from the laminin B1 chain mediates cell adhesion and binds the 67,000 laminin receptor. *Biochemistry* **26**, 6896-6900.
- Grandbois, M., Beyer, M., Rief, M., Clausen-Schaumann, H., and Gaub, H.E.** (1999). How strong is a covalent bond? *Science* **283**, 1727-1730.
- Greenspan, D.S.** (2005). Biosynthetic Processing of Collagen Molecules/ Collagen, J. Brinckmann, H. Notbohm, and P.K. Müller, eds (Springer Berlin / Heidelberg), pp. 149-183.

- Gross, J., and Schmitt, F.O.** (1948). The structure of human skin collagen as studied with the electron microscope. *J Exp Med* **88**, 555-568.
- Grundel, R., and Rubin, H.** (1988). Maintenance of multiplication rate stability by cell populations in the face of heterogeneity among individual cells. *J Cell Sci* **91 ( Pt 4)**, 571-576.
- Guidry, C., Miller, E.J., and Hook, M.** (1990). A second fibronectin-binding region is present in collagen alpha chains. *J Biol Chem* **265**, 19230-19236.
- Gullberg, D., Gehlsen, K.R., Turner, D.C., Ahlen, K., Zijenah, L.S., Barnes, M.J., and Rubin, K.** (1992). Analysis of alpha 1 beta 1, alpha 2 beta 1 and alpha 3 beta 1 integrins in cell-collagen interactions: identification of conformation dependent alpha 1 beta 1 binding sites in collagen type I. *EMBO J* **11**, 3865-3873.
- Gupta, S.K., Meiri, K.F., Mahfooz, K., Bharti, U., and Mani, S.** Coordination between extrinsic extracellular matrix cues and intrinsic responses to orient the centrosome in polarizing cerebellar granule neurons. *J Neurosci* **30**, 2755-2766.
- Harburger, D.S., and Calderwood, D.A.** (2009). Integrin signalling at a glance. *J Cell Sci* **122**, 159-163.
- Harburger, D.S., Bouaouina, M., and Calderwood, D.A.** (2009). Kindlin-1 and -2 directly bind the C-terminal region of beta integrin cytoplasmic tails and exert integrin-specific activation effects. *J Biol Chem* **284**, 11485-11497.
- Hattori, K., Sugiura, S., and Kanamori, T.** (2010). On-chip cell culture on a microarray of extracellular matrix with surface modification of poly(dimethylsiloxane). *Biotechnol J* **5**, 463-469.
- Hattori, K., Sugiura, S., and Kanamori, T.** (2011). Microenvironment array chip for cell culture environment screening. *Lab Chip* **11**, 212-214.
- Hay, E.D.** (1991). *Cell Biology of Extracellular Matrix*. (New York: Plenum Press).
- HAY, E.D.** (1999). Biogenesis and organization of extracellular matrix. *The FASEB Journal* **13**, S281-S283.
- Heino, J.** (2000). The collagen receptor integrins have distinct ligand recognition and signaling functions. *Matrix Biol* **19**, 319-323.
- Helenius, J., Heisenberg, C.P., Gaub, H.E., and Muller, D.J.** (2008). Single-cell force spectroscopy. *J Cell Sci* **121**, 1785-1791.
- Heppner, G.H.** (1984). Tumor heterogeneity. *Cancer Res* **44**, 2259-2265.
- Hinterdorfer, P., and Dufrene, Y.F.** (2006). Detection and localization of single molecular recognition events using atomic force microscopy. *Nat Meth* **3**, 347-355.
- Hochmuth, F.M., Shao, J.Y., Dai, J., and Sheetz, M.P.** (1996). Deformation and flow of membrane into tethers extracted from neuronal growth cones. *Biophys J* **70**, 358-369.
- Hodivala-Dilke, K.M., DiPersio, C.M., Kreidberg, J.A., and Hynes, R.O.** (1998). Novel roles for alpha3beta1 integrin as a regulator of cytoskeletal assembly and as a trans-dominant inhibitor of integrin receptor function in mouse keratinocytes. *J Cell Biol* **142**, 1357-1369.
- Hoh, J.H., and Hansma, P.K.** (1992). Atomic force microscopy for high-resolution imaging in cell biology. *Trends Cell Biol* **2**, 208-213.
- Honda, S., Shirogami-Ikejima, H., Tadokoro, S., Maeda, Y., Kinoshita, T., Tomiyama, Y., and Miyata, T.** (2009). Integrin-linked kinase associated with integrin activation. *Blood* **113**, 5304-5313.
- Hopker, V.H., Shewan, D., Tessier-Lavigne, M., Poo, M., and Holt, C.** (1999). Growth-cone attraction to netrin-1 is converted to repulsion by laminin-1. *Nature* **401**, 69-73.
- Hou, S., Li, X.X., Li, X.Y., Feng, X.Z., Guan, L., Yang, Y.L., and Wang, C.** (2009). Patterning of 293T fibroblasts on a mica surface. *Anal Bioanal Chem* **394**, 2111-2117.
- Hudson, B.G., Tryggvason, K., Sundaramoorthy, M., and Neilson, E.G.** (2003). Alport's syndrome, Goodpasture's syndrome, and type IV collagen. *N Engl J Med* **348**, 2543-2556.
- Hui, C.Y., Jagota, A., Lin, Y.Y., and Kramer, E.J.** (2002). Constraints on Microcontact Printing Imposed by Stamp Deformation. *Langmuir* **18**, 1394-1407.
- Hulmes, D.J.** (2002). Building collagen molecules, fibrils, and suprafibrillar structures. *J Struct Biol* **137**, 2-10.

- Humphries, M.J.** (2000). Integrin structure. *Biochem Soc Trans* **28**, 311-339.
- Humphries, M.J., Symonds, E.J., and Mould, A.P.** (2003). Mapping functional residues onto integrin crystal structures. *Curr Opin Struct Biol* **13**, 236-243.
- Huth, J.R., Olejniczak, E.T., Mendoza, R., Liang, H., Harris, E.A., Lupper, M.L., Jr., Wilson, A.E., Fesik, S.W., and Staunton, D.E.** (2000). NMR and mutagenesis evidence for an I domain allosteric site that regulates lymphocyte function-associated antigen 1 ligand binding. *Proc Natl Acad Sci U S A* **97**, 5231-5236.
- Hutter, J.L., and Bechhoefer, J.** (1993). Calibration of atomic force microscope tips. *Review of Scientific Instruments* **64**, 1868-1873.
- Huvneers, S., and Danen, E.H.** (2009). Adhesion signaling - crosstalk between integrins, Src and Rho. *J Cell Sci* **122**, 1059-1069.
- Huxley - Jones, J., Robertson, D.L., and Boot-Handford, R.P.** (2007). On the origins of the extracellular matrix in vertebrates. *Matrix Biology* **26**, 2-11.
- Hynes, R.O.** (1987). Integrins: a family of cell surface receptors. *Cell* **48**, 549-554.
- Hynes, R.O.** (2002). Integrins: bidirectional, allosteric signaling machines. *Cell* **110**, 673-687.
- Hynes, R.O.** (2009). The extracellular matrix: not just pretty fibrils. *Science* **326**, 1216-1219.
- Ishijima, A., Kojima, H., Higuchi, H., Harada, Y., Funatsu, T., and Yanagida, T.** (1996). Multiple- and single-molecule analysis of the actomyosin motor by nanometer-piconewton manipulation with a microneedle: unitary steps and forces. *Biophysical Journal* **70**, 383-400.
- Ivaska, J., Reunanen, H., Westermarck, J., Koivisto, L., Kahari, V.M., and Heino, J.** (1999). Integrin  $\alpha 2\beta 1$  mediates isoform-specific activation of p38 and upregulation of collagen gene transcription by a mechanism involving the  $\alpha 2$  cytoplasmic tail. *J Cell Biol* **147**, 401-416.
- James, C.D., Davis, R.C., Kam, L., Craighead, H.G., Isaacson, M., Turner, J.N., and Shain, W.** (1998). Patterned Protein Layers on Solid Substrates by Thin Stamp Microcontact Printing. *Langmuir* **14**, 741-744.
- Jeon, S.I., Lee, J.H., Andrade, J.D., and De Gennes, P.G.** (1991). Protein—surface interactions in the presence of polyethylene oxide: I. Simplified theory. *Journal of Colloid and Interface Science* **142**, 149-158.
- Jiang, F., Horber, H., Howard, J., and Muller, D.J.** (2004). Assembly of collagen into microribbons: effects of pH and electrolytes. *J Struct Biol* **148**, 268-278.
- Jinka, R., Kapoor, R., Sistla, P.G., Raj, T.A., and Pande, G.** (2012). Alterations in Cell-Extracellular Matrix Interactions during Progression of Cancers. *Int J Cell Biol* **2012**, 219196.
- Johnston, S., Bramble, J., Yeung, C., Mendes, P., and Machesky, L.** (2008). Arp2/3 complex activity in filopodia of spreading cells. *BMC Cell Biology* **9**, 65.
- Jokinen, J., Dadu, E., Nykvist, P., Kapyla, J., White, D.J., Ivaska, J., Vehvilainen, P., Reunanen, H., Larjava, H., Hakkinen, L., and Heino, J.** (2004). Integrin-mediated cell adhesion to type I collagen fibrils. *J Biol Chem* **279**, 31956-31963.
- Jungbauer, S., Kemkemer, R., Gruler, H., Kaufmann, D., and Spatz, J.P.** (2004). Cell shape normalization, dendrite orientation, and melanin production of normal and genetically altered (haploinsufficient NF1)-melanocytes by microstructured substrate interactions. *Chemphyschem* **5**, 85-92.
- Kadler, K.E., Hojima, Y., and Prockop, D.J.** (1987). Assembly of collagen fibrils de novo by cleavage of the type I pC-collagen with procollagen C-proteinase. Assay of critical concentration demonstrates that collagen self-assembly is a classical example of an entropy-driven process. *J Biol Chem* **262**, 15696-15701.
- Kadler, K.E., Hill, A., and Canty-Laird, E.G.** (2008). Collagen fibrillogenesis: fibronectin, integrins, and minor collagens as organizers and nucleators. *Curr Opin Cell Biol* **20**, 495-501.
- Kadler, K.E., Holmes, D.F., Trotter, J.A., and Chapman, J.A.** (1996). Collagen fibril formation. *Biochem J* **316 ( Pt 1)**, 1-11.

- Kadler, K.E., Baldock, C., Bella, J., and Boot-Handford, R.P.** (2007). Collagens at a glance. *J Cell Sci* **120**, 1955-1958.
- Kaern, M., Elston, T.C., Blake, W.J., and Collins, J.J.** (2005). Stochasticity in gene expression: from theories to phenotypes. *Nat Rev Genet* **6**, 451-464.
- Kanchanawong, P., Shtengel, G., Pasapera, A.M., Ramko, E.B., Davidson, M.W., Hess, H.F., and Waterman, C.M.** (2010). Nanoscale architecture of integrin-based cell adhesions. *Nature* **468**, 580-584.
- Kane, R.S., Takayama, S., Ostuni, E., Ingber, D.E., and Whitesides, G.M.** (1999). Patterning proteins and cells using soft lithography. *Biomaterials* **20**, 2363-2376.
- Kaplanski, G., Farnarier, C., Tissot, O., Pierres, A., Benoliel, A.M., Alessi, M.C., Kaplanski, S., and Bongrand, P.** (1993). Granulocyte-endothelium initial adhesion. Analysis of transient binding events mediated by E-selectin in a laminar shear flow. *Biophysical Journal* **64**, 1922-1933.
- Karp, G.C.** (2010). *Cell Biology*. (Singapore: John Wiley & Sons, Inc).
- Kaupp, G.** (2006). *Atomic Force Microscopy, Scanning Nearfield Optical Microscopy and Nanoscratching*. (Heidelberg: Springer-Verlag Berlin Heidelberg).
- Keely, P.J., Fong, A.M., Zutter, M.M., and Santoro, S.A.** (1995). Alteration of collagen-dependent adhesion, motility, and morphogenesis by the expression of antisense alpha 2 integrin mRNA in mammary cells. *J Cell Sci* **108 ( Pt 2)**, 595-607.
- Kern, A., Eble, J., Golbik, R., and Kuhn, K.** (1993). Interaction of type IV collagen with the isolated integrins alpha 1 beta 1 and alpha 2 beta 1. *Eur J Biochem* **215**, 151-159.
- Kern, A., Briesewitz, R., Bank, I., and Marcantonio, E.E.** (1994). The role of the I domain in ligand binding of the human integrin alpha 1 beta 1. *J Biol Chem* **269**, 22811-22816.
- Khoshnoodi, J., Pedchenko, V., and Hudson, B.G.** (2008). Mammalian collagen IV. *Microsc Res Tech* **71**, 357-370.
- Kielosto, M., Nummela, P., Järvinen, K., Yin, M., and Hölttä, E.** (2009). Identification of integrins  $\alpha 6$  and  $\beta 7$  as c-Jun- and transformation-relevant genes in highly invasive fibrosarcoma cells. *International Journal of Cancer* **125**, 1065-1073.
- Kirchhofer, D., Languino, L.R., Ruoslahti, E., and Pierschbacher, M.D.** (1990). Alpha 2 beta 1 integrins from different cell types show different binding specificities. *J Biol Chem* **265**, 615-618.
- Kishino, A., and Yanagida, T.** (1988). Force measurements by micromanipulation of a single actin filament by glass needles. *Nature* **334**, 74-76.
- Klebe, R.J.** (1974). Isolation of a collagen-dependent cell attachment factor. *Nature* **250**, 248-251.
- Knight, C.G., Morton, L.F., Peachey, A.R., Tuckwell, D.S., Farndale, R.W., and Barnes, M.J.** (2000). The collagen-binding A-domains of integrins alpha(1)beta(1) and alpha(2)beta(1) recognize the same specific amino acid sequence, GFOGER, in native (triple-helical) collagens. *J Biol Chem* **275**, 35-40.
- Knupp, C., and Squire, J.M.** (2005). Molecular Packing in Network-Forming Collagens. In *Advances in Protein Chemistry*, A.D.P. David and M.S. John, eds (Academic Press), pp. 375-403.
- Koch, M., Olson, P.F., Albus, A., Jin, W., Hunter, D.D., Brunken, W.J., Burgeson, R.E., and Champlaud, M.F.** (1999). Characterization and expression of the laminin gamma3 chain: a novel, non-basement membrane-associated, laminin chain. *J Cell Biol* **145**, 605-618.
- Kollmannsberger, P., and Fabry, B.** (2007). High-force magnetic tweezers with force feedback for biological applications. *Rev Sci Instrum* **78**, 114301.
- Kostenuik, P.J., Sanchez-Sweatman, O., Orr, F.W., and Singh, G.** (1996). Bone cell matrix promotes the adhesion of human prostatic carcinoma cells via the alpha 2 beta 1 integrin. *Clin Exp Metastasis* **14**, 19-26.
- Kramer, R.H., Cheng, Y.F., and Clyman, R.** (1990). Human microvascular endothelial cells use beta 1 and beta 3 integrin receptor complexes to attach to laminin. *J Cell Biol* **111**, 1233-1243.

- Kramer, R.H., Vu, M.P., Cheng, Y.F., Ramos, D.M., Timpl, R., and Waleh, N.** (1991). Laminin-binding integrin alpha 7 beta 1: functional characterization and expression in normal and malignant melanocytes. *Cell Regul* **2**, 805-817.
- Kumar, A., and Whitesides, G.M.** (1993). Features of gold having micrometer to centimeter dimensions can be formed through a combination of stamping with an elastomeric stamp and an alkanethiol "ink" followed by chemical etching. *Applied Physics Letters* **63**, 2002-2004.
- Kumar, A., Biebuyck, H.A., and Whitesides, G.M.** (1994). Patterning Self-Assembled Monolayers: Applications in Materials Science. *Langmuir* **10**, 1498-1511.
- Kuschel, C., Steuer, H., Maurer, A.N., Kanzok, B., Stoop, R., and Angres, B.** (2006). Cell adhesion profiling using extracellular matrix protein microarrays. *Biotechniques* **40**, 523-531.
- Kussell, E., and Leibler, S.** (2005). Phenotypic diversity, population growth, and information in fluctuating environments. *Science* **309**, 2075-2078.
- Languino, L.R., Gehlsen, K.R., Wayner, E., Carter, W.G., Engvall, E., and Ruoslahti, E.** (1989). Endothelial cells use alpha 2 beta 1 integrin as a laminin receptor. *J Cell Biol* **109**, 2455-2462.
- Larson, R.S., Corbi, A.L., Berman, L., and Springer, T.** (1989). Primary structure of the leukocyte function-associated molecule-1 alpha subunit: an integrin with an embedded domain defining a protein superfamily. *J Cell Biol* **108**, 703-712.
- Latchman, D.S.** (1997). Transcription factors: An overview. *The International Journal of Biochemistry & Cell Biology* **29**, 1305-1312.
- Lauer, J.L., Gendron, C.M., and Fields, G.B.** (1998). Effect of ligand conformation on melanoma cell alpha3beta1 integrin-mediated signal transduction events: implications for a collagen structural modulation mechanism of tumor cell invasion. *Biochemistry* **37**, 5279-5287.
- Lauffenburger, D.A., and Horwitz, A.F.** (1996). Cell migration: a physically integrated molecular process. *Cell* **84**, 359-369.
- Lauffenburger, D.A., and Wells, A.** (2001). Getting a grip: new insights for cell adhesion and traction. *Nat Cell Biol* **3**, E110-112.
- Laukaitis, C.M., Webb, D.J., Donais, K., and Horwitz, A.F.** (2001). Differential dynamics of alpha 5 integrin, paxillin, and alpha-actinin during formation and disassembly of adhesions in migrating cells. *J Cell Biol* **153**, 1427-1440.
- Lawson, M.A., and Maxfield, F.R.** (1995). Ca(2+)- and calcineurin-dependent recycling of an integrin to the front of migrating neutrophils. *Nature* **377**, 75-79.
- Le Grimellec, C., Lesniewska, E., Giocondi, M.-C., Finot, E., Vié, V., and Gouidonnet, J.-P.** (1998). Imaging of the Surface of Living Cells by Low-Force Contact-Mode Atomic Force Microscopy. *Biophysical Journal* **75**, 695-703.
- Lee, C.H., Singla, A., and Lee, Y.** (2001). Biomedical applications of collagen. *Int J Pharm* **221**, 1-22.
- Lee, J.O., Bankston, L.A., Arnaout, M.A., and Liddington, R.C.** (1995). Two conformations of the integrin A-domain (I-domain): a pathway for activation? *Structure* **3**, 1333-1340.
- Lee, M.H., Brass, D.A., Morris, R., Composto, R.J., and Ducheyne, P.** (2005). The effect of non-specific interactions on cellular adhesion using model surfaces. *Biomaterials* **26**, 1721-1730.
- Lehenkari, P.P., and Horton, M.A.** (1999). Single integrin molecule adhesion forces in intact cells measured by atomic force microscopy. *Biochem Biophys Res Commun* **259**, 645-650.
- Lehmann, M., Rigot, V., Seidah, N.G., Marvaldi, J., and Lissitzky, J.C.** (1996). Lack of integrin alpha-chain endoproteolytic cleavage in furin-deficient human colon adenocarcinoma cells LoVo. *Biochem J* **317 ( Pt 3)**, 803-809.
- Lehnert, D., Wehrle-Haller, B., David, C., Weiland, U., Ballestrem, C., Imhof, B.A., and Bastmeyer, M.** (2004). Cell behaviour on micropatterned substrata: limits of extracellular matrix geometry for spreading and adhesion. *J Cell Sci* **117**, 41-52.
- Leitinger, B.** (2011). Transmembrane collagen receptors. *Annu Rev Cell Dev Biol* **27**, 265-290.
- Leitinger, B., and Hohenester, E.** (2007). Mammalian collagen receptors. *Matrix Biology* **26**, 146-155.

- Li, H., Zhang, F., Zhang, Y., Ye, M., Zhou, B., Tang, Y.Z., Yang, H.J., Xie, M.Y., Chen, S.F., He, J.H., Fang, H.P., and Hu, J. (2009). Peptide diffusion and self-assembly in ambient water nanofilm on mica surface. *J Phys Chem B* **113**, 8795-8799.
- Li, R., Mitra, N., Gratkowski, H., Vilaire, G., Litvinov, R., Nagasami, C., Weisel, J.W., Lear, J.D., DeGrado, W.F., and Bennett, J.S. (2003). Activation of integrin  $\alpha$ 11 $\beta$ 3 by modulation of transmembrane helix associations. *Science* **300**, 795-798.
- Liang, Y.L., Fu, Y., Chen, S.G., Cai, X.M., Su, J.M., Jin, J.W., Ma, D.Z., Li, Z.X., Zhang, W., and Zha, X. (2004). Integrin  $\beta$ 1 subunit overexpressed in the SMMC-7721 cells regulates the promoter activity of p21(CIP1) and enhances its transcription. *FEBS Lett* **558**, 107-113.
- Lichtner, R.B., Howlett, A.R., Lerch, M., Xuan, J.A., Brink, J., Langton-Webster, B., and Schneider, M.R. (1998). Negative cooperativity between  $\alpha$ 3  $\beta$ 1 and  $\alpha$ 2  $\beta$ 1 integrins in human mammary carcinoma MDA MB 231 cells. *Exp Cell Res* **240**, 368-376.
- Lin, C.S., Chen, Y., Huynh, T., and Kramer, R. (1997). Identification of the human  $\alpha$ 6 integrin gene promoter. *DNA Cell Biol* **16**, 929-937.
- Lotz, M.M., Korzelius, C.A., and Mercurio, A.M. (1990). Human colon carcinoma cells use multiple receptors to adhere to laminin: involvement of  $\alpha$ 6  $\beta$ 4 and  $\alpha$ 2  $\beta$ 1 integrins. *Cell Regul* **1**, 249-257.
- Lotz, M.M., Burdsal, C.A., Erickson, H.P., and McClay, D.R. (1989). Cell adhesion to fibronectin and tenascin: quantitative measurements of initial binding and subsequent strengthening response. *J Cell Biol* **109**, 1795-1805.
- Lu, C., Takagi, J., and Springer, T.A. (2001). Association of the membrane proximal regions of the  $\alpha$  and  $\beta$  subunit cytoplasmic domains constrains an integrin in the inactive state. *J Biol Chem* **276**, 14642-14648.
- Lu, X., Lu, D., Scully, M., and Kakkar, V. (2008). The role of integrins in cancer and the development of anti-integrin therapeutic agents for cancer therapy. *Perspect Medicin Chem* **2**, 57-73.
- Luo, B.H., and Springer, T.A. (2006). Integrin structures and conformational signaling. *Curr Opin Cell Biol* **18**, 579-586.
- Luo, B.H., Carman, C.V., and Springer, T.A. (2007). Structural basis of integrin regulation and signaling. *Annu Rev Immunol* **25**, 619-647.
- Lynch, M. (2010). Evolution of the mutation rate. *Trends Genet* **26**, 345-352.
- Ma, W., Tavakoli, T., Derby, E., Serebryakova, Y., Rao, M.S., and Mattson, M.P. (2008a). Cell-extracellular matrix interactions regulate neural differentiation of human embryonic stem cells. *BMC Dev Biol* **8**, 90.
- Ma, Y.Q., Qin, J., Wu, C., and Plow, E.F. (2008b). Kindlin-2 (Mig-2): a co-activator of  $\beta$ 3 integrins. *J Cell Biol* **181**, 439-446.
- Maamar, H., Raj, A., and Dubnau, D. (2007). Noise in gene expression determines cell fate in *Bacillus subtilis*. *Science* **317**, 526-529.
- Maeda, T., Titani, K., and Sekiguchi, K. (1994). Cell-adhesive activity and receptor-binding specificity of the laminin-derived YIGSR sequence grafted onto Staphylococcal protein A. *J Biochem* **115**, 182-189.
- Maheshri, N., and O'Shea, E.K. (2007). Living with noisy genes: how cells function reliably with inherent variability in gene expression. *Annu Rev Biophys Biomol Struct* **36**, 413-434.
- Malinoff, H.L., McCoy, J.P., Jr., Varani, J., and Wicha, M.S. (1984). Metastatic potential of murine fibrosarcoma cells is influenced by cell surface laminin. *Int J Cancer* **33**, 651-655.
- Marcus, W.D., McEver, R.P., and Zhu, C. (2004). Forces required to initiate membrane tether extrusion from cell surface depend on cell type but not on the surface molecule. *Mech Chem Biosyst* **1**, 245-251.
- Martin, Y., Williams, C.C., and Wickramasinghe, H.K. (1987). Atomic force microscope--force mapping and profiling on a sub 100- $\text{\AA}$  scale. *Journal of Applied Physics* **61**, 4723-4729.

- Massia, S.P., Rao, S.S., and Hubbell, J.A.** (1993). Covalently immobilized laminin peptide Tyr-Ile-Gly-Ser-Arg (YIGSR) supports cell spreading and co-localization of the 67-kilodalton laminin receptor with alpha-actinin and vinculin. *J Biol Chem* **268**, 8053-8059.
- McDevitt, T.C., Angello, J.C., Whitney, M.L., Reinecke, H., Hauschka, S.D., Murry, C.E., and Stayton, P.S.** (2002). In vitro generation of differentiated cardiac myofibers on micropatterned laminin surfaces. *J Biomed Mater Res* **60**, 472-479.
- Mecham, R.P.** (1991). Laminin receptors. *Annu Rev Cell Biol* **7**, 71-91.
- Meighan, C.M., and Schwarzbauer, J.E.** (2008). Temporal and spatial regulation of integrins during development. *Curr Opin Cell Biol* **20**, 520-524.
- Mendelsohn, A.D., Bernards, D.A., Lowe, R.D., and Desai, T.A.** Patterning of Mono- and Multilayered Pancreatic beta-Cell Clusters. *Langmuir*.
- Mercurio, A.M.** (1995). Laminin receptors: achieving specificity through cooperation. *Trends Cell Biol* **5**, 419-423.
- Mercurio, A.M., and Rabinovitz, I.** (2001). Towards a mechanistic understanding of tumor invasion--lessons from the alpha6beta 4 integrin. *Semin Cancer Biol* **11**, 129-141.
- Meyer, G., and Amer, N.M.** (1988). Novel optical approach to atomic force microscopy. *Applied Physics Letters* **53**, 1045-1047.
- Michler, G.H.** (2008). *Electron Microscopy of Polymers.* (Springer-Verlag Berlin Heidelberg).
- Miller, A., and Wray, J.S.** (1971). Molecular Packing in Collagen. *Nature* **230**, 437-439.
- Millon-Fremillon, A., Bouvard, D., Grichine, A., Manet-Dupe, S., Block, M.R., and Albiges-Rizo, C.** (2008). Cell adaptive response to extracellular matrix density is controlled by ICAP-1-dependent beta1-integrin affinity. *J Cell Biol* **180**, 427-441.
- Miner, J.H., and Yurchenco, P.D.** (2004). Laminin functions in tissue morphogenesis. *Annu Rev Cell Dev Biol* **20**, 255-284.
- Mirtti, T., Nylund, C., Lehtonen, J., Hiekkanen, H., Nissinen, L., Kallajoki, M., Alanen, K., Gullberg, D., and Heino, J.** (2006). Regulation of prostate cell collagen receptors by malignant transformation. *Int J Cancer* **118**, 889-898.
- Mitra, S.K., Hanson, D.A., and Schlaepfer, D.D.** (2005). Focal adhesion kinase: in command and control of cell motility. *Nat Rev Mol Cell Biol* **6**, 56-68.
- Monier-Gavelle, F., and Duband, J.L.** (1997). Cross talk between adhesion molecules: control of N-cadherin activity by intracellular signals elicited by beta1 and beta3 integrins in migrating neural crest cells. *J Cell Biol* **137**, 1663-1681.
- Monroe, M., Li, Y., Ajinkya, S., Gower, L., and Douglas, E.** (2009). Directed collagen patterning on gold-coated silicon substrates via micro-contact printing. *Materials Science and Engineering C* **29**, 2365-2369.
- Morris, V.J., Kirby, A.R., and Gunning, A.P.** (2010). *Atomic Force Microscopy for Biologists.* (London: Imperial College Press).
- Mould, A.P., Hulmes, D.J.S., Holmes, D.F., Cummings, C., Sear, C.H.J., and Chapman, J.A.** (1990). D-periodic assemblies of type I procollagen. *Journal of Molecular Biology* **211**, 581-594.
- Muller, D.J., Helenius, J., Alsteens, D., and Dufrene, Y.F.** (2009a). Force probing surfaces of living cells to molecular resolution. *Nat Chem Biol* **5**, 383-390.
- Muller, D.J., Krieg, M., Alsteens, D., and Dufrene, Y.F.** (2009b). New frontiers in atomic force microscopy: analyzing interactions from single-molecules to cells. *Curr Opin Biotechnol* **20**, 4-13.
- Myllyharju, J.** (2005). Intracellular Post-Translational Modifications of Collagens/ Collagen, J. Brinckmann, H. Notbohm, and P.K. Müller, eds (Springer Berlin / Heidelberg), pp. 115-147.
- Myllyharju, J., and Kivirikko, K.I.** (2001). Collagens and collagen-related diseases. *Ann Med* **33**, 7-21.
- Neuman, K.C., and Nagy, A.** (2008). Single-molecule force spectroscopy: optical tweezers, magnetic tweezers and atomic force microscopy. *Nat Meth* **5**, 491-505.



- Neuman, K.C., Lionnet, T., and Allemand, J.-F.** (2007). Single-Molecule Micromanipulation Techniques. *Annual Review of Materials Research* **37**, 33-67.
- Nicholas A, G.** AFM and combined optical techniques. *Materials Today* **12**, 40-45.
- Niepel, M., Spencer, S.L., and Sorger, P.K.** (2009). Non-genetic cell-to-cell variability and the consequences for pharmacology. *Curr Opin Chem Biol* **13**, 556-561.
- Niyibizi, C., and Eyre, D.R.** (1989). Bone type V collagen: chain composition and location of a trypsin cleavage site. *Connect Tissue Res* **20**, 247-250.
- Nurcombe, V., Aumailley, M., Timpl, R., and Edgar, D.** (1989). The high-affinity binding of laminin to cells. Assignment of a major cell-binding site to the long arm of laminin and of a latent cell-binding site to its short arms. *Eur J Biochem* **180**, 9-14.
- Nykvist, P., Tu, H., Ivaska, J., Kapyla, J., Pihlajaniemi, T., and Heino, J.** (2000). Distinct recognition of collagen subtypes by alpha(1)beta(1) and alpha(2)beta(1) integrins. Alpha(1)beta(1) mediates cell adhesion to type XIII collagen. *J Biol Chem* **275**, 8255-8261.
- Ohashi, P.S., Mak, T.W., Van den Elsen, P., Yanagi, Y., Yoshikai, Y., Calman, A.F., Terhorst, C., Stobo, J.D., and Weiss, A.** (1985). Reconstitution of an active surface T3/T-cell antigen receptor by DNA transfer. *Nature* **316**, 606-609.
- Palecek, S.P., Huttenlocher, A., Horwitz, A.F., and Lauffenburger, D.A.** (1998). Physical and biochemical regulation of integrin release during rear detachment of migrating cells. *J Cell Sci* **111 ( Pt 7)**, 929-940.
- Pankov, R., Cukierman, E., Katz, B.Z., Matsumoto, K., Lin, D.C., Lin, S., Hahn, C., and Yamada, K.M.** (2000). Integrin dynamics and matrix assembly: tensin-dependent translocation of alpha(5)beta(1) integrins promotes early fibronectin fibrillogenesis. *J Cell Biol* **148**, 1075-1090.
- Patarroyo, M., Tryggvason, K., and Virtanen, I.** (2002). Laminin isoforms in tumor invasion, angiogenesis and metastasis. *Seminars in Cancer Biology* **12**, 197-207.
- Paulo, Á.S., and García, R.** (2002). Unifying theory of tapping-mode atomic-force microscopy. *Physical Review B* **66**, 041406.
- Paulsson, M.** (1988). The role of Ca<sup>2+</sup> binding in the self-aggregation of laminin-nidogen complexes. *J Biol Chem* **263**, 5425-5430.
- Pawelek, J.M., and Chakraborty, A.K.** (2008). The cancer cell--leukocyte fusion theory of metastasis. *Adv Cancer Res* **101**, 397-444.
- Pawley, J.P.** (2006). *Handbook of Biological Confocal Microscopy*. (New York: Springer Science+Business Media, LLC).
- Pedchenko, V., Zent, R., and Hudson, B.G.** (2004). Alpha(v)beta3 and alpha(v)beta5 integrins bind both the proximal RGD site and non-RGD motifs within noncollagenous (NC1) domain of the alpha3 chain of type IV collagen: implication for the mechanism of endothelial cell adhesion. *J Biol Chem* **279**, 2772-2780.
- Peyton, S.R., Raub, C.B., Keschrumus, V.P., and Putnam, A.J.** (2006). The use of poly(ethylene glycol) hydrogels to investigate the impact of ECM chemistry and mechanics on smooth muscle cells. *Biomaterials* **27**, 4881-4893.
- Pfaff, M., Gohring, W., Brown, J.C., and Timpl, R.** (1994). Binding of purified collagen receptors (alpha 1 beta 1, alpha 2 beta 1) and RGD-dependent integrins to laminins and laminin fragments. *Eur J Biochem* **225**, 975-984.
- Pignatelli, M., and Stamp, G.** (1995). Integrins in tumour development and spread. *Cancer Surv* **24**, 113-127.
- Porter, J.C., and Hogg, N.** (1998). Integrins take partners: cross-talk between integrins and other membrane receptors. *Trends in Cell Biology* **8**, 390-396.
- Poste, G., Tzeng, J., Doll, J., Greig, R., Rieman, D., and Zeidman, I.** (1982). Evolution of tumor cell heterogeneity during progressive growth of individual lung metastases. *Proc Natl Acad Sci U S A* **79**, 6574-6578.

- Prime, K.L., and Whitesides, G.M.** (1993). Adsorption of proteins onto surfaces containing end-attached oligo(ethylene oxide): a model system using self-assembled monolayers. *Journal of the American Chemical Society* **115**, 10714-10721.
- Prockop, D.J., and Fertala, A.** (1998). Inhibition of the Self-assembly of Collagen I into Fibrils with Synthetic Peptides. *Journal of Biological Chemistry* **273**, 15598-15604.
- Puech, P.H., Poole, K., Knebel, D., and Muller, D.J.** (2006). A new technical approach to quantify cell-cell adhesion forces by AFM. *Ultramicroscopy* **106**, 637-644.
- Puech, P.H., Taubenberger, A., Ulrich, F., Krieg, M., Muller, D.J., and Heisenberg, C.P.** (2005). Measuring cell adhesion forces of primary gastrulating cells from zebrafish using atomic force microscopy. *J Cell Sci* **118**, 4199-4206.
- Quist, A.P., Pavlovic, E., and Oscarsson, S.** (2005). Recent advances in microcontact printing. *Anal Bioanal Chem* **381**, 591-600.
- Radisky, D.C.** (2005). Epithelial-mesenchymal transition. *J Cell Sci* **118**, 4325-4326.
- Ramshaw, J.A., Peng, Y.Y., Glattauer, V., and Werkmeister, J.A.** (2009). Collagens as biomaterials. *J Mater Sci Mater Med* **20 Suppl 1**, S3-8.
- Rando, O.J., and Verstrepen, K.J.** (2007). Timescales of genetic and epigenetic inheritance. *Cell* **128**, 655-668.
- Reyes, C.D., and García, A.J.** (2003). A centrifugation cell adhesion assay for high-throughput screening of biomaterial surfaces. *Journal of Biomedical Materials Research Part A* **67A**, 328-333.
- Ricard-Blum, S., Ruggiero, F., and van der Rest, M.** (2005). The Collagen Superfamily/ Collagen, J. Brinckmann, H. Notbohm, and P.K. Müller, eds (Springer Berlin / Heidelberg), pp. 35-84.
- Riederer, M.A., Ginsberg, M.H., and Steiner, B.** (2002). Blockade of platelet GPIIb-IIIa (Integrin  $\alpha$ IIb $\beta$ 3) in flowing human blood leads to passivation of prothrombotic surfaces. *Thromb Haemost* **88**, 858-864.
- Rigot, V., Andre, F., Lehmann, M., Lissitzky, J.C., Marvaldi, J., and Luis, J.** (1999). Biogenesis of  $\alpha$ 6 $\beta$ 4 integrin in a human colonic adenocarcinoma cell line involvement of calnexin. *Eur J Biochem* **261**, 659-666.
- Riikonen, T., Westermarck, J., Koivisto, L., Broberg, A., Kahari, V.M., and Heino, J.** (1995). Integrin  $\alpha$ 2 $\beta$ 1 is a positive regulator of collagenase (MMP-1) and collagen  $\alpha$ 1(I) gene expression. *J Biol Chem* **270**, 13548-13552.
- Roughley, P.J.** (2008). Lecture 36. Skin 1: Collagen and Extracellular Matrix (Montréal: McGill Molson Medical Informatics).
- Rubin, H.** (1990). The significance of biological heterogeneity. *Cancer Metastasis Rev* **9**, 1-20.
- Rubin, H., and Hatie, C.** (1968). Increase in the size of chick embryo cells upon cultivation in serum-containing medium. *Dev Biol* **17**, 603-616.
- Ryan, D., Ren, K., and Wu, H.** (2011). Single-cell assays. *Biomicrofluidics* **5**, 21501.
- Sasaki, T., Larsson, H., Tisi, D., Claesson-Welsh, L., Hohenester, E., and Timpl, R.** (2000). Endostatins derived from collagens XV and XVIII differ in structural and binding properties, tissue distribution and anti-angiogenic activity. *Journal of Molecular Biology* **301**, 1179-1190.
- Scheele, S., Nystrom, A., Durbeej, M., Talts, J.F., Ekblom, M., and Ekblom, P.** (2007). Laminin isoforms in development and disease. *J Mol Med* **85**, 825-836.
- Schimmel, T., Koch, T., Küppers, J., and Lux-Steiner, M.** (1999). True atomic resolution under ambient conditions obtained by atomic force microscopy in the contact mode. *Applied Physics A: Materials Science & Processing* **68**, 399-402.
- Schreiner, C., Bauer, J., Margolis, M., and Juliano, R.L.** (1991). Expression and role of integrins in adhesion of human colonic carcinoma cells to extracellular matrix components. *Clin Exp Metastasis* **9**, 163-178.
- Shahin, V., Ludwig, Y., Schafer, C., Nikova, D., and Oberleithner, H.** (2005). Glucocorticoids remodel nuclear envelope structure and permeability. *Journal of Cell Science* **118**, 2881-2889.

- Shimaoka, M., Lu, C., Palframan, R.T., von Andrian, U.H., McCormack, A., Takagi, J., and Springer, T.A. (2001). Reversibly locking a protein fold in an active conformation with a disulfide bond: integrin alphaL I domains with high affinity and antagonist activity in vivo. *Proc Natl Acad Sci U S A* **98**, 6009-6014.
- Sieg, D.J., Hauck, C.R., Ilic, D., Klingbeil, C.K., Schaefer, E., Damsky, C.H., and Schlaepfer, D.D. (2000). FAK integrates growth-factor and integrin signals to promote cell migration. *Nat Cell Biol* **2**, 249-256.
- Simson, D.A., Ziemann, F., Strigl, M., and Merkel, R. (1998). Micropipet-based pico force transducer: in depth analysis and experimental verification. *Biophys J* **74**, 2080-2088.
- Singh, D.K., Ku, C.J., Wichaidit, C., Steininger, R.J., 3rd, Wu, L.F., and Altschuler, S.J. (2010). Patterns of basal signaling heterogeneity can distinguish cellular populations with different drug sensitivities. *Mol Syst Biol* **6**, 369.
- Smith, J.W. (1968). Molecular Pattern in Native Collagen. *Nature* **219**, 157-158.
- Snijder, B., and Pelkmans, L. (2011). Origins of regulated cell-to-cell variability. *Nat Rev Mol Cell Biol* **12**, 119-125.
- Sonnenberg, A., Linders, C.J., Daams, J.H., and Kennel, S.J. (1990a). The alpha 6 beta 1 (VLA-6) and alpha 6 beta 4 protein complexes: tissue distribution and biochemical properties. *J Cell Sci* **96** ( Pt 2), 207-217.
- Sonnenberg, A., Linders, C.J., Modderman, P.W., Damsky, C.H., Aumailley, M., and Timpl, R. (1990b). Integrin recognition of different cell-binding fragments of laminin (P1, E3, E8) and evidence that alpha 6 beta 1 but not alpha 6 beta 4 functions as a major receptor for fragment E8. *J Cell Biol* **110**, 2145-2155.
- Sonnenberg, A., Calafat, J., Janssen, H., Daams, H., van der Raaij-Helmer, L.M., Falcioni, R., Kennel, S.J., Aplin, J.D., Baker, J., Loizidou, M., and et al. (1991). Integrin alpha 6/beta 4 complex is located in hemidesmosomes, suggesting a major role in epidermal cell-basement membrane adhesion. *J Cell Biol* **113**, 907-917.
- Sotomayor Torres, C.M. (2003). *Alternative Lithography: Unleashing the Potentials of Nanotechnology* (New York: Kluwer Academic/Plenum Publishers).
- Spiller, D.G., Wood, C.D., Rand, D.A., and White, M.R. (2010). Measurement of single-cell dynamics. *Nature* **465**, 736-745.
- Stallmach, A., von Lampe, B., Matthes, H., Bornhoft, G., and Riecken, E.O. (1992). Diminished expression of integrin adhesion molecules on human colonic epithelial cells during the benign to malign tumour transformation. *Gut* **33**, 342-346.
- Staniszewska, I., Walsh, E.M., Rothman, V.L., Gaathon, A., Tuszyński, G.P., Calvete, J.J., Lazarovici, P., and Marcinkiewicz, C. (2009). Effect of VP12 and viperistatin on inhibition of collagen-receptor-dependent melanoma metastasis. *Cancer Biol Ther* **8**, 1507-1516.
- Suel, G.M., Kulkarni, R.P., Dworkin, J., Garcia-Ojalvo, J., and Elowitz, M.B. (2007). Tunability and noise dependence in differentiation dynamics. *Science* **315**, 1716-1719.
- Sun, H., Santoro, S.A., and Zutter, M.M. (1998). Downstream events in mammary gland morphogenesis mediated by reexpression of the alpha2beta1 integrin: the role of the alpha6 and beta4 integrin subunits. *Cancer Res* **58**, 2224-2233.
- Sun, M., Graham, J.S., Hegedus, B., Marga, F., Zhang, Y., Forgacs, G., and Grandbois, M. (2005). Multiple membrane tethers probed by atomic force microscopy. *Biophys J* **89**, 4320-4329.
- Tadokoro, S., Shattil, S.J., Eto, K., Tai, V., Liddington, R.C., de Pereda, J.M., Ginsberg, M.H., and Calderwood, D.A. (2003). Talin binding to integrin beta tails: a final common step in integrin activation. *Science* **302**, 103-106.
- Takada, Y., Ye, X., and Simon, S. (2007). The integrins. *Genome Biol* **8**, 215.
- Takagi, J., and Springer, T.A. (2002). Integrin activation and structural rearrangement. *Immunol Rev* **186**, 141-163.

- Takagi, J., Erickson, H.P., and Springer, T.A.** (2001a). C-terminal opening mimics 'inside-out' activation of integrin alpha5beta1. *Nat Struct Biol* **8**, 412-416.
- Takagi, J., Petre, B.M., Walz, T., and Springer, T.A.** (2002). Global conformational rearrangements in integrin extracellular domains in outside-in and inside-out signaling. *Cell* **110**, 599-511.
- Takagi, J., Beglova, N., Yalamanchili, P., Blacklow, S.C., and Springer, T.A.** (2001b). Definition of EGF-like, closely interacting modules that bear activation epitopes in integrin beta subunits. *Proc Natl Acad Sci U S A* **98**, 11175-11180.
- Takaoka, A.S., Yamada, T., Gotoh, M., Kanai, Y., Imai, K., and Hirohashi, S.** (1998). Cloning and characterization of the human beta4-integrin gene promoter and enhancers. *J Biol Chem* **273**, 33848-33855.
- Tan, J.L., Tien, J., and Chen, C.S.** (2001). Microcontact Printing of Proteins on Mixed Self-Assembled Monolayers. *Langmuir* **18**, 519-523.
- Tani, T., Karttunen, T., Kiviluoto, T., Kivilaakso, E., Burgeson, R.E., Sipponen, P., and Virtanen, I.** (1996). Alpha 6 beta 4 integrin and newly deposited laminin-1 and laminin-5 form the adhesion mechanism of gastric carcinoma. Continuous expression of laminins but not that of collagen VII is preserved in invasive parts of the carcinomas: implications for acquisition of the invading phenotype. *Am J Pathol* **149**, 781-793.
- Taubenberger, A.** (2009). Quantifying adhesive interactions between cells and extracellular matrix by single-cell force spectroscopy In *Fakultät Maschinenwesen (Dresden: Technische Universitaet Dresden)*, pp. 187.
- Taubenberger, A., Cisneros, D.A., Friedrichs, J., Puech, P.H., Muller, D.J., and Franz, C.M.** (2007). Revealing early steps of alpha2beta1 integrin-mediated adhesion to collagen type I by using single-cell force spectroscopy. *Mol Biol Cell* **18**, 1634-1644.
- Taupier, M.A., Kearney, J.F., Leibson, P.J., Loken, M.R., and Schreiber, H.** (1983). Nonrandom escape of tumor cells from immune lysis due to intraclonal fluctuations in antigen expression. *Cancer Res* **43**, 4050-4056.
- Taylor, M.E.** (1993). Dynamics of piezoelectric tube scanners for scanning probe microscopy. *Review of Scientific Instruments* **64**, 154-158.
- Terranova, V.P., Williams, J.E., Liotta, L.A., and Martin, G.R.** (1984). Modulation of the metastatic activity of melanoma cells by laminin and fibronectin. *Science* **226**, 982-985.
- Than, M.E., Henrich, S., Huber, R., Ries, A., Mann, K., Kuhn, K., Timpl, R., Bourenkov, G.P., Bartunik, H.D., and Bode, W.** (2002). The 1.9-A crystal structure of the noncollagenous (NC1) domain of human placenta collagen IV shows stabilization via a novel type of covalent Met-Lys cross-link. *Proc Natl Acad Sci U S A* **99**, 6607-6612.
- Thery, M., Pepin, A., Dressaire, E., Chen, Y., and Bornens, M.** (2006). Cell distribution of stress fibres in response to the geometry of the adhesive environment. *Cell Motil Cytoskeleton* **63**, 341-355.
- Thornton, J.** (1998). *Scanning Probe Microscopy Training Notebook* (Digital Instruments, Veeco Metrology Group,).
- Tiger, C.F., Fougere, F., Grundstrom, G., Velling, T., and Gullberg, D.** (2001). alpha11beta1 integrin is a receptor for interstitial collagens involved in cell migration and collagen reorganization on mesenchymal nonmuscle cells. *Dev Biol* **237**, 116-129.
- Timpl, R.** (1989). Structure and biological activity of basement membrane proteins. *Eur J Biochem* **180**, 487-502.
- Timpl, R., Rohde, H., Robey, P.G., Rennard, S.I., Foidart, J.M., and Martin, G.R.** (1979). Laminin--a glycoprotein from basement membranes. *J Biol Chem* **254**, 9933-9937.
- Tomatis, D., Echtermayer, F., Schober, S., Balzac, F., Retta, S.F., Silengo, L., and Tarone, G.** (1999). The muscle-specific laminin receptor alpha7 beta1 integrin negatively regulates alpha5 beta1 fibronectin receptor function. *Exp Cell Res* **246**, 421-432.

- Tortonese, M.** (1997). Cantilevers and tips for atomic force microscopy. *Engineering in Medicine and Biology Magazine, IEEE* **16**, 28-33.
- Tuckwell, D., Calderwood, D.A., Green, L.J., and Humphries, M.J.** (1995). Integrin alpha 2 I-domain is a binding site for collagens. *J Cell Sci* **108 ( Pt 4)**, 1629-1637.
- Tulla, M., Helenius, J., Jokinen, J., Taubenberger, A., Muller, D.J., and Heino, J.** (2008a). TPA primes alpha2beta1 integrins for cell adhesion. *FEBS Lett* **582**, 3520-3524.
- Tulla, M., Pentikainen, O.T., Viitasalo, T., Kapyla, J., Impola, U., Nykvist, P., Nissinen, L., Johnson, M.S., and Heino, J.** (2001). Selective binding of collagen subtypes by integrin alpha 1I, alpha 2I, and alpha 10I domains. *J Biol Chem* **276**, 48206-48212.
- Tulla, M., Lahti, M., Puranen, J.S., Brandt, A.M., Kapyla, J., Domogatskaya, A., Salminen, T.A., Tryggvason, K., Johnson, M.S., and Heino, J.** (2008b). Effects of conformational activation of integrin alpha 1I and alpha 2I domains on selective recognition of laminin and collagen subtypes. *Exp Cell Res* **314**, 1734-1743.
- Tunggal, P., Smyth, N., Paulsson, M., and Ott, M.C.** (2000). Laminins: structure and genetic regulation. *Microsc Res Tech* **51**, 214-227.
- Vakonakis, I., and Campbell, I.D.** (2007). Extracellular matrix: from atomic resolution to ultrastructure. *Current Opinion in Cell Biology* **19**, 578-583.
- Valles, A.M., Boyer, B., Tarone, G., and Thiery, J.P.** (1996). Alpha 2 beta 1 integrin is required for the collagen and FGF-1 induced cell dispersion in a rat bladder carcinoma cell line. *Cell Adhes Commun* **4**, 187-199.
- Van de Walle, G.R., Vanhoorelbeke, K., Majer, Z., Illyes, E., Baert, J., Pareyn, I., and Deckmyn, H.** (2005). Two functional active conformations of the integrin {alpha}2{beta}1, depending on activation condition and cell type. *J Biol Chem* **280**, 36873-36882.
- van der Rest, M., and Garrone, R.** (1991). Collagen family of proteins. *The FASEB Journal* **5**, 2814-2823.
- Vandenberg, P., Kern, A., Ries, A., Luckenbill-Edds, L., Mann, K., and Kuhn, K.** (1991). Characterization of a type IV collagen major cell binding site with affinity to the alpha 1 beta 1 and the alpha 2 beta 1 integrins. *J Cell Biol* **113**, 1475-1483.
- Vihinen, P., Riikonen, T., Laine, A., and Heino, J.** (1996). Integrin alpha 2 beta 1 in tumorigenic human osteosarcoma cell lines regulates cell adhesion, migration, and invasion by interaction with type I collagen. *Cell Growth Differ* **7**, 439-447.
- Voigt, S., Gossrau, R., Baum, O., Loster, K., Hofmann, W., and Reutter, W.** (1995). Distribution and quantification of alpha 1-integrin subunit in rat organs. *Histochem J* **27**, 123-132.
- Volk, T., Geiger, B., and Raz, A.** (1984). Motility and adhesive properties of high- and low-metastatic murine neoplastic cells. *Cancer Res* **44**, 811-824.
- von Ardenne, M.** (1938). Das Elektronen-Rastermikroskop. *Zeitschrift für Physik A Hadrons and Nuclei* **109**, 553-572.
- von der Mark, H., Durr, J., Sonnenberg, A., von der Mark, K., Deutzmann, R., and Goodman, S.L.** (1991). Skeletal myoblasts utilize a novel beta 1-series integrin and not alpha 6 beta 1 for binding to the E8 and T8 fragments of laminin. *J Biol Chem* **266**, 23593-23601.
- von Philipsborn, A.C., Lang, S., Bernard, A., Loeschinger, J., David, C., Lehnert, D., Bastmeyer, M., and Bonhoeffer, F.** (2006a). Microcontact printing of axon guidance molecules for generation of graded patterns. *Nat Protoc* **1**, 1322-1328.
- von Philipsborn, A.C., Lang, S., Loeschinger, J., Bernard, A., David, C., Lehnert, D., Bonhoeffer, F., and Bastmeyer, M.** (2006b). Growth cone navigation in substrate-bound ephrin gradients. *Development* **133**, 2487-2495.
- Wallraff, G.M., and Hinsberg, W.D.** (1999). Lithographic Imaging Techniques for the Formation of Nanoscopic Features. *Chem Rev* **99**, 1801-1822.

- Walter, N., Selhuber, C., Kessler, H., and Spatz, J.P.** (2006). Cellular unbinding forces of initial adhesion processes on nanopatterned surfaces probed with magnetic tweezers. *Nano Lett* **6**, 398-402.
- Wang, H., Yang, Y., and Erie, D.** (2007). Characterization of Protein–Protein Interactions Using Atomic Force Microscopy/ Protein Interactions, P. Schuck, ed (Springer US), pp. 39-77.
- Weder, G., Voros, J., Giazson, M., Matthey, N., Heinzemann, H., and Liley, M.** (2009). Measuring cell adhesion forces during the cell cycle by force spectroscopy. *Biointerphases* **4**, 27-34.
- Wegener, K.L., Partridge, A.W., Han, J., Pickford, A.R., Liddington, R.C., Ginsberg, M.H., and Campbell, I.D.** (2007). Structural basis of integrin activation by talin. *Cell* **128**, 171-182.
- Weghuber, J., Brameshuber, M., Sunzenauer, S., Lehner, M., Paar, C., Haselgrubler, T., Schwarzenbacher, M., Kaltenbrunner, M., Hesch, C., Paster, W., Heise, B., Sonnleitner, A., Stockinger, H., and Schutz, G.J.** (2010). Detection of protein-protein interactions in the live cell plasma membrane by quantifying prey redistribution upon bait micropatterning. *Methods Enzymol* **472**, 133-151.
- Werb, Z., and Chin, J.R.** (1998). Extracellular Matrix Remodeling during Morphogenesis. *Annals of the New York Academy of Sciences* **857**, 110-118.
- White, D.J., Puranen, S., Johnson, M.S., and Heino, J.** (2004). The collagen receptor subfamily of the integrins. *Int J Biochem Cell Biol* **36**, 1405-1410.
- Wojcikiewicz, E.P., Zhang, X., and Moy, V.T.** (2004). Force and Compliance Measurements on Living Cells Using Atomic Force Microscopy (AFM). *Biol Proced Online* **6**, 1-9.
- Xia, Y., Mrksich, M., Kim, E., and Whitesides, G.M.** (1995). Microcontact Printing of Octadecylsiloxane on the Surface of Silicon Dioxide and Its Application in Microfabrication. *Journal of the American Chemical Society* **117**, 9576-9577.
- Xiong, J.-P., Stehle, T., Goodman, S.L., and Arnaout, M.A.** (2003). New insights into the structural basis of integrin activation. *Blood* **102**, 1155-1159.
- Xiong, J.P., Stehle, T., Diefenbach, B., Zhang, R., Dunker, R., Scott, D.L., Joachimiak, A., Goodman, S.L., and Arnaout, M.A.** (2001). Crystal structure of the extracellular segment of integrin alpha Vbeta3. *Science* **294**, 339-345.
- Xu, J., Rodriguez, D., Petitclerc, E., Kim, J.J., Hangai, M., Moon, Y.S., Davis, G.E., and Brooks, P.C.** (2001). Proteolytic exposure of a cryptic site within collagen type IV is required for angiogenesis and tumor growth in vivo. *J Cell Biol* **154**, 1069-1079.
- Xu, X., Nagarajan, H., Lewis, N.E., Pan, S., Cai, Z., Liu, X., Chen, W., Xie, M., Wang, W., Hammond, S., Andersen, M.R., Neff, N., Passarelli, B., Koh, W., Fan, H.C., Wang, J., Gui, Y., Lee, K.H., Betenbaugh, M.J., Quake, S.R., Famili, I., and Palsson, B.O.** (2011). The genomic sequence of the Chinese hamster ovary (CHO)-K1 cell line. *Nat Biotechnol* **29**, 735-741.
- Yamada, K.M., and Kennedy, D.W.** (1984). Dualistic nature of adhesive protein function: fibronectin and its biologically active peptide fragments can autoinhibit fibronectin function. *The Journal of Cell Biology* **99**, 29-36.
- Yang, W., Shimaoka, M., Salas, A., Takagi, J., and Springer, T.A.** (2004). Intersubunit signal transmission in integrins by a receptor-like interaction with a pull spring. *Proc Natl Acad Sci U S A* **101**, 2906-2911.
- Yang, X., Pursell, B., Lu, S., Chang, T.K., and Mercurio, A.M.** (2009). Regulation of beta 4-integrin expression by epigenetic modifications in the mammary gland and during the epithelial-to-mesenchymal transition. *J Cell Sci* **122**, 2473-2480.
- Yang, Z., Galloway, J.A., and Yu, H.** (1999). Protein Interactions with Poly(ethylene glycol) Self-Assembled Monolayers on Glass Substrates: Diffusion and Adsorption. *Langmuir* **15**, 8405-8411.
- Yasumura, K.Y., Stowe, T.D., Chow, E.M., Pfafman, T., Kenny, T.W., Stipe, B.C., and Rugar, D.** (2000). Quality factors in micron- and submicron-thick cantilevers. *Microelectromechanical Systems, Journal of* **9**, 117-125.

- Yurchenco, P.D., and Ruben, G.C.** (1988). Type IV collagen lateral associations in the EHS tumor matrix. Comparison with amniotic and in vitro networks. *Am J Pathol* **132**, 278-291.
- Yurchenco, P.D., Cheng, Y.S., and Colognato, H.** (1992). Laminin forms an independent network in basement membranes. *J Cell Biol* **117**, 1119-1133.
- Yurchenco, P.D., Tsilibary, E.C., Charonis, A.S., and Furthmayr, H.** (1985). Laminin polymerization in vitro. Evidence for a two-step assembly with domain specificity. *J Biol Chem* **260**, 7636-7644.
- Zaidel-Bar, R., Itzkovitz, S., Ma'ayan, A., Iyengar, R., and Geiger, B.** (2007). Functional atlas of the integrin adhesome. *Nat Cell Biol* **9**, 858-867.
- Zamir, E., Katz, M., Posen, Y., Erez, N., Yamada, K.M., Katz, B.Z., Lin, S., Lin, D.C., Bershadsky, A., Kam, Z., and Geiger, B.** (2000). Dynamics and segregation of cell-matrix adhesions in cultured fibroblasts. *Nat Cell Biol* **2**, 191-196.
- Zang, Q., and Springer, T.A.** (2001). Amino acid residues in the PSI domain and cysteine-rich repeats of the integrin beta2 subunit that restrain activation of the integrin alpha(X)beta(2). *J Biol Chem* **276**, 6922-6929.
- Zarnitsyna, V.I., Huang, J., Zhang, F., Chien, Y.H., Leckband, D., and Zhu, C.** (2007). Memory in receptor-ligand-mediated cell adhesion. *Proc Natl Acad Sci U S A* **104**, 18037-18042.
- Zhang, W.M., Kapyla, J., Puranen, J.S., Knight, C.G., Tiger, C.F., Pentikainen, O.T., Johnson, M.S., Farndale, R.W., Heino, J., and Gullberg, D.** (2003). alpha 11beta 1 integrin recognizes the GFOGER sequence in interstitial collagens. *J Biol Chem* **278**, 7270-7277.
- Zhang, X., Wojcikiewicz, E., and Moy, V.T.** (2002). Force spectroscopy of the leukocyte function-associated antigen-1/intercellular adhesion molecule-1 interaction. *Biophys J* **83**, 2270-2279.
- Zhao, C., and Meng, A.** (2005). Sp1-like transcription factors are regulators of embryonic development in vertebrates. *Dev Growth Differ* **47**, 201-211.
- Zhou, J., and Reeders, S.T.** (1996). The alpha chains of type IV collagen. *Contrib Nephrol* **117**, 80-104.
- Zutter, M.M., and Santoro, S.A.** (1990). Widespread histologic distribution of the alpha 2 beta 1 integrin cell-surface collagen receptor. *Am J Pathol* **137**, 113-120.
- Zutter, M.M., Santoro, S.A., Staatz, W.D., and Tsung, Y.L.** (1995). Re-expression of the alpha 2 beta 1 integrin abrogates the malignant phenotype of breast carcinoma cells. *Proc Natl Acad Sci U S A* **92**, 7411-7415.
- Zutter, M.M., Santoro, S.A., Painter, A.S., Tsung, Y.L., and Gafford, A.** (1994). The human alpha 2 integrin gene promoter. Identification of positive and negative regulatory elements important for cell-type and developmentally restricted gene expression. *J Biol Chem* **269**, 463-469.

## Appendix

---

### Movie (included in CD)

#### **Movie 1. Comparative SCFS of a CHO cell performed on a laminin/fibrillar collagen I bifunctional substrate.**

A single CHO cell attached to an AFM cantilever is alternately brought into contact with laminin (red stripes) and fibrillar collagen I (transparent stripes) for a total of 8 force cycles using a retract speed of 10  $\mu\text{m/s}$  and a contact time of 10 s (top panel). The corresponding force signal (laminin in red and collagen in green) is displayed over time.



## Curriculum Vitae

### Personal Data:

**Name:** Lu DAO  
**Date of Birth:** 21.08.1983  
**Nationality:** China  
**Contact:** dolphinroad@gmail.com  
**Gender:** Female

### Education:

**Apr. 2008— now** PhD student in Center for Functional Nanostructures, Karlsruhe Institute of Technology  
**Jan. 2007** Obtained Master of Science degree, University of Ulm, Germany  
**Oct. 2005—Mar. 2007** Dept. of Advanced Materials, University of Ulm, Germany (as a formal student pursuing Master of Science degree)  
**Jun. 2005** Obtained Bachelor of Engineering degree, Southeast University, China  
**Sept. 2004—Sept. 2005** Dept. of Advanced Materials, University of Ulm, Germany (as an exchange student)  
**Sept. 2001—Aug. 2004** Dept. of Biomedical Engineering, Southeast University, China  
**Sept. 1998—Jun. 2001** Jiangsu Provincial Zhenjiang NO.1 High School, China  
**Sept. 1995—Jun. 1998** Jianbi Power Plant Middle School, China

### Professional & research experience:

**Apr. 2008—now** PhD student working with projects “Revealing adhesive variations in clonal populations by comparative single cell force spectroscopy”, “Comparative single cell force spectroscopy on different bifunctional substrates” and “Inverse regulation between integrin  $\alpha_2\beta_1$  and laminin receptors”  
**Feb. 2007—Sep. 2007** For internship, involved in the project “Mechanism of stem cell fusion and applications for regenerative therapies” in Fraunhofer Institute for Cell Therapy and Immunology, Leipzig  
**Oct. 2006—Jan. 2007** Research assistant in Max-Planck Institute for Metal Research, Dept. of Prof. Spatz, on the topic of “Using micro contact printed pattern to research fibroblasts morphology”  
**Apr. 2006—Sept. 2006** Master thesis research on the topic “Manipulation of cell shape polarity and nucleus oscillations of melanocytes from healthy donors and NF1 patients by micro contact printing ( $\mu$ CP) methods”, in Dept. of Prof. Spatz, Max-Planck Institute for Metal Research

## List of publications

### Articles:

**Lu Dao, Ulrich Weiland, Mario Hauser, Irina Nazarenko, Heinz Kalt, Martin Bastmeyer and Clemens M. Franz.** (2012). Revealing non-genetic adhesive variations in clonal populations by comparative single-cell force spectroscopy. **Experimental Cell Research**.

**Lu Dao, Martin Bastmeyer and Clemens M. Franz.** Inverse regulation between integrin  $\alpha_2\beta_1$  and laminin receptors. In preparation

**Lu Dao and Clemens M. Franz.** Comparative single-cell force spectroscopy on bifunctional substrates. In preparation,

### Posters:

**Lu Dao, Ulrich Weiland, Thomas Striebel, Martin Bastmeyer and Clemens M. Franz.** Micropatterned substrates for single-cell force spectroscopy. 7<sup>th</sup> international symposium SPM in life science. Berlin (Germany), October, 2008.

**Lu Dao, Ulrich Weiland, Thomas Striebel, Martin Bastmeyer and Clemens M. Franz.** Micropatterned substrates for single-cell force spectroscopy. CFN summer school on nano-biology. Bad Herrenalb (Germany), September, 2009.

**Lu Dao and Clemens M. Franz.** Inverse regulation between integrin  $\alpha_2\beta_1$  and laminin receptors. Gordon-Kenan research seminar and Gordon research conference on fibronectin, integrins & related molecules. Lucca (Italy), April-May, 2011.

**Lu Dao, Ulrich Weiland, Mario Hauser, Heinz Kalt, Martin Bastmeyer and Clemens M. Franz.** Bifunctional cell adhesion substrates for comparative single-cell force spectroscopy. Gordon-Kenan research seminar and Gordon research conference on science of adhesion. Bates College (USA), July, 2011.

**Lu Dao and Clemens M. Franz.** Inverse regulation between integrin  $\alpha_2\beta_1$  and laminin receptors. CFN summer school on nano-biology. Bad Herrenalb (Germany), September, 2011.

**Lu Dao, Ulrich Weiland, Mario Hauser, Heinz Kalt, Martin Bastmeyer and Clemens M. Franz.** Bifunctional cell adhesion substrates for comparative single-cell force spectroscopy. The XIV. Annual Linz Winter Workshop and Hands-on Winter School. Linz (Austria), January-February, 2012

**Lu Dao and Clemens M. Franz.** Inverse regulation between integrin  $\alpha_2\beta_1$  and laminin receptors. Gordon research seminar and Gordon research conference on signaling by adhesion receptors. Colby College (USA), June, 2012.

## Acknowledgements

I would like to acknowledge all people who have helped and inspired me during my doctoral study.

Dr. Clemens M. Franz, I would like to express my sincere and full gratitude to you for offering me the opportunity to research this interesting and interdisciplinary topic. Thank you very much for your academic and personal support all along. It's a great honor to be your first PhD student.

I am indebted to Prof. Dr. Martin Bastmeyer for sharing your scientific expertise with me and generously providing me with the access to many cutting edge microscopy and Microcontact printing techniques.

Prof. Dr. Doris Wedlich, as an outstanding female scientist, you are an idol for me.

Dr. Ralf Kemkemer and PD Dr. Dieter Kaufmann, I profoundly thank you for your kind care and support for so many years. You helped me tremendously when I was in a deep life rut and for that I am always thankful.

Dr. Wilko Thiele, Dr. Irina Nazarenko and Dr. Mario Hauser and Dr. Anna Müller, it is a great experience collaborating with you. I appreciate all the effort you made for the joint projects.

All my colleagues from AG Franz and zoology institute I supported my research work. Thank you for all your generous help and stimulating suggestions. I enjoy the time I spent together with you. Especially I am obliged to Dr. Anna Müller, Dr. Dimitar Stamo, Dr. Anna Burcza, Tetyana Gudzenko and Ramona Ring.

I thank Gregorij Grabovskij for software support.

My friends Dr. Zhongxiang Jiang, Dr. Fei Qiao, Dr. Rui Yang, Dr. Xiaoli Chang, Yi Su and Yuhan Liu, your care and encouragement helped me overcome many difficulties and stay focused on my research work. I cherish your friendship and appreciate your faith in me.

Finally, my deepest gratitude goes to my parents, Shuyuan Dao and Hedi Chen. I can never be me without your unflagging love and patience. My dear brother Liang Dao, thanks for your company and always being a good example for me. My husband Puyi Zhao, you have been a constant source of support and strength all these years. I love you all.